PARTS OF THE ORIGINAL DOCUMENT

ARE OF POOR REPRODUCTIVE QUALITY

CERTAINES PARTIES DU DOCUMENT ORIGINAL

SONT DE PIÈTRE QUALITÉ DE REPRODUCTION

Canada Mortgage and Housing Corporation

Société canadienne d'hypothèques et de logement

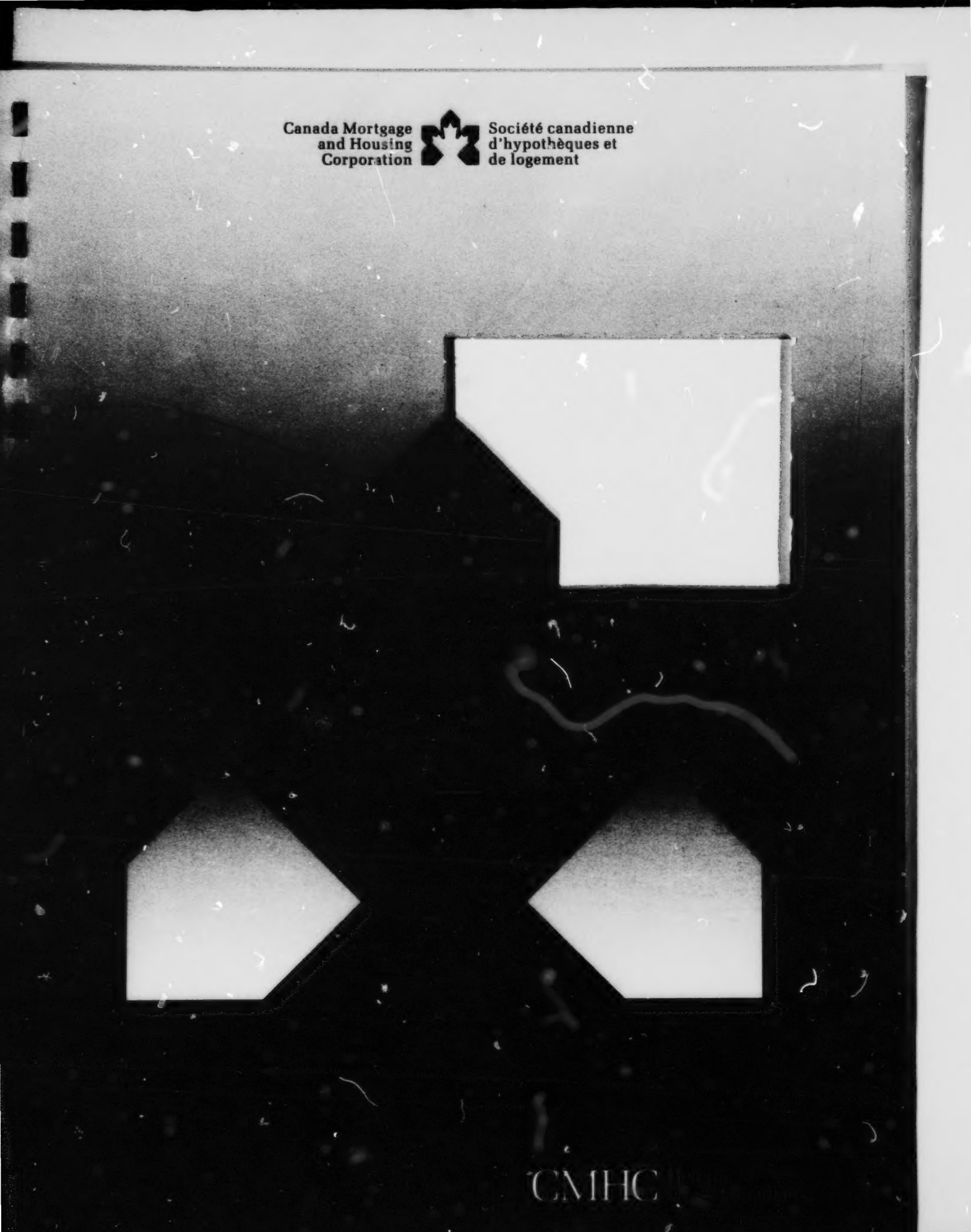

CMHC

DRYING CHARACTERISTICS IN TIMBER FRAME WALLS OF LOW-RISE RESIDENTIAL HOUSING - FINAL REPORT

April 5, 1988

Rowan Williams
Davies & Irwin Inc.

DRYING CHARACTERISTICS IN TIMBER FRAME WALLS OF LOW-RISE RESIDENTIAL HOUSING FINAL REPORT

Report 487-1400-1

April 5, 1988

Submitted to:
THE RESEARCH DIVISION
POLICY DEVELOPMENT AND RESEARCH SECTOR
CANADA MORTGAGE AND HOUSING CORPORATION

By:
ROWAN WILLIAMS DAVIES & IRWIN Inc.
CONSULTING ENGINEERS
GUELPH, ONTARIO

Vincent Ferraro, P.Eng.
Project Engineer

Glenn D. Schuyler, P.Eng.
Principal

and

SCANADA CONSULTANTS LIMITED
OAKVILLE, ONTARIO

Michael C. Swinton, P.Eng.

COPYRIGHT - CMHC 1988

650 Woodlawn Road West, Guelph, Ontario N1K 1B8 • Tel. (519) 823-1311, Telex 069-56639, Fax (519) 823-1316

TABLE OF CONTENTS

	Page No.
ABSTRACT	1
EXECUTIVE SUMMARY	2
1. INTRODUCTION	4
2. PROJECT SCOPE AND OBJECTIVES	6
3. COMPUTER MODEL DEVELOPMENT	7
3.1 General	8
3.2 Modelling Details	10
3.2.1 The Heat Transport Submodel	10
3.2.2 The Moisture Transport Submodel	11
3.2.3 The Air Flow Submodel	13
3.2.4 Linking the Three Submodels	14
3.2.5 Space and Time Domains	16
4. FULL SCALE LABORATORY WALL DRYING TEST	17
4.1 General	17
4.2 The Test Chamber	17
4.3 The Wall Assembly	19
4.4 Instrumentation and Test Parameters	20
4.5 Results of Drying of Laboratory Test Walls	21
5. VALIDATION OF THE COMPUTER MODEL WITH LABORATORY TEST WALL DATA	22
5.1 General	22
5.2 Validation Procedure	22
5.3 Comparison of Computer Simulations and Test Results for a 5mm Airspace	25
5.3.1 First Comparison	25
5.3.2 Second Comparison	28
5.3.3 Third Comparison	28
5.4 Simulation of Wall Drying With a Narrower Air Space	29

6. SIMULATION OF WALL DRYING IN THE HALIFAX CLIMATE 30
6.1 Simulation for a Full Year 30
6.2 Wall Drying of the Laboratory Wall Using Assumed Versus Benchtop Parameters 32

7. CONCLUSIONS 34

REFERENCES

FIGURES

TABLES

APPENDICES
A - Property of Materials Database
B - Milestone Report for Task 1 and 2
C - Milestone Report for Task 3
D - Milestone Report for Task 4
E - Milestone Report for Task 5
F - Milestone Report for Task 6

ABSTRACT

The main objective of the project, as described in this report, has been the development of an analytical model to represent the wetting/drying characteristics in outer portions of walls in low-rise timber frame residential housing. Initiated to improve the understanding of the causes of moisture damage in real walls the study provides the basis for developing practical design information regarding outer-wall moisture performance. Previous theoretical and field studies, including the reporting from Atlantic Canada moisture troubled houses, indicated a need for a comprehensive analytical model to represent the entire wetting and drying cycle in real walls. This study was comprised of two phases, with the first phase, analysis and model development, reported upon in December 1986. The second phase consisted of model improvement and verification.

The essential output from both phases of research is an analytical computer simulation program, called WALLDRY. It is based on currently available moisture movement theories and supported with key parameters, required in the governing equations, determined from bench top tests. The simulation program has been validated with data gathered from laboratory measurements on a full scale timber frame wall assembly.

Results of the validation work are encouraging. Despite the complexities associated with moisture movement issues, the computer model is able to closely follow the drying of sheathing and studs as measured in the full scale laboratory wall, over a 19 day test period. Similar computer runs on a hypothetical wall using one year of Halifax weather data indicated that the model is sufficiently sensitive to track important moisture changes in the wall and that the modelling complexity is warranted. Because of efficient formulation and implementation, the computer program is able to achieve these results economically and in a reasonably short time period.

EXECUTIVE SUMMARY

Introduction

This project was initiated in response to observed moisture related damage in Canadian timber frame housing[1, 2, 3, 4] where moisture induced damage of outer walls was correlated with cool, high humidity climates and increased indoor humidities. Higher indoor moisture levels result from the use of heating systems without flues as well as the improved airtightness emphasized in more recent house construction practices. Differences of opinion among the players involved, over causes and the availability of practical solutions, emphasized the need for a more detailed and comprehensive study of outer-wall moisture movement.

Objectives

Rowan Williams Davies & Irwin Inc. (RWDI) of Guelph, together with Scanada Consultants Limited of Ottawa, were requested to develop a comprehensive model in the form of a computer simulation program based on available theories. Where available theories or system parameters were insufficient or not available new data was to be estimated through bench top testing. The hygroscopic nature of wood was to be an essential feature of the modelling, developed also to incorporate outdoor weather data.

Methodology

The work, comprised Phases I and II, and included:

Phase I
- attendance at a technical workshop and the development of a "Research Design";
- a survey of the international literature;
- a preliminary analysis from that literature;
- development of a first generation computer model; and
- an assessment of the approach chosen.

Phase II
- improvement and refinement to the computer model;
- experimental determination of the air flow coefficients behind and across the siding;
- experimental determination of moisture adsorption and evaporation rate from building materials; and
- validation of the computer model using full scale wall simulation.

Discussion

The literature survey highlighted the current level of understanding concerning moisture damage in timber frame walls. Although substantial experimental and theoretical studies had been performed by others, a comprehensive moisture transport model, along with an understanding of the wall as a system were lacking. Analytical models developed by others fell short of realistic representations of real walls. Deficiences with these models in simulating the wetting and

drying of actual walls resulted from a combination of the following factors, including: absences of airflows in the outer-wall cavities as they affected moisture movement, moisture balances in all wall components and air leakages from the indoor space; lack of modelling the hygroscopic storage capacity of porous building materials and, representation of real walls with one dimensional "lumped" mass models.

The computer model now developed addresses these issues.

Findings

To assure the development of a realistic analytical model to predict outer-wall drying, it was necessary to generate at least rough estimates of required material properties and air flow characteristics for a typical wall. The analytical model so developed addresses the deficiencies previously listed by representing all aspects of wetting and drying thought to exist as interrelated processes in a real wall.

Simulations using this new computer model and parameters from the bench top tests show that the surrounding layers of material in an outer-wall system could absorb large quantities of moisture relative to air. Accordingly, any change of vapour pressures or relative humidities would result in negligible moisture content variations in these materials over a one hour period; the dominant time step in the program. These findings imply that the material layers act as slowly varying moisture boundary conditions and that the air layer is an important and dynamic component reaching steady state early in the hour interval. Based on this insight, the moisture flow model was subsequently developed.

Satisfactory validation of the analytical simulation model with comparisons of predicted versus measured drying in a laboratory full scale wall assembly under measured exterior and indoor conditions has been carried out.

Conclusions

Comparisons of the measured and predicted laboratory wall drying indicate that, despite the complexities of the interrelated processes governing moisture transport in timber frame walls, the computer simulation program is capable of closely representing drying in the wood studs and the sheathing layer.

Comparisons between simulation and laboratory test results indicate that representative practical moisture performances of studs and sheathing in timber framed walls of low-rise housing can be predicted.

The model can also produce drying times that are indicative of actual drying times of real walls in a given climate.

The model can be used to evaluate and quantify test data. This is perhaps the best use of the model at this stage and through this process, both the test data and the simulated results are better understood.

1. INTRODUCTION

The incidence of moisture related damage in outer walls of low-rise timber frame residential houses has increased in recent years. The causes are partly attributed to improved airtightness, increased insulation levels in houses as well as an increase in the use of heating systems without flues. In addition, surveys of moisture related damage in houses indicate that a large proportion of the damaged outer walls occur in coastal areas, suggesting that climate is an important aspect of the problem. Over the course of this study it has become apparent that an understanding of moisture issues can only be achieved by considering the complex interaction of the wall components in relation to climatic conditions and construction practices.

In an attempt to resolve the moisture related problems identified by numerous surveys(1, 2, 3, 4), CMHC issued Builders' Bulletins T-4 in 1982 and T-6 in 1984 requiring the use of furring strips, i.e. strapping, for all the Atlantic provinces. The intention of this remedial measure was to reduce wall moisture problems by increasing the ventilation within the air space behind the siding. At the same time, recognizing the complexity of the problem, CMHC initiated a comprehensive research project to study the outer wall moisture performance of timber frame walls.

The research work described in this present report, comprises an analytical study supported with laboratory experiments and validation. A field study, reported in (5), comprising erection and observation of three test huts, was carried out in parallel with the present program and has provided some further insights for use in this research work. The main objective of the work described herein is the development of an analytical computer simulation model supported with experimental data and validated with laboratory measurements on a full-scale wall assembly. This project has been divided into two contract phases, I and II. The Phase I segment included a state-of-the-art 'Literature Review', the development of a 'Research Design', and the development of a framework for the analytical computer simulation of wetting and drying processes in the outer wall. These

RWDI

activities are referred to as Tasks 1, 2 and 3 of Phase I respectively. Phase II work is comprised of Tasks 1 through 7 which include refinement of the computer model, experimental determination of key parameters and experimental validation of the improved simulation program.

The computer model of wall drying as developed in the first phase and as modified in this, the second phase, includes all the essential features thought to affect the systems process of wall wetting and drying. The key algorithm in the model as described in reference 8, page 31, is the one that determines the absolute humidity in the air space behind the outer wall siding and is the one that is thought to have a significant impact on the overall wetting and drying of the total outer wall system. The algorithm for the absolute humidity in that air space was derived by linking the three sub-models -- thermal, air flow and moisture flow -- and includes one of the key parameters in this system model: the characteristic length of vapour diffusion at the surface of a porous material.

In order to determine the characteristic length of vapour diffusion into the air space from adjacent building materials, the following three factors had to be determined:

- the effective evaporation rate at the surface of a material and the development of an understanding of what factors control it;

- the resistance to air leakage through gaps between outer siding boards and in the air space behind these siding boards;

- the quantity of moisture which a wood-based material can adsorb before it forms a water film on the surface of the material thereby affecting this surface moisture transfer.

The laboratory work done in this regard was directed to the specific and key modelling questions listed above. This new work incldued:

- benchtop tests determining the air flow resistance through and behind siding materials, as described in Appendices C and D;

- benchtop tests on water adsorption of various building materials, as described in Appendix E;

- benchtop tests on the surface evaporation rates of building materials, as described in Appendix F.

The results of these benchtop tests were parameterized and used directly in the computer model. As part of the analysis which followed from the laboratory work, realistic characteristic lengths of surface vapour diffusion were developed for an example siding material using the benchtop test data, as described in Section 6.2.

The resulting overall systems model, now calibrated with test-derived parameters, was validated against the results of a test of a full scale wall, with drying rates measured and recorded specifically for model verification purposes, as described in Section 4.

2. PROJECT SCOPE AND OBJECTIVES

The fundamental objective of the Phase I and Phase II contracts was to develop an analytical computer model capable of assessing the drying performance on a seasonal basis of timber frame outer walls in low-rise residential housing. The 'Literature Survey' and 'Research Design' tasks of Phase I along with the initial computer program development provide the background and starting point for the Phase II work reported on here.

The Phase II tasks were:

Task 1: Improvement of the computer simulation program to include an inner wall model representing the studs and insulation.

Task 2: Further improvement and refinement of the computer program, to include an enhanced wind model, an improved air leakage model and a surface drainage and condensation model.

Task 3: Experimental determination of air flow coefficients vertically along the wall in the air space, relating volume flow rate to pressure drop for various airspace thicknesses.

Task 4: Experimental determination of air flow coefficients across the siding gaps, relating volume flow rate to pressure drop, with the siding in dry and in wet conditions.

Task 5: Experimental determination of the moisture adsorption capacity of various building materials and the level at which surface drainage occurs.

Task 6: Experimental determination of rates of evaporation from various building materials at temperatures above and below freezing.

Task 7: Experimental validation of the computer simulation program with the use of a 2.4m wide full-scale wall segment.

The program skeleton, in modular format, was developed in Phase I and includes all essential features of a representative wall system which influence wetting and drying of its components. Generally, these features include the ability to represent; air, moisture and heat transport in the wall, a variable outdoor or indoor climate, if desired, air leakage from the indoors, as well as the hygroscopic behaviour of porous building materials.

The present tasks collectively were intended to produce a refined computer model sufficiently sensitive to discern the influences of varying one or more parameters describing a wall assembly on drying performance. With the intention of validating the model, the role of benchtop tests was to provide at least order of magnitude estimates of numerous flow and material parameters required by the

computer model and otherwise unavailable. The resulting laboratory-validated computer model will be used as a practical design tool, regarding moisture damage resistance, to assess the relative value of different materials or arrangements of wall components. Validation of model predictions against field measurements on actual walls will be desirable to accumulate experience and confidence with the model.

3. COMPUTER MODEL DEVELOPMENT

3.1 General

The goal of this task of the work was to develop, in modular form, a program which would predict drying in various components of a timber frame wall on a seasonal basis, given the outdoor climatic conditions, the indoor environment and the wall construction details.

This computer simulation program has been implemented in Task 3 of the Phase I contract and refined in Tasks 1 and 2 of the Phase II contract. The model is based on the 'Research Design' task of Phase I and describes the essential flow quantities that govern the moisture transport, i.e. wetting and drying, in the outer portion of the timber frame walls. The three essential transport mechanisms are: air flow, heat flow and vapour flow as shown in Figure 1.

The computer program represents an actual timber frame wall with a simplified quasi two-dimensional model. The model selected is based on considerations of the important flow directions indicated by the governing equations and by the geometry of the wall assembly. Two dimensions only are considered necessary to represent the phenomena occurring within a wall. One direction, X, always points perpendicular to the plane of the wall. Depending on the wall construction and the pressure regime, the Y direction can either point vertically or horizontally in the plane of the wall. For instance, with a pressure gradient up the wall and the use of vertical strapping the important flow directions are considered to be through the wall and vertically up the wall. Similarly, with the use of horizontal strapping

RWDI

and a horizontal pressure gradient the important directions are taken to be through the wall and horizontally along the wall.

A finite difference approach is used to represent a wall with 20 layers through its thickness and 9 vertically stacked wall elements for each layer. Flow through the wall layers in each element is one dimensional. In any layer, the nine vertical elements can represent variations in material properties and flow parameters vs the wall height. Air flow in the air space behind the siding, with or without furring strips is also represented by nine vertical elements with the main flow direction being vertical, i.e. the Y direction. This level of detail for the vertical direction is chosen to allow sufficient resolution for the modelling of the characteristic lengths of moisture and heat transport up the wall while maintaining practical limits on the computational effort.

Temperature and pressure gradients provide the fundamental driving forces for the transport mechanisms including heat, air and moisture. Interaction among vertical elements in the model is made possible by the airspace which can convect moisture and heat vertically from one element to another. Horizontal moisture transport, which occurs by diffusion and capillarity through porous components, combined with vertical convection in the air space gives the model its quasi two-dimensional capability. Moisture accumulation beyond a certain saturation level in one element may be transferred to an element below by gravity drainage, also represented in the model.

Air leakage occurring through layers across the wall, has been addressed in the model with sources and sinks connected in pairs within vertical elements across all layers. This interrelation of elements and layers give the model an ability to represent complex flow paths.

Running the program requires a 'wall' file which describes the wall regarding among other items; materials used, thicknesses, gap spacings, and wind pressure coefficients. Table 1 is an example of such a file. The first line of the table is a title that gives a brief description of the wall. The reference to a Halifax South

wall indicates that the pre-processed hourly weather data is for a south facing wall located in Halifax. The appropriate weather data file is specified within the table. A prompt in the program asks if weather data is to be used, i.e. real or artifical. If not, it asks for a set of fixed weather conditions, and ignores the weather data file, named in the table. The material properties are specified by numbers from a materials data base shown in Appendix A. Those properties are handbook values subject to modification if desired, as in the benchtop and laboratory validation tests.

3.2 Modelling Details

3.2.1 The Heat Transport Submodel

The purpose of the heat transport model is to predict mean hourly temperatures anywhere within the wall as governed by conduction through the wall layers, convection of air behind the siding, and radiation on the external face of the siding. These predictions depend on the boundary conditions, which may change from hour to hour, including: the temperature gradient across the wall, solar radiation on the siding, latent heat effects arising from moisture phase changes and heat storage changes in the material.

The heat transfer in the wall has been formulated as a one dimensional transport model, including a correction term for stored heat. The main heat flow is assumed to occur along the X direction. Conduction heat transfer vertically along the wall, in a material layer, is assumed negligible in comparison to conduction along the main flow direction as well as to convective transfer in the air layer, and is therefore not modelled.

The heat energy balance applied to each layer of material is an expression of the conservation of energy taking into account convection, conduction, radiation, capillary and diffusion transport as well as latent and sensible heat storage.

Applying this principle to all layers in each of the 9 elements produces a 'banded' matrix solved by standard matrix methods. The outcome of this solution is a set of temperatures for each layer of each element up the wall for each hour. Sensible heat stored in a layer as a result of a temperature change from one hour to the next is applied as a correction term to the following hour. Latent heat from phase changes is treated as a heat source, i.e. condensation, or heat sink, i.e. evaporation.

Applying this equation to the air layer demonstrates the interrelation between the air and heat transport submodels. Connection between the two sub models exists by virtue of air leaking from the outside and flowing vertically along the air space. The Research Design(6) and Literature Survey(7) reports describe details of the governing heat transport equations.

Considering the heat balance equation for the air layer, further leads to characteristic 'time' and 'length' scales for convection heat transfer vertically along the air space and conduction heat transfer from adjacent layers to the air. These factors, along with similar parameters for moisture transport, are important because their relative magnitudes determine how heat transport processes interact to arrive at the equilibrium temperature.

3.2.2 The Moisture Transport Submodel

In similar fashion to the heat flow submodel, the moisture transport submodel is fundamentally influenced by the air layer. The studies shows that the surrounding layers of material in an outer wall system can adsorb large quantities of moisture relative to air. Accordingly any change in vapour pressures, or relative humidities will result in negligible moisture content variations in these materials over the hour calculation interval. This implies that the material layers act as slowly varying moisture boundary conditions and the air layer is an important and a dynamic component reaching steady state early in the hour interval. Based on this the moisture flow model was developed to follow a five point procedure with the

conservation of mass principle applied to the absolute humidity when formulating the moisture transport equations for the air layer.

These steps include:

(i) establishing the psychrometric conditions at the surface of layers containing moisture from the previous interval and the temperature as obtained from the heat flow submodel

(ii) calculating equilibrium properties of the air space (vapour pressure, absolute humidity) as it responds to changes in the adjacent layers

(iii) calculating the rates of moisture flow, including the influence of air flow, that result in equilibrium conditions for the air layer

(iv) summing the moisture flow quantities over each hour and updating the moisture contents of the boundaries for the next hour calculations

(v) repeating these calculations for each hour in a full year and assembling moisture content time histories for the various hygroscopic components

Transport of vapour from the material boundaries to the air is assumed to occur purely by vapour pressure gradients. Diffusion of vapour from a material surface, i.e. evaporation, was the subject of Task 6 of the Phase II contract and is included as Appendix F of this report. As discussed therein, evaporation from a surface is taken to occur in two steps: migration of moisture towards an equilibrium surface moisture layer by internal diffusion and capillarity and then diffusion into the air by vapour pressure gradients. The Task 6 report includes measurements of moisture evaporation rates ($kg/m^2 \times sec \times Pa$) or, inversely, surface evaporation resistivities ($m^2 \times sec \times Pa)/kg$) for a variety of building materials and for a range of temperature from -5.6°C to 23.2°C. The results are used directly by the moisture flow submodel. Applying the above equation to each of 9 vertical elements in the air layer, generates 9 simultaneous equations for

absolute humidities along the wall for each hour. The moisture equation describes three characteristic time scales, namely, the moisture convection time scale, the diffusion time scale between air and sheathing and the diffusion time scale between air and the siding back surface.

Corresponding length scales of the flows can be derived by multiplying the velocity of the moving air by the time scales. Both scales are useful in assessing the relative importance of processes occuring in the wall. The relationships among the moisture flow submodel and the heat and air flow submodels are discussed in Section 3.2.4. Further details are described in References (6) and (7).

3.2.3 The Air Flow Submodel

An air flow submodel is the third essential component required to describe moisture related processes in a wall system. Its purpose is to calculate the air velocities and mass flow rates in the air space. The same principle of conservation of mass is applied, as for the moisture flow model, to determine velocities in each of the 9 vertical elements. In addition, mass conservation and air space velocity are influenced by pressure drops due to air leaking through siding gaps as well as to friction and form losses along the air space. Buoyancy effects caused by differing temperature up the wall are also influential, particularly when the wind induced pressure gradient is small. Three equations are needed to describe the air flow in each element, a mass balance equation and two flow versus pressure drop equations, one including the buoyancy term. These relations are presented and described in Reference (6).

Although the mass balance equation can be derived exactly from first principles, the pressure drop equations for air flow through the siding gaps and along the air space require determination of empirical flow coefficients. These empirical studies are the subject of Tasks 3 and 4 of the Phase II contract. The results are described in the milestone reports included as Appendices C and D respectively of this report. Task 4, considering flow coefficients across the siding gaps, also looks at the effect of water, rain for instance, on air flow behaviour past

the siding gaps. The general form of the pressure drop equation used in the model, irregardless of the cause of pressure drop is

$$Q = K1 * \Delta P + K2 * \Delta P^{0.5}$$

where K1 and K2 are the experimentally determined parameters, Q is the volume flow rate in meters^3/sec and ΔP is the pressure drop in Pascals. As described in (6), the buoyancy term is treated as a component of the pressure drop along the air space and is of the following form

$$\Delta P = g\,(\rho_{oi} \times H_i - \rho_{ai} \times H_i)$$

where ρ_{oi} and ρ_{ai} are air densities outside (o) and in the airspace (a) respectively at level i, H is the height of the wall, g is the gravitational acceleration and ΔP is pressure drop as before.

An iterative technique is used to solve the system of three equations for each element under the constraint that the pressure difference, between the lowest and highest elements describing the air space, must be equal to the pressure induced by exterior wind flows and buoyancy.

The air flow submodel requires a number of user supplied inputs including gap spacings between siding members, air space width, the distribution of wind pressures over the exterior surface of the siding, and the orientation of the wall under investigation relative to true north. The program has the ability to include various wind induced pressure distributions depending on differing wall orientations relative to the wind.

3.2.4 Linking the Three SubModels

Depending on the external conditions imposed on a wall and the relative importance of the moisture transport processes, the three submodels may be interrelated in differing degrees. For instance, the temperature regime across and

vertically up the wall will control whether or not buoyant convection is generated in the airspace. Thus, temperature generated buoyancy convection provides one link from the heat flow submodel to the air flow submodel. In the reverse direction, air flow generated either by buoyancy or pressure gradients affects the heat flow mainly by mixing of air streams. The moisture flow submodel is also connected to both the heat flow and air flow submodels. Air flow in the air space influences the moisture content of the space by air exchange with the exterior. This can occur either by air leakage through the siding gaps or by air flow towards the top or bottom of the wall. Two terms are included in the moisture balance expressions for the elements of the air layer to model these effects. Similarly the heat transport model will influence the moisture content in the air space and drying of wall components. Heat flow directly affects moisture content in the air space by influencing moisture exchange, i.e. evaporation or condensation, between the air space and adjacent material layers through changes in vapour pressure of hygroscopic materials. Heat and moisture also interact through latent heat effects.

Although the model has been formulated with the ability to represent these rather complex interactions, actual wall systems usually offer simplifications to the drying processes. For instance, numerous hypothetical model investigations have indicated short length scales for heat conduction in the air space. This suggests that average hourly temperatures in the air space are insignificantly affected by air flow velocities commonly found in walls. Further, sensible heat has also been found to have a small effect on the temperature field because of the small thermal mass forming the outer wall. Regarding the interaction of the heat and moisture transport submodels, it is also clear that the effects of latent heats of condensation or evaporation are also small in influencing the temperature field.

These simplifications result in an overall model formulation which can be solved by sequential calculation, Figure 2 illustrates a simplified flow chart of the major steps followed by the program.

3.2.5 Space and Time Domains

Consideration of the governing moisture and heat transport equations, discussed in References 6 and 7, offers indications of time and length scales controlling the drying of timber frame walls. Events directly associated with the air layer of the wall commonly have short time and length scales. For instance, exchange of moisture or heat from the sheathing to adjacent air can occur on the order of seconds. The distance, associated with this time scale gives rise to the concept of a 'characteristic length' - a distance within which any change, at a boundary or in the air, comes into moisture or thermal equilibrium with its surroundings.

Field observations of timber frame walls suggest that wetting and drying are intimately dependant on climate and its associated diurnal, weekly and annual cycles. In regard to overall drying performance, important time scales should be, at most, on the order of several hours in order to adequately define the shortest diurnal changes. As indicated in the 'Research Design'(6), some types of construction practices produce unvented cavitities where diffusion time constants can be on the order of a month.

The vast disparity in time scales dictated by the underlying processes and external factors, such as climate and wall construction, are suitably handled, in the program, with an hour time interval. Dynamic processes with time scales much less than an hour are treated as average 'lumped' steady state events occurring uniformily over the hour. Processes having time scales longer than an hour are monitored and updated at every hour. The topic of time and length scales for heat and moisture flow are discussed further in the Research Design (6) and the computer model description (8).

4. FULL SCALE LABORATORY WALL DRYING TEST

4.1 General

This section describes the laboratory simulation of a full-scale wall segment subjected to known and controllable test conditions. The purpose of the simulation is to validate the computer model of drying in residential timber-framed walls by comparing measured quantities from the simulation to those predicted by the program.

This section describes the laboratory test, including details of the wall assembly and test procedure, as well as the controlling test parameters and the output results. The controlling parameters comprise measured hourly indoor and outdoor relative humidity (RH) and temperature as well as static pressure distribution on the outside surfaces. The measured test results include relative humidity (RH) at numerous locations within the wall assembly as well as moisture content (i.e. MC, % by weight) at many locations in the sheathing and the wood studs. By applying the hourly values of the test parameters, a useful comparison can be made between model predictions and actual wall measurements of relative humidities and moisture contents. Several comparisons are presented and discussed in Section 5 of this report.

Numerous runs of the computer model were required to represent the natural variability in such items as gap spacings between and behind siding boards. Thus a range of theoretical results are compared to the single set of measured results.

4.2 The Test Chamber

The chamber used for the simulation comprises an insulated wooden box having interior dimensions of 3m long by 2.5m wide by 2.7m high. Tracks on the floor and ceiling divided the chamber in two along its length and held the test wall in place. The test wall therefore divided the chamber into two independant compartments whose environments were controlled to represent any real or

artificial weather conditions. Figures 3(a) and 3(b) illustrate the test chamber interior, the baffle and the test wall.

In the present experiment one compartment represented the exterior and the second compartment, the roomside of a timber frame house. The exterior compartment contained a baffle which served to control air movement along the exterior surface of the test wall. Air flows were generated by a fan driven by a 5 kilowatt motor and providing air at a rate of 85,000 L/min (liter/minute). The fan was located outside the chamber and adjacent to the exterior compartment. Air flow was directed through this compartment and into the baffle through flexible 0.25m diameter hosing. The baffle constrained air flow to occur from bottom to top of the test wall. The triangular shape of the baffle, created by a pivot at its quarter height, generated the pressure distribution with the highest pressure at the pivot and decreasing towards both top and bottom.

Gradients of temperature across the wall and pressure gradients vertically along the exterior surface were established and measured twice daily at 9:00 a.m. and 6:00 p.m. This information was subsequently provided as input into the analytical computer model. The validation involved the comparison of predictions from the analytical calculations to measured values of moisture contents in the sheathing and wood studs.

Dry bulb temperature was roughly controlled for the indoor environment to fall between 38° C and 45° C using common 100 Watt light bulbs and 250 Watt heating bulbs. The relative humidity was allowed to reach levels determined by the slowly varying indoor chamber temperature and any moisture infiltrating with the laboratory air. The range of RH corresponding to these temperatures and laboratory conditions was between 15% to 25% by weight. Similarly, only relative humidity was controlled in the exterior compartment using a water bath and a dehumidifier, and ranged between 25% and 40% RH. The temperature in this compartment was not controlled but determined by the heat input of the fan and cooling from the chamber towards the laboratory air. The resulting temperature range in this compartment was 32 C to 37 C. Insulation in the outside walls of the

test chamber slowed down variations in temperature imposed in either compartment. Further, temperature and RH in one compartment followed those in the other compartment so that the differences in these two parameters, across the test wall, remained relatively constant. The difference in temperature and RH ranged approximately between 5° C to 8° C and 10% to 20% respectively. Figure 4 illustrates a chart recording of temperature and RH in both compartments over a week. Hourly recordings of these inputs formed the input for the computer simulation.

4.3 The Wall Assembly

The wall assembly used in the simulation was typical of residential timber frame walls found across Canada including the East coast. The wall was constructed of commercially available components including hardboard siding layered horizontally on the exterior, followed by building paper on half the wall, fiberboard sheathing board, 50 mm x 90mm spruce studs, 90 mm of glass fiber insulation, 0.1 mm thick polyethylene sheet and 10 mm thick gypsum board on the indoors. In order to investigate the effects of building paper, half of the 2.4 m wide test wall contained it between the siding and the sheathing board while the other half did not. Strapping was not included in either half of the assembly. The assembled wall,set in the test chamber, is illustrated in Figure 3(a).

The framing of each half wall comprised four vertical spruce studs spaced on 400 mm centers with stud base and header plates as well as horizontal spacers at approximately the mid-height of the wall. Thus each half wall contained three insulated cavities. Partial views of this arrangement are illustrated in Figures 5(a) and 5(b).

With a view to maintaining simplicity in the test and in the computer model, the bulk pressure difference between the room-side and outside compartments of the test apparatus was eliminated. A 2 cm hole near the bottom of the test wall connected the two compartments and kept the pressure gradient across the wall to a near-zero value. This feature reduced and simplified the pressure measurements

on the exterior surface of the test wall which were required as inputs to the computer model.

4.4 Instrumentation and Test Parameters

As discussed previously, test parameters consisted of imposed parameters which describe the testing envelope and output parameters which describe the drying response of the wall. The imposed parameters including indoor and outdoor chamber temperatures and relative humidities were measured with two thermohygrographs calibrated against a secondary standard traceable to the National Bureau of Standards (NBS). The thermohygrographs used bimetallic strips to sense temperature and hair to measure RH. Within the range of 20% to 80% RH the accuracy of the relative humidity measurements was $\pm$5%. Accuracy of temperature measurements in the operating range between -5 C and 50 C was $\pm$2 C.

Measurements of the response or output parameters were made in the middle cavity of each half wall segment. These measurements included dry bulb temperature, relative humidity and moisture contents of the sheathing and the studs. Dry bulb temperature and RH measurements were made between all components comprising the wall (i.e. 5 measurements and 4 measurements each for half walls with and without building paper respectively) and on both inside and outside test wall surfaces. Dry bulb temperatures were measured with type 'T' thermocouples. Relative humidities were derived from dry bulb and dew point temperatures and the governing relations. Dew point temperatures were measured with a dew point meter considered a secondary standard traceable to the NBS. Measuring locations for dry bulb and dew point temperatures are illustrated in Figures 6(a) through 6(f) and 7(a) through 7(f) respectively for the numerous layers comprising the wall. Moisture content measurements were also taken in the middle cavity of each half wall in the fiberboard and the wood stud framing. These locations are illustrated in Figure 8 for both half walls. Moisture measurements were taken with a Delmhorst resistivity moisture meter using two metallic pins inserted to a certain depth in the material. Below fiber saturation, and above 6% MC, the instrument was accurate to $\pm$1% MC. Stud moisture measurements were taken at a depth of 5mm and

corrected for wood specie. Sheathing moisture contents were also taken at a depth of approximately 5mm from the room-side surface. The resulting measured variations in moisture content over a nineteen day period were subsequently compared to analytically predicted values.

These comparisons are discussed in Section 5 of this report. Moisture content measurements were not recorded in the siding boards.

4.5 Results of Drying of Laboratory Test Walls

As described in the previous sections of this report, the measured data comprise dry bulb and dew point temperatures to give relative humidity as well as moisture contents in the studs and sheathing to indicate drying of the wall. The two nominally identical half walls differ in that one half contains a sheathing paper layer, i.e. building paper, between the siding and the sheathing while the other half does not. Figures 9(a) through 9(e) and 10(a) through 10(d) illustrate relative humidity measurements over the nineteen day test period on walls with and without the sheathing paper as derived from dry bulb and dew point temperatures. Each figure illustrates groups of measurements through the wall between all layers for one location on the wall. Measuring locations are identified with a number location on the wall shown in Figure 9(a) and an RHn designation where n is a layer number from 0 to 5, to indicate the layer. Wall layers in the context of this laboratory wall test are not to be confused with the layers used to represent a wall in the computer simulation. Thus, layer 0 corresponds to the measurements on the outside siding surface, layer 1 correspond to measurements between the siding and the sheathing paper and so on until layer 5 corresponds to measurements on the room side surface of the drywall. It should be noted that layer 1 does not exist for the half test wall not containing a sheathing paper layer. In this case, measurements are made between the sheathing and the siding which is designated as layer 2, i.e. RH2.

Moisture pin locations in these laboratory test walls, are identified in Figure 8. Figures 11(a) through 11(d) and 12(a) through 12(d) illustrate actual drying, i.e.

moisture content (%), of wood studs and sheathing in these walls for both the test cases, with sheathing paper absent and present. Moisture pin measurements are grouped according to their location in the test walls. For instance, Figure 11(a) illustrates the drying of moisture pins M1, M2 and M4 located in the upper stud area of the wall containing building paper. In Figures 11(b) and 12(b) sheathing moisture pins M3, M6 and M9 as well as M15, M20 and M23 are grouped according to the walls with and without sheathing paper respectively. The artificial, 'laboratory' weather conditions, imposed on the walls for the entire nineteen day, 457 hour test period, are plotted in Figure 13. Only the temperature difference and outdoor relative humidity are displayed because the room side RH, although recorded, is assumed to be isolated as a drying influence on the wall by the vapour barrier.

5. VALIDATION OF THE COMPUTER MODEL WITH LABORATORY TEST WALL DATA

5.1 General

As indicated in previous sections the intended purpose of computer model validation was to assess the model's ability to predict wetting and drying behaviour of a wall under controlled but arbitrary test conditions. The task was performed by comparing model simulated moisture contents in the sheathing and studs with corresponding measured values on a full size laboratory constructed wall segment as described in Section 4. Although the materials and fabrication procedure were typical of walls constructed in the field, the care taken in erecting the laboratory wall was probably greater. As well, the weather conditions imposed on this test wall in the laboratory were not intended to be, nor were they actually, representative of conditions expected in the field.

5.2 Validation Procedure

The following steps were performed as part of the validation procedure:

RWDI

(i) Characteristics of the test wall were entered into the wall specifications file of the WALLDRY program. These specifications included:

- wall dimensions
- construction materials and their thicknesses
- flow coefficients generated by benchtop tests for reconstituted wood siding. The flow coefficients for the siding with a 5 mm air space behind the siding were used to reflect the poorly fitting siding of the test wall (warping of the boards was evident)
- wind pressure coefficients on the face of the wall, as measured in Task 7

(ii) The weather file required by WALLDRY, that normally contains hour-by-hour weather data for a specific location, Halifax for instance, was replaced by a file of measured conditions (temperature, wind speed, RH) on the "weathered" side of the test wall. This file was generated using data measured over the course of the test. Two additional hourly inputs not normally available in a weather file, indoor temperature and indoor RH, were also included in this file.

(iii) The library of material properties, an example of which is included in Appendix A, was updated to contain results of the benchtop tests of surface evaporation rates. Results of the tests were included in terms of effective resistances to surface evaporation. This was done to characterize the measured performance in terms that were comparable to the vapour diffusion resistances already in the database. These test values were entered into the properties database and used by the model.

The evaporation performance of the inside face of reconstituted wood siding was not tested in the benchtop tests; however, that of a pine board was. Thus, the surface resistance tested for pine was assumed to apply for the reconstituted wood surface facing the air space between the siding and sheathing paper. This is a major but not a critical assumption in terms of

model validation since the drying rate of the siding was not the focus of this test.

The drying performance of sheathing paper and fiberboard sheathing was evaluated in the benchtop test. The resulting effective surface resistances determined by the tests were included in the materials properties database. All other vapour diffusion resistances in the database are from the ASHRAE FUNDAMENTALS Handbook.

(iv) The initial moisture contents of the sheathing and studs were specified, in the wall specification file of step (i), to be those measured at the start of the test. The siding moisture content was not measured and was therefore assumed to be at the same moisture content as that of the sheathing at the start of the test.

(v) The test wall had 12 rows of siding in the vertical direction. The model was set up to analyze nine vertical elements, and it had been assumed in previous analyses that there was one siding row per element in the reference walls analyzed. To analyze the test wall with 12 rows, the model had to be modified to analyze the effect of more than one row per vertical element.

Increasing the number of elements to match the number of boards would increase the number of computations and computation time dramatically and needlessly. Thus, the flow coefficients that account for friction pressure drop through and behind the siding were adjusted to account for the fact that there are on average 1.33 rows per vertical element for the test wall, i.e. 12/9. This adjustment was made to be general so that any number of rows of siding can now be specified and the program will account for these automatically,

(vi) The test wall had a specific number of vertical studs as well as a top plate, bottom plate, and mid-height bracing members. The program was modified to accept a user specified number of equivalent full-height studs to account

for all of the wood and wood surfaces of the studs. (Originally, the program estimated this number.)

5.3 Comparison of Computer Simulations and Test Results for a 5mm Airspace

As described, the test wall had two halves: one with sheathing paper and one without.

The comparisons are presented in three sets. These are:

- first comparison, no adjustments
- second comparison, Moisture Content vs Equilibrium RH curve adjusted by 1.5% Moisture Content points
- third comparison, simulated test wall without sheathing

Each comparison is reported on two figures, one for the drying of the sheathing, and one for the drying of the studs. The solid lines are the computer simulation results; the superimposed symbols are test results. (Test results were recorded more frequently as shown in Figures 11(a) through 12(d)).

5.3.1 First Comparison

Sheathing Drying

The simulated drying rate of the sheathing is shown in Figure 14. The drying rate was uniform from the bottom of the wall to the top, and this uniformity was also observed in the test data. The simulated bottom, mid-height, and top drying curves are so close that they do not require differentiation. The actual measured sheathing drying rates as shown in Figures 11(a) through 11(d) are also so uniform that only the average tested drying rate is presented in Figure 14(a) for clarity.

It is interesting to note that uniform drying of the sheathing has been observed in previous simulations, during Phase I of this study, to be the result of

generous air flow behind the siding. The very fast and uniform drying of the sheathing of the test wall is a good indication that generous air movement is occurring behind the siding.

The simulated rate of drying and the final equilibrium moisture content of the sheathing are not well matched to the test results. The actual drying rate is much faster and the equilibrium moisture content significantly higher than the simulated results.

The slower simulated drying rate may be due to:

- the evaporation resistance of the sheathing paper that is too high (this is the value derived from the benchtop tests)
- not enough simulated air flow behind the siding
- the simulated drying rate of the studs could be too high (thereby loading up the sheathing too quickly)
- air circulation around the sheathing paper may be reducing its effect

The uniformity of the drying rate of the sheathing suggests that the simulated air flow behind the siding is adequate. Also, as will be seen, the simulated stud drying rate is slower than measured. This points to either high evaporative resistance in the model or possible air flow behind the paper in the actual test. Examination of the test results for the half of the wall without sheathing paper shows virtually identical drying rates as the half with sheathing paper. This suggests that air could have been short circuiting the building paper - a theory that as tested with the model in a third set of comparisons as described in Section 5.3.3. This hypothesis is also reinforced by similar measured relative humidity on both sides of the sheathing paper as shown in Figure 9(c) indicating intimate communication between airspaces in either side of the paper.

The underpredicted equilibrium moisture content could be due to:

- actual hygroscopic properties of the wood and sheathing being different than published values
- the calibration of the moisture sensors being high by about 1.5 moisture content points, i.e. moisture content values were adjusted for the wood specie
- instrument accuracy degrading for low moisture content measurments

Any one of these requires an adjustment before comparisons of the drying rates can be made fairly. This adjustment was made in the second comparison.

Drying of the Studs

Since the drying of the studs is in series with the drying of the sheathing, it would be expected that the simulated drying rates of the studs would also be slower than tested. This is in fact the case, as shown in Figure 14(b), although the discrepancy was smaller than the one indicated for the sheathing. As well, there are a number of encouraging similarities between test and simulation results for the drying of the studs. The slow drying rate over the first ten hours was picked up by the model. Examination of temperature differences in Figure 13 shows that this gradient was inward over the first 10 hours or so. For that 10 hour period, the model shows the sheathing to be drying both inward towards the cooler surfaces and outward to the dryer air. This explains the very steep drying curve of the sheathing. It is thought on the other hand that the studs are loading up with moisture from the sheathing and are prevented from significant indoor drying by the polyethylene vapour barrier. The only reason the studs show some drying at the surface under this regime is that the layers with the studs are dryer than the surface layers and the moisture is migrating from the surface to the inner layers of the stud. In fact, some portions of the studs in the test wall showed wetting during this initial period, suggesting that those portions had wet inner layers and could not dry at the surface. If the model had started with uniform stud moisture content then wetting of the surface layers would have been predicted for this initial period. The attempt to induce a uniform high moisture content in the wall including the

studs at the beginning of the test was responsible for the initial moisture gradient being inwards into the studs.

5.3.2 Second Comparison

A second simulation was undertaken in which the Moisture Content vs RH curve for wood was adjusted upward by 1.5 moisture content points to match tested equilibrium conditions. Note that this adjustment is not permanent since the discrepancy may be a result of a small calibration error. Nevertheless, for purposes of comparison, the adjustment was made temporarily to ensure that the model has a consistent calibration with the test apparatus since the model uses the initial test reading as initial conditions for the simulation. Implicit in this adjustment is the fact that for the same initial moisture content as the unadjusted case, the simulated wall now has less drying to do to reach the tested equilibrium moisture content.

With the proper equilibrium moisture content, the sheathing drying curve in Figure 15(a) shows very clearly that the simulated drying time is too high by a factor of about 3. However, since the simulated sheathing now has less drying to do than in the first case, the simulated studs dry more quickly and at a rate that is closer to actual drying rates, as shown in Figure 15(b).

5.3.3 Third Comparison

A final simulation was undertaken in which the moisture content adjustment indicated above was retained and the sheathing paper was removed from the simulated wall so that the sheathing surface is in contact with air space behind the siding. The result is that the simulated sheathing drying time is now very close to the drying time derived from tests, as illustrated in Figure 16(a). This is not surprising since the other half of the test wall without sheathing paper had the same drying time. There is, therefore, strong evidence - both from the model and from the test - that air is getting behind the paper, minimizing the effect of the sheathing paper on the drying rate of the sheathing. A final supporting argument

for this theory is that the simulated stud drying profiles are now very close to the tested results over the whole drying period, as shown in Figure 16(b).

Based on the comparisons presented, it is our opinion that the modelled moisture flow system of the wall is represented accurately in all its essential features.

It is emphasized that the purpose of these comparisons is to validate the computer model using a laboratory controlled test wall as described in Section 4.3, and not to infer specific behaviour about the wall. The test wall represents an ideal wall segment carefully assembled under controlled laboratory conditions. Under these specific conditions the sheathing paper is seen to behave as intended, providing air movement to the sheathing and at the same time apparently capable to serve as a second rain screen. The ability of a real wall assembled under field conditions, to perform these functions is expected to vary considerably depending, among other factors, on weather conditions, materials and installation procedures used and experience of the contractor. Outcomes from the laboratory test wall should not be used to infer full scale wall behaviour.

One anomaly remains at this point of the analysis. Given the very fast drying response of the sheathing, why does the tested moisture content of the sheathing not fluctuate according to fluctuations in the "outdoor" RH as does the simulated moisture content? (Note: As shown in Figures 11 and 12, the tested results do fluctuate more than shown since only the conditions at every 50 hours or so are plotted here; nevertheless, the fluctuation in the tested moisture content is less dramatic and not correlated to fluctuations in outdoor RH, as in the case with the simulated result.)

5.4 Simulation of Wall Drying with a Narrower Air Space

Figure 17(a) illustrates the drying pattern of the sheathing for the same wall as was previously simulated, but now with only three millimetres average clearance behind the siding, down from the five millimetres used previously. The net result

of this reduced clearance is the slightly greater accumulation of moisture in the air stream behind the siding towards the top of the wall. The simulated result thus predicts slower drying for the mid and top portions of the wall compared to the bottom portion. The previous simulation, i.e. the one with the five millimetre clearance behind the siding, exhibited a more uniform drying pattern for the sheathing.

The drying rate of the studs as illustrated in Figure 17(b) was affected by this change. The comparison between the simulated and tested result is still very good for the bottom, mid height and top. One can observe that the top portions of the studs in the simulated case are now slightly slower at drying than was tested, especially in the region of 100 hours into the test.

6. SIMULATION OF WALL DRYING IN THE HALIFAX CLIMATE

The same wall as used in the laboratory simulation and described in Table 1 has also been run with weather data from Halifax for a full year on a south facing wall. The wall was initially assumed to be soaked, with moisture contents of all hygroscopic wood based components having a moisture content in excess of fiber saturation. The geometry, airspace, gap spacings between siding boards, etc. are identical to the wall used for the comparison with laboratory measurements as described in Table 1. For completeness, these characteristics are also included in Table 2 describing the full scale wall.

6.1 Simulation for a Full Year

Figure 18(a) illustrates the siding moisture content time histories for the drying of siding in a south-facing wall in Halifax, as simulated by WALLDRY. The tightness and evaporative resistance characteristics of the wall were specified using the benchtop test results. The drying characteristics of that wall are reported in Figures 18(a) through 18(d).

Figure 18(a) illustrates the drying time histories of the inside surface of the reconstituted wood siding in the Halifax south wall. It will be noted that the bottom of the wall dries steadily and gradually and reaches approximate equilibrium after 100 days. The mid portion of the wall initially lags behind the bottom but eventually dries out in approximately the same number of days. The top portion of the wall is initially exposed to an accumulation of moisture in the air stream behind the siding, coming from both the siding and the sheathing located in the lower portion of the wall. The top portion of the wall does not start drying until a major portion of the initial moisture in the lower portion of the outer wall has been eliminated. The top portion of the wall takes approximately 150 days to dry as a result.

The drying time histories of the sheathing are presented in Figure 18(b).

Note that the maximum moisture content that the fibreboard sheathing can tolerate before surface films and beading start to form has been set for illustrative purposes only at 75% in the model. The actual maximum level tested as part of Task 5 for fibreboard sheathing was in the order of 280%. The 75% level, which was shown as a typical moisture level in this simulation, was selected to illustrate the formation of surface films as indicated in Figure 18(c). As well the horizontal line at 75% moisture content in Figure 18(b) indicates that the sheathing cannot begin drying until the condensed moisture layer evaporates. As before the progression of drying occurs from bottom, to mid height, to top because air flow, created largely by wind induced pressure gradients and buoyancy, is mainly upwards. Once drying has begun in the sheathing the process proceeds rapidly requiring about 160 days to reach minimum moisture content.

Figure 18(c) illustrates the growth of the water film layer of water/ice trapped between the sheathing paper and the sheathing. The thickness of this film actually increases over a 50 to 75 day period in the early part of the year (i.e. mid winter). This is a result of the fact that the moisture flow into the film layer due to temperature gradients in the inner wall was greater than the moisture flow out of the film layer across the sheathing paper into the cold air stream behind the

siding. Had this trend continued for another month, the model would have predicted drying of the film by gravity action.

After about 50 to 75 days, the water/ice film begins to shrink. This is a result of two factors. The temperature gradients across the inner wall diminish, thereby slowing the flow of moisture into the film layer, and the drying conditions of the outer wall improve. Drying continues until the films disappear, at which point the sheathing drying begins, as illustrates in Figure 18(b). This occurs between day 75 and 125 depending on the location in the wall.

Figure 18(d) illustrates the drying performance of the studs. As can be seen, the studs have a rather uniform drying rate through the first 100 days of the year. Over late spring and summer, the stud at the top of the wall apparently picks up moisture from the sheathing which is not yet quite dried, while the mid and bottom portions of the stud are now facing dry sheathing so that these stud continue to dry in a low RH environment. The re-wetting of the top of the studs is a function of the fact that the house, simulated in the program, is assumed to be air conditioned in the summer. The temperature gradients are therefore inward on average for the summer, and any excess moisture in the sheathing is driven back into the studs. Once the sheathing is totally dry after 150 days, the stud drying resumes. This particular simulation result illustrates the importance of drying the outer portion of the wall before summer, especially in air conditioned houses.

A final stage of stud drying seems to occur after about 300 days, when the wall temperature gradients are again predominantly outward.

6.2 Wall Drying of the Laboratory Wall Using Assumed Versus Bench Top Parameters

Improvements and refinements in the computer model have taken place over the course of the project including: improvements in technique, correction of errors, and implementation of parameters from benchtop tests. The combined effects of these changes on the model's ability to represent actual drying behaviour

can be illustrated by comparing drying curves of the sheathing and the studs before and after the changes were implemented. Figures 19(a) and 19(b) illustrate comparative drying curves between simulations with the computer model in its early stages of development using assumed parameters and the test results from the present laboratory study. Similarly corresponding Figures 16(a) and 16(b) compare simulations using the latest computer model to results from the present study. The improved comparisons due to the combined effects of the changes, are evident.

A specific comparison of the measured benchtop parameters versus those derived from theory or otherwise assumed is worthwhile. Tables 3, 4 and 5 illustrate the progress made in this phase of the work as a result of benchtop testing.

Table 3 is a comparison of the surface evaporation resistances derived from the benchtop testing and those that had been derived from ASHRAE materials properties. These are for fibreboard sheathing, pine board and building paper. The effective surface evaporation resistances from the benchtop tests are considerably lower than the derived values by a factor of between three for fibreboard sheathing and building paper, and over 40 times lower for the pine board. This means that early modelling efforts during the present study were underestimating the ability of those materials to rid themselves of moisture when exposed to air.

Table 4 compares the air velocities in the airspace behind the siding as theoretically estimated during the initial phases of this project and as practically obtained from the benchtop testing described in Appendix C. These benchtop tests indicate that estimated airspace velocities could have been excessive by a factor between 2 to 3. This suggests that the siding as tested is offering more resistance to flow than previously expected and that drying rates correspondingly decrease.

Regarding the simulation of drying in outer walls using the early version of the computer model, the effect of over-estimating air flow quantities as seen in Table 4 approximately cancelled the effect of under-estimating surface evapor-

ation rates of the various materials as summarized in Table 3. The end result was to produce simulations of drying in sheathing and studs which were not greatly different from those using the latest version of the computer model and parameters developed from benchtop tests. It should be clear that this outcome is fortuitious and obscures the radically different way in which the wall would be rated given the results of the benchtop tests.

Table 5 presents a calculation of characteristic lengths of moisture accumulation in the air stream behind the siding of the test wall. Based on the benchtop results, the characteristic lengths are of the order of two metres for a 30 km/h wind. This compares to about 15 metres based on derived wall characteristics developed for preliminary versions of the WALLDRY model. The new characteristic length of surface evaporation is only about 12 board widths, not 76. The wall can therefore be expected to have marginally good drying characteristics, but is much closer to being a poorly drying wall than would have been previously assessed. As the characteristic length of the air stream approaches the width of one siding board, the air change behind the siding is no longer sufficient to avoid saturating that air with the moisture evaporating from the surface. This results in lower moisture transport rates away from the wall surfaces and allows wet sheathing to saturate the air stream and wet the siding. The drying characteristics of the wall could be improved with strapping, even though the simulated drying performance was noted to be good already. Based on the previously derived characteristic lengths, strapping would not have been recommended but after reducing the evaporative resistance of the sheathing paper it would have been.

7. CONCLUSIONS

The following conclusions are drawn from the above comparisons:

1. Comparisons between simulation and laboratory test results indicate that the computer model can predict stud and sheathing moisture contents with a degree of accuracy sufficient to represent practical moisture performance of timber framed walls of low-rise housing.

2. As a result of benchtop tests and validation work the model can produce drying times that are indicative of actual drying times of real walls in a given climate. Comparisons of simulations with actual field data are now possible as the next step in the validation process and should prove to be informative both in the process of validating the model and in the interpretation of the field results.

3. As demonstrated in the discussion about the effectiveness of the sheathing paper, the model can be used to evaluate and qualify test data. Through this process, both the test data and the simulated results are better understood. This is perhaps the best use of the model at this stage.

4. The system interactions discussed in this report play different roles in different seasons and at different levels of moisture content of the materials. The following combinations of occurrences have been observed over the course of the annual simulation:

   - studs drying while sheathing (or surface film) is wetting
   - studs drying while sheathing is drying also
   - studs wetting while sheathing is drying
   - top and bottom of outer wall are wetting
   - top is wetting while bottom is drying
   - top and bottom dry together

The complexity of these interactions give credibility to the fact that the complexity of the system model developed is warranted.

5. Regarding the annual simulation, the temperature gradients during cold weather in the inner wall tend to take care of the drying of the inner wall outward. (We can speculate at this point that highly insulating sheathings, which tend to lessen the thermal gradients in the inner wall, may reduce the inner wall drying action). The first goal in drying the total wall is therefore to rid the sheathing and siding of excess moisture in winter so that there is no

excess moisture left to be driven back into the inner wall in warm weather. (Wet sheathing in late spring is a very bad sign in that, even though it will likely dry over the summer, some of the drying will be inward to the studs).

6. The key elements of drying the outer portion of the wall are the evaporative resistance of the material and the quantity of air flow behind the siding, both of which have been addressed by the benchtop tests and modelling in this phase. As discussed in the previous phase of this work, the characteristic length is a key parameter that relates evaporative resistance to air flow rate behind the siding. Analysis of benchtop results in terms of the characteristic length has indicated that the typical wall tested in the lab has a characteristic length of the order of two metres in 30 km/h winds. (This is smaller than what had been previously estimated without the benefit of testing by a factor of seven). In that a siding board width is about .2 metres, the much larger characteristic length indicates that there is enough air flow behind the siding, given the evaporative resistance of the sheathing paper; however, on calmer days the characteristic length may be approaching the magnitude of the board width. This explains why the top portion of the siding experienced wetting in the early portion of the simulation.

Therefore, whereas previously we would have concluded that there is generous air flow behind the siding for this unstrapped siding, the relatively low characteristic length derived for this wall indicates that it may be on the margin of good drying performance and that strapping could be warranted to improve this margin.

7. The above discussion also indicates that field testing of the drying of walls should be done under marginal or poor drying conditions (i.e. sheltered, shaded, damp climates) to highlight drying differences that will not show up under ideal drying conditions.

References

1. Scanada Consultants Ltd. "A Survey of Moisture Problems in New Housing", for technical research division, CMHC, May 1980.

2. Scanada Consultants Ltd. "Survey of MP in Thermally Upgraded Existing Housing, Prepared for the Division of Building Research, National RC, Contract 078-042-8-4452, September 1979.

3. Marshall Macklin Monaghan Limited "Moisture Induced Problems in NHA Housing, Part 1, Analysis of Field Survey Reports and Projections of Fugure Problem (J.H. Van Poorten) for Canada MHC, 1983.

4. Thermocan Limited "Moisture Induced Structural Damage in NLHC Units, St. John's, Newfoundland, 1982.

5. Field Study of Test Huts

6. Morrison Hershfield Limited with Scanada Consultants Ltd., "Research Design for the Study of Drying Characteristics in Outer Walls of Low Rise Residential Housing", for CMHC, September 1985.

7. Morrison Hershfield Limited with Scanada Consultants Limited, "Drying Characteristics in Outer Walls of Low Rise Residential Housing, II State-of-the-Art Literature Review", for CMHC, August 1985.

8. Scanada Consultants Limited, "Computer Model of the Drying of the Exterior Portion of Wood Frame Walls - Updated Version", for Morrison Hershfield Limited, October 1986.

Note: RWDI was formerly the microclimate division of Morrison Hershfield Limited under which name the first phase of the contract was completed.

TABLES

TABLE 1
TYPICAL WALL FILE: LABORATORY TEST

```
TITLE:
COMPARISON OF WALLENY SIMULATION RESULTS TO BADI FULL WALL TEST DATA: W/O SHEATHING PAPER
-------------------------------------------------------------------------------
NUMBER OF RUNS OF SIDING UP THE WALL (NV) AND LAYERS THROUGH THE WALL (NZ)
12,19

NUMBER OF SHEATHING LAYERS: 2 (OR )  (USE 2 FOR LIGHT SHEATHING; 3 FOR HEAVY)
2

SELECTION OF MATERIALS FOR EACH LAYER  (SEE PROPERTIES DATABASE FOR #)
1,15,20,13,13,4,5,4,4,4,24,7,17,17,17,19,21,4,9

THICKNESS OF EACH LAYER (in m)
1,0.002,0.003,0.003,0.003,0.0005,0.004,0.0001,0.0001,0.0001,0.0075,0.0075,0.030,0.030,0.030,0.000127,0.0095,0.002,1

SELECTION OF MATERIALS FOR THE STUD LAYERS (SEE PROPERTIES DATA BASE FOR #)
18,18

LATERAL THICKNESS OF STUD LAYERS
0.019,0.019

LOCATION OF THE STUDS: NEXT TO THE INSULATION LAYER (LAYER #)
14

WALL HEIGHT (m), WALL LENGTH (m), No. EQUIVALENT FULL LENGTH STUDS
2.44,1.22,5.5

Siding GAP Characteristics: K1 (Pa/(L/min)/m)) : bottom to top (9 elements + opening)
.1097,.1097,.1097,.1097,.1097,.1097,.1097,.1097,.1097,.1097

Siding GAP Characteristics: K2 (Pa/((L/min)/m)^2) : bottom to top (9 + opening)
.000192,.000192,.000192,.000192,.000192,.000192,.000192,.000192,.000192,.000192

Siding AIR SPACE Characteristics: K1 (Pa/gap)/(L/min/m))   : bottom to top (9 elements + opening)
.051,.051,.051,.051,.051,.051,.051,.051,.051,.051

Siding AIR SPACE Characteristics: K2 (Pa/gap)/(L/min/m)^2)   : bottom to top (9 + opening)
.0001,.0001,.0001,.0001,.0001,.0001,.0001,.0001,.0001,.0001

INWARD LEAK: ELEMENT # (0 IF NONE), INDEX WIND PRESSURE COEFF, HEIGHT OF NPP(m)
0,-0.3,3

AIR SPACE CHARACTERISTICS: NUMBER OF THE LAYER, FLOW EXPONENT
7

(+/- 22.5) WIND PRESSURE COEFFICIENTS : bottom to top (9 elements + opening)
22.5,  0.1,0.5,1.0,0.9,0.75,0.6,0.5,0.3,0.2,0.1

(+/- 45)  WIND PRESSURE COEFFICIENTS : bottom to top (9 elements + opening)
45.0,  0.05,0.1,0.15,0.2,0.25,0.25,0.2,0.15,0.1,0.05

(+/- 67.5) WIND PRESSURE COEFFICIENTS : bottom to top (9 elements + opening)
67.5,  0.025,0.05,0.075,0.1,0.125,0.125,0.1,0.075,0.05,0.025

((OTHER DIRECTIONS) WIND PRESSURE COEFF: bottom to top (9 elements + opening)
180.,  0.0,0.0,0.0,0.0,0.0,0.0,0.0,0.0,0.0,0.0,0.0,0.0,0.0

WALL ORIENTATION (DEGREES FROM NORTH): N:360, E:90, S:180, W:270
360

MOISTURE SOURCE STRENGTH IN kg/hr, & LOCATION: LAYER #  &  ELEMENT NUMBER
0.,10,6

MOISTURE CONTENT FOR FORMATION OF SURFACE FILM, FILM THICKNESS THRESHOLD(mm)
75,1.0

NUMBER OF LAYERS FACING AIR (OR INSULATION),  WHICH LAYERS
6,  3,5,9,11,12,20

SIMULATION START AND END (DAY OF THE YEAR)
1,18.75

NUMBER OF ITERATIONS BETWEEN THE 3 MAJOR SUB MODELS
8

NUMER OF LAYERS DISPLAYED IN SCREEN (MAX 12): SPECIFY LAYER NUMBERS
12,  1,2,3,4,5,6,7,11,12,20,21,19

NAME OF THE WEATHER DATA FILE  (INCLUDE THE DRIVE SPEC:  e.g.  A:DMEATH.SOU)
TESTWALL.WTH

NAME OF OUTPUT FILE FOR PLOTTING (e.g. GRAPH.PRN)
GRF.PRN

NAME OF THE TABULAR OUTPUT FILE (e.g. DR3.PRN; "LPT1:" PRINTS TO PRINTER)
BADITEST.PRN
```

TABLE 2
TYPICAL WALL FILE: HALIFAX RUNS

```
TITLE:
HALIFAX / SOUTH FACING / STRAPPED SIDING  / NO OPENING AT TOP
-------------------------------------------------------------------------------
NUMBER OF ROWS OF SIDING UP THE WALL (NV) AND LAYERS THROUGH THE WALL (NZ)
12,20

NUMBER OF LAYERS OF SHEATHING: 2 OR 3 (USE 2 FOR LIGHT MATERIAL 3 FOR HEAVY)
3

SELECTION OF MATERIALS FOR EACH LAYER  (SEE PROPERTIES DATABASE FOR #)
1,15,20,13,13,4,5,4,22,6,7,7,17,17,17,19,21,4,9

THICKNESS OF EACH LAYER (in m)
1,0.002,0.003,0.003,0.003,0.0005,0.004,0.0005,0.0005,0.0005,0.005,0.005,0.005,0.030,0.030,0.030,0.000127,0.0095,0.002,1

SELECTION OF MATERIALS FOR THE STUD LAYERS (SEE PROPERTIES DATA BASE FOR #)
18,18

LATERAL THICKNESS OF STUD LAYERS
0.019,0.019

LOCATION OF THE STUDS: NEXT TO THE INSULATION LAYER (LAYER #)
15

WALL HEIGHT (m), WALL LENGTH (m), No. OF EQUIVALENT FULL LENGTH STUDS
2.44,6,5.5

Siding GAP Characteristics: K1 (Pa/(L/min)/m))  : bottom to top (9 elements + opening)
.1097,.1097,.1097,.1097,.1097,.1097,.1097,.1097,.1097,.1097

Siding GAP Characteristics: K2 (Pa/((L/min)/m)^2) : bottom to top (9 + opening)
.0001925,.0001925,.0001925,.0001925,.0001925,.0001925,.0001925,.0001925,.0001925,.0001925

Siding AIR SPACE Characteristics: K1 (Pa/gap)/(L/min/m))   : bottom to top (9 elements + opening)
.051,.051,.051,.051,.051,.051,.051,.051,.051,.051

Siding AIR SPACE Characteristics: K2 (Pa/gap)/(L/min/m)^2)   : bottom to top (9 + opening)
.0001,.0001,.0001,.0001,.0001,.0001,.0001,.0001,.0001,.0001

INWARD LEAK: ELEMENT # (0 IF NONE), INDEX WIND PRESSURE COEFF, HEIGHT OF NPP(m)
0,-0.3,3

NUMBER OF THE AIR SPACE LAYER
7

(+/- 22.5) WIND PRESSURE COEFFICIENTS : bottom to top (9 elements + opening)
22.5,  0.1,0.5,1.0,0.9,0.75,0.6,0.5,0.3,0.2,0.1

(+/- 45)  WIND PRESSURE COEFFICIENTS : bottom to top (9 elements + opening)
45.0,  0.05,0.25,0.5,0.45,0.35,0.3,0.25,0.15,0.1,0.05

(+/- 67.5) WIND PRESSURE COEFFICIENTS : bottom to top (9 elements + opening)
67.5,  0.025,0.125,0.25,0.225,0.175,0.15,0.125,0.075,0.05,0.025

(OTHER DIRECTIONS) WIND PRESSURE COEFF: bottom to top (9 elements + opening)
180.,  0.0,0.0,0.0,0.0,0.0,0.0,0.0,0.0,0.0,0.0

WALL ORIENTATION (DEGREES FROM NORTH): N:360, E:90, S:180, W:270
180

MOISTURE SOURCE STRENGTH IN kg/hr, & LOCATION: LAYER #  &  ELEMENT NUMBER
0.,10,6

MOISTURE CONTENT FOR FORMATION OF SURFACE FILM, FILM THICKNESS THRESHOLD(mm)
75,1.0

NUMBER OF LAYERS FACING AIR (OR INSULATION),  WHICH LAYERS
6,  3,5,9,11,13,21

SIMULATION START AND END (DAY OF THE YEAR)
1,365

NUMBER OF ITERATIONS BETWEEN THE 3 MAJOR SUB MODELS
3

NUMBER OF LAYERS DISPLAYED IN SCREEN (MAX 12); SPECIFY LAYER NUMBERS
12,  1,2,3,5,6,7,11,12,13,21,22,20

NAME OF THE WEATHER DATA FILE  (INCLUDE THE DRIVE SPEC:  e.g.  A:DARTH.SOU)
D:HAL.SOU

NAME OF OUTPUT FILE FOR PLOTTING (e.g. GRAPH.PRN)
HALGRF.PRN

NAME OF THE TABULAR OUTPUT FILE (e.g. DATA.PRN; "LPT1:" PRINTS TO PRINTER)
HALSUM.PRN
```

TABLE 3

COMPARISON OF EFFECTIVE SURFACE EVAPORATION RESISTANCES MEASURED WITH BENCHTOP TESTS AND VALUES DERIVED FROM PUBLISHED DIFFUSION RESISTIVITIES

	Surface Evaporation Resistances (m^2 .s. Pa/kg)	
	Benchtop	**Derived**
Fibreboard Sheathing	0.05×10^9	0.15×10^9
Pine Board	0.054×10^9	2.4×10^9
Building Paper	0.33×10^9	0.85×10^9

TABLE 4

SIMULATED AIR VELOCITIES BEHIND THE SIDING
ASSUMING A 3mm AVERAGE AIRSPACE: VALUES BASED ON
BENCHTOP TESTS VS VALUES BASED ON FLUID MECHANICS THEORY

	Based on Benctop (m/s)	Based on Fluid Mechanics (m/s)
Top	0.25	0.64
Mid	0.33	0.85
Bottom	-0.66	-1.45

TABLE 5

CHARACTERISTIC LENGTH OF SURFACE EVAPORATION OVER WET SHEATHING PAPER IN A 3mm AIR SPACE

WALL CHARACTERISTICS

Air Space Width = 0.003m
Siding Board Width (W) = 0.203 m
Wall Section Width = 1.220 m
Volume of Air Space (V) = 0.00074 m^3
Evaporating Surface (A) = 0.248 m^2
Gas Constant of Water Vapour (R) = 462 Joules/kg.^oK
Air Temperature (T) = 303 ^oK

The characteristic length of surface evaporation L is:

$$L = R_e \times V \times U/A \times R \times T$$

where

R_e = evaporative resistance (Pa.m^2.sec)/kg
U = air velocity (m/sec)

Characteristic Lengths (L) Based on Bench Top Tests

Sheathing Paper Evaporation Resistance = 3.3×10^8 (Pa/m^2.sec)/kg

	U(m/sec)	L(m)	L/W
Bottom of Wall	-0.66	-4.67	23.0
Mid Height	0.33	2.33	11.5
Top of Wall	0.25	1.77	8.7

TABLE 5 (con't)

Characteristic Lengths (L) Based on Best Estimates Used in Early Version of 'WALLDRY' Program

Sheathing Paper Evaporative Resistance = 8.5×10^8 $(Pa/m^2.sec)/kg$

	U(m/sec)	L(M)	L/W
Bottom of Wall	-1.45	-26.41	129.9
Mid Height	0.85	15.48	76.1
Top of Wall	0.64	11.66	57.3

FIGURES

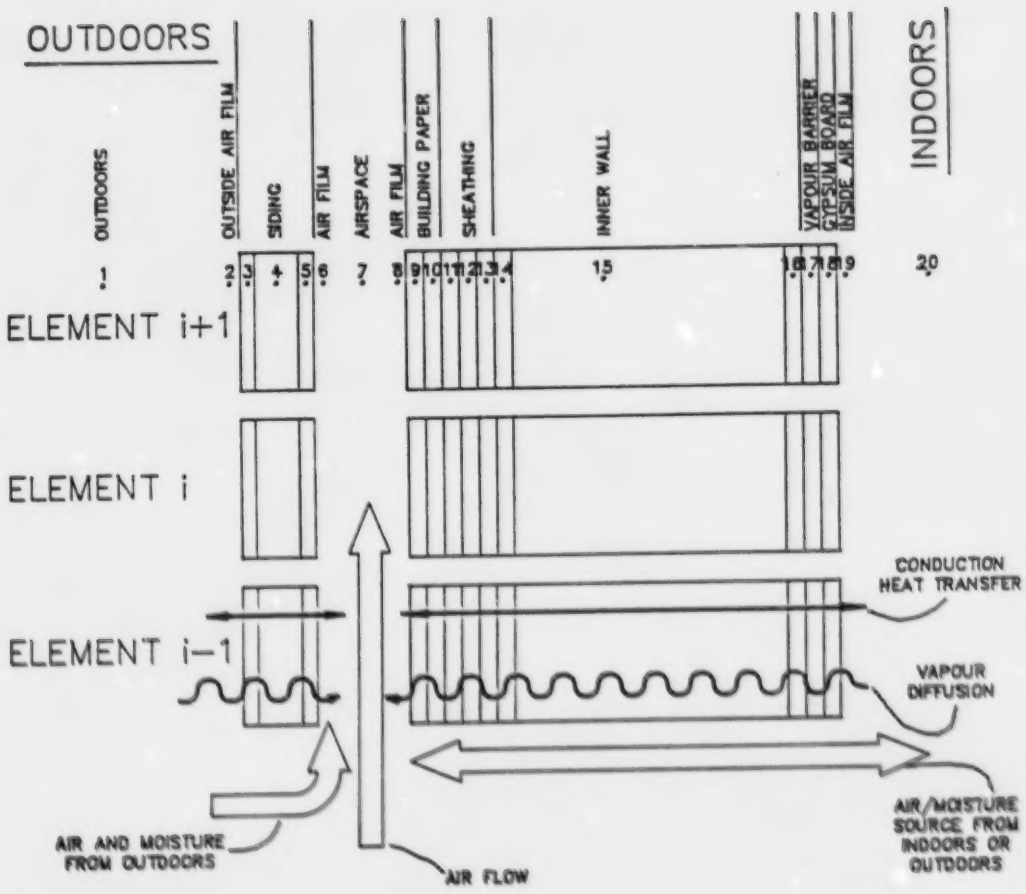

FIGURE 1
COMPUTER MODEL SCHEMATIC

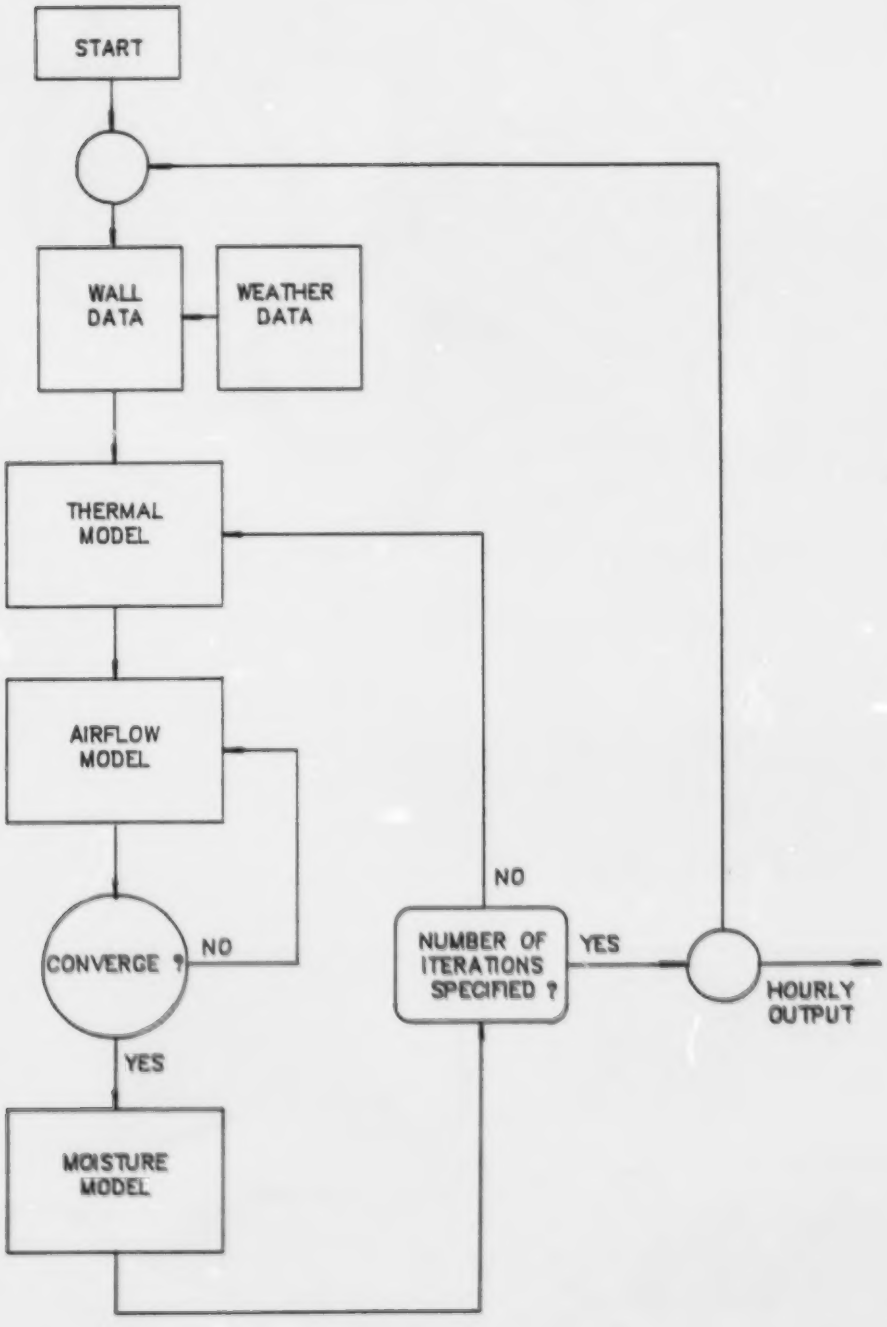

FIGURE 2
MODEL FLOW CHART

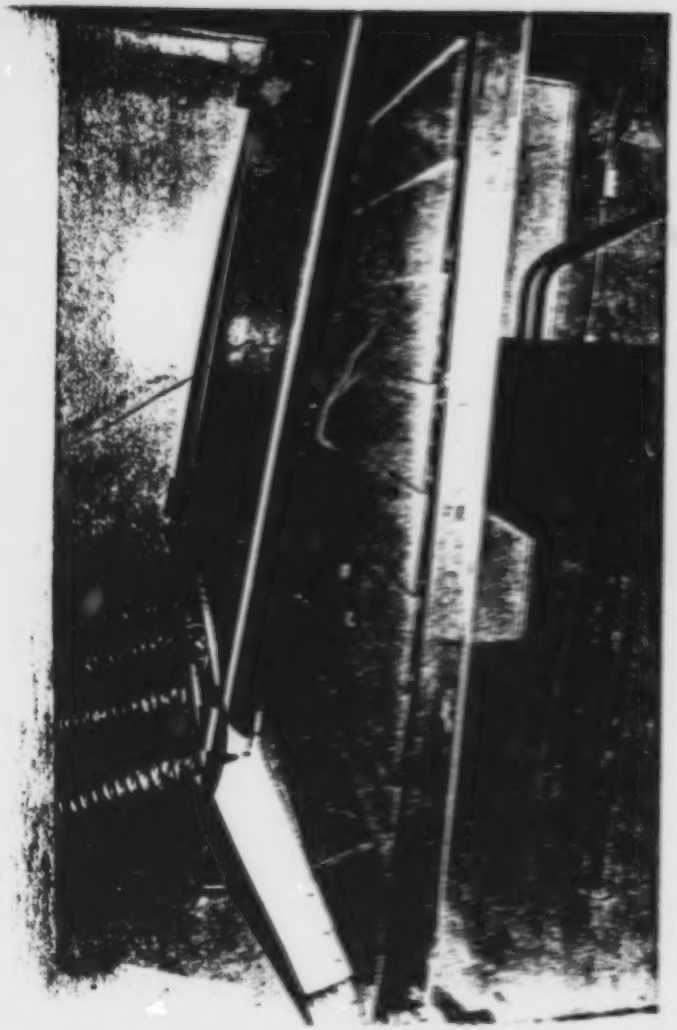

FLOW ARRANGEMENT OVER
TEST WALL

FIGURE 3(a)

THERMOCOUPLES ON INSULATION (ROOM--SIDE)

FIGURE 3(b)

RWMD

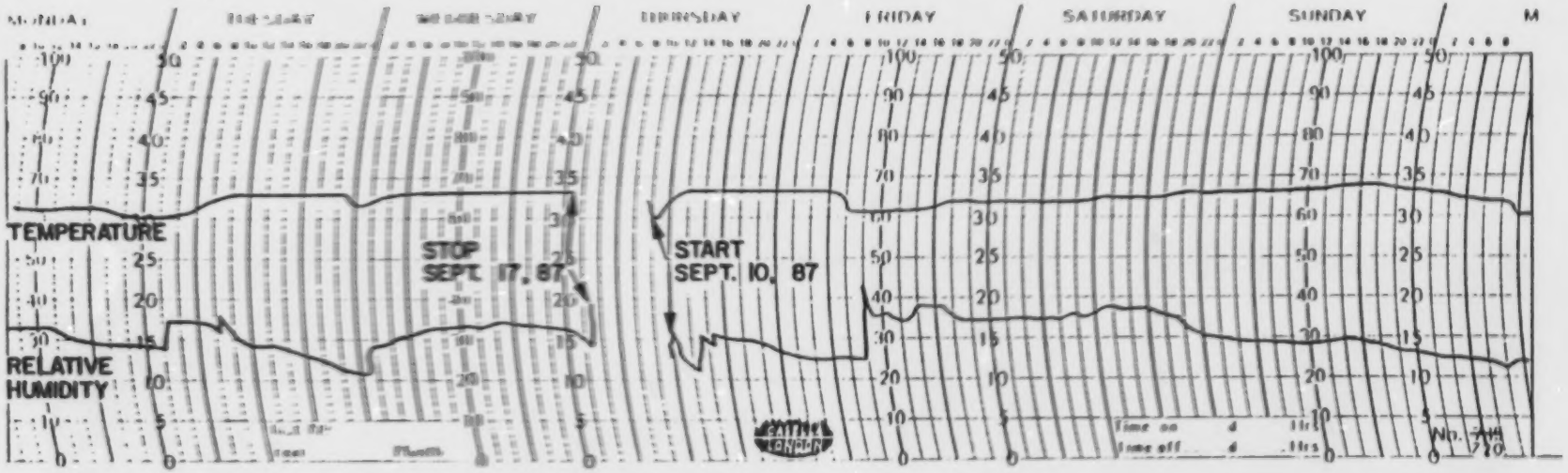

EXTERIOR

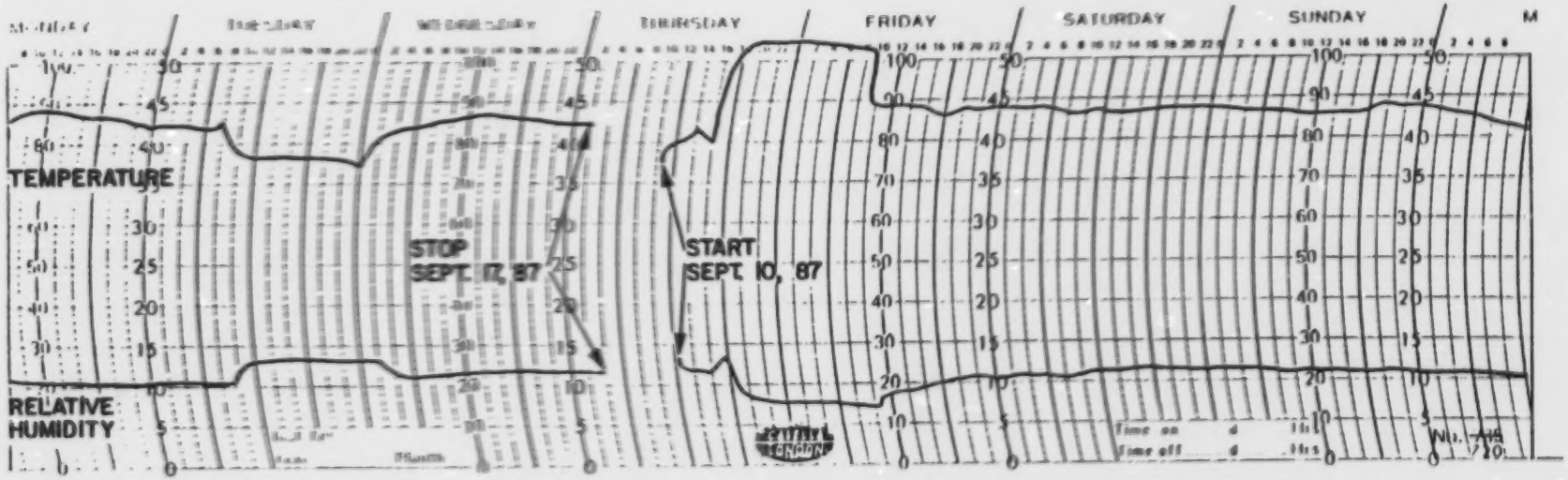

INTERIOR

FIGURE 4

TYPICAL LABORATORY TEST CONDITIONS:
RELATIVE HUMIDITY (%), TEMPERATURE (C)

RWDI

FIGURE 5(a)

FIGURE 5(b)

INSTRUMENTATION OF TEST WALL

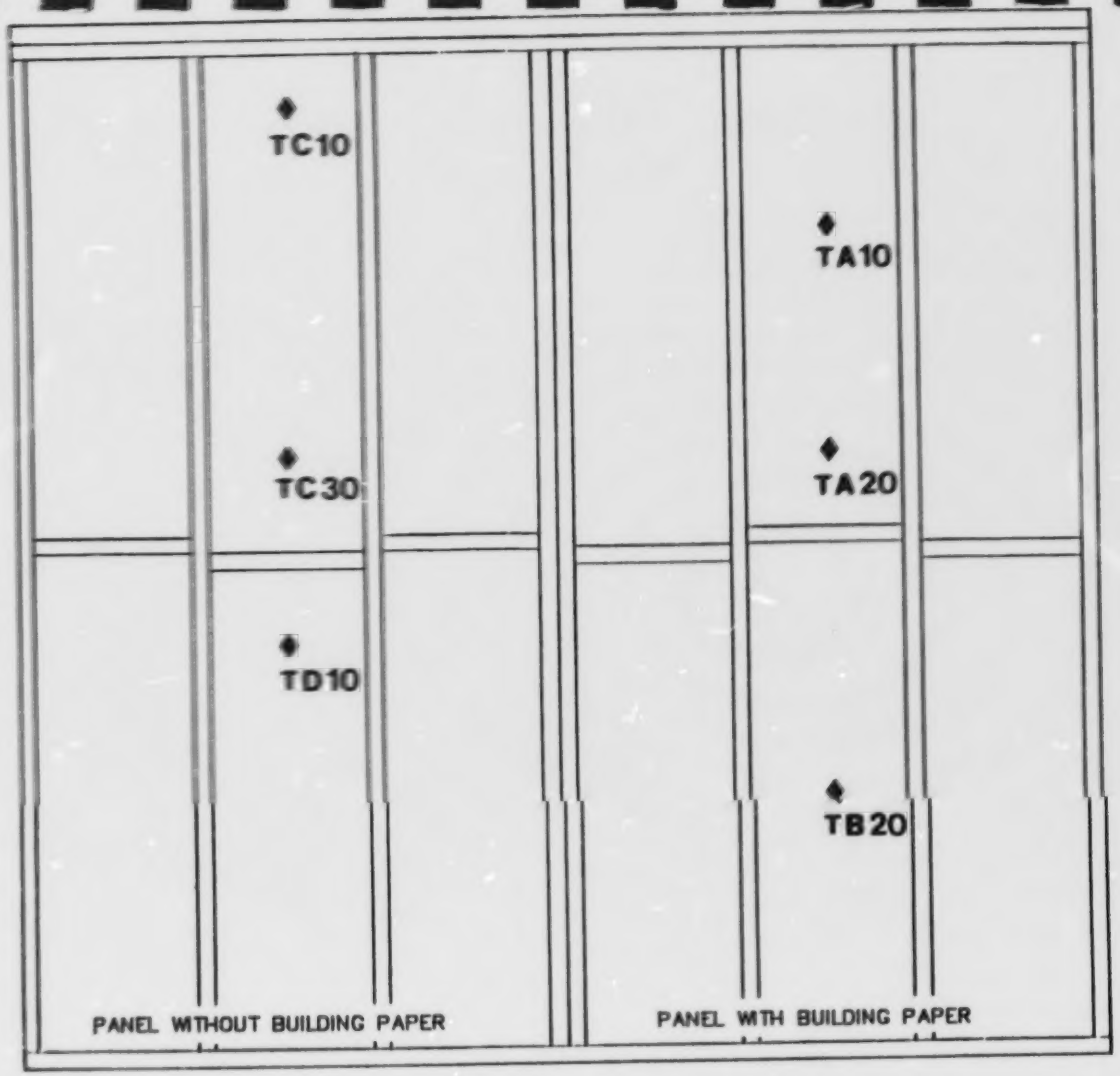

SENSORS LOCATED ON OUTSIDE SURFACE OF SIDING

FIGURE 6(a)

WALL ELEVATION (EXTERIOR VIEW) – THERMOCOUPLES

APPROX. SCALE 3/4"=1'

RWDI

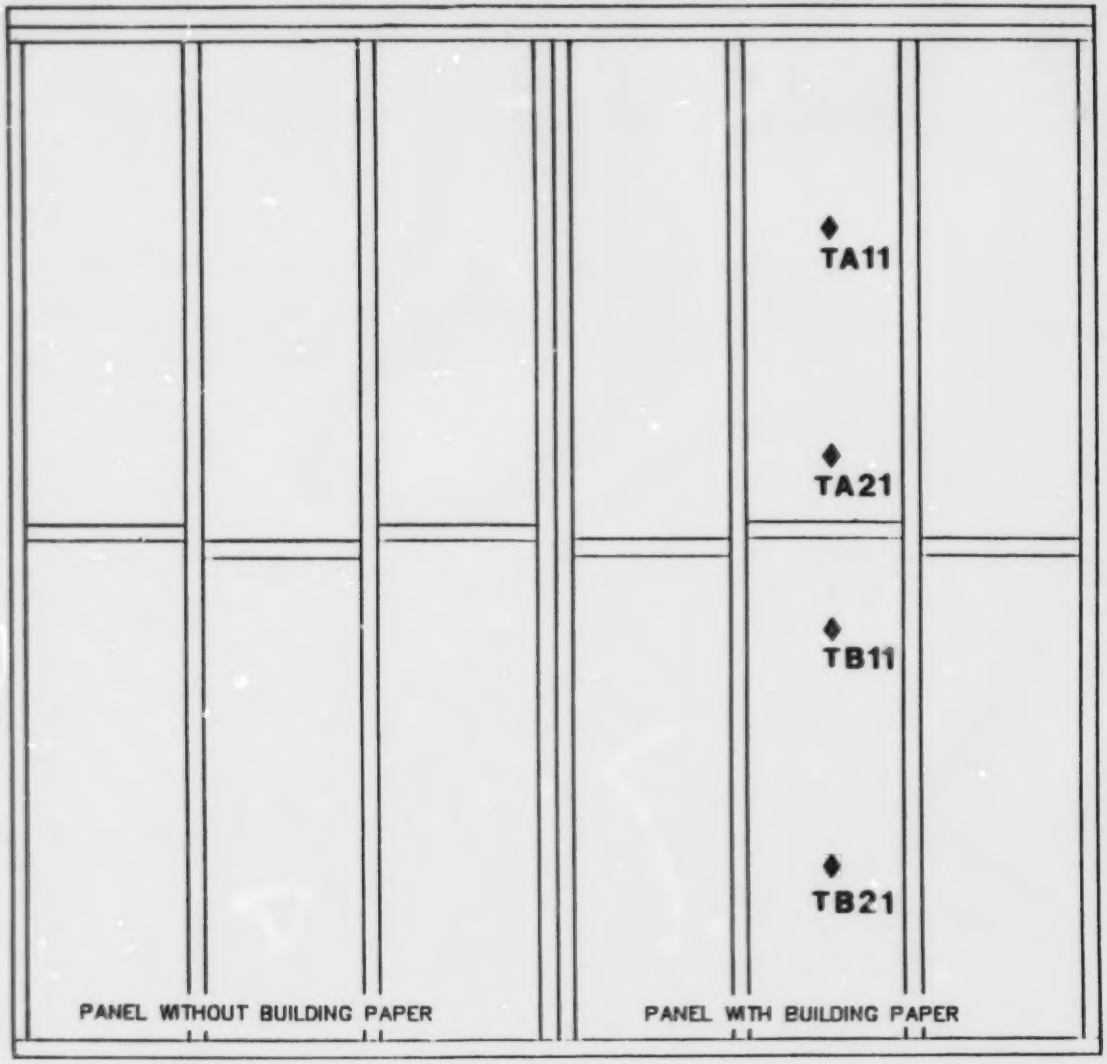

SENSORS LOCATED BETWEEN
SIDING AND BUILDING PAPER

FIGURE 6(b)

WALL ELEVATION (EXTERIOR VIEW) – THERMOCOUPLES

APPROX. SCALE 3/4"=1'

RWDI

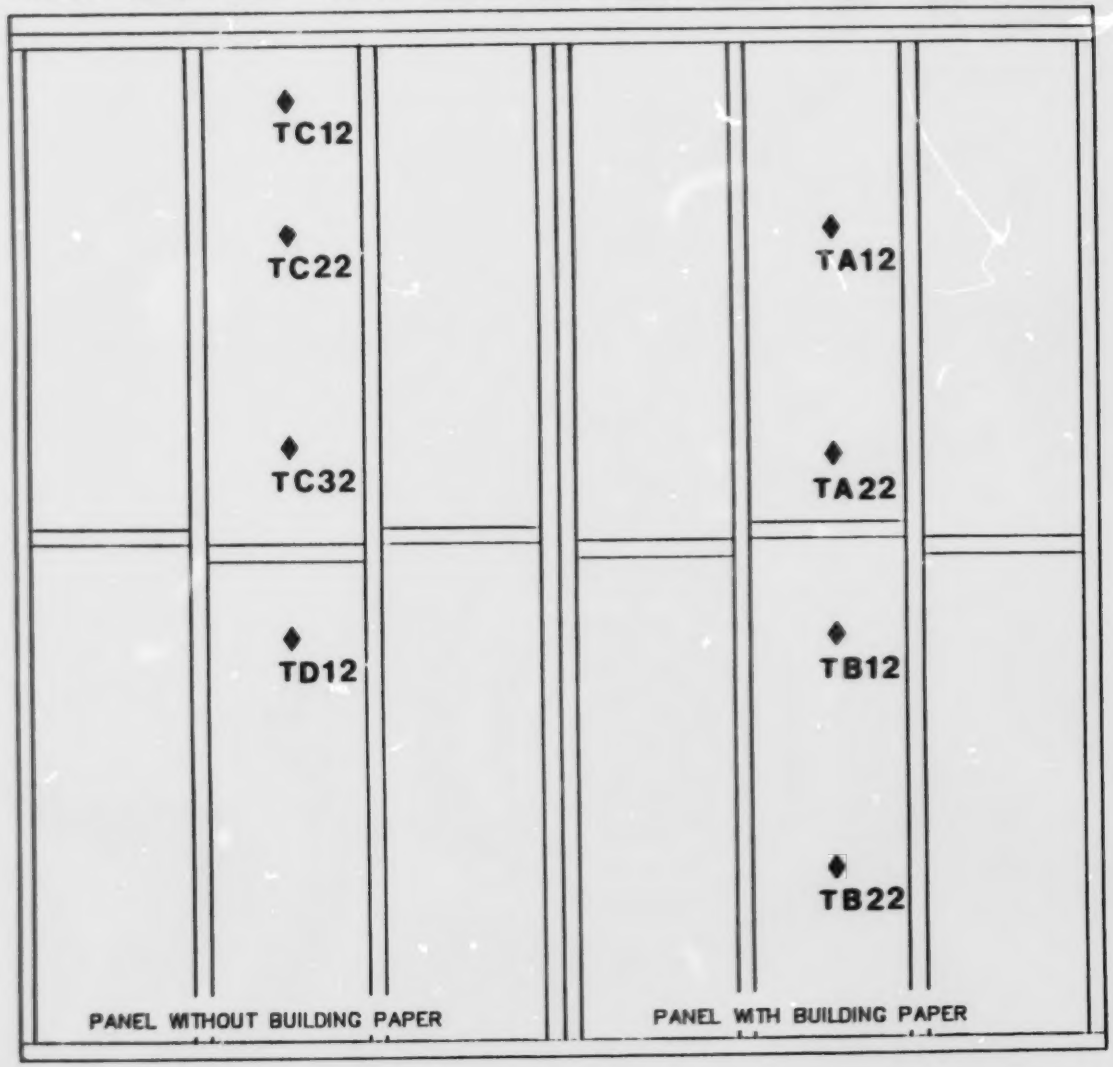

SENSORS LOCATED BETWEEN SIDING AND TENTEST

SENSORS LOCATED BETWEEN BUILDING PAPER & TENTEST

FIGURE 6(c)

WALL ELEVATION (EXTERIOR VIEW) – THERMOCOUPLES

APPROX. SCALE 3/4"=1'

RWDI

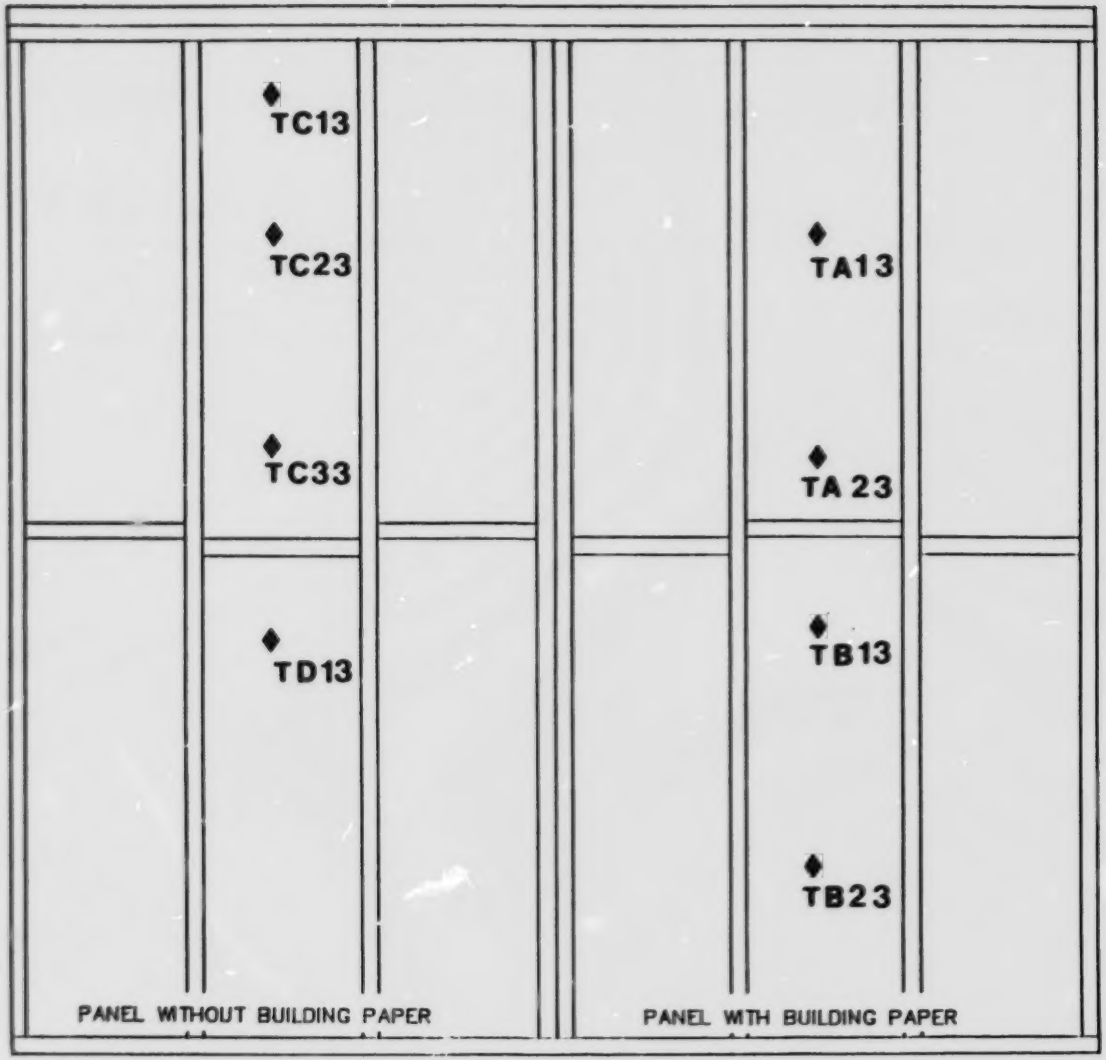

SENSORS LOCATED BETWEEN TENTEST AND INSULATION

FIGURE 6(d)

WALL ELEVATION (EXTERIOR VIEW) – THERMOCOUPLES

APPROX. SCALE 3/4"=1'

RWDI

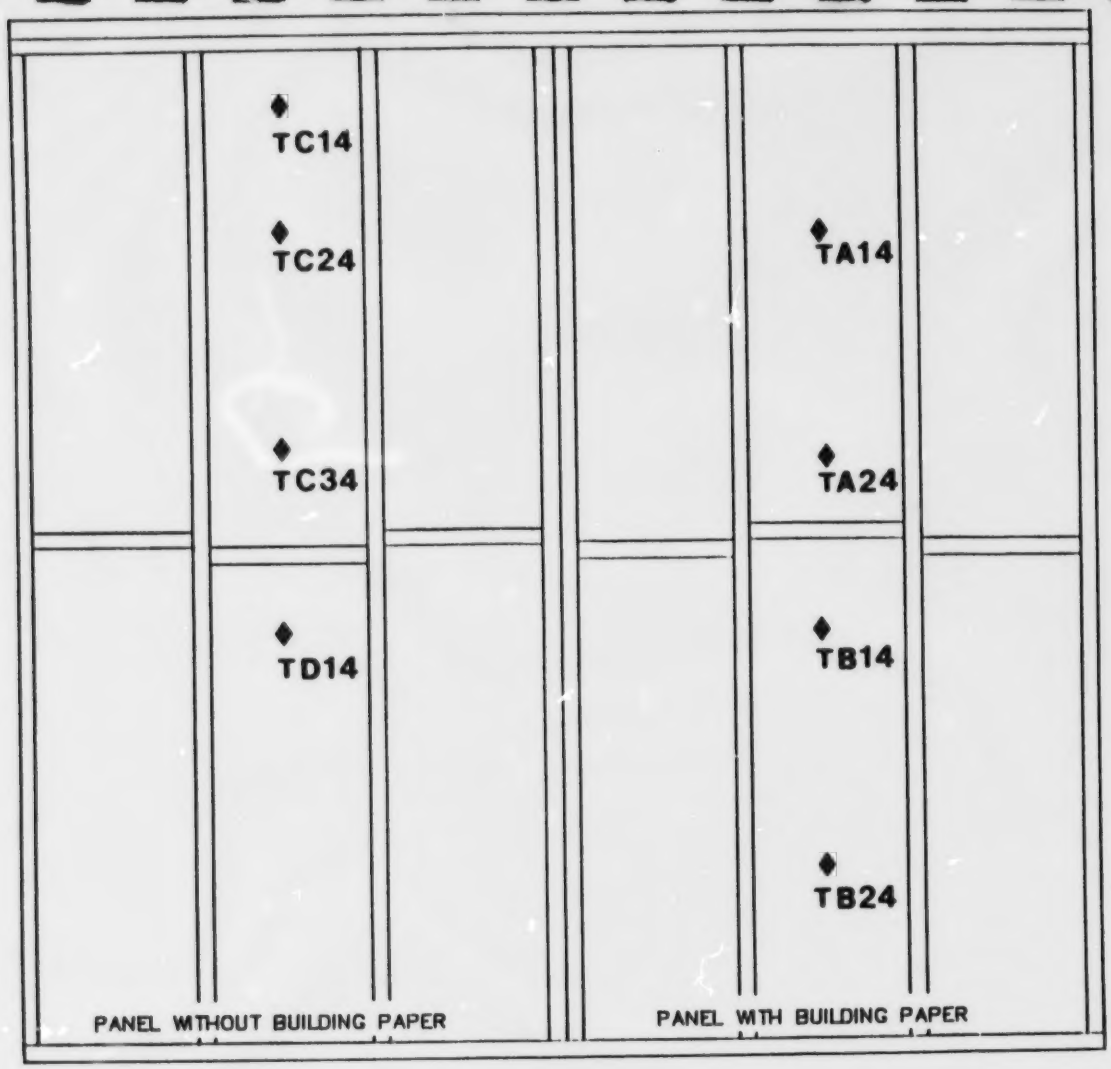

SENSORS LOCATED BETWEEN INSULATION AND MOISTURE BARRIER

FIGURE 6(e)

WALL ELEVATION (EXTERIOR VIEW) – THERMOCOUPLES

APPROX. SCALE 3/4"=1'

RWDI

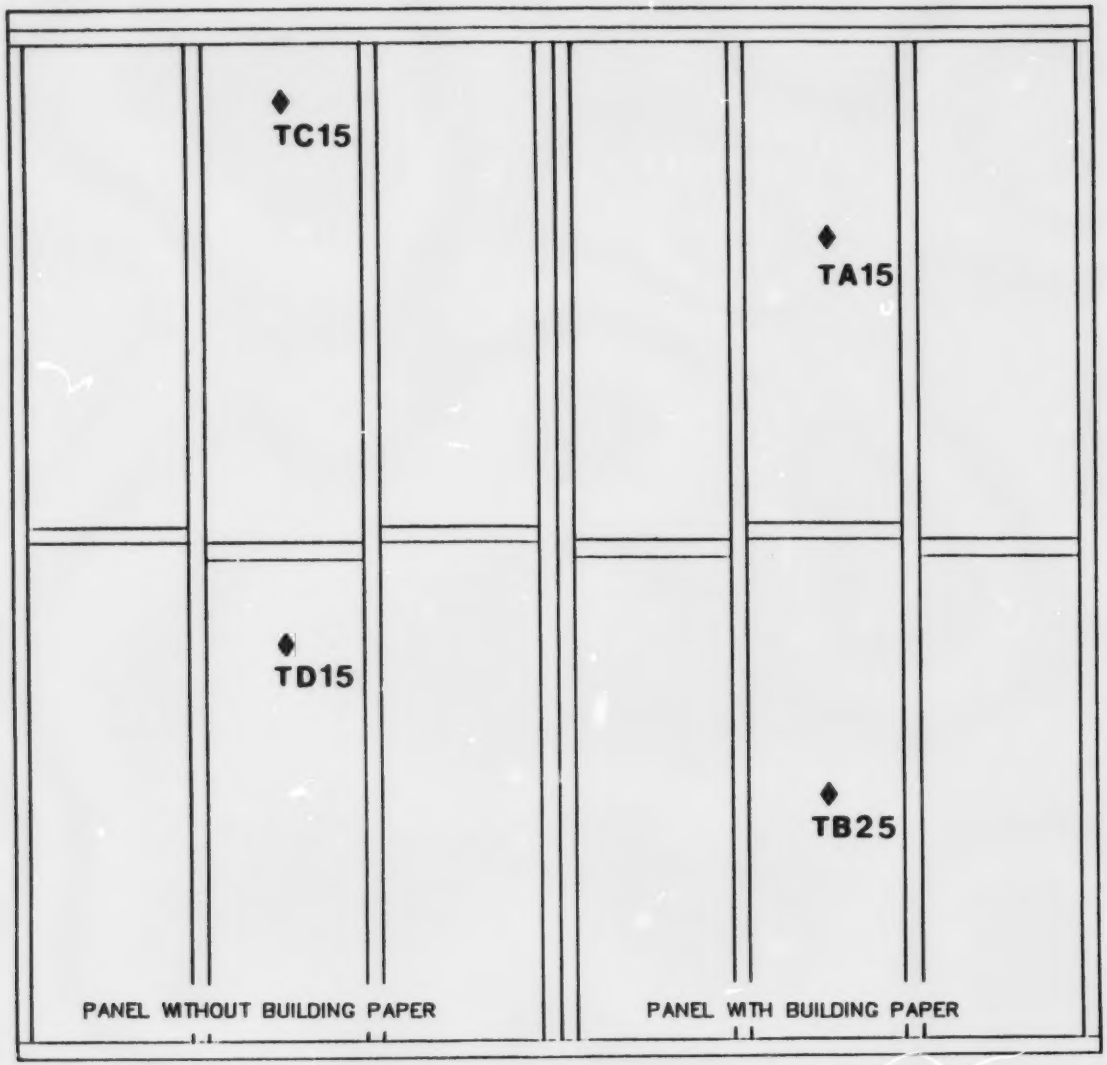

SENSORS LOCATED ON ROOM–SIDE SURFACE OF DRY WALL

FIGURE 6(f)

WALL ELEVATION (EXTERIOR VIEW) – THERMOCOUPLES

APPROX. SCALE 3/4"=1'

RWDI

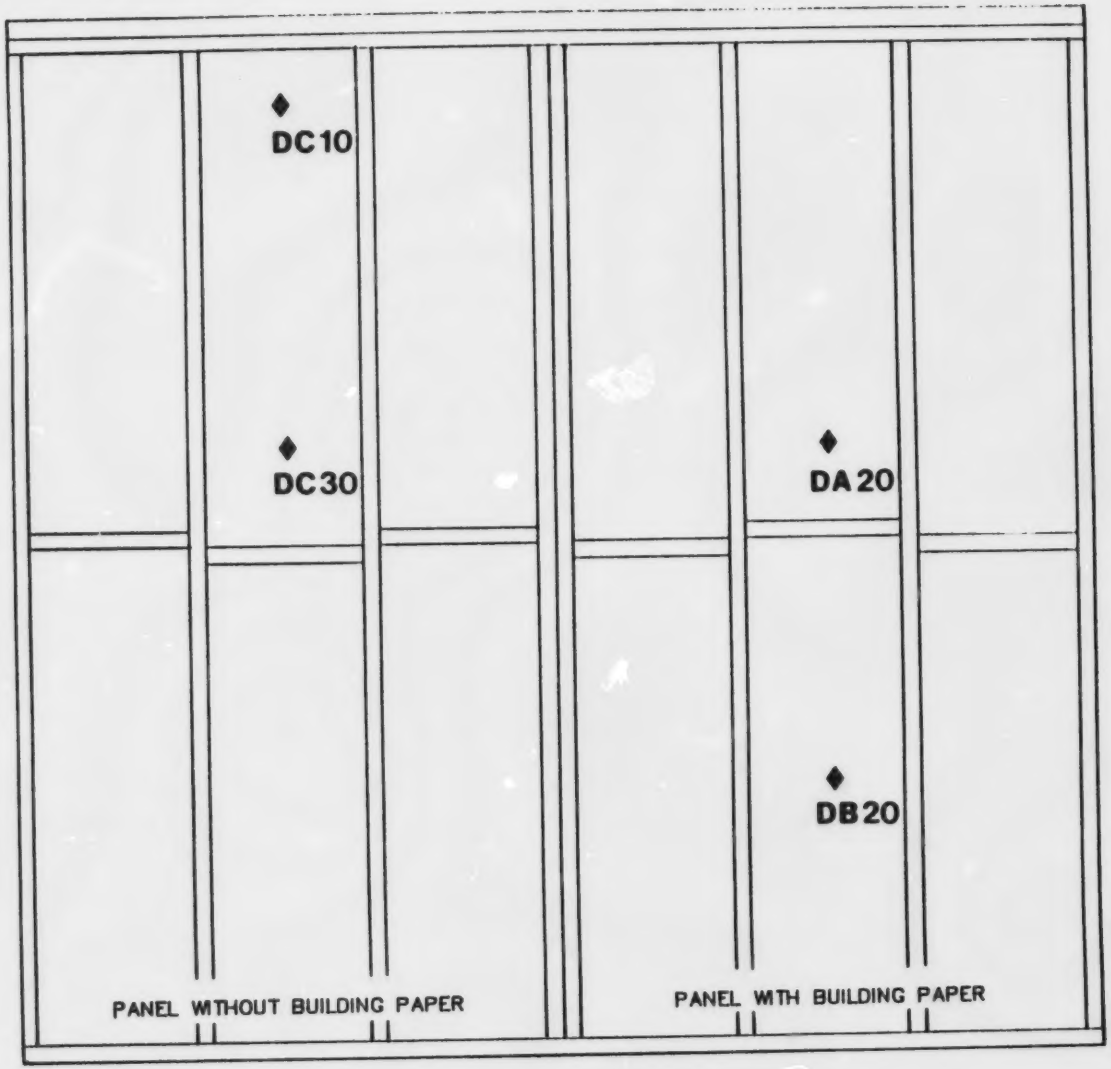

SENSORS LOCATED ON OUTSIDE SURFACE OF SIDING

FIGURE 7(a)

WALL ELEVATION (EXTERIOR VIEW) – DEW POINT SENSORS

APPROX. SCALE 3/4"=1'

RWDI

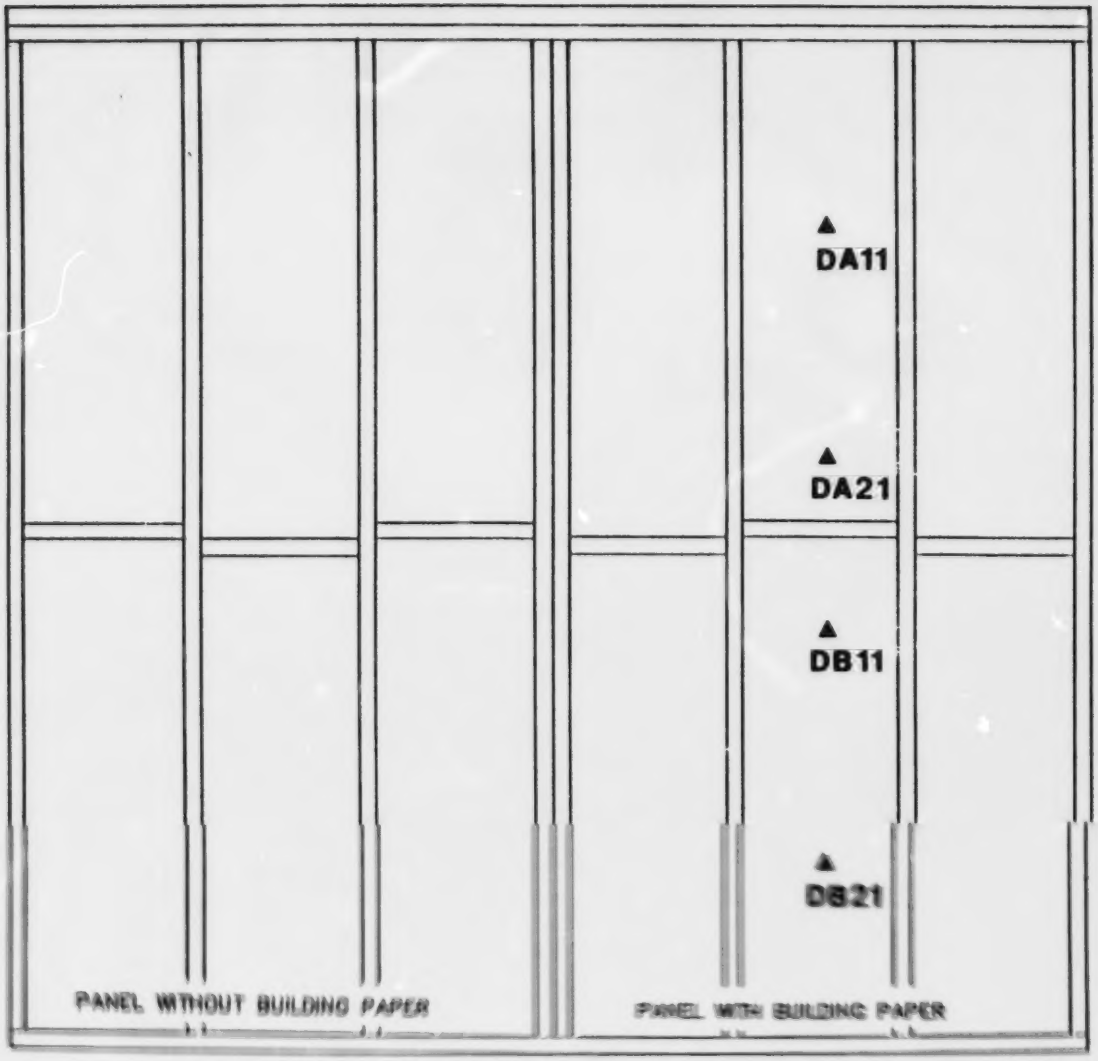

SENSORS LOCATED BETWEEN
SIDING AND BUILDING PAPER

FIGURE 7(b)

WALL ELEVATION (EXTERIOR VIEW) – DEW POINT SENSORS

APPROX. SCALE 3/4"=1'

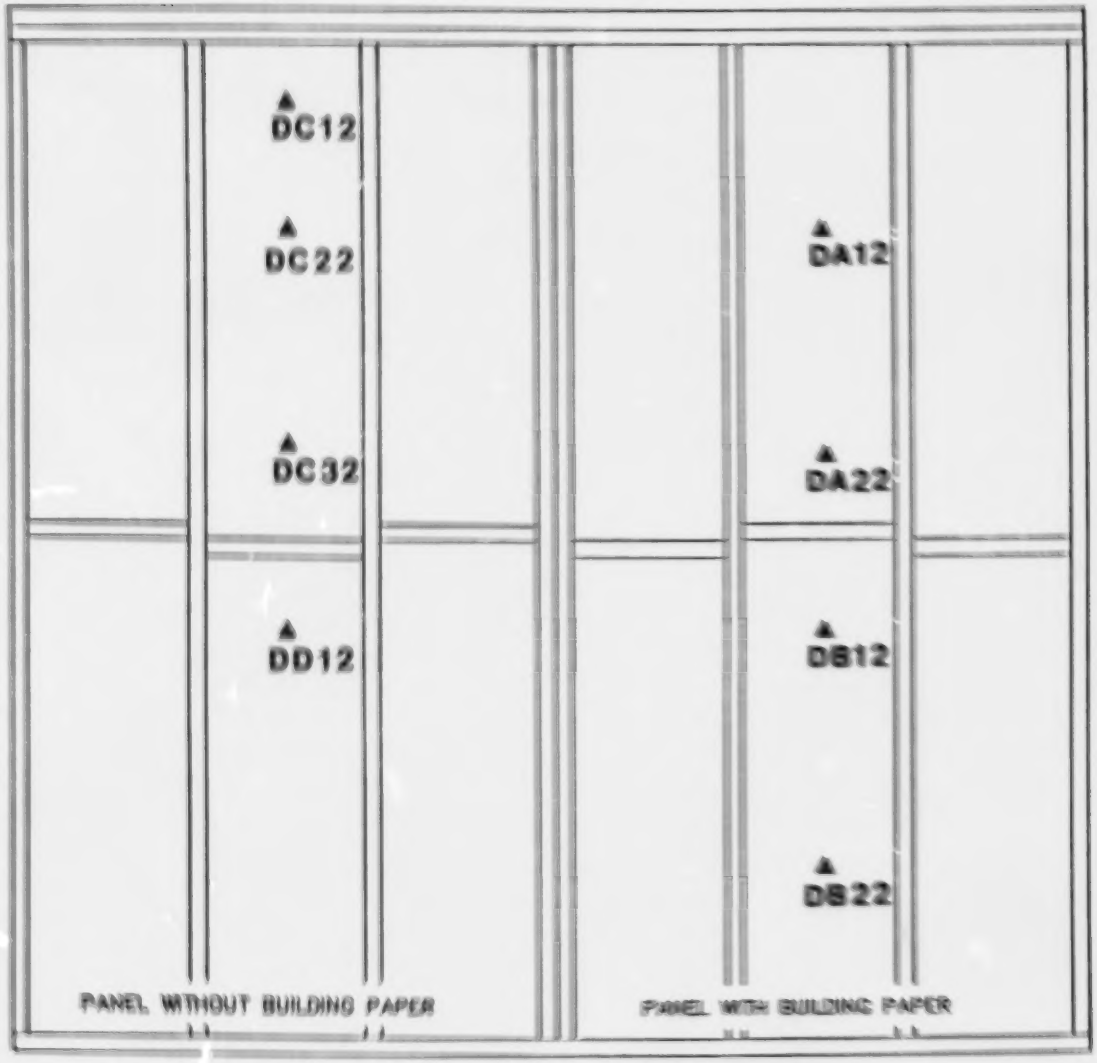

FIGURE 7(c)

WALL ELEVATION (EXTERIOR VIEW) – DEW POINT SENSORS

APPROX. SCALE 3/4"=1'

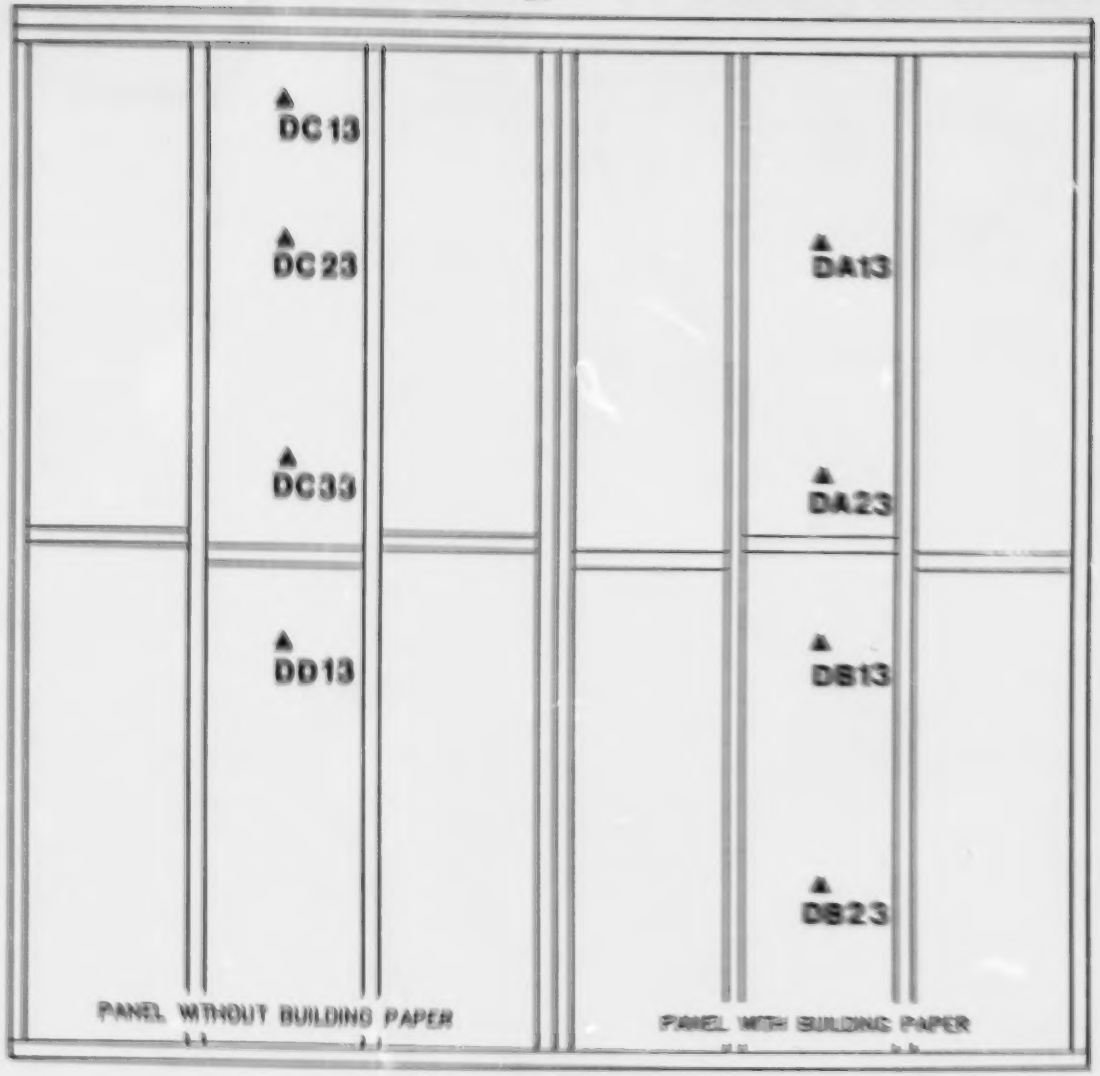

SENSORS LOCATED BETWEEN TENTEST AND INSULATION

FIGURE 7(d)

WALL ELEVATION (EXTERIOR VIEW) – DEW POINT SENSORS

APPROX. SCALE 3/4"=1'

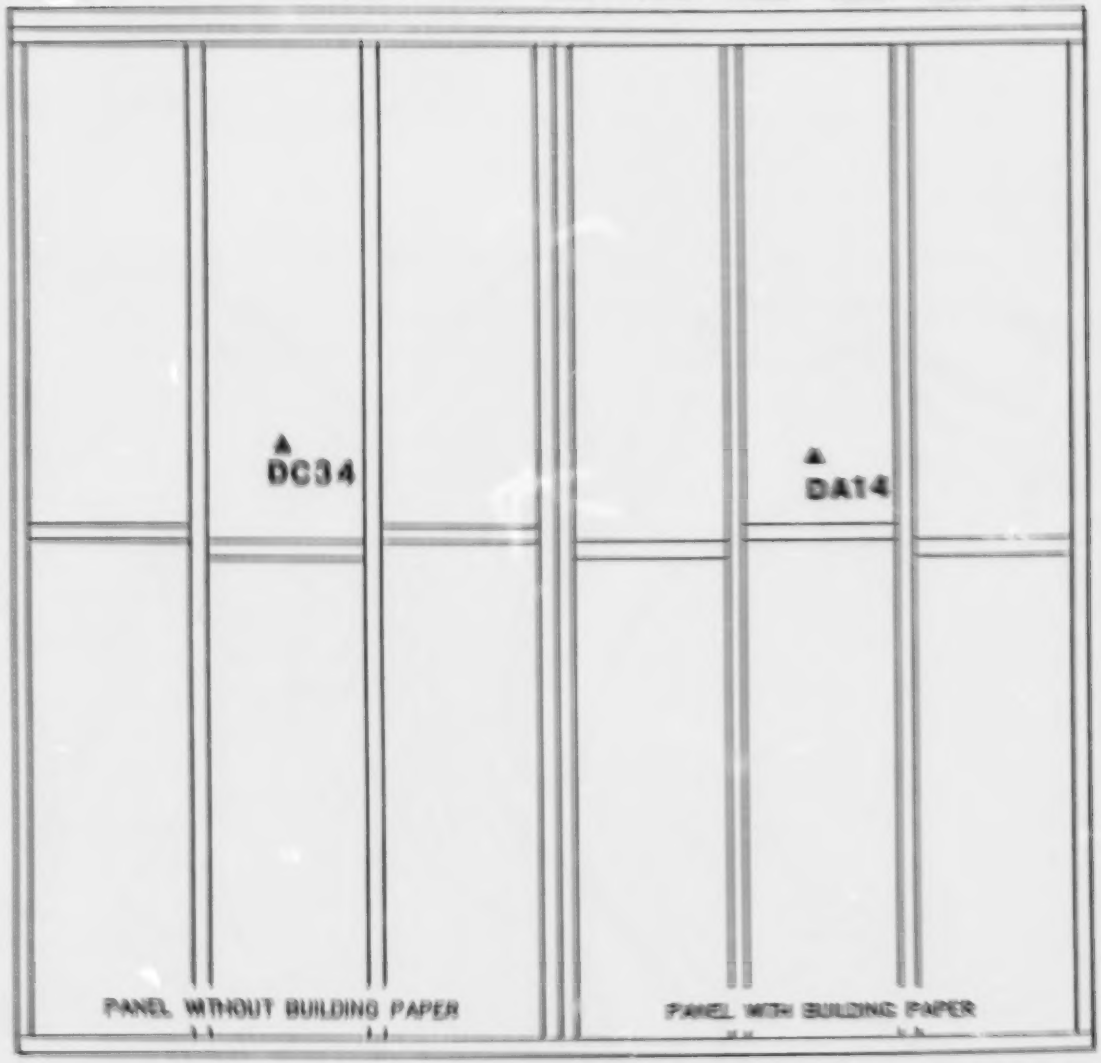

SENSORS LOCATED BETWEEN INSULATION AND MOISTURE BARRIER

FIGURE 7(e)

WALL ELEVATION (EXTERIOR VIEW) – DEW POINT SENSORS

APPROX. SCALE 3/4"=1'

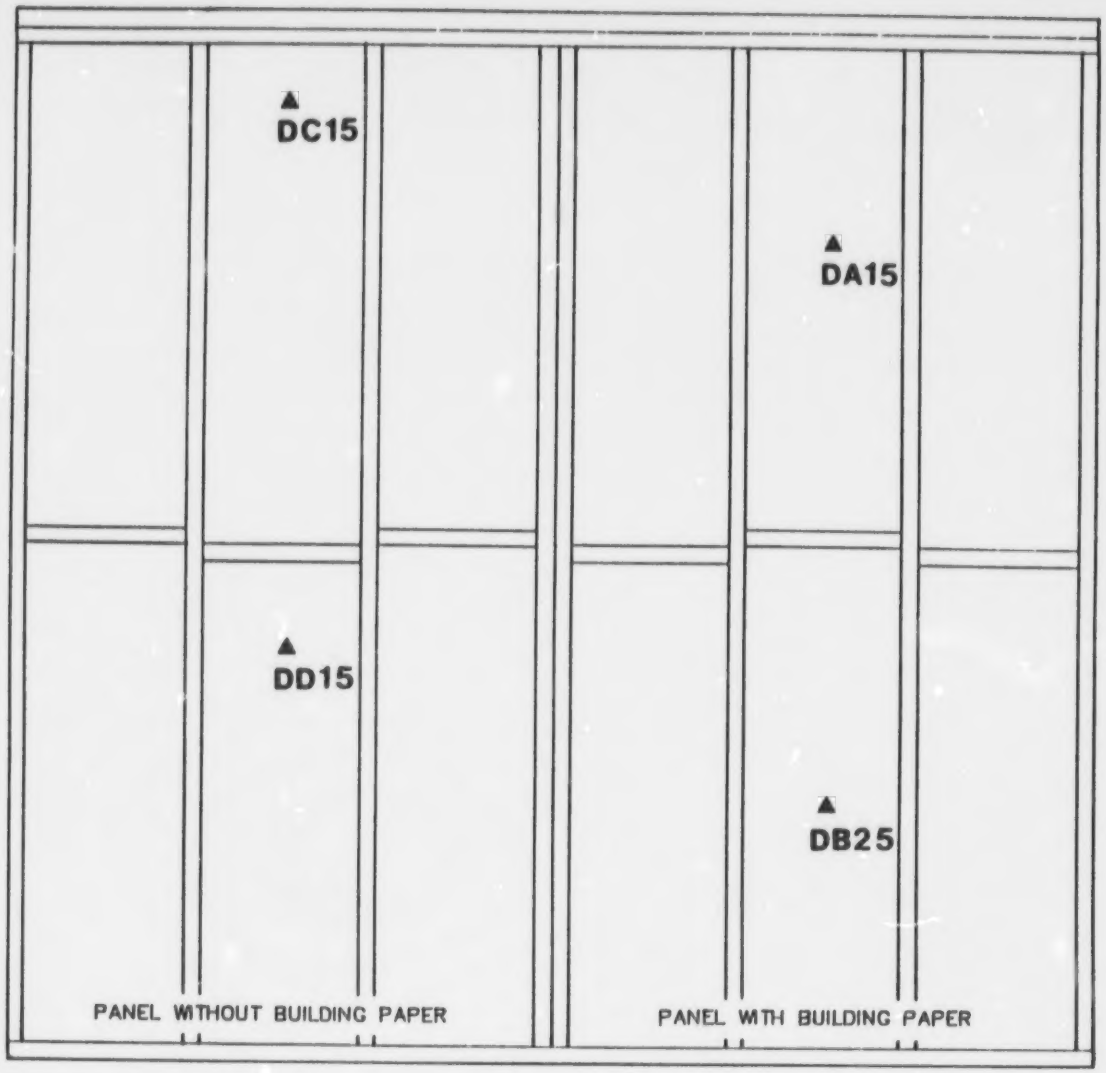

SENSORS LOCATED ON ROOM–SIDE SURFACE OF DRY WALL

FIGURE 7(f)

WALL ELEVATION (EXTERIOR VIEW) – DEWPOINT SENSORS

APPROX. SCALE 3/4"=1'

RWDI

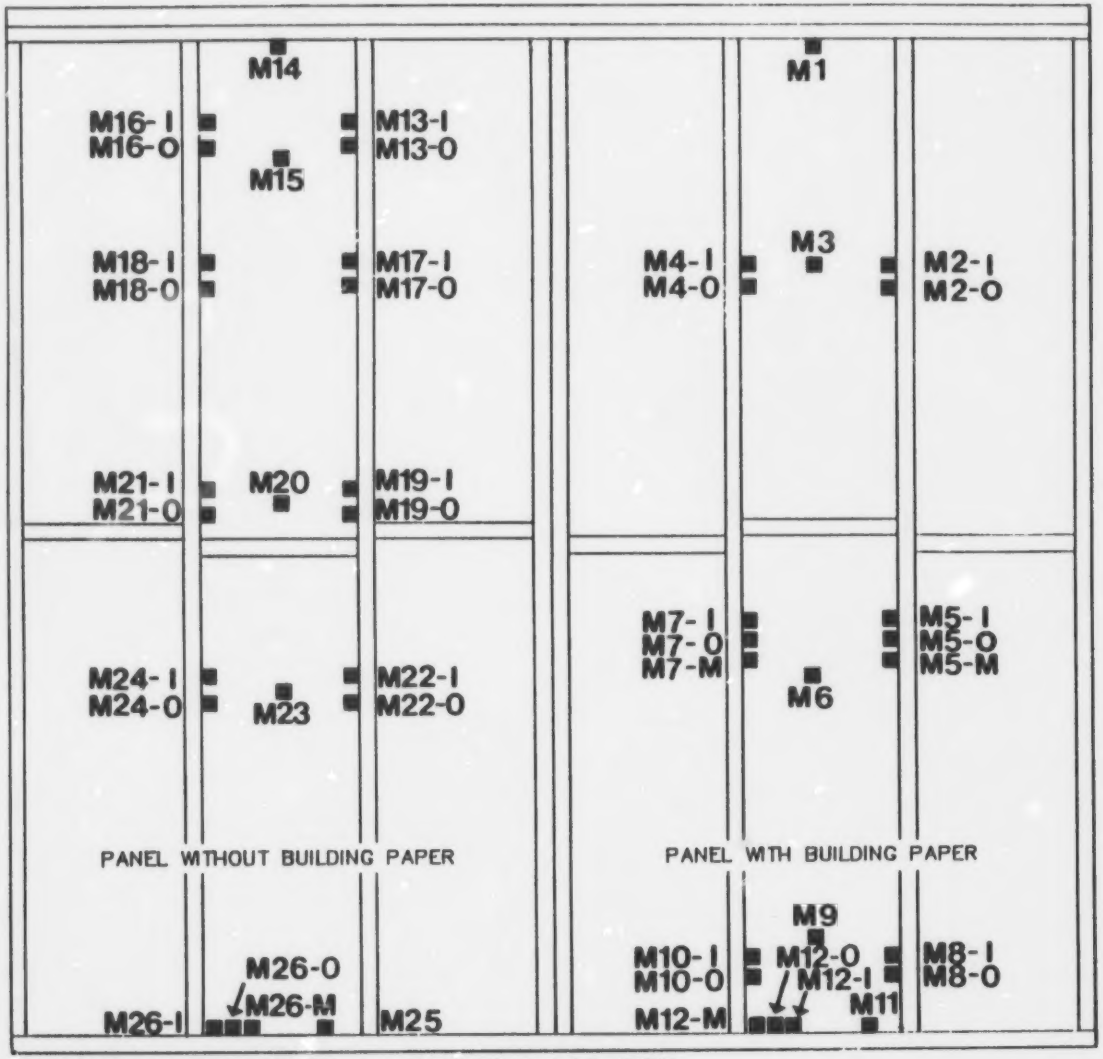

NOTES: EACH SQUARE REPRESENTS A MEASURING LOCATION
ALL PINS IN A GROUP OF TWO OR THREE ARE AT SAME HEIGHT ALONG WIDE DIRECTION OF STUD
PIN DEPTHS ARE 5mm INTO MATERIAL

FIGURE 8

WALL ELEVATION (EXTERIOR VIEW) – MOISTURE PINS

APPROX. SCALE 3/4"=1'

RWDI

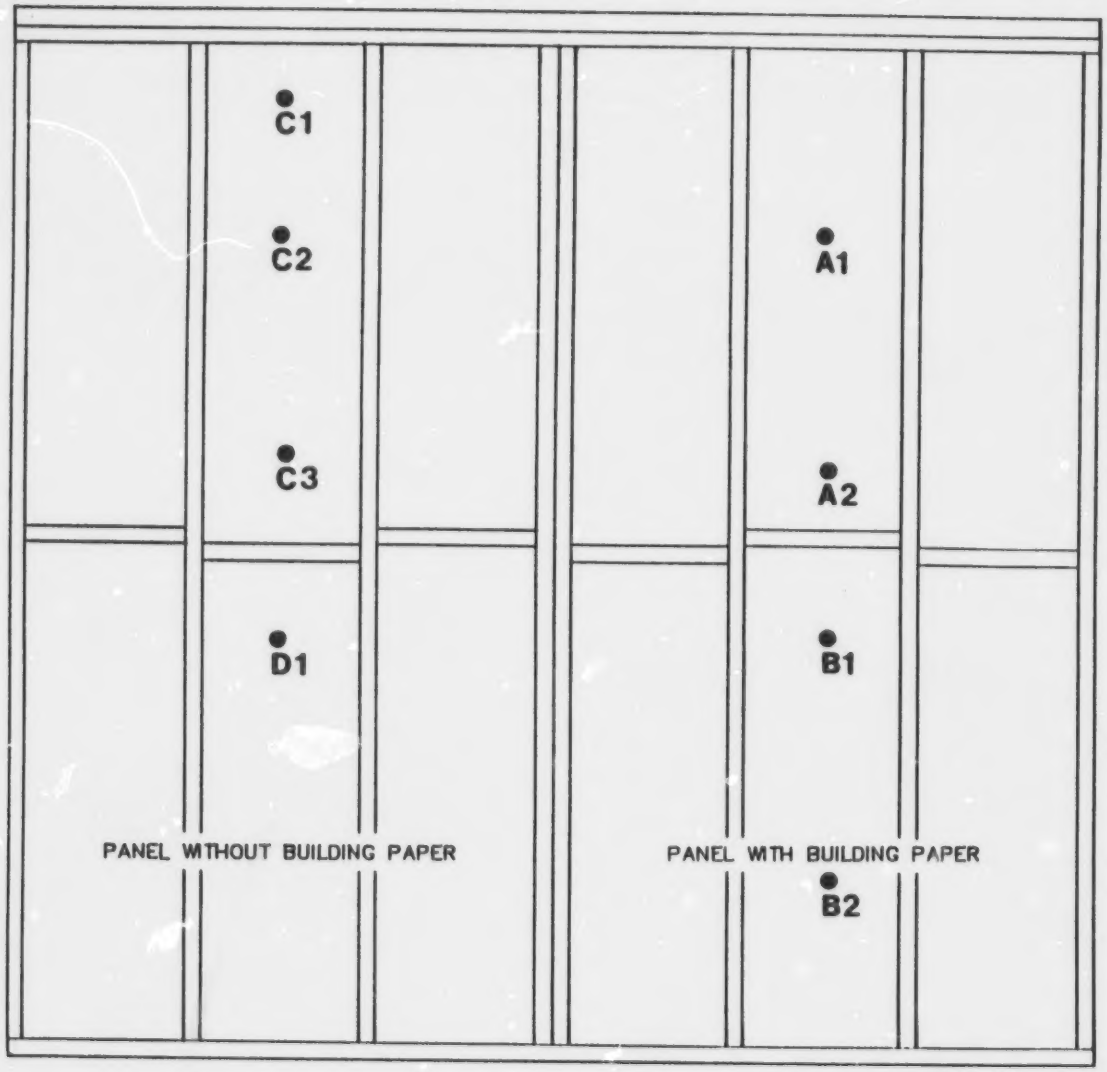

FIGURE 9(a)

LOCATIONS OF RELATIVE HUMIDITY MEASUREMENTS

APPROX. SCALE 3/4"=1'

RWDI

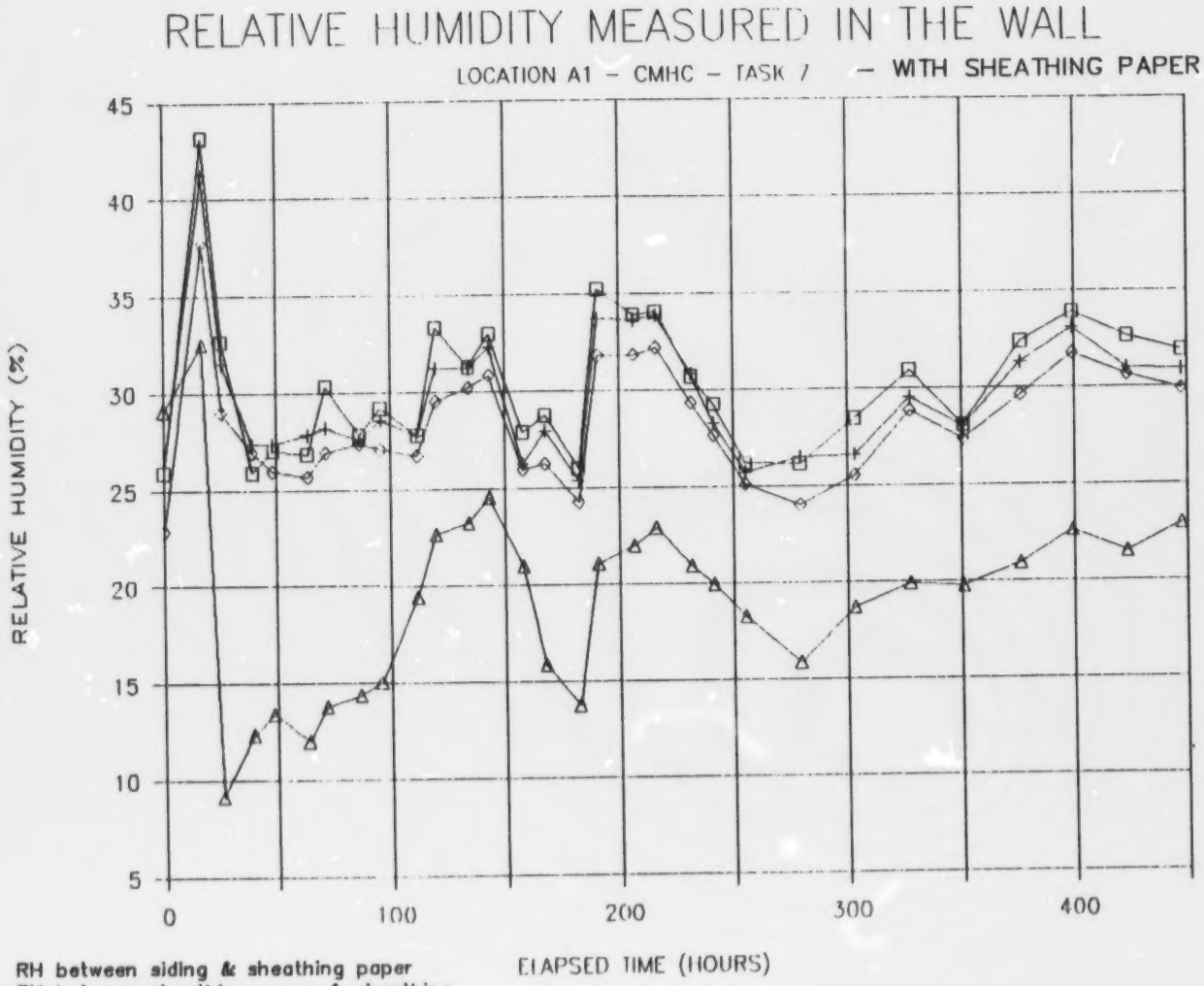

FIGURE 9(b)

RWDI

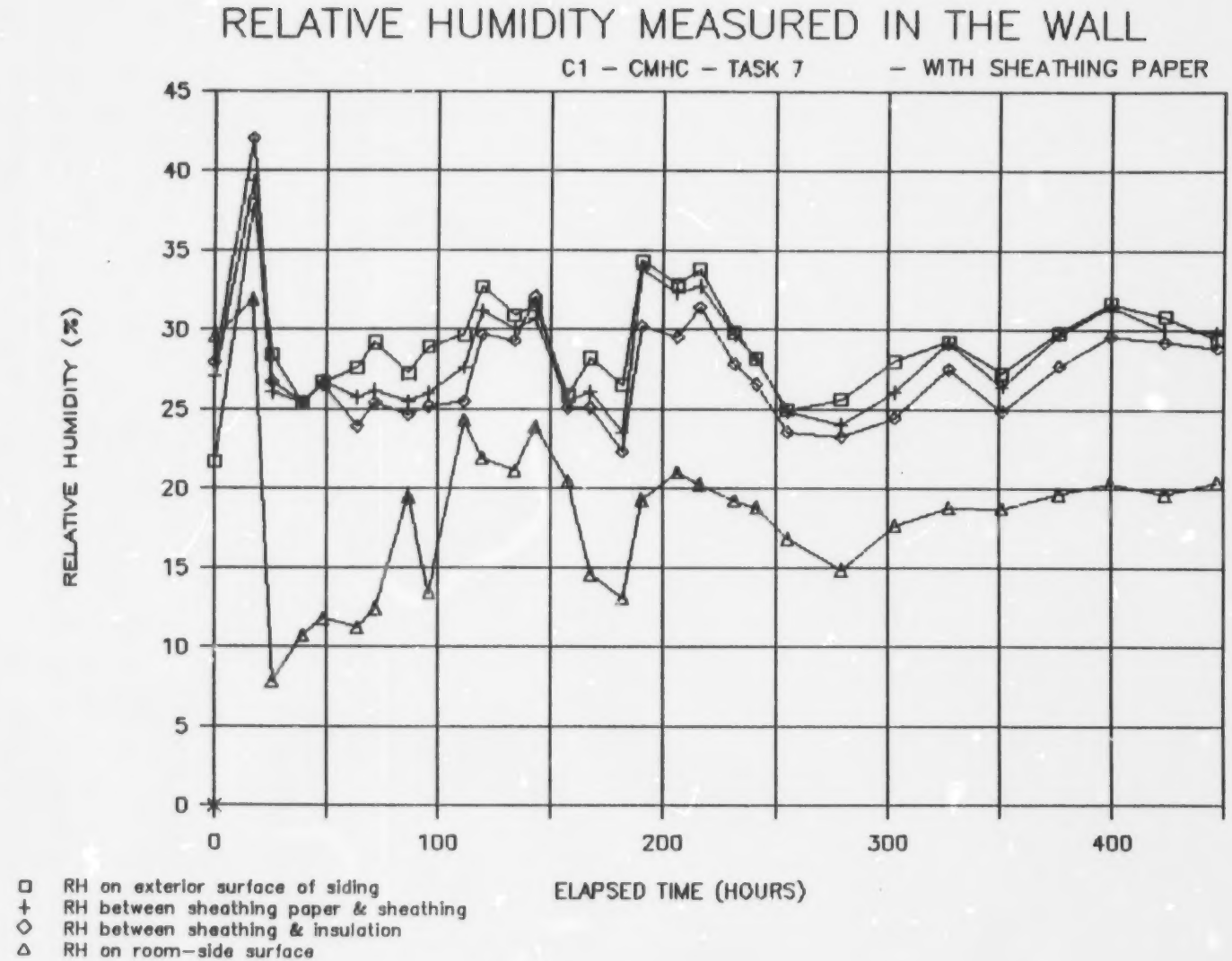
RELATIVE HUMIDITY MEASURED IN THE WALL
C1 – CMHC – TASK 7 – WITH SHEATHING PAPER
RELATIVE HUMIDITY (%)
45
40
35
30
25
20
15
10
5
0
0
100
200
300
400
ELAPSED TIME (HOURS)
RH on exterior surface of siding
RH between sheathing paper & sheathing
RH between sheathing & insulation
RH on room–side surface

FIGURE 9(c)

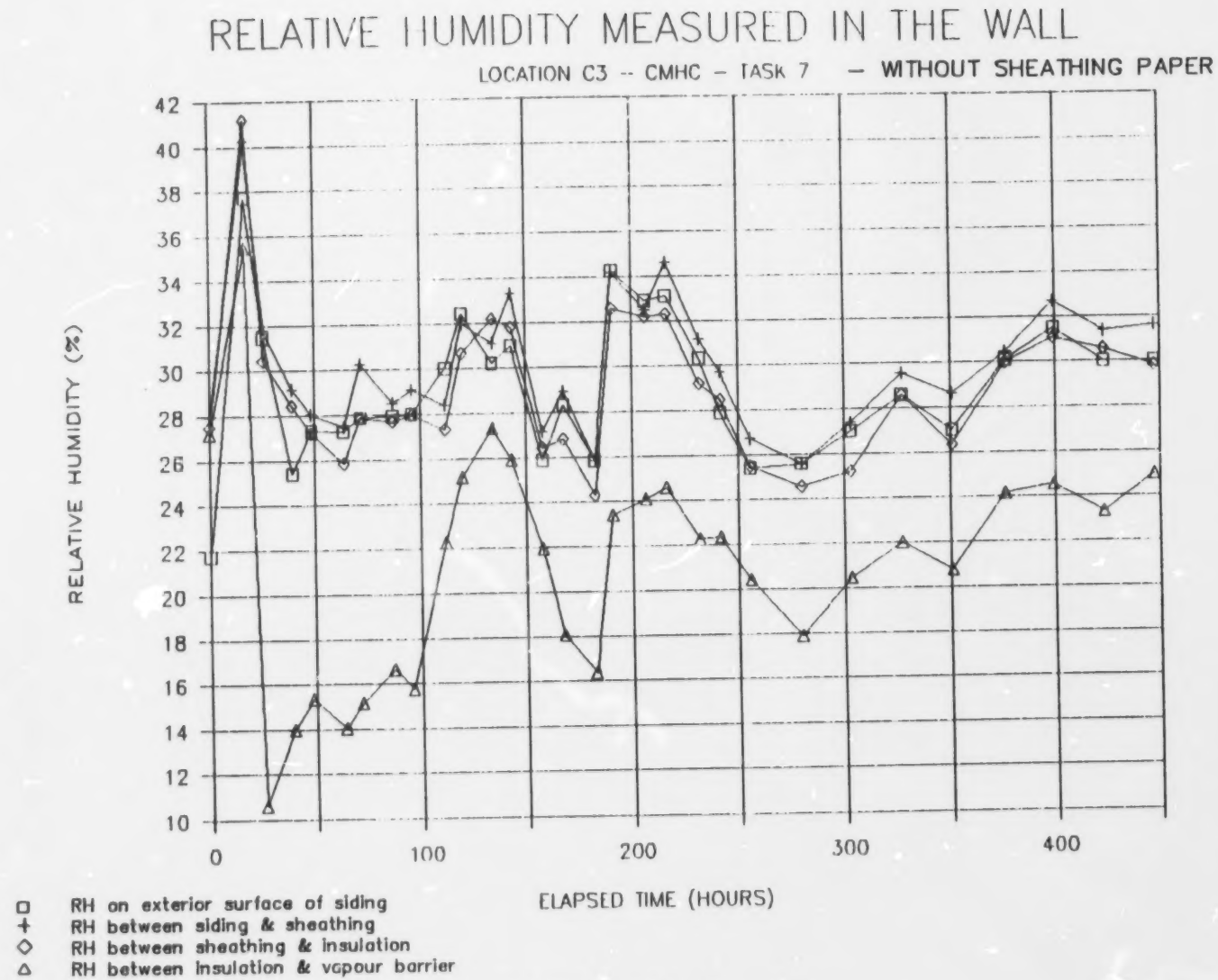

FIGURE 10(a)

RWDI

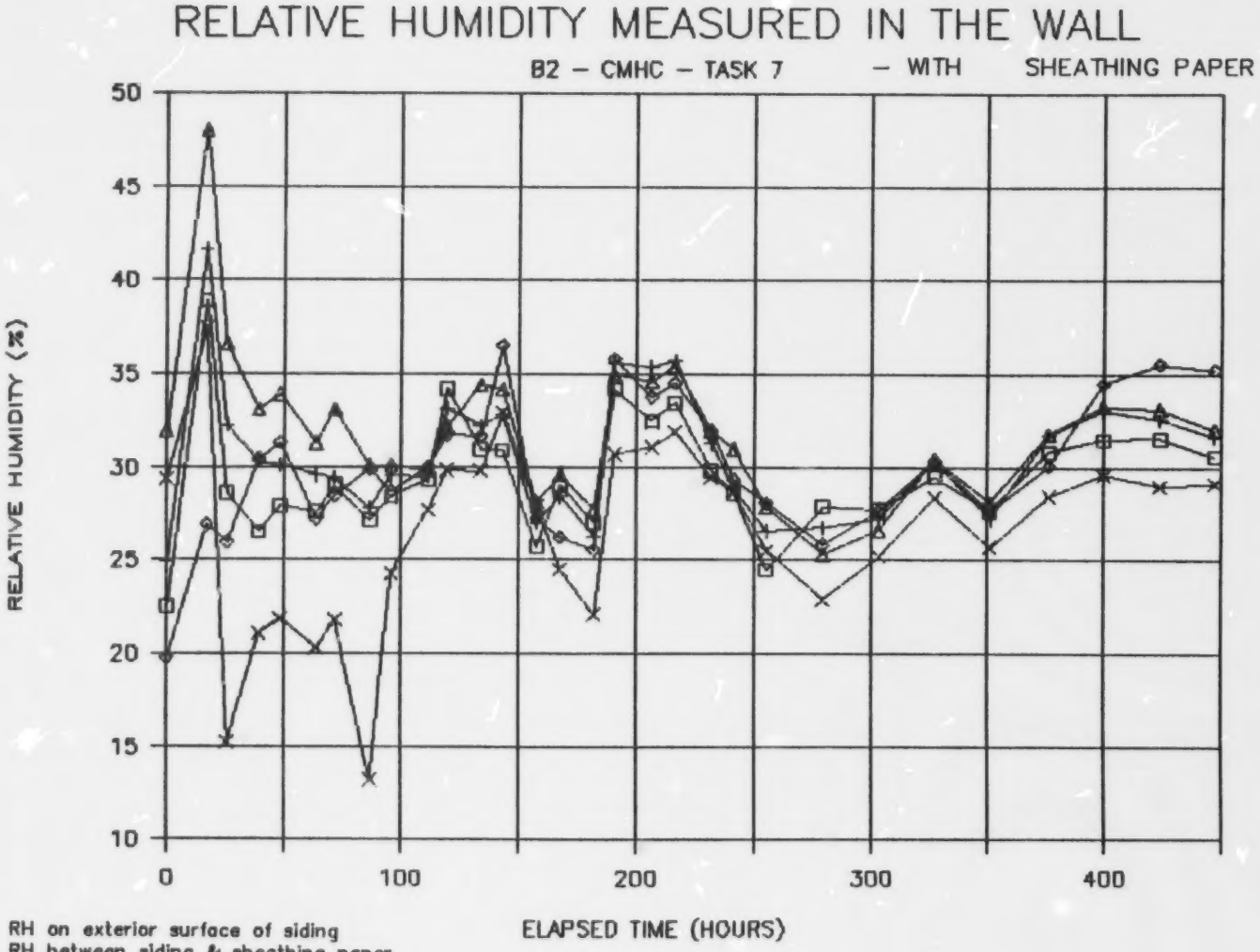

FIGURE 10(b)

RWDI

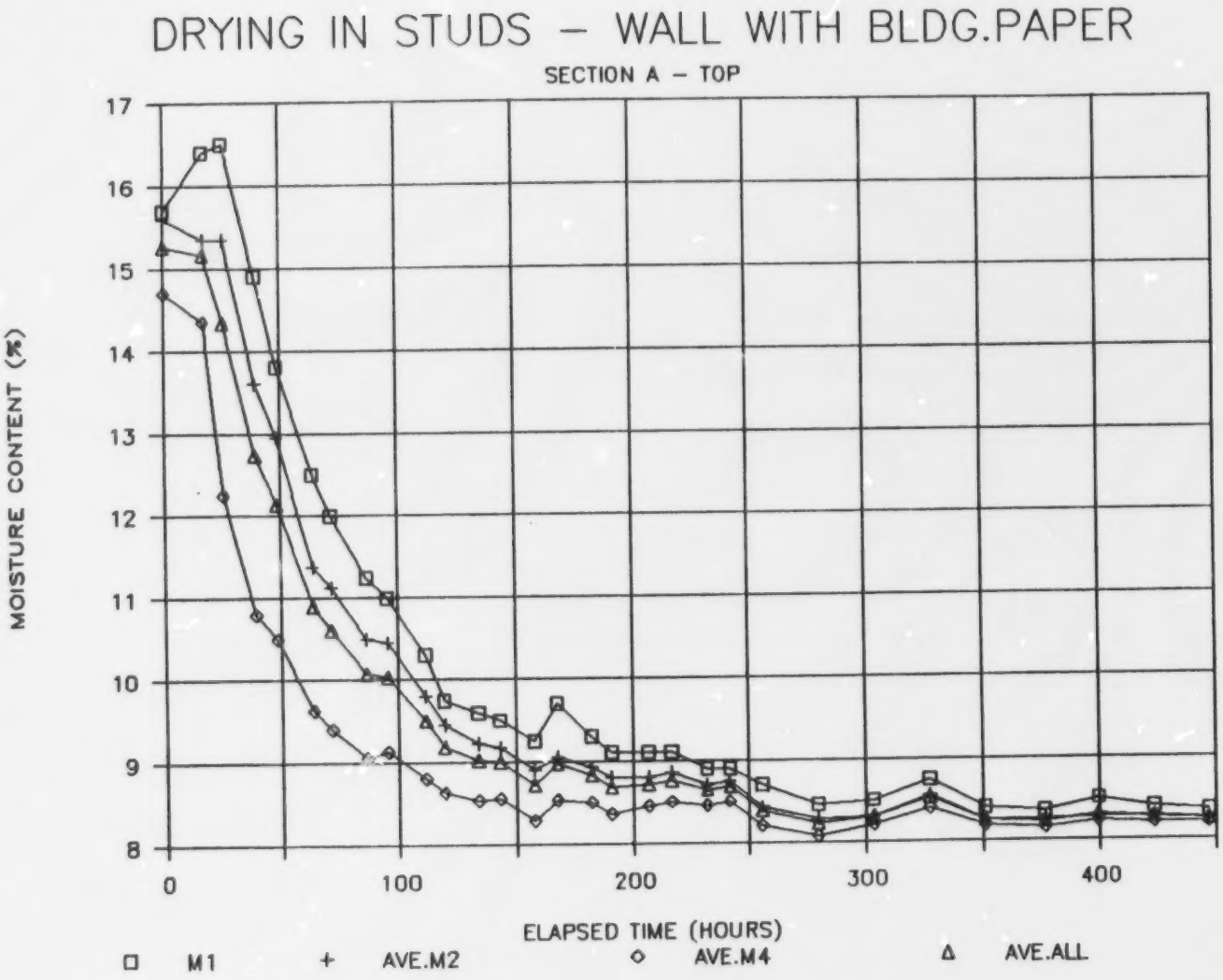

FIGURE 11(a)

RWDI

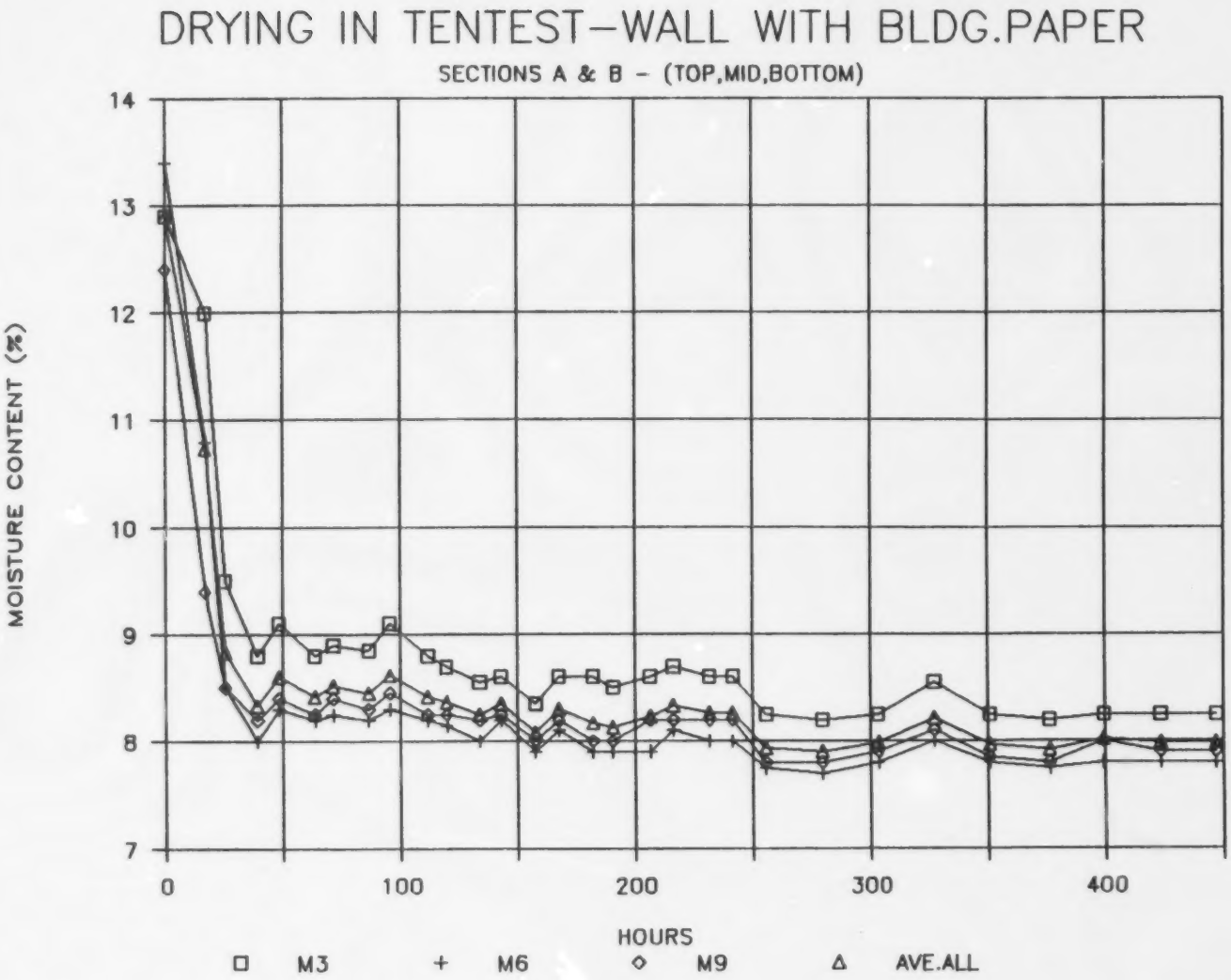
DRYING IN TENTEST–WALL WITH BLDG.PAPER
SECTIONS A & B – (TOP,MID,BOTTOM)
MOISTURE CONTENT (%)
14
13
12
11
10
9
8
7
0
100
200
300
400
HOURS
M3
M6
M9
AVE.ALL

FIGURE 11(b)

DRYING IN STUDS – WALL WITH BLDG. PAPER

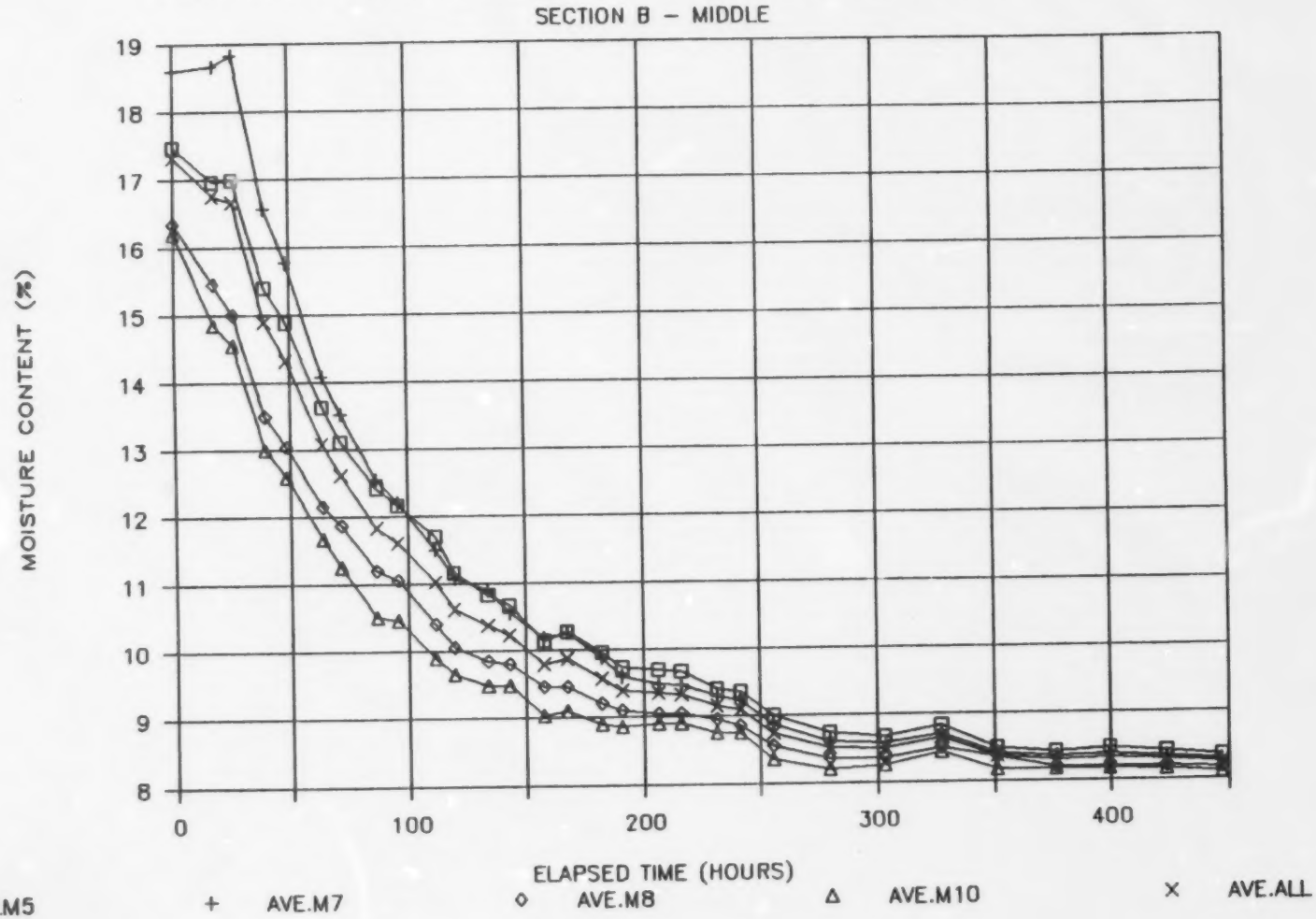

FIGURE 11(c)

RWDI

DRYING IN STUDS – WALL WITH BLDG. PAPER

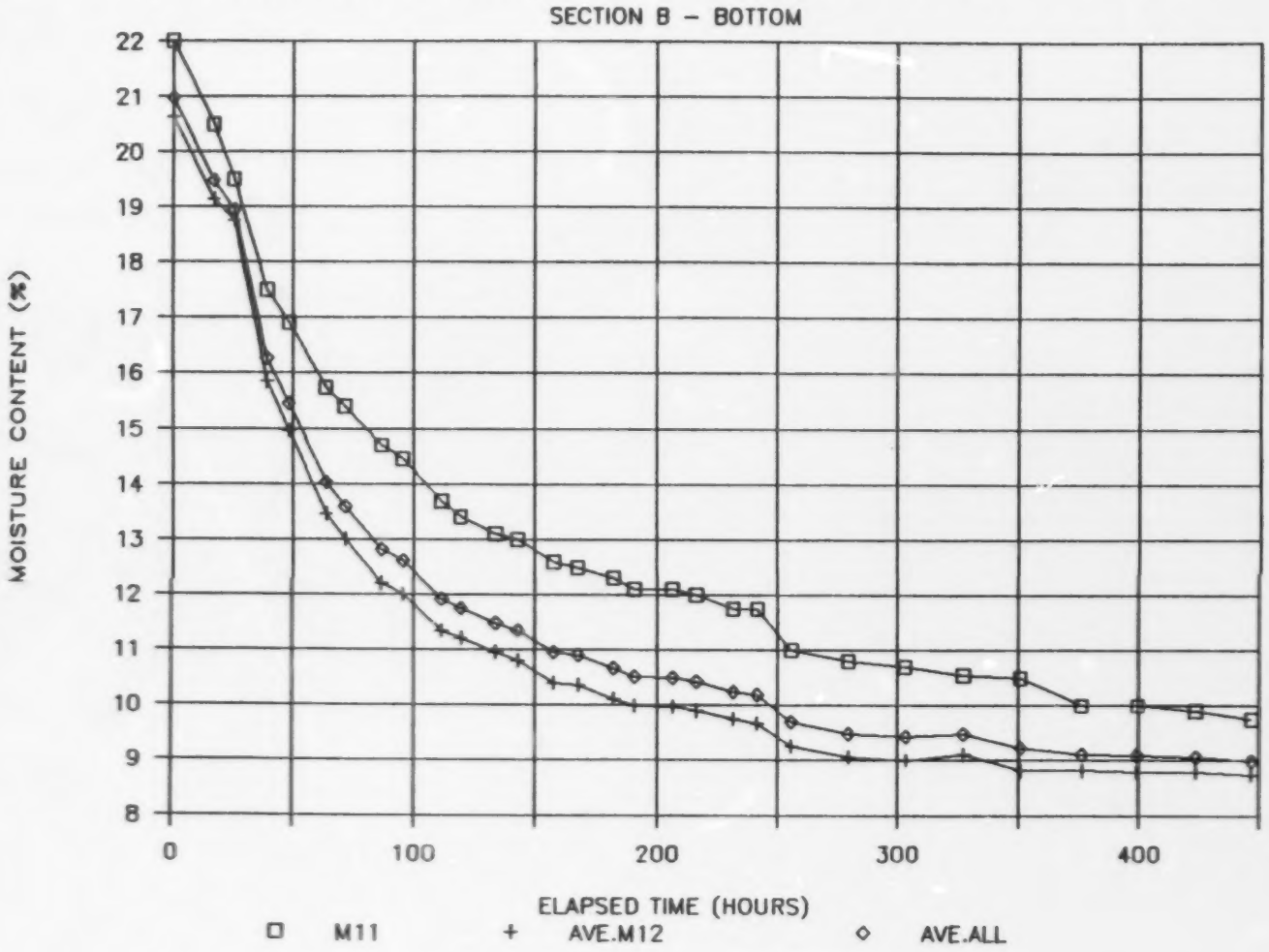

FIGURE 11(d)

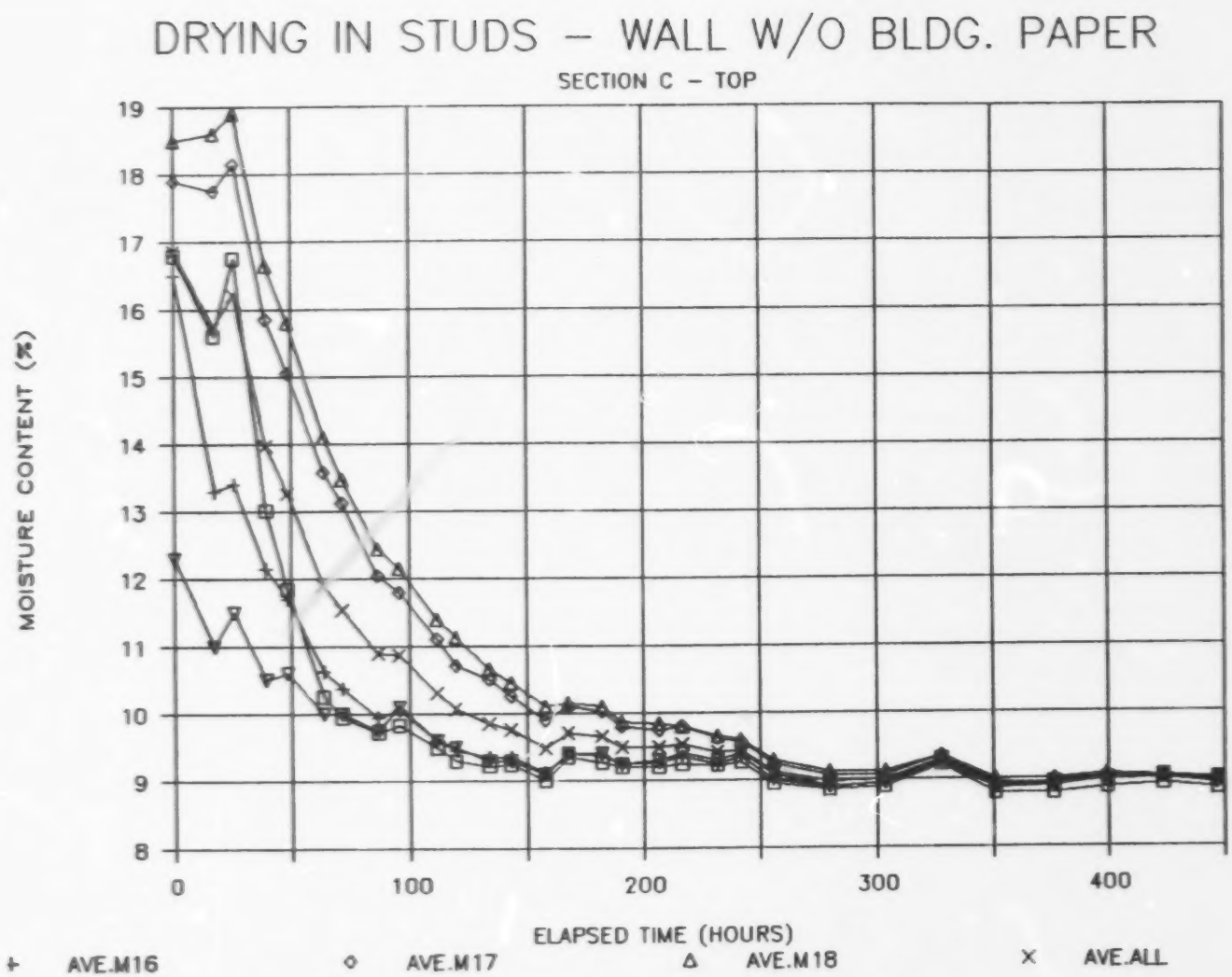
DRYING IN STUDS – WALL W/O BLDG. PAPER
SECTION C – TOP
MOISTURE CONTENT (%)
19
18
17
16
15
14
13
12
11
10
9
8
0
100
200
300
400
ELAPSED TIME (HOURS)
+ AVE.M16
◇ AVE.M17
△ AVE.M18
× AVE.ALL

FIGURE 12(a)

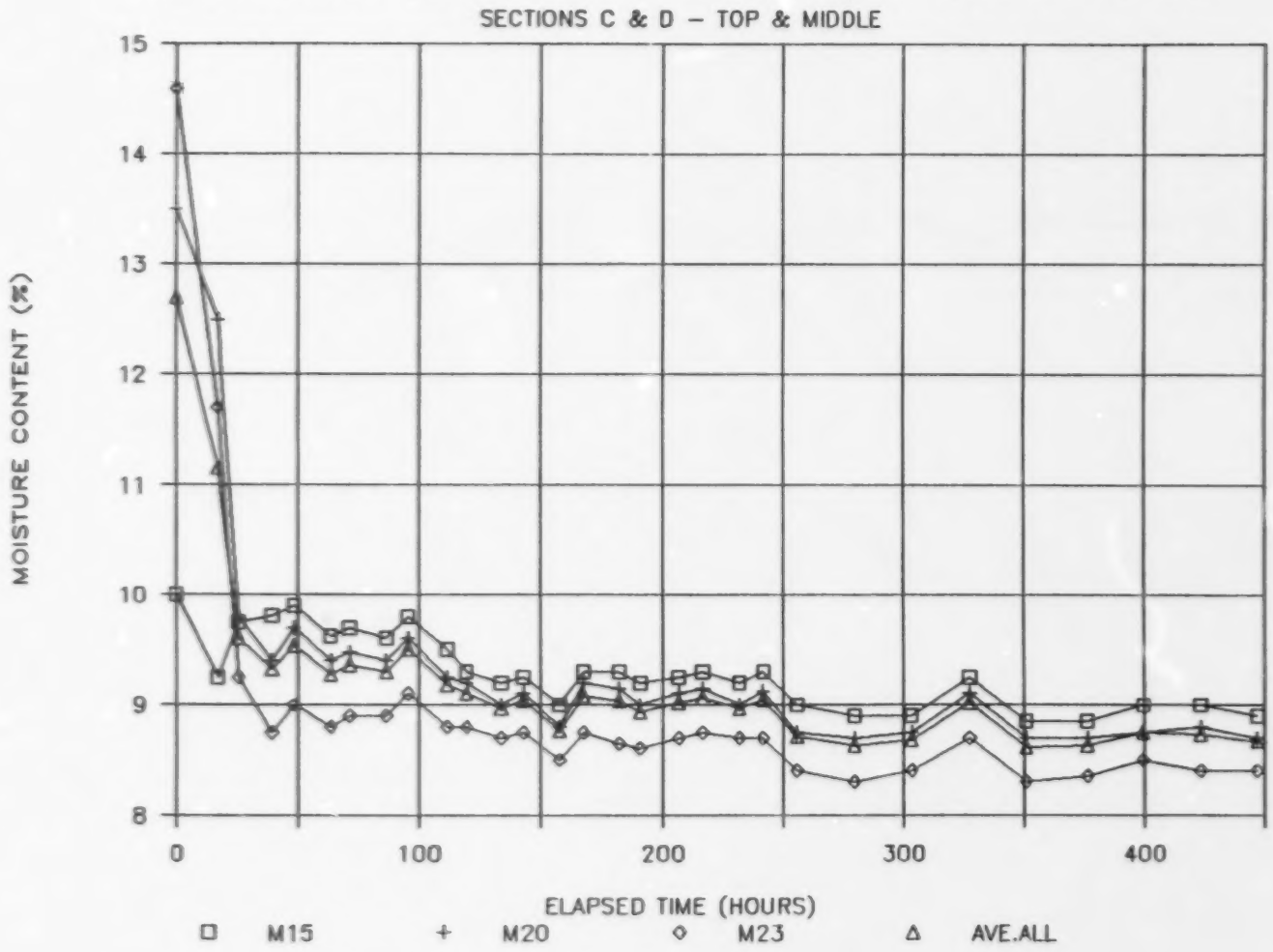
DRYING IN TENTEST – WALL W/O BLDG.PAPER
SECTIONS C & D – TOP & MIDDLE
MOISTURE CONTENT (%)
15
14
13
12
11
10
9
8
0
100
200
300
400
ELAPSED TIME (HOURS)
M15
M20
M23
AVE.ALL

FIGURE 12(b)

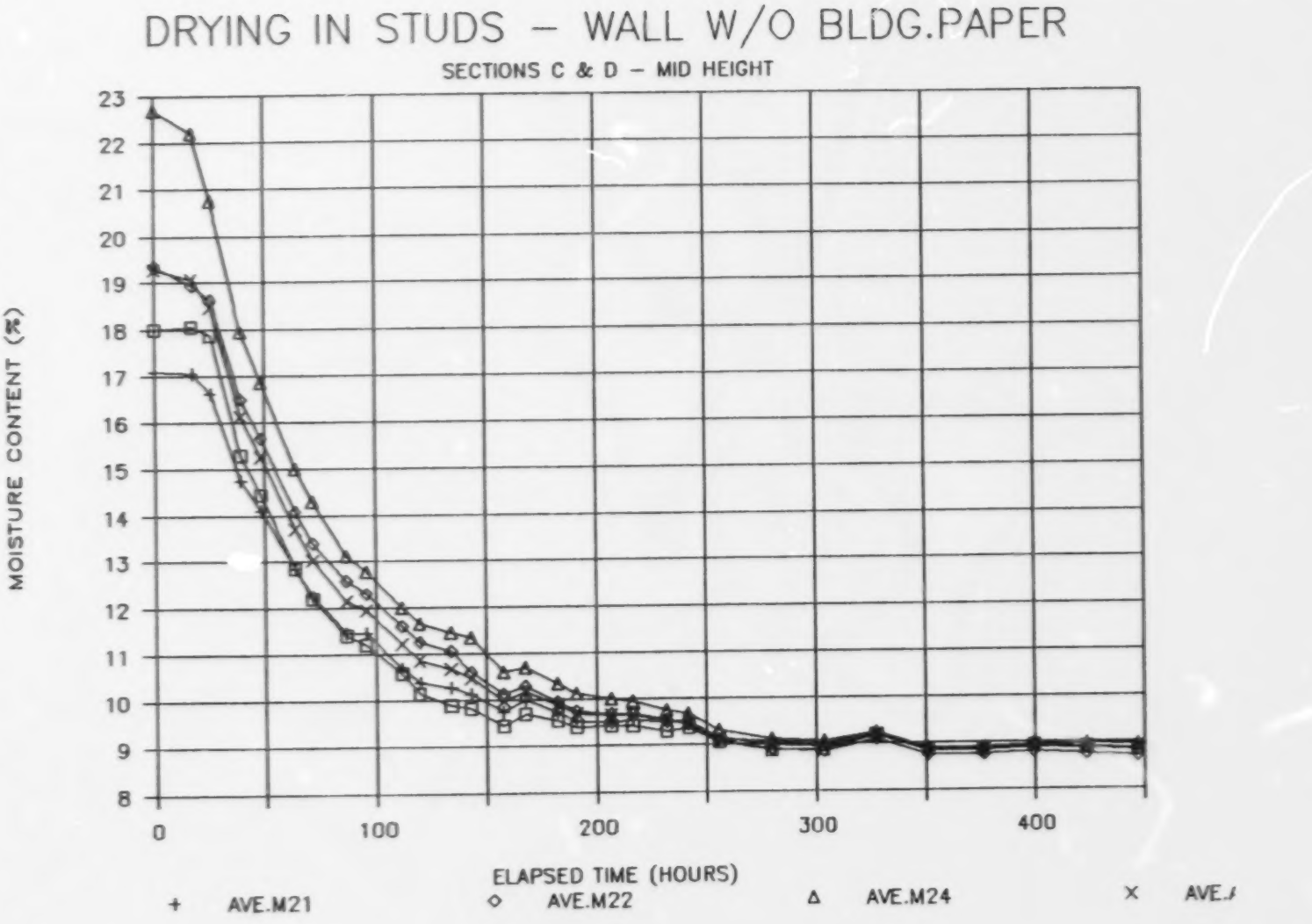

FIGURE 12(c)

RWDI

DRYING IN STUDS – WALL W/O BLDG. PAPER

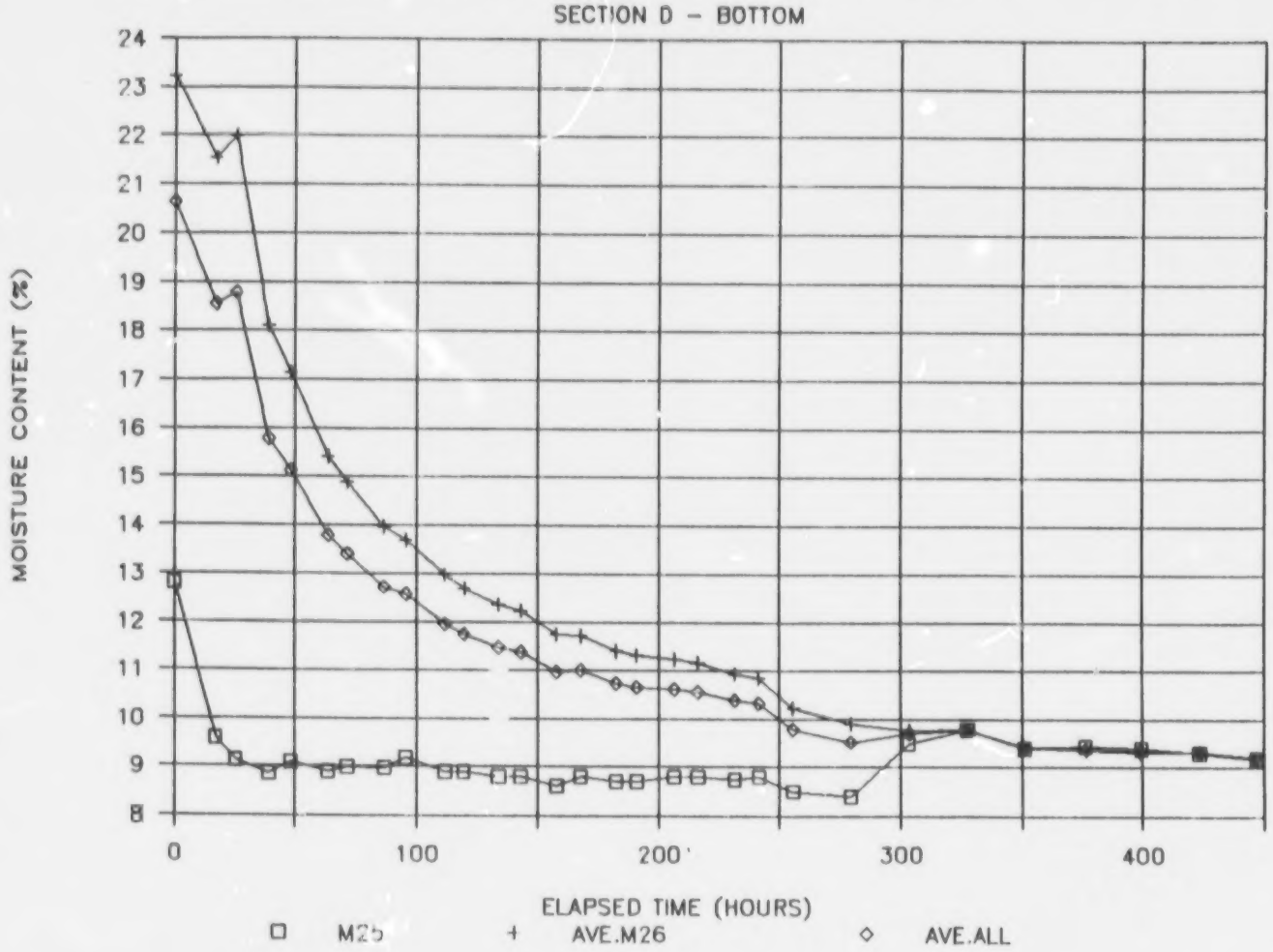

FIGURE 12(d)

KWDI

TEST CONDITIONS – FULL SCALE LAB TEST

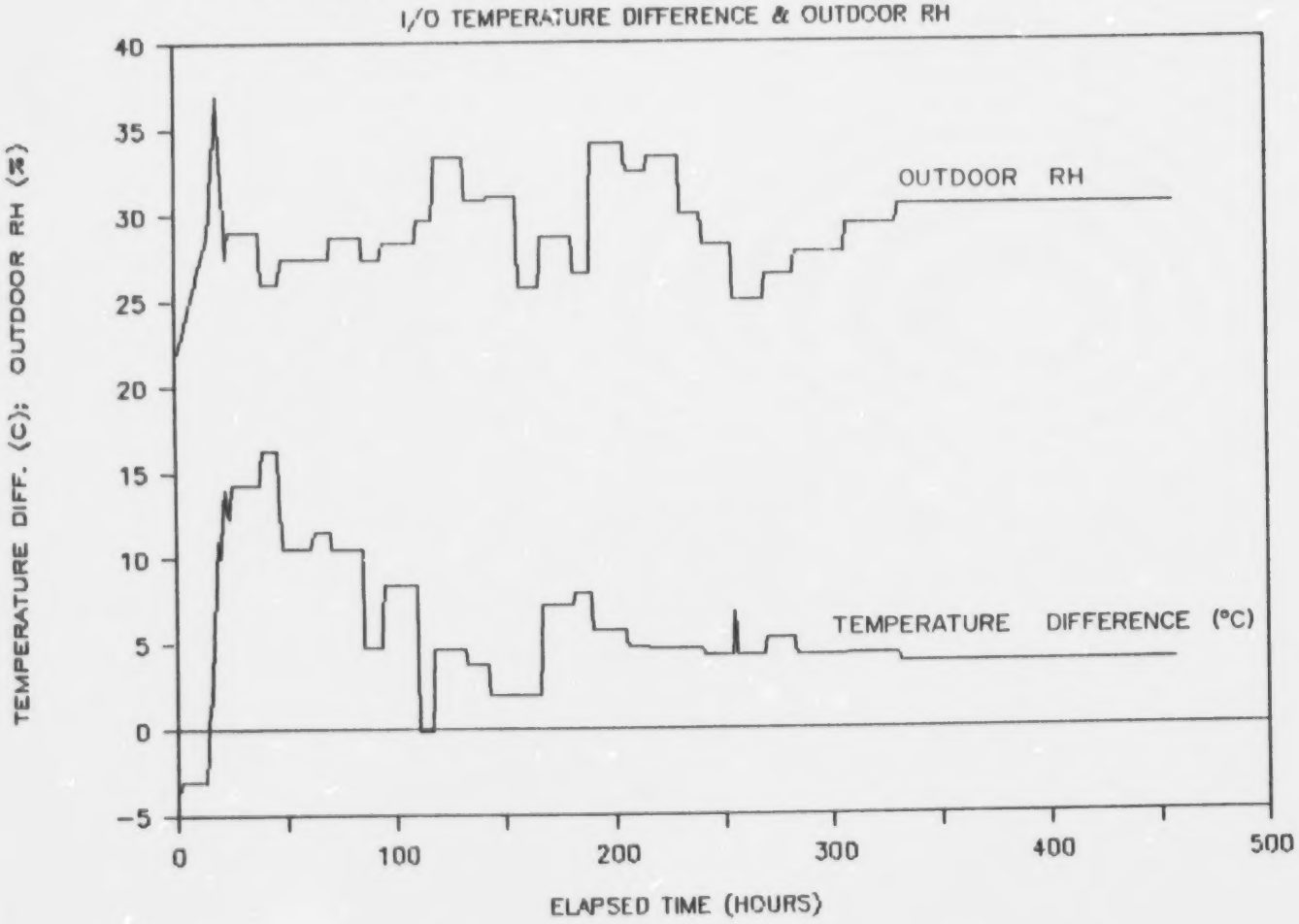

FIGURE 13

RWDI

COMPARISON OF SIMULATION & TEST RESULTS

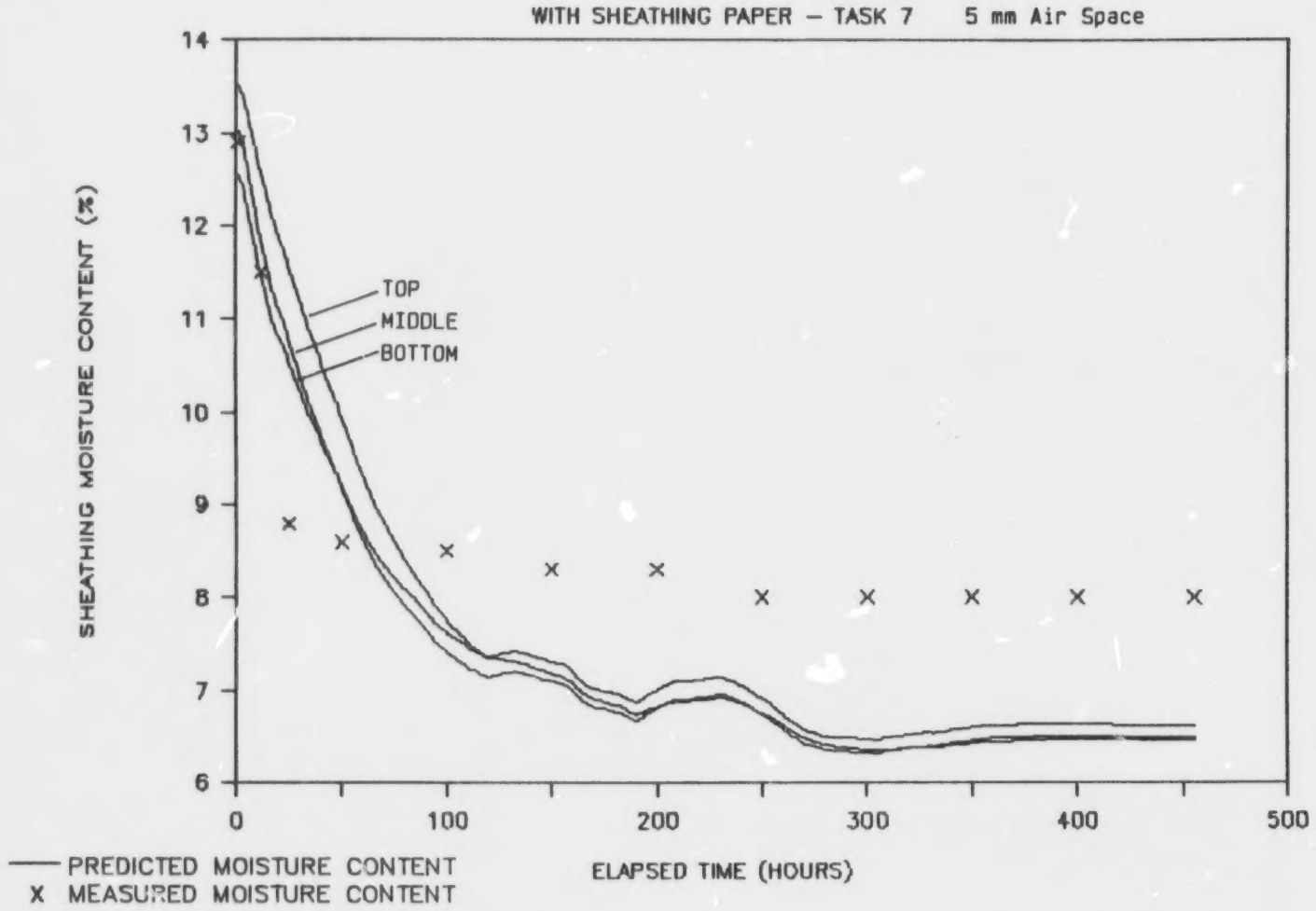

FIGURE 14(a)

RWDI

COMPARISON OF SIMULATION & TEST RESULTS

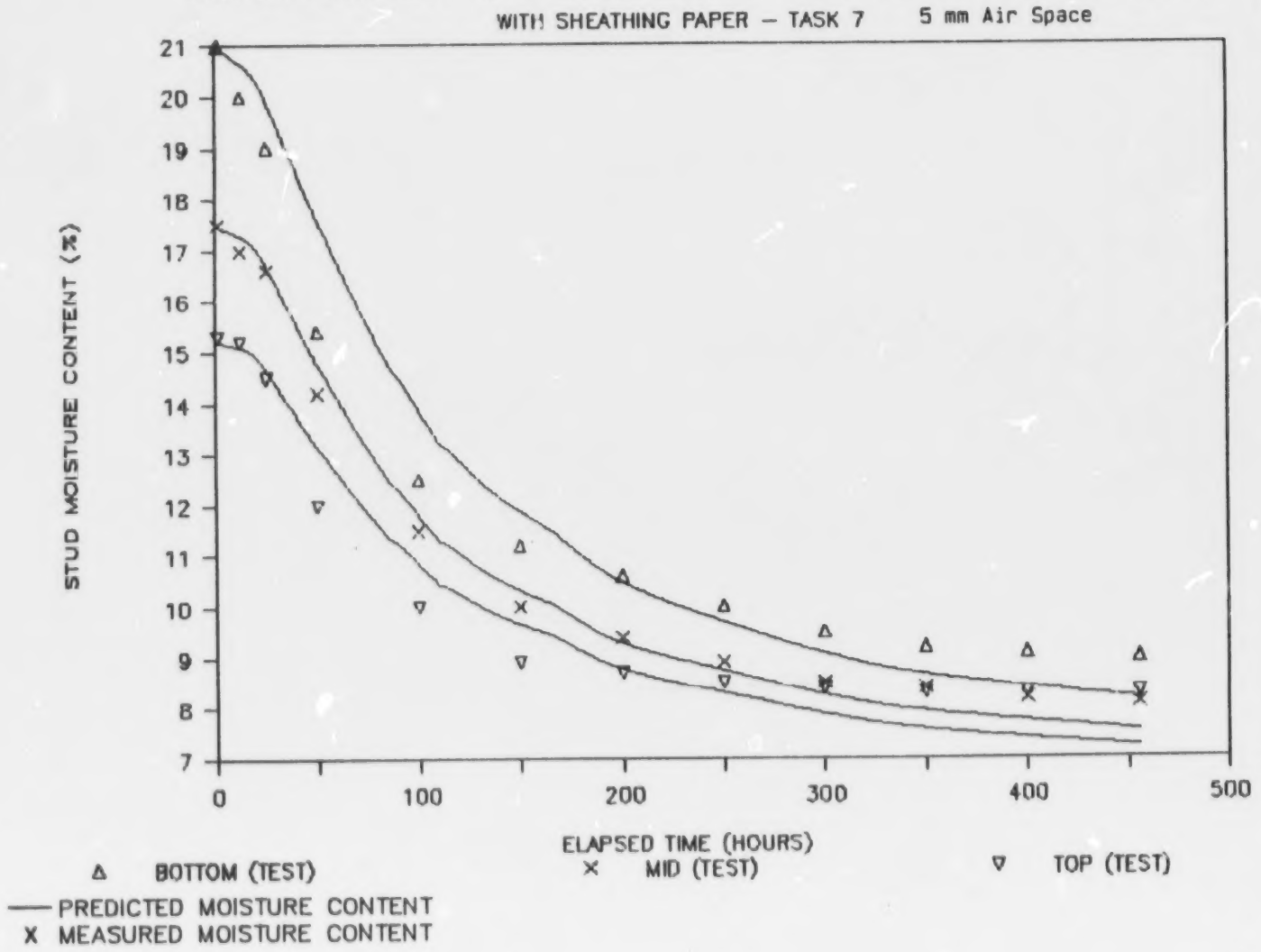

FIGURE 14(b)

RWDI

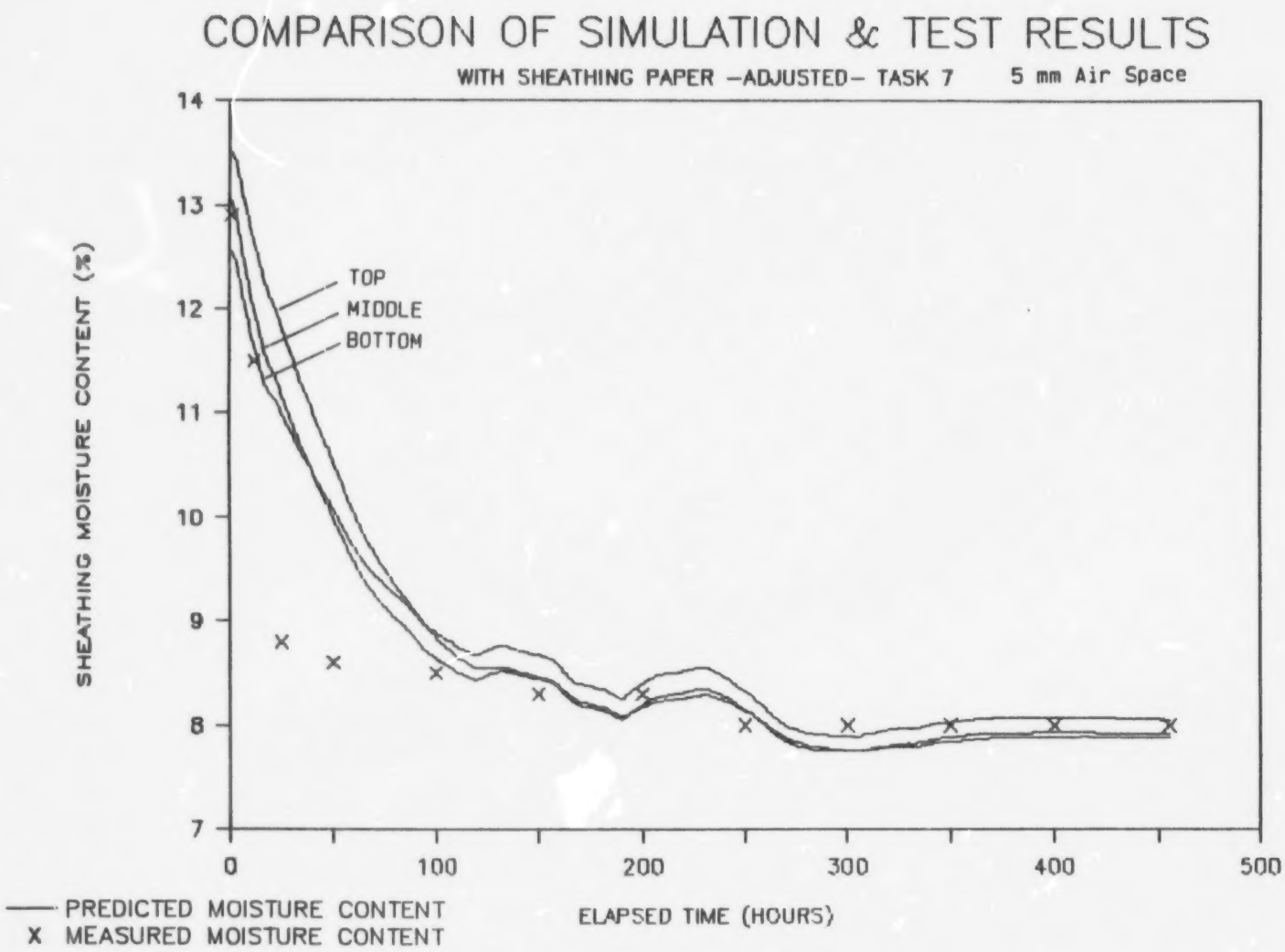

FIGURE 15(a)

RWDI

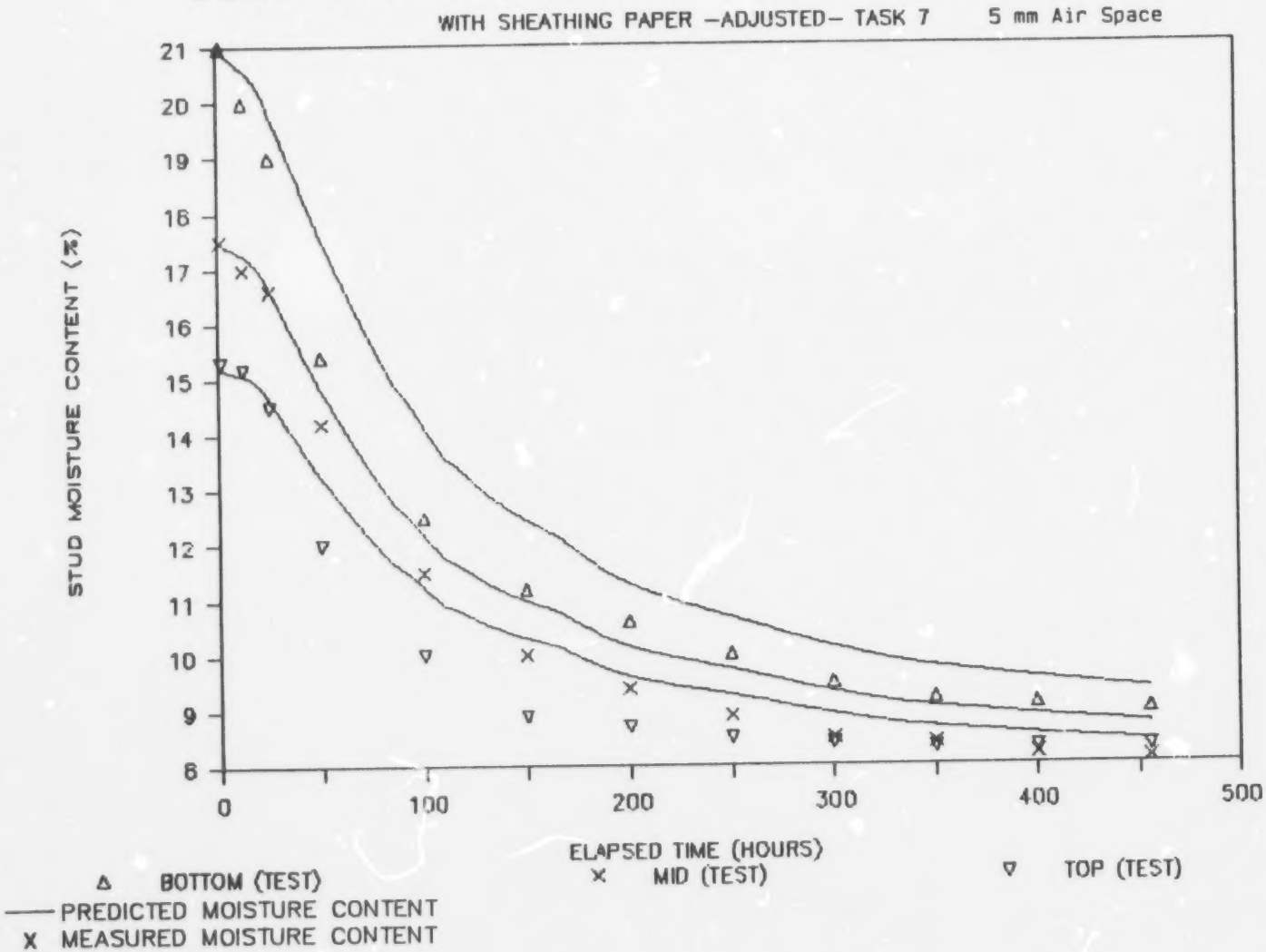

FIGURE 15(b)

RWDI

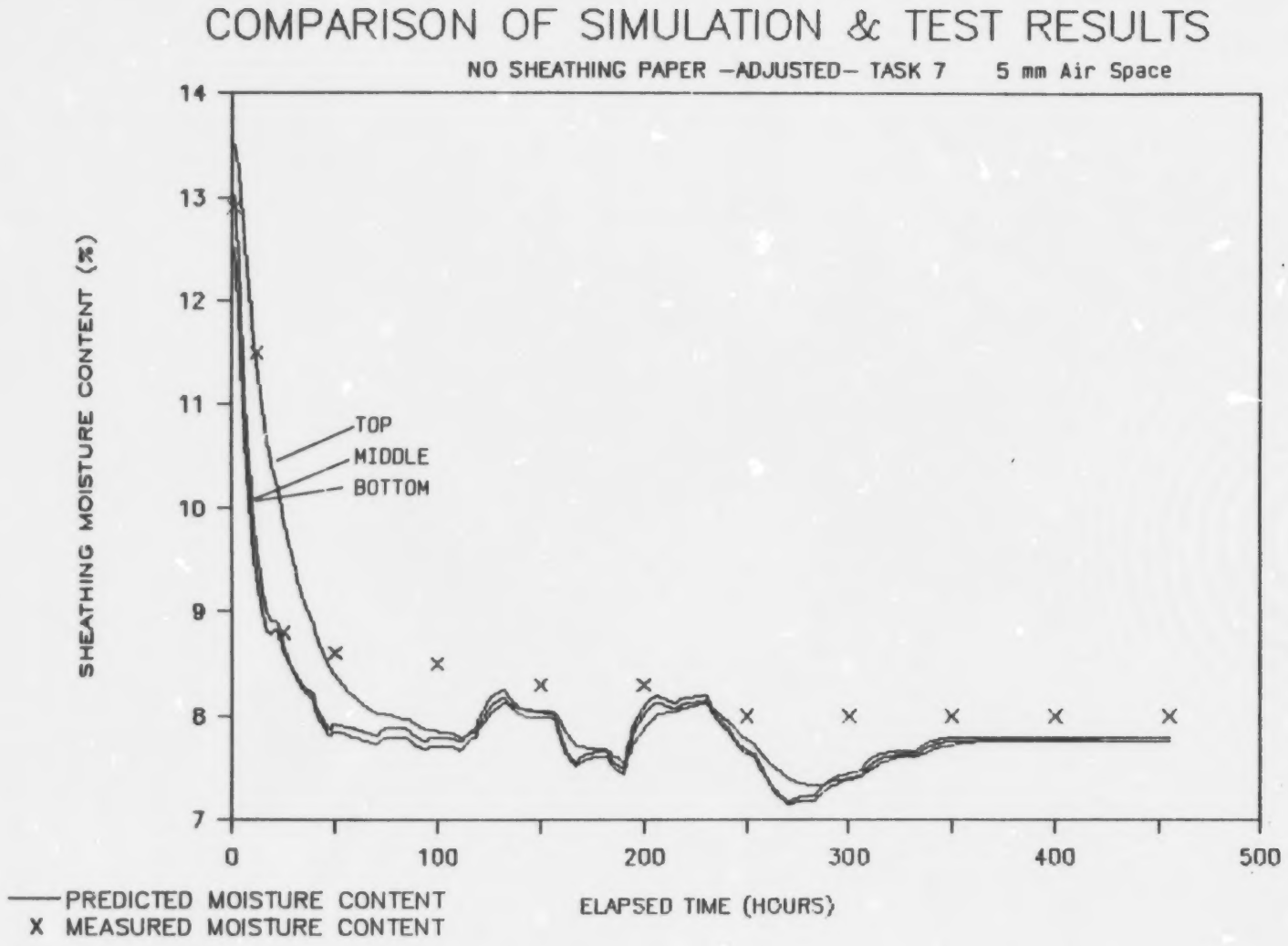
COMPARISON OF SIMULATION & TEST RESULTS
NO SHEATHING PAPER –ADJUSTED– TASK 7 5 mm Air Space
SHEATHING MOISTURE CONTENT (%)
14
13
12
11
10
9
8
7
0
100
200
300
400
500
TOP
MIDDLE
BOTTOM
ELAPSED TIME (HOURS)
PREDICTED MOISTURE CONTENT
X MEASURED MOISTURE CONTENT

FIGURE 16(a)

COMPARISON OF SIMULATION & TEST RESULTS

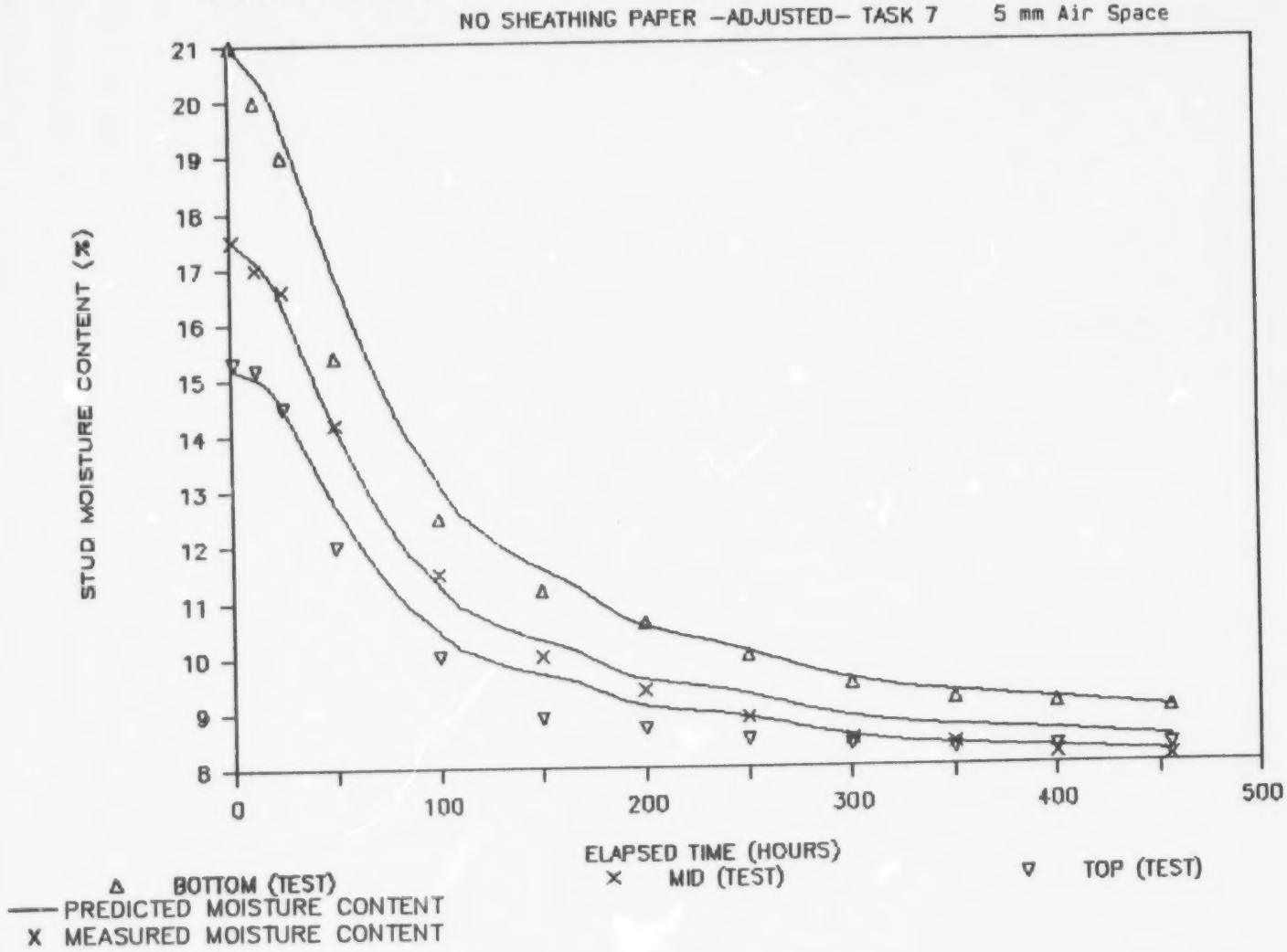

FIGURE 16(b)

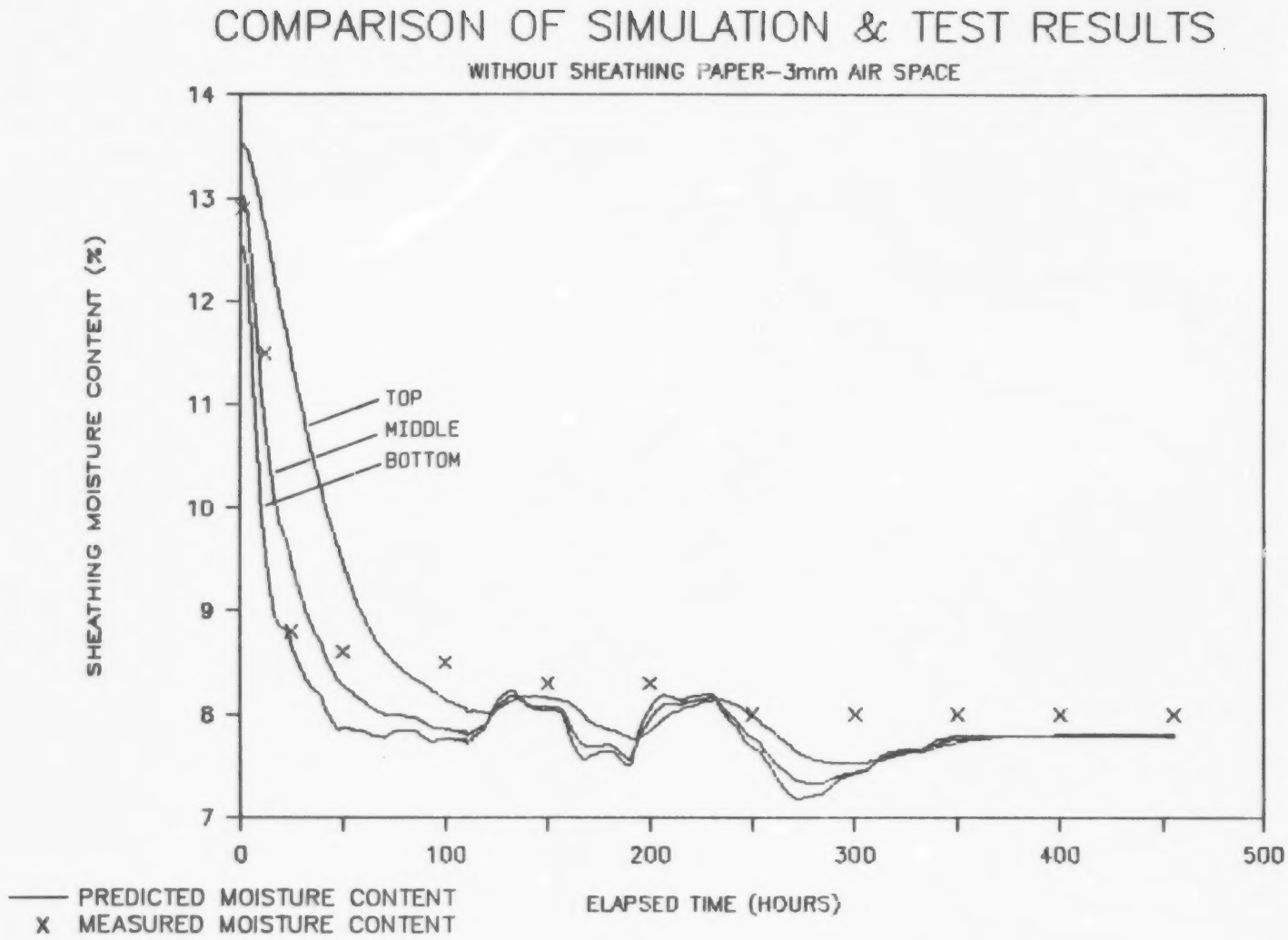
COMPARISON OF SIMULATION & TEST RESULTS
WITHOUT SHEATHING PAPER–3mm AIR SPACE
SHEATHING MOISTURE CONTENT (%)
14
13
12
11
10
9
8
7
0
100
200
300
400
500
TOP
MIDDLE
BOTTOM
PREDICTED MOISTURE CONTENT
MEASURED MOISTURE CONTENT
ELAPSED TIME (HOURS)

FIGURE 17(a)

COMPARISON OF SIMULATION & TEST RESULTS

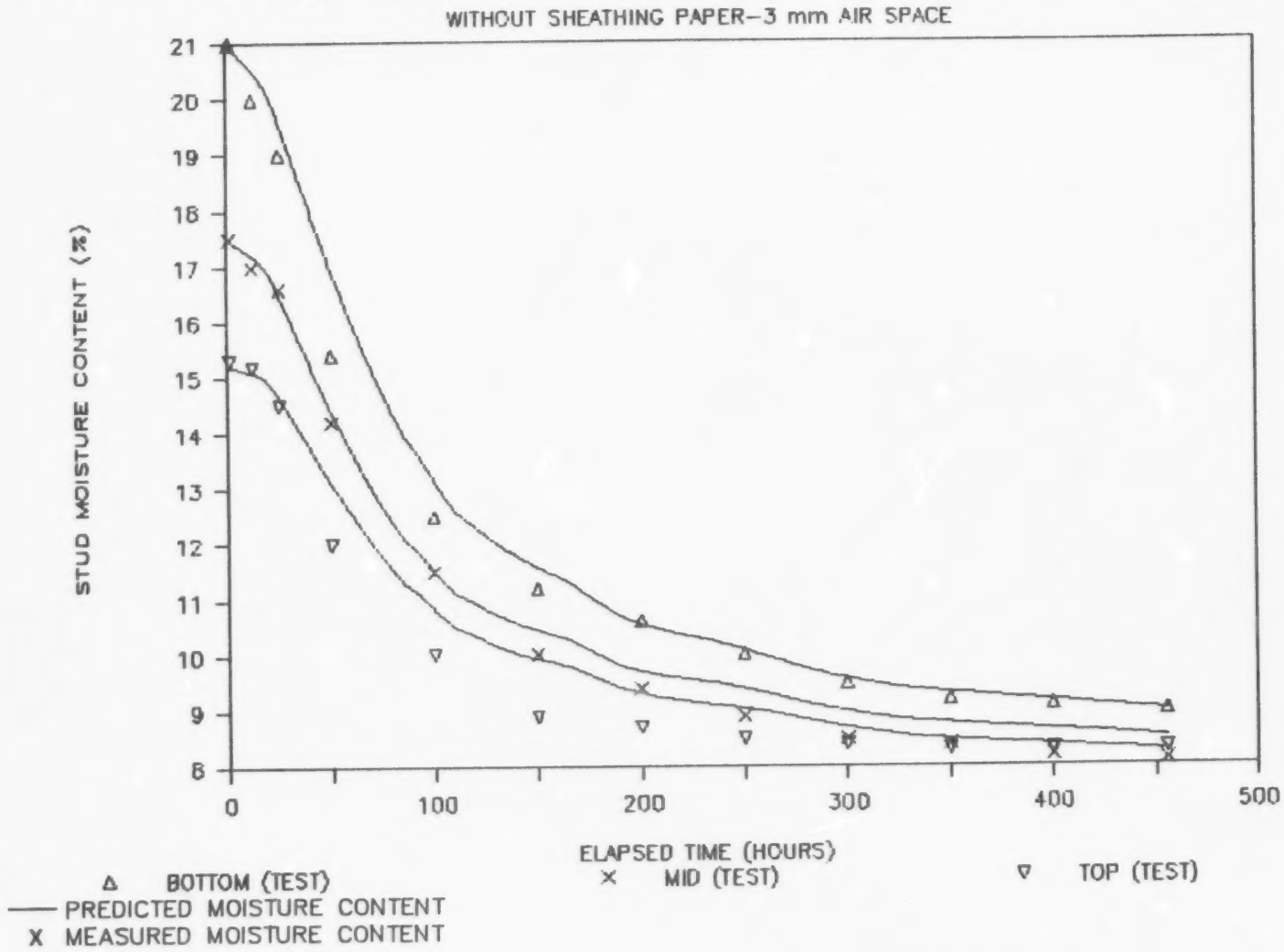

FIGURE 17(b)

RWDI

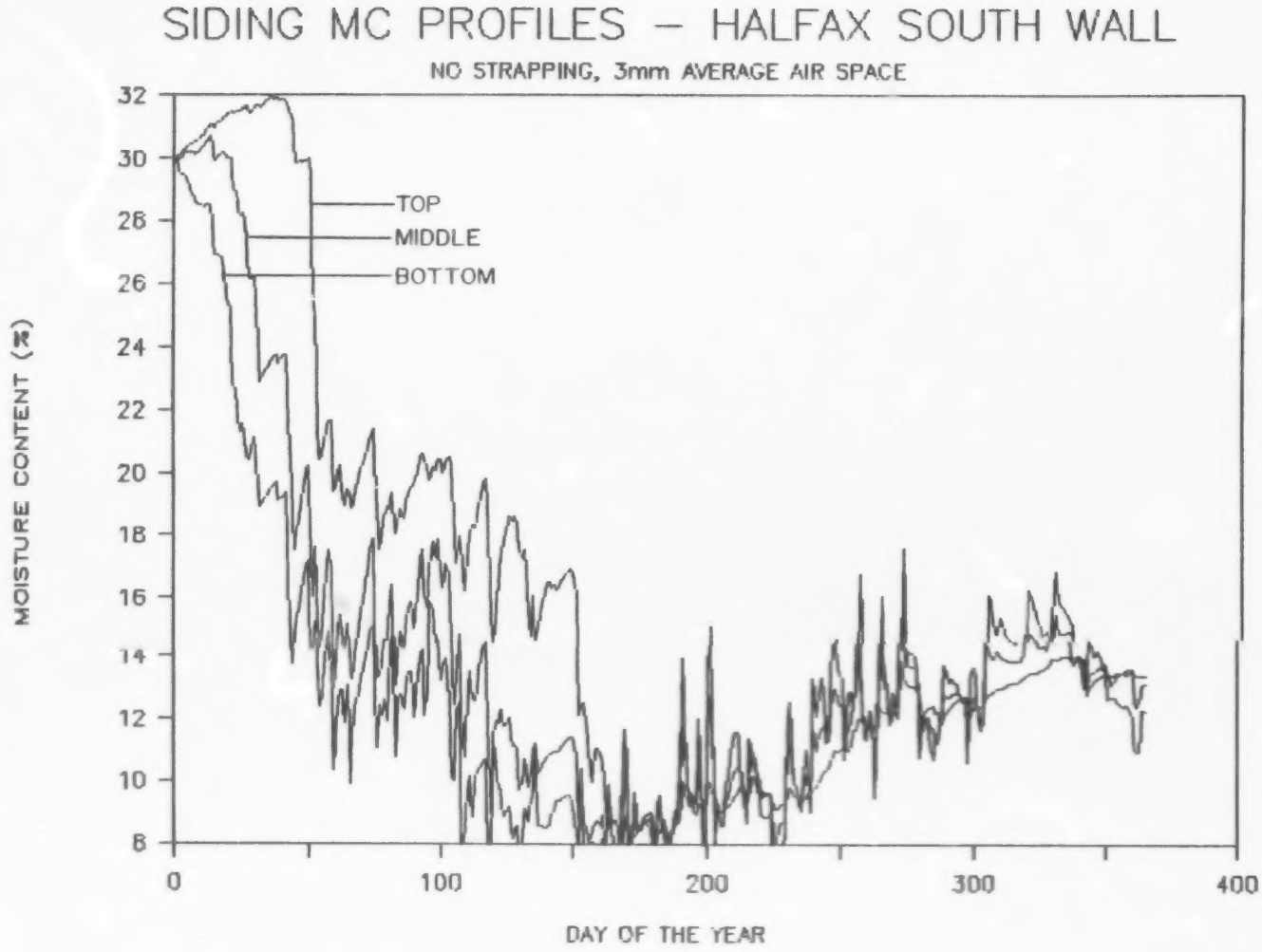
SIDING MC PROFILES – HALFAX SOUTH WALL
NO STRAPPING, 3mm AVERAGE AIR SPACE
MOISTURE CONTENT (%)
32
30
28
26
24
22
20
18
16
14
12
10
8
TOP
MIDDLE
BOTTOM
0
100
200
300
400
DAY OF THE YEAR

FIGURE 18(a)

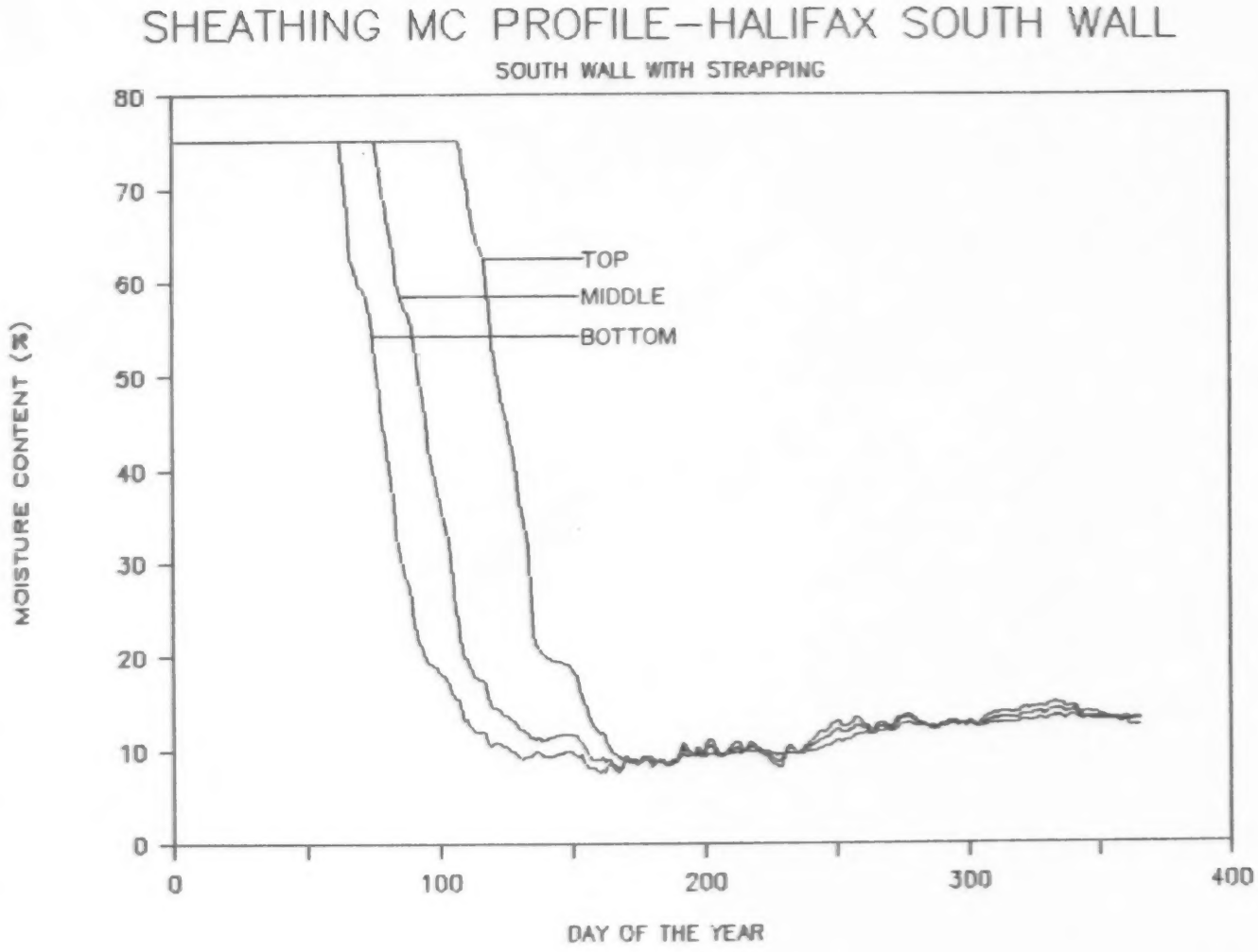

FIGURE 18(b)

RWDI

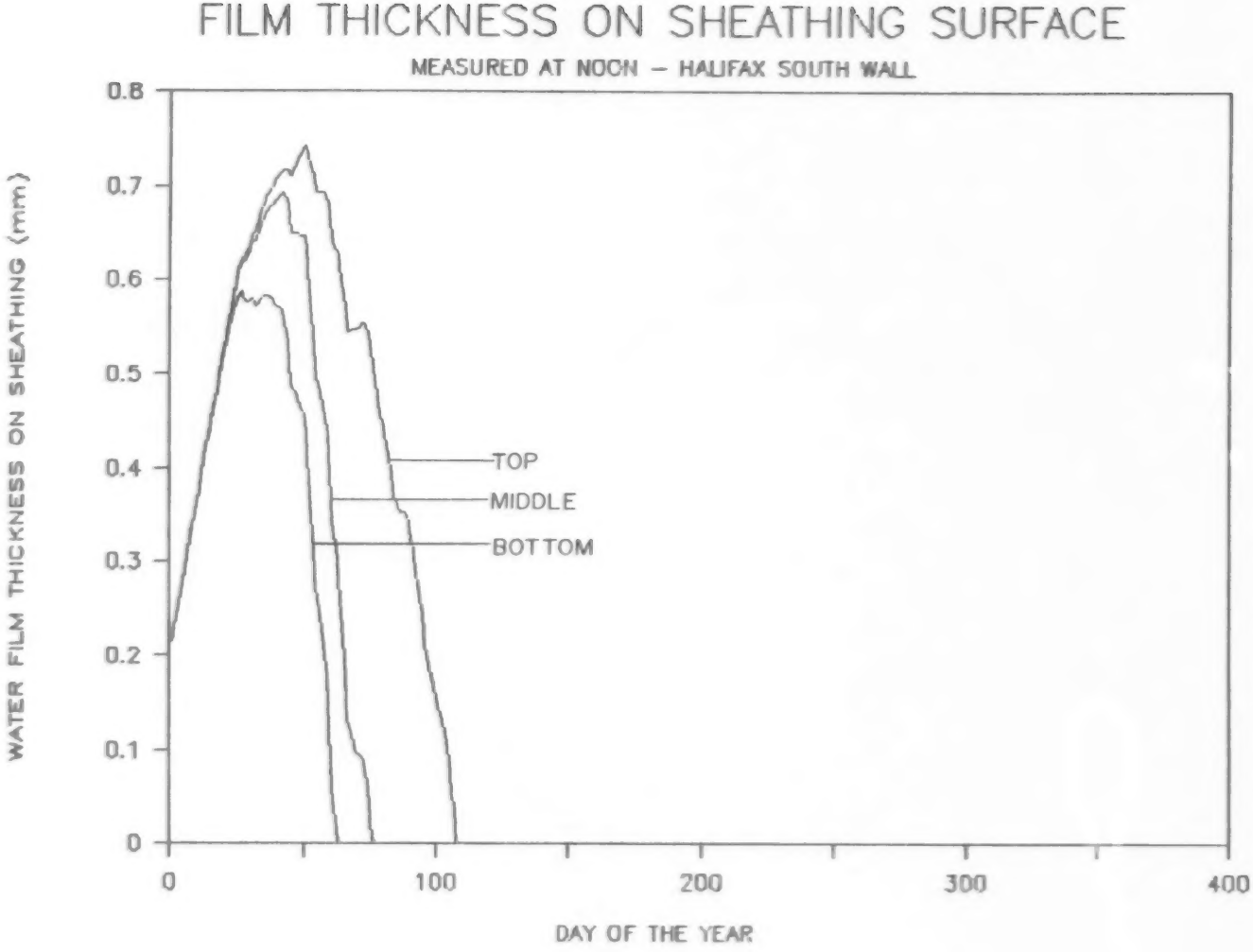
FILM THICKNESS ON SHEATHING SURFACE
MEASURED AT NOON – HALIFAX SOUTH WALL
WATER FILM THICKNESS ON SHEATHING (mm)
0.8
0.7
0.6
0.5
0.4
0.3
0.2
0.1
0
TOP
MIDDLE
BOTTOM
0
100
200
300
400
DAY OF THE YEAR

FIGURE 18(c)

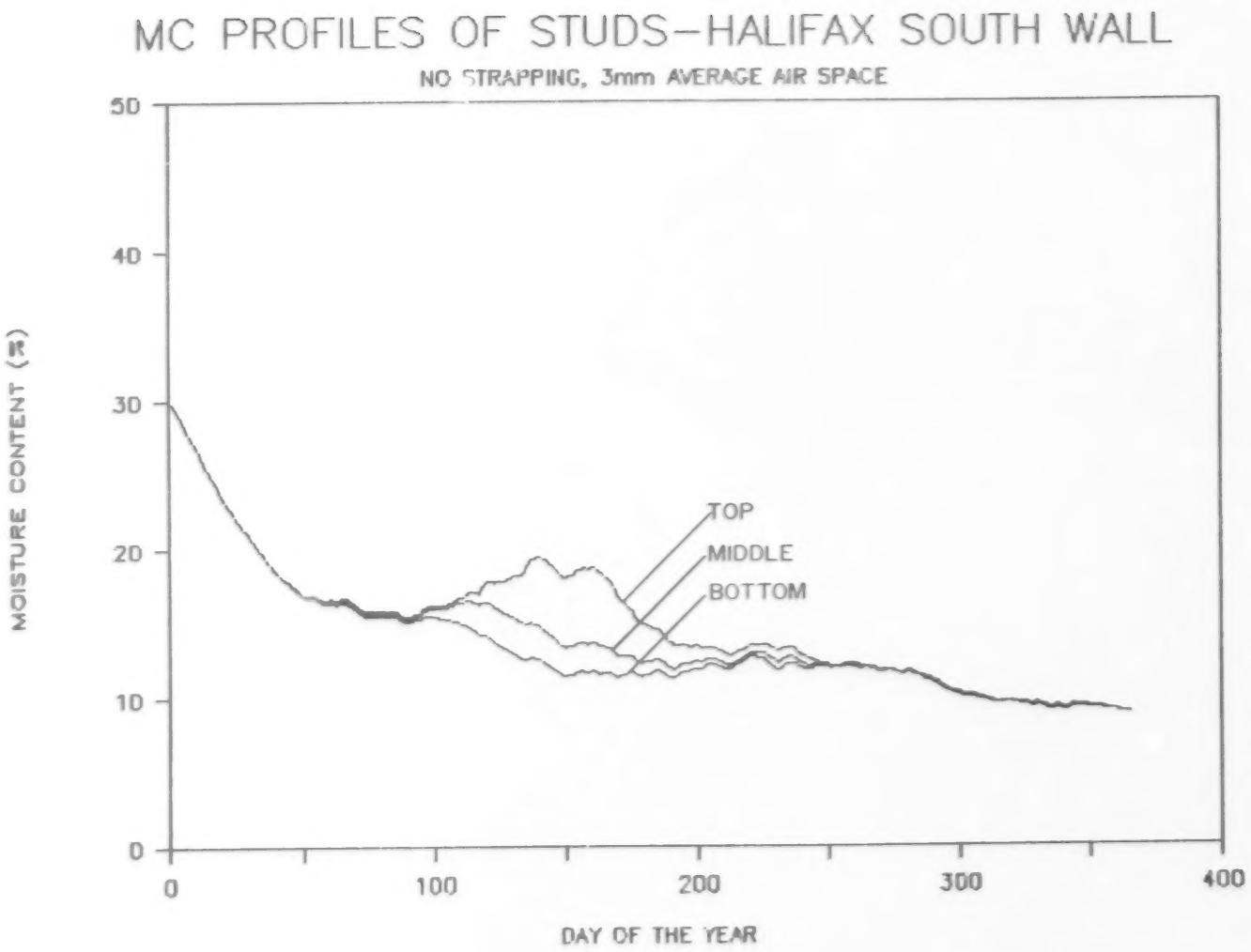

FIGURE 18(d)

RWDI

ORIGINAL SIMULATION vs TEST RESULTS

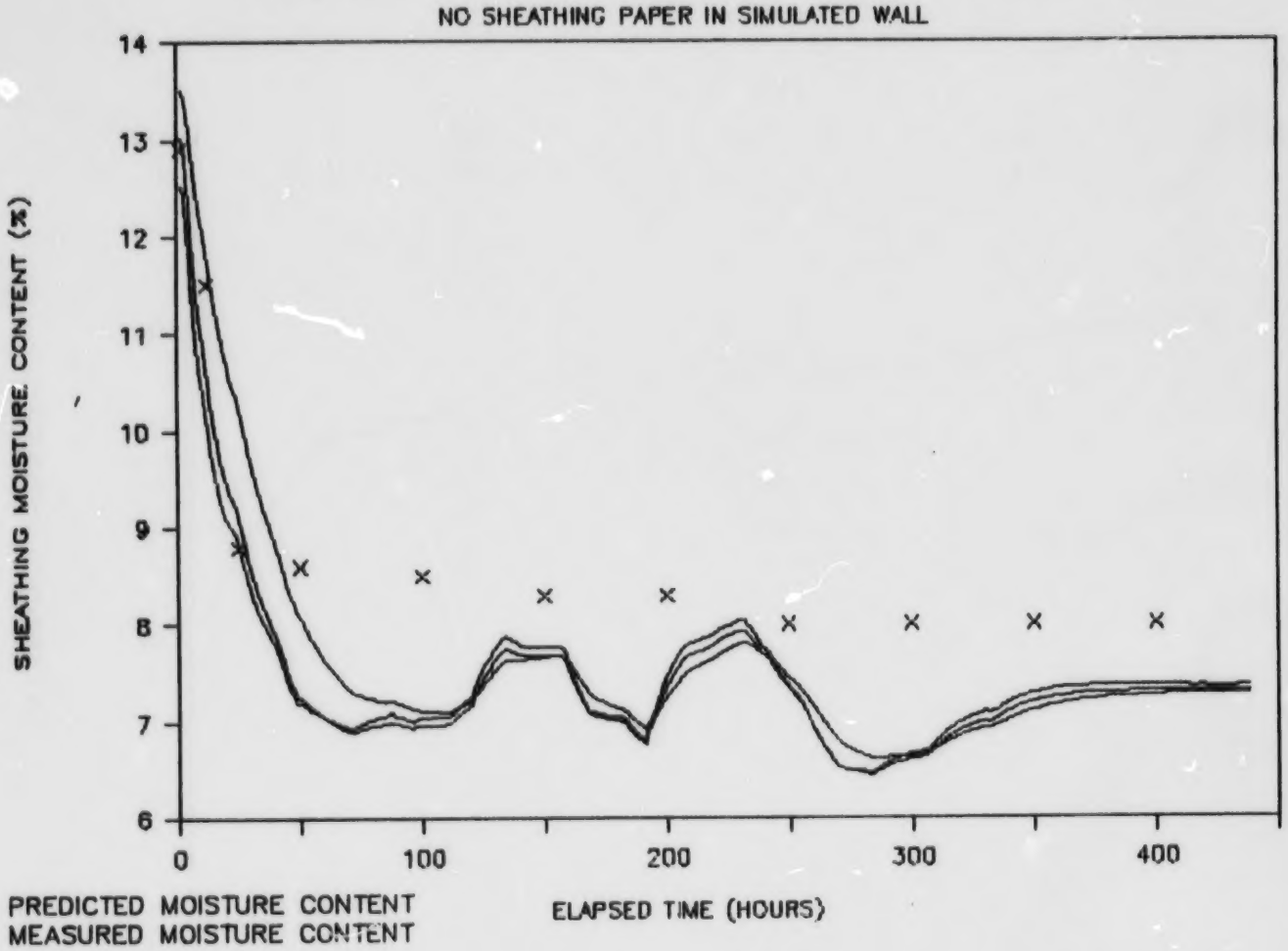

FIGURE 19(a)

RWDI

ORIGINAL SIMULATION vs TEST RESULTS

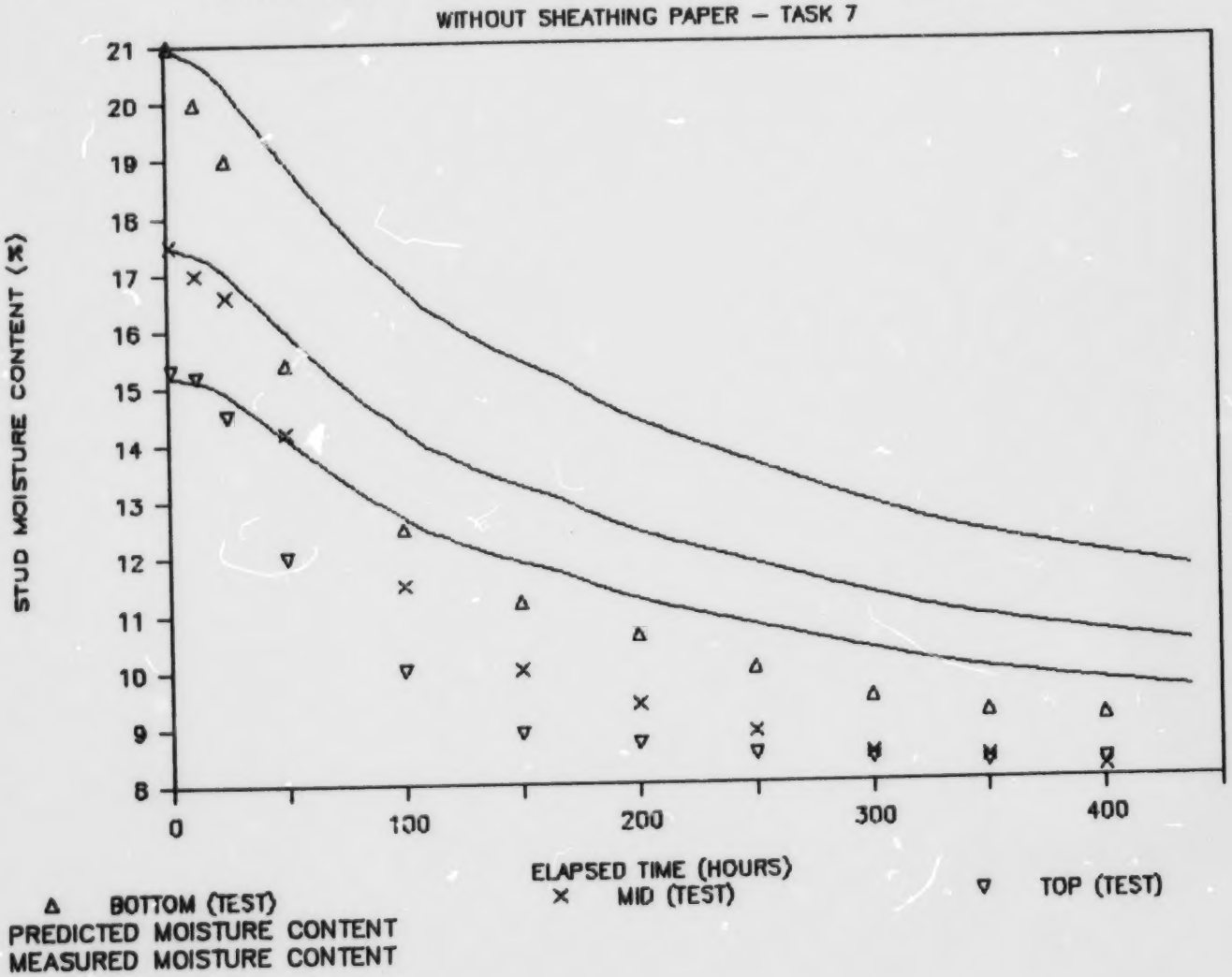

FIGURE 19(b)

RWDI

APPENDICES

APPENDIX A
PROPERTY OF MATERIALS DATABASE

APPENDIX A - PROPERTY OF MATERIALS DATABASE 01-01-1980

RECORD NO. 1

NAME	: OUTDOOR AIR
DENSITY (Kg/m3)	: 1.21
HEAT CAPACITY (W.s)/(Kg.K)	: 1005
THERMAL RESISTIVITY ((m2.C)/W)/m	: 0
DIFFUSION RESISTIVITY ((Pa.m2.s)/Kg)/m	: 5.7E9
GAS CONSTANT (Pa.m3)/(Kg.K)	: 287.055
CLASS (1-AIR/2-WATER/3-WOOD/4-OTHER)	: 1

RECORD NO. 2

NAME	: WATER VAPOUR
DENSITY (Kg/m3)	: .598
HEAT CAPACITY (W.s)/(Kg.K)	: 2050
THERMAL RESISTIVITY ((m2.C)/W)/m	: 18.
DIFFUSION RESISTIVITY ((Pa.m2.s)/Kg)/m	: 0
GAS CONSTANT (Pa.m3)/(Kg.K)	: 461.52
CLASS (1-AIR/2-WATER/3-WOOD/4-OTHER)	: 1

RECORD NO. 3

NAME	: LIQUID WATER
DENSITY (Kg/m3)	: 998
HEAT CAPACITY (W.s)/(Kg.K)	: 4180
THERMAL RESISTIVITY ((m2.C)/W)/m	: 1.66
DIFFUSION RESISTIVITY ((Pa.m2.s)/Kg)/m	: 0
GAS CONSTANT (Pa.m3)/(Kg.K)	: 0
CLASS (1-AIR/2-WATER/3-WOOD/4-OTHER)	: 2

RECORD NO. 4

NAME	: INTERIOR AIR FILM
DENSITY (Kg/m3)	: 1.21
HEAT CAPACITY (W.s)/(Kg.K)	: 1005
THERMAL RESISTIVITY ((m2.C)/W)/m	: 20
DIFFUSION RESISTIVITY ((Pa.m2.s)/Kg)/m	: 5.7E9
GAS CONSTANT (Pa.m3)/(Kg.K)	: 287.055
CLASS (1-AIR/2-WATER/3-WOOD/4-OTHER)	: 1

RECORD NO. 5

NAME	: AIR SPACE
DENSITY (Kg/m3)	: 1.21
HEAT CAPACITY (W.s)/(Kg.K)	: 1005
THERMAL RESISTIVITY ((m2.C)/W)/m	: 5
DIFFUSION RESISTIVITY ((Pa.m2.s)/Kg)/m	: 5.7E9
GAS CONSTANT (Pa.m3)/(Kg.K)	: 287.055
CLASS (1-AIR/2-WATER/3-WOOD/4-OTHER)	: 1

RECORD NO. 11	
NAME	: PARTICLE BOARD
DENSITY (Kg/m3)	: 800
HEAT CAPACITY (W.s)/(Kg.K)	: 1300
THERMAL RESISTIVITY ((m2.C)/W)/m	: 7.4
DIFFUSION RESISTIVITY ((Pa.m2.s)/Kg)/m	: 3900E9
GAS CONSTANT (Pa.m3)/(Kg.K)	: 0
CLASS (1-AIR/2-WATER/3-WOOD/4-OTHER)	: 3
RECORD NO. 12	
NAME	: SEMI-RIGID FIBREGLASS
DENSITY (Kg/m3)	: 100
HEAT CAPACITY (W.s)/(Kg.K)	: 960
THERMAL RESISTIVITY ((m2.C)/W)/m	: 30.5
DIFFUSION RESISTIVITY ((Pa.m2.s)/Kg)/m	: 5.9E9
GAS CONSTANT (Pa.m3)/(Kg.K)	: 0
CLASS (1-AIR/2-WATER/3-WOOD/4-OTHER)	: 1
RECORD NO. 13	
NAME	: FIBERBOARD SIDING
DENSITY (Kg/m3)	: 800
HEAT CAPACITY (W.s)/(Kg.K)	: 1300
THERMAL RESISTIVITY ((m2.C)/W)/m	: 10.7
DIFFUSION RESISTIVITY ((Pa.m2.s)/Kg)/m	: 503E9
GAS CONSTANT (Pa.m3)/(Kg.K)	: 0
CLASS (1-AIR/2-WATER/3-WOOD/4-OTHER)	: 3
RECORD NO. 14	
NAME	: METAL SIDING
DENSITY (Kg/m3)	: 2740
HEAT CAPACITY (W.s)/(Kg.K)	: 896
THERMAL RESISTIVITY ((m2.C)/W)/m	: .004
DIFFUSION RESISTIVITY ((Pa.m2.s)/Kg)/m	: 1E20
GAS CONSTANT (Pa.m3)/(Kg.K)	: 0
CLASS (1-AIR/2-WATER/3-WOOD/4-OTHER)	: 2
RECORD NO. 15	
NAME	: EXTERIOR AIR FILM
DENSITY (Kg/m3)	: 1.21
HEAT CAPACITY (W.s)/(Kg.K)	: 1005
THERMAL RESISTIVITY ((m2.C)/W)/m	: 15
DIFFUSION RESISTIVITY ((Pa.m2.s)/Kg)/m	: 5.7E9
GAS CONSTANT (Pa.m3)/(Kg.K)	: 287.055
CLASS (1-AIR/2-WATER/3-WOOD/4-OTHER)	: 1

RECORD NO. 16

NAME	: WOOD-BASED SIDING
DENSITY (Kg/m3)	: 544
HEAT CAPACITY (W.s)/(Kg.K)	: 1170
THERMAL RESISTIVITY ((m2.C)/W)/m	: 11.9
DIFFUSION RESISTIVITY ((Pa.m2.s)/Kg)/m	: 800E9
GAS CONSTANT (Pa.m3)/(Kg.K)	: 0
CLASS (1-AIR/2-WATER/3-WOOD/4-OTHER)	: 3

RECORD NO. 17

NAME	: GLASS FIBER INSULATION
DENSITY (Kg/m3)	: 25
HEAT CAPACITY (W.s)/(Kg.K)	: 657
THERMAL RESISTIVITY ((m2.C)/W)/m	: 26
DIFFUSION RESISTIVITY ((Pa.m2.s)/Kg)/m	: 5.9E9
GAS CONSTANT (Pa.m3)/(Kg.K)	: 0
CLASS (1-AIR/2-WATER/3-WOOD/4-OTHER)	: 1

RECORD NO. 18

NAME	: WOOD STUD
DENSITY (Kg/m3)	: 430
HEAT CAPACITY (W.s)/(Kg.K)	: 1200
THERMAL RESISTIVITY ((m2.C)/W)/m	: 9.1
DIFFUSION RESISTIVITY ((Pa.m2.s)/Kg)/m	: 800E9
GAS CONSTANT (Pa.m3)/(Kg.K)	: 0
CLASS (1-AIR/2-WATER/3-WOOD/4-OTHER)	: 3

RECORD NO. 19

NAME	: POLYETHYLENE
DENSITY (Kg/m3)	: 0
HEAT CAPACITY (W.s)/(Kg.K)	: 0
THERMAL RESISTIVITY ((m2.C)/W)/m	: 0
DIFFUSION RESISTIVITY ((Pa.m2.s)/Kg)/m	: 2.1E15
GAS CONSTANT (Pa.m3)/(Kg.K)	: 0
CLASS (1-AIR/2-WATER/3-WOOD/4-OTHER)	: 4

RECORD NO. 20

NAME	: PAINTED WOOD SIDING
DENSITY (Kg/m3)	: 544
HEAT CAPACITY (W.s)/(Kg.K)	: 1170
THERMAL RESISTIVITY ((m2.C)/W)/m	: 11.9
DIFFUSION RESISTIVITY ((Pa.m2.s)/Kg)/m	: 3E12
GAS CONSTANT (Pa.m3)/(Kg.K)	: 0
CLASS (1-AIR/2-WATER/3-WOOD/4-OTHER)	: 3

RECORD NO. 21

NAME	: GYPSUM
DENSITY (Kg/m3)	: 1200
HEAT CAPACITY (W.s)/(Kg.K)	: 1080
THERMAL RESISTIVITY ((m2.C)/W)/m	: 2.33
DIFFUSION RESISTIVITY ((Pa.m2.s)/Kg)/m	: 37E9
GAS CONSTANT (Pa.m3)/(Kg.K)	: 0
CLASS (1-AIR/2-WATER/3-WOOD/4-OTHER)	: 4

RECORD NO. 22

NAME	: SHEATHING PAPER (SURFACE LAYER)
DENSITY (Kg/m3)	: 193
HEAT CAPACITY (W.s)/(Kg.K)	: 1200
THERMAL RESISTIVITY ((m2.C)/W)/m	: 10
DIFFUSION RESISTIVITY ((Pa.m2.s)/Kg)/m	: 6.5E11
GAS CONSTANT (Pa.m3)/(Kg.K)	: 0
CLASS (1-AIR/2-WATER/3-WOOD/4-OTHER)	: 4

RECORD NO. 23

NAME	: FIBREBOARD SIDING (SURFACE LAYER)
DENSITY (Kg/m3)	: 800
HEAT CAPACITY (W.s)/(Kg.K)	: 1300
THERMAL RESISTIVITY ((m2.C)/W)/m	: 10.7
DIFFUSION RESISTIVITY ((Pa.m2.s)/Kg)/m	: 18E9
GAS CONSTANT (Pa.m3)/(Kg.K)	: 0
CLASS (1-AIR/2-WATER/3-WOOD/4-OTHER)	: 3

RECORD NO. 24

NAME	: FIBREBOARD SHEATHING (SURFACE)
DENSITY (Kg/m3)	: 352
HEAT CAPACITY (W.s)/(Kg.K)	: 1300
THERMAL RESISTIVITY ((m2.C)/W)/m	: 16.5
DIFFUSION RESISTIVITY ((Pa.m2.s)/Kg)/m	: 6.6E9
GAS CONSTANT (Pa.m3)/(Kg.K)	: 0
CLASS (1-AIR/2-WATER/3-WOOD/4-OTHER)	: 3

APPENDIX B

DRYING CHARACTERISTICS IN WALLS OF LOW RISE RESIDENTIAL HOUSING MILESTONE REPORT NUMBER 2

Report 48714001

March 31, 1987

Submitted to:

CANADA MORTGAGE AND HOUSING CORPORATION

By:

ROWAN WILLIAMS DAVIES & IRWIN Inc.

Carolyn R. Fraser, P.Eng.
Project Enginer

Glenn D. Schuyler, P.Eng.
Principal

1. INTRODUCTION

As described in the statement of work for the present contract which is part 2 of a 2 part research program, Tasks 1 and 2 involve further development of the computer model of the drying mechanisms in the outer portion of a wood frame envelope developed in Part 1 of this research program. Task 1 is the enhancement of wind effects as they affect the subject wall. Task 2 is the creation of an "inner wall" model and its addition to the existing model of the outer wall. These two computer programming tasks have been completed and are described in this report which will serve as contract deliverables for Tasks I and II. Appendices A and B are reports describing the model changes. These reports as well as the programming changes were prepared by Scanada Consultants Limited under contract to RWDI.

2. BACKGROUND

The computer model, as developed prior to this contract, contained several simplifications upon which it was felt necessary to improve in order to increase the flexibility and predictive accuracy of the model. Accordingly the bulk of this work consists of computer programming changes. The wood frame wall section being modelled in the computer program is illustrated in Figure 1.

The computer model consists of a stack of one-dimensional models of heat and moisture flow connected by a one-dimensional airflow model. The basic structure of the computer program, which is illustrated in Figure 2, consists of three sub-models that are solved interactively. The air pressure patterns at the siding outer surface that, along with solar heating, provide the driving forces for air movement in the airspace behind the siding, are produced by wind impinging on the wall. Those patterns vary with wind direction with respect to the plane of the wall. In the original model, this variation was simplified to a simple "on or off" algorithm based on whether or not the wind would impinge on the wall. Task 1 was the extension of this model to be more realistic in its response to wind direction.

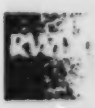

Task 2 consists of expanding the inner portion of the wall, layer 11, (shown on Figure 1) to describe a standard frame wall and to include air leakage.

Task 1 - Enhancement of Wind Model

Air movement in the wall air spaces, specifically between the siding and the sheathing provides one of the major mechanisms for moisture transfer between air and materials. These air flows are due to thermal and wind induced pressures and have the capacity to carry heat and moisture along or up the wall. Therefore, since the wind induced pressures on the wall significantly affect the moisture behaviour in the wall, the accurate modelling of these pressures will affect the accuracy of the wall model. Figure 3 is a representation of the wind model as previously developed. The two zones shown on this figure represent either "wind off" or "wind on". In the case of "wind off" there are uniform pressure coefficients up the wall. For the case of "wind on" one fixed pressure coefficient pattern was used and the pressure at each element in the wall was derived by multiplying those pressure coefficient values by the approaching wind pressure. Hourly weather data is used as input to derive the wind pressures approaching the wall, obtained from available weather data.

The newly developed computer program incorporates two main changes to this model, which improve its flexibility and predictive accuracy. The first is the ability to vary the wind pressure coefficients with wind direction. The second enhancement allows the resistance to air flow at each of the openings in the siding to be made independantly settable. These enhancements provide more accuracy. More importantly, they allow the model to be turned on its side to represent a horizontal slice of wall. This allows investigation of lateral flows behind the siding.

The newly developed wind model is illustrated in Figure 4. This figure shows the variation of the wind pressure coefficient pattern with wind direction in relation to the normal to the wall. Since wind is considered the main driving force for air movement in the airspace behind the siding, and air movement may be the

major drying mechanism in the air space, this new development will provide considerably more accuracy on the simulation.

Making individually settable air flow resistances enables the computer model to be turned on its side so that lateral flow behind the siding can be represented. Figure 5 illustrates the wall model on its side, thus representing lateral flow. For this case, there would be large variations in the pressure patterns with changes in wind direction. These large pressure variations would significantly affect airflow patterns and thus the moisture movement in the wall.

The investigation of lateral air movement, especially at corners, behind the siding, is important in modelling the three-dimensional aspect of the moisture problem. Data obtained from studies in Atlantic Canada, show that leeward walls and corners suffer the worst moisture problems. The aspect of corner moisture problems illustrates the three-dimensional nature of the problem and by the enhancements described above this aspect can now be modelled more accurately.

Task 2 - Development of Inner Wall Model

It was found necessary to extend the program to include an accurate representation of the inner wall moisture movement behaviour by including the interaction between the studs and the adjacent insulated cavities. The inclusion of both studs and insluation in the same model implies two dimensional flow in each of the stack of nine wall elements in the model.

It was considered inadvisable to enlarge each of the nine one-dimensional wall elements into a two-dimensional element because this would cause a great deal of increased complexity and greatly reduced computational speed. In order to avoid this, the stud and insulation were added as three separate layers. Half of the cavity insulation was placed in a layer on one side of the stud layer and half on the other. In this way the model was still one-dimensional in its analysis, but was able to represent a two-dimensional behaviour. The layers of insulation, on either side of the stud layer, were required to have equal vapour pressures and the stud layer

RWDI

was given zero thermal resistance. This eliminated the stud from acting as a series resistance for heat or moisture flow. Instead it acts simply as a moisture storage device and is always at the mean temperature of the cavity. These layers with their special combination of properties, are equivalent to the system shown in Figure 6. The moisture capacity of the insulation and that of the stud must be chosen to reflect their respective volumes within the wall in order for this inner wall model to accurately predict the moisture behaviour within it.

One important mechanism of heat and moisture transport through the wall is air leakage. Previously the computer model included only diffusion from the inner surface to the airspace. In Task 2, air leakage paths have been added. These were added through the use of a set of source/sink pairs that respond to the pressure difference through the wall. These source/sink pairs can be placed to represent a leakage path from any layer in any model element to any other layer or element.

Moisture decay plots were generated with both the enhanced wind model and with the inner wall model in place. Figure 7 shows samples of the moisture decay with time in a stud as well as in the sheathing material and siding. The air leakage paths are not demonstrated in Figure 7.

3. CONCLUSIONS

The tasks described above have enhanced the accuracy and flexibility of the model as well as extended the simulation to the inner portion of the wall. The results show the decay of moisture in the stud as well as in the sheathing. The enhanced wind pressure model increases accuracy, and allows the model to be used for the simulation of a horizontal slice of wall. The air leakage paths will be useful in modelling construction errors in the wall.

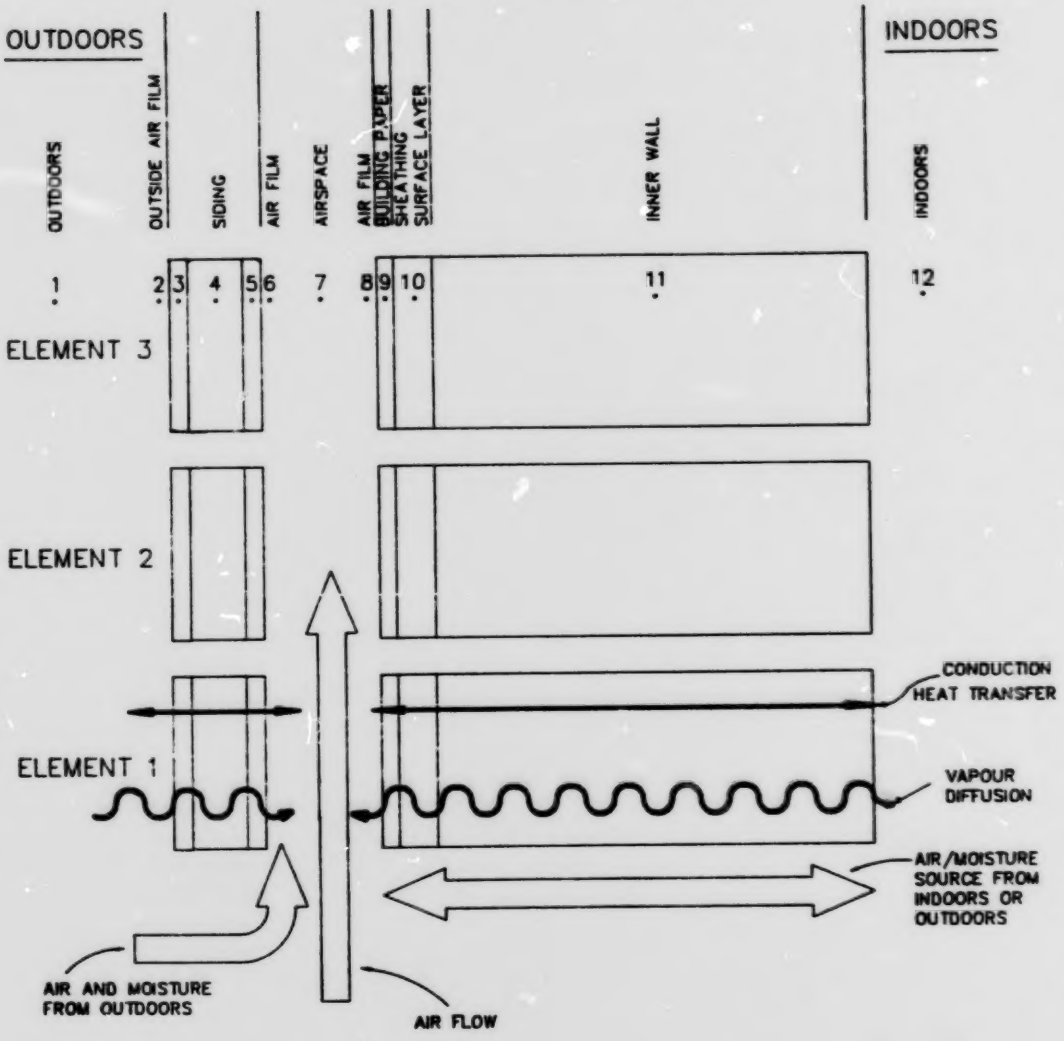

FIGURE 1
MODEL SCHEMATIC

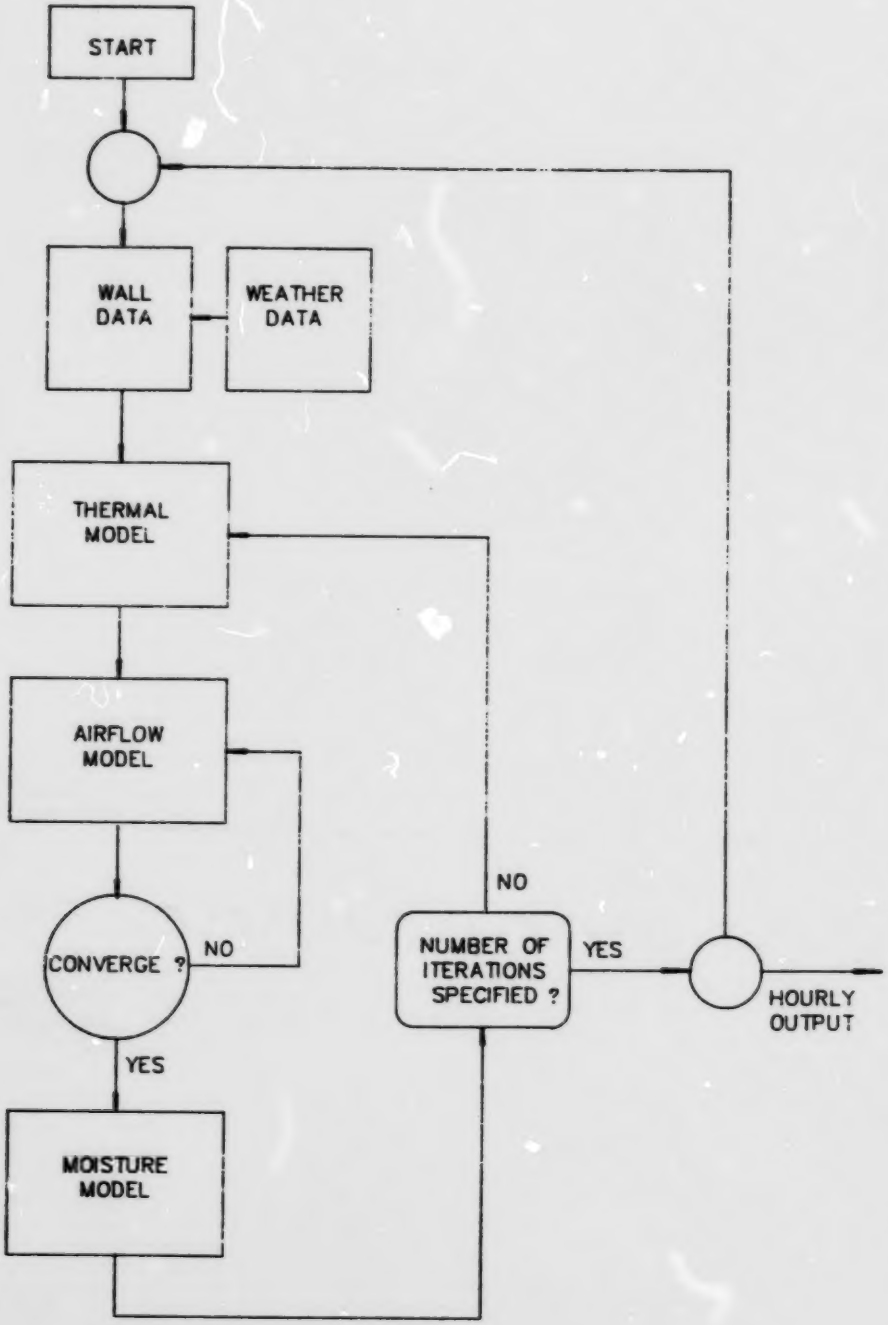

FIGURE 2
MODEL FLOW CHART

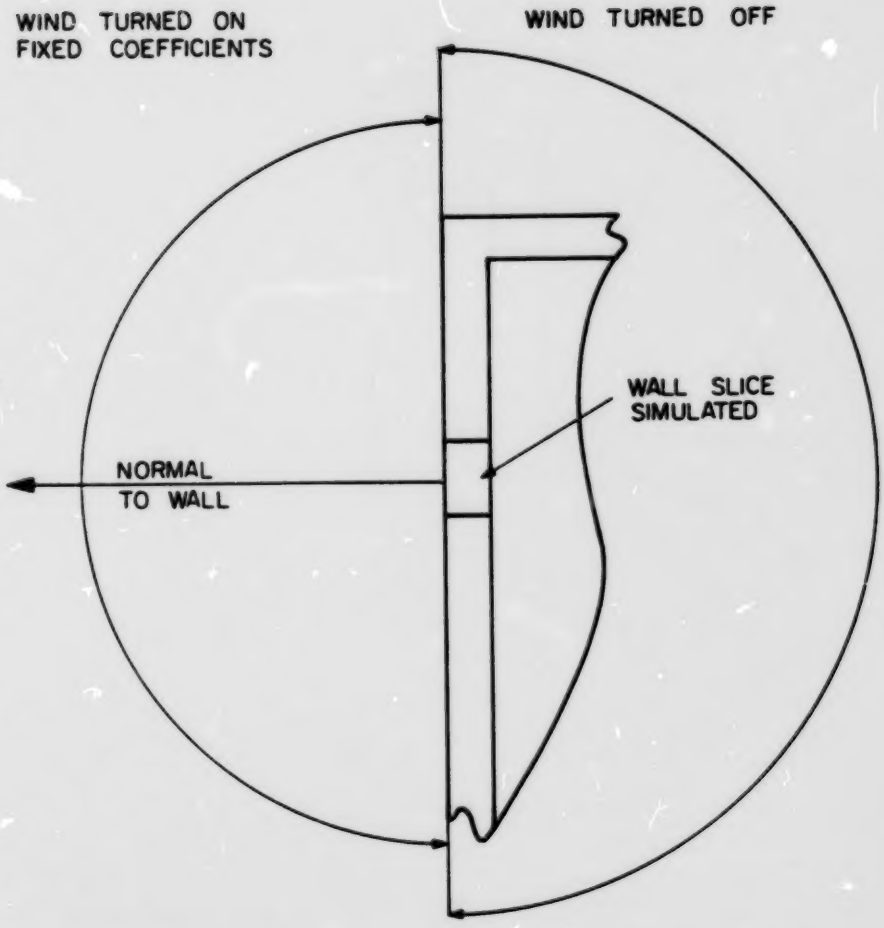

FIGURE 3
OLD WIND MODEL

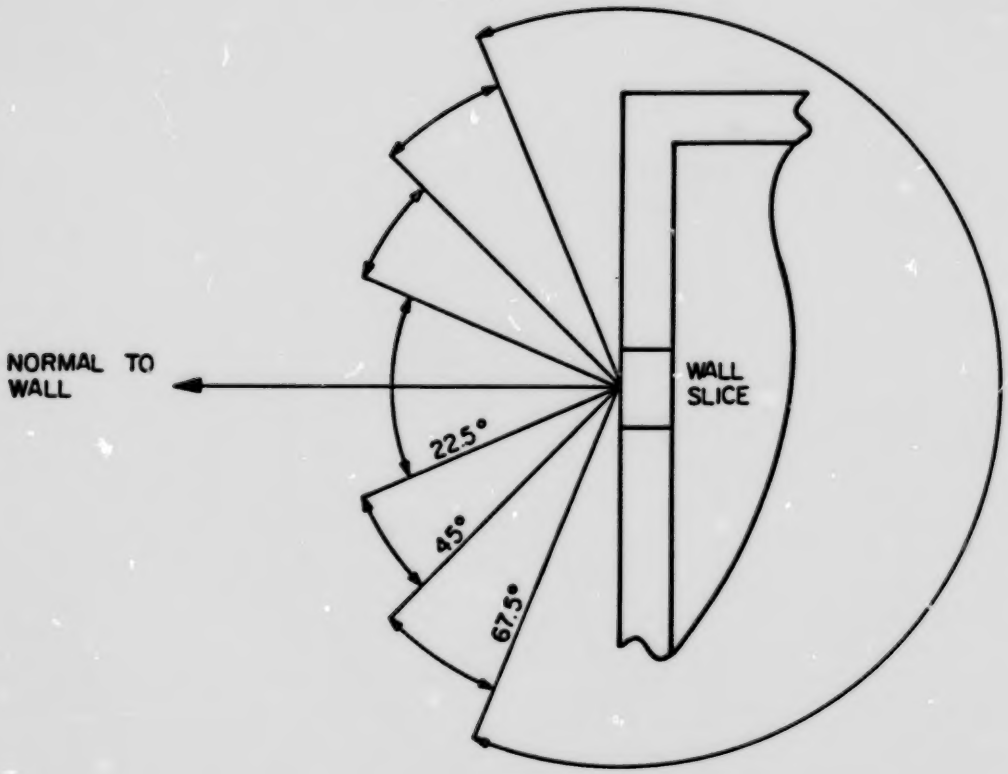

NOTE:

EACH ZONE ABOUT THE NORMAL HAS AN INDIVIDUAL COEFFICIENT PATTERN

FIGURE 4
NEW WIND MODEL

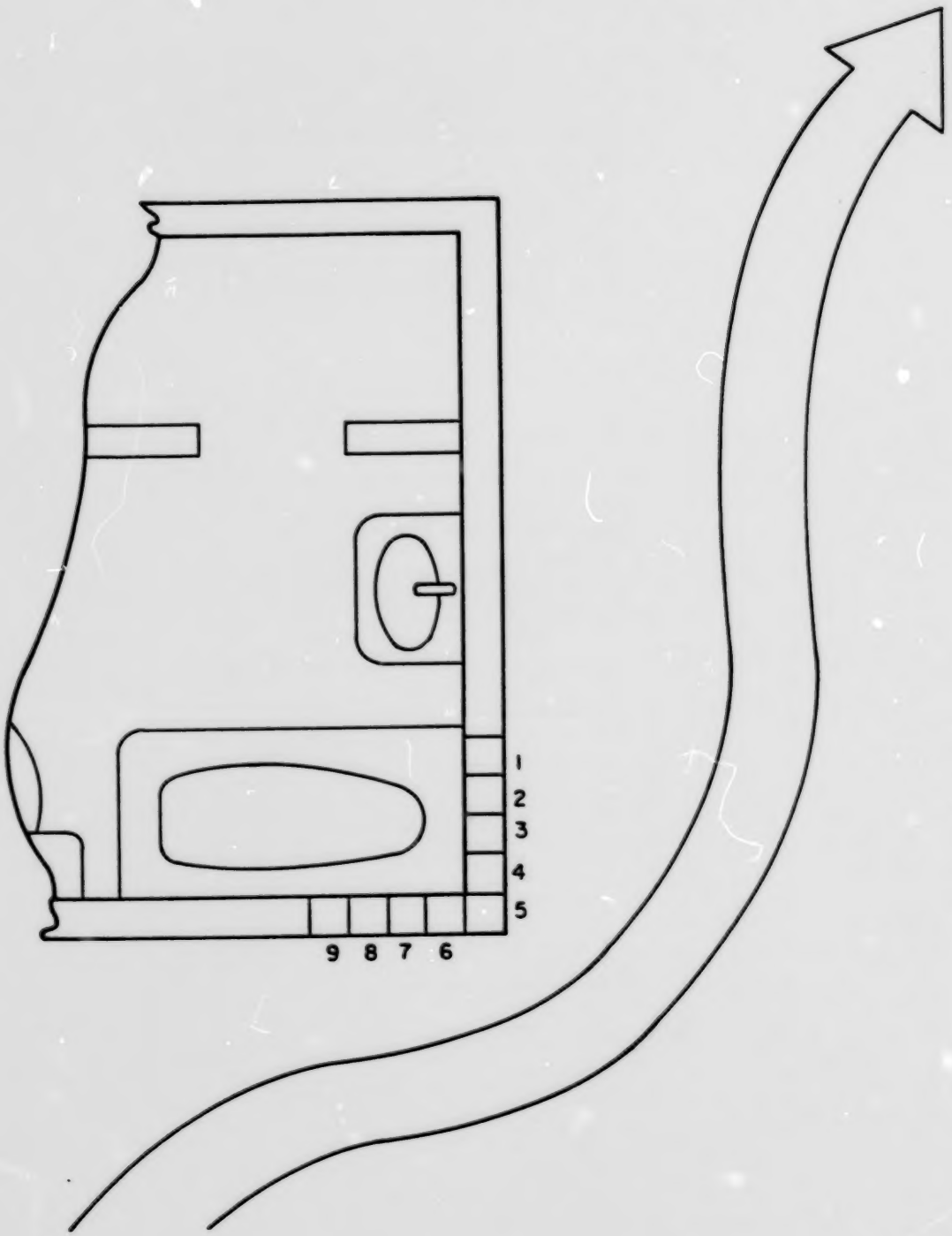

FIGURE 5
MODEL TURNED SIDEWAYS

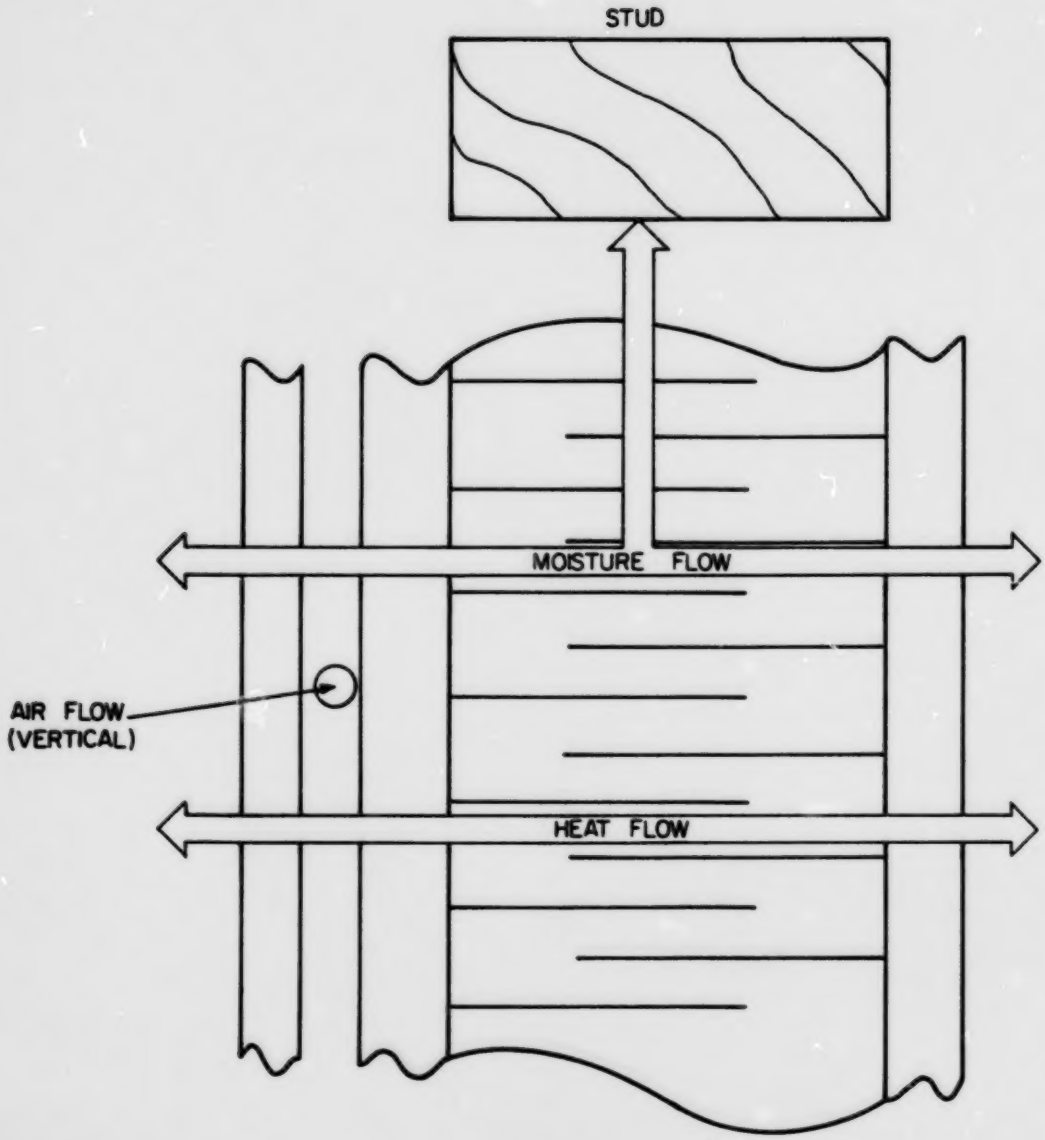

FIGURE 6
EQUIVALENT INNER WALL MODEL

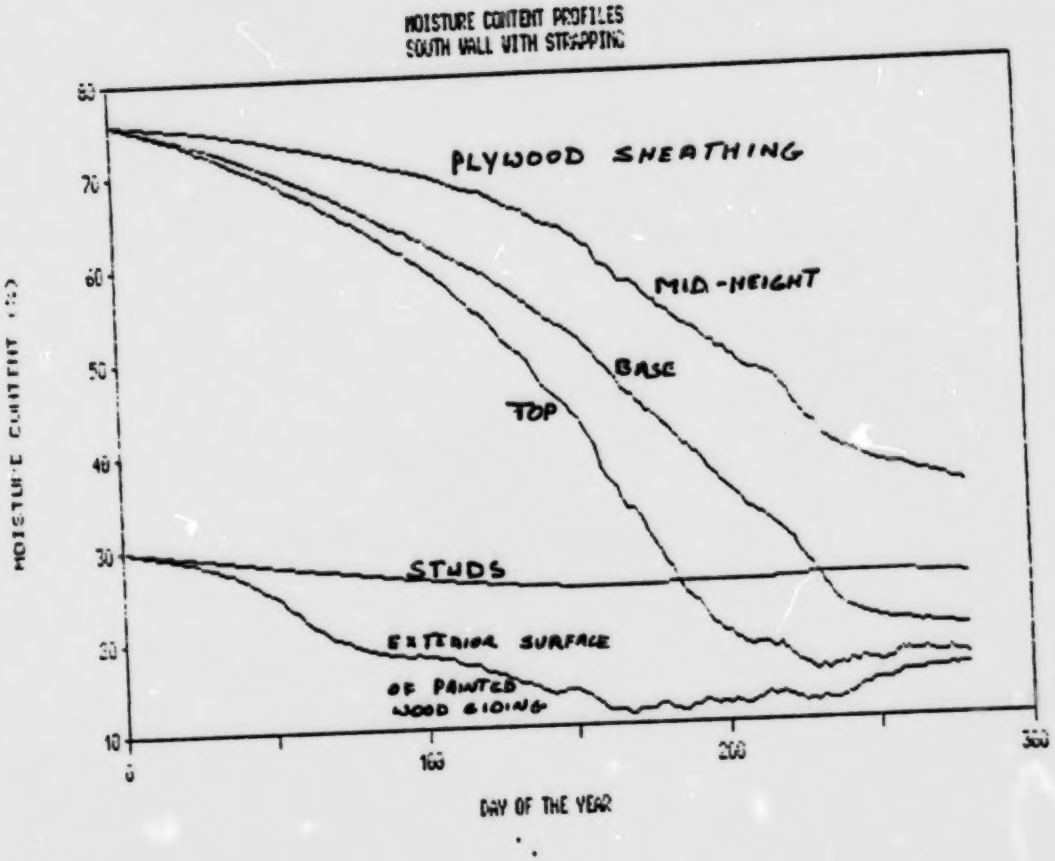

FIGURE 7

MOISTURE CONTENT TIME HISTORIES
GENERATED BY ENHANCED COMPUTER MODEL

APPENDIX A

SUBCONSULTANT REPORT
TASK 1

Scanada
Consultants
Limited

436 MacLaren Street
Ottawa, Ontario
K2P 0M8

Tel: (613) 236-7179
Envoy ID. Scanada.Ott

January 16, 1987

Mr. Glen D. Schuyler, P. Eng.
R.W.D.I.
650 Woodlawn Road West
Guelph, Ontario
N1K 1B8

Dear Glen:

Re: Progress Report #1: Drying Wall Model Refinement

We have recently completed the modifications to the Drying Wall program that have to do with the improvements to the Air Flow Model. We have modified:

- the input data file
- the input routine in the program, and
- the algorithms

to handle the following modifications:

- Four sets of wind pressure coefficients can be specified. These act on the wall for a range of wind directions specified by the user. For now we have specified the following ranges:

  ± 22½° from the direction normal to the wall
  ± 45° from the direction normal to the wall
  ± 67½° from the direction normal to the wall
  all other directions.

- The characteristics of all 10 gaps or openings in the siding can now be specified by the user. This will permit investigation of corner effects in horizontal flows.

- Any set of friction factors can be specified for different outer wall configurations:

  - strapped and unstrapped
  - vertical and horizontal flow.

A copy of the new input file is attached for your interest.

The above changes have been successfully integrated into the program. This completes Task #1 of our agreement dated October 27, 1986.

Yours truly,

SCANADA CONSULTANTS LIMITED

Michael C. Swinton, P. Eng.

MCS/wl
Encls.

```
TITLE:
HALIFAX SOUTH WALL - NO STRAPPING:  PAINTED EXTERIOR SURFACE OF THE SIDING
-------------------------------------------------------------

NUMBER OF ELEMENTS UP THE WALL (NV) AND LAYERS THROUGH THE WALL (NE)
9,20

SELECTION OF MATERIALS FOR EACH LAYER  (SEE PROPERTIES DATABASE FOR #)
1,15,20,16,16,4,5,4,6,6,7,7,7,17,17,17,19,21,4,9

THICKNESS OF EACH LAYER (in m)
1,0.002,0.005,0.005,0.005,0.002,0.003,0.002,0.00025,0.00025,0.003,0.003,0.003,0.030,0.030,0.030,0.0001,0.0095,0.002,1

SELECTION OF MATERIALS FOR THE STUD LAYERS (SEE PROPERTIES DATA BASE FOR #)
18,18

LATERAL THICKNESS OF STUD LAYERS
0.019,0.019

WALL HEIGHT (m), WALL LENGTH (m)
6,9

Siding Gap Characteristics: WIDTH(m)  ¦ bottom to top (9 elements + opening)
0.001,0.001,0.001,0.001,0.001,0.001,0.001,0.001,0.001,0.001

Siding Gap Characteristics: FLOW PATH LENGTH(m) ¦ bottom to top (9 + opening)
0.01,0.01,0.01,0.01,0.01,0.01,0.01,0.01,0.01,0.01

Siding Gap Characteristics: FLOW EXPONENT ¦ bottom to top (9 elements + opening)
0.9,0.9,0.9,0.9,0.9,0.9,0.9,0.9,0.9,0.9

AIR SPACE CHARACTERISTICS: NUMBER OF THE LAYER, FLOW EXPONENT
7,0.8

(+/- 22.5) WIND PRESSURE COEFFICIENTS ¦ bottom to top (9 elements + opening)
22.5,  0.1,0.2,0.3,0.4,0.5,0.5,0.4,0.3,0.2,0.1

(+/- 45)  WIND PRESSURE COEFFICIENTS ¦ bottom to top (9 elements + opening)
45.0,  0.05,0.1,0.15,0.2,0.25,0.25,0.2,0.15,0.1,0.05

(+/- 67.5) WIND PRESSURE COEFFICIENTS ¦ bottom to top (9 elements + opening)
67.5,  0.025,0.05,0.075,0.1,0.125,0.125,0.1,0.075,0.05,0.025

(OTHER DIRECTIONS) WIND PRESSURE COEFF¦ bottom to top (9 elements + opening)
180.,  0.0,0.0,0.0,0.0,0.0,0.0,0.0,0.0,0.0,0.0

WALL ORIENTATION (DEGREES FROM NORTH): N:360, E:90, S:180, W:270
180

MOISTURE SOURCE STRENGTH IN kg/hr, & LOCATION: LAYER # & ELEMENT NUMBER
0.,10,6

SIMULATION START AND END (DAY OF THE YEAR)
1,365

NUMBER OF ITERATIONS BETWEEN THE 3 MAJOR SUB MODELS
3

NUMBER OF LAYERS DISPLAYED IN SCREEN (MAX 12); SPECIFY LAYER NUMBERS
12, 1,2,3,5,6,7,9,10,11,13,15,20

NAME OF THE WEATHER DATA FILE  (INCLUDE THE DRIVE SPEC:  e.g.  A:DWEATH.SOU)
D:HAL.SOU
```

APPENDIX B

SUBCONSULTANT REPORT
TASK 2

Scanada
Consultants
Limited

436 MacLaren Street
Ottawa, Ontario
K2P 0M8

Tel: (613) 236-7179
Envoy ID: Scanada Ott

March 30, 1987

Mr. Glen D. Schuyler, P. Eng.
R.W.D.I.
650 Woodlawn Road West
Guelph, Ontario
N1K 1B8

Dear Glen:

Re: Progress Report #2: Drying Wall Model Refinement

We have now completed the modifications to the following modules of the drying wall program:

- the air flow model (reported to you in a letter of January 16, 1987),
- the inside wall model,
- the interior air leakage module and
- the surface condensation and drainage module.

As evidence of our work, we have run the model through a nine month simulation period starting on January 1 and ending on September 30 for a typical year of Halifax weather data. Reproduced as an addendum to this letter are the input data file that was used in this run and various model outputs that highlight many of the changes that we have performed. The highlights of the results are described briefly below.

Changes to the Input Data File

The input data file indicates to what extent the user is now able to change or influence the data used in the program that pertains to the various modifications listed above. In the new input data file the second data entry is the number of layers through the wall, which is now quoted at 20. The number of layers through the wall used to be 12; therefore, the model now accounts for 8 additional layers starting from the sheathing inside face, inward through the insulation, gypsum and interior of the house. The selection of those materials from the material properties data base is specified as before. The thickness of those additional materials is also specified as before.

The next set of entries indicate the selection of materials for the stud layers. We have accounted for 2 stud layers in the model that are acting in parallel to the insulation layers. Incidentally, the properties for the stud layers are stored in elements #21 and #22 of the model. The lateral thickness of the stud layers is specified and the location of those studs relative to the chosen insulation layer in the selection of materials list. In this case, the insulation layer next to the studs is layer #15.

The next new entry into the data base is the specification of the location for the inward air leak in the wall assembly. Specified is the vertical element number where the leak is located, the indoor wind pressure coefficient (i.e. the wind pressure coefficient that affects the air pressure inside the house) and the height of the neutral pressure plane of the wall. These inputs are used in the model to calculate the leakage flow into or out of the house from the air space. The model accounts for conservation of mass of the air, for the effect of this leak on the moisture balance of the air space behind the siding.

The next addition to the data base is the specification of the surface moisture content threshold and the film thickness threshold. These are quantities required to determine when the moisture that is condensing on the face remains on the face as a surface film. The film thickness threshold determines how much moisture can adhere to the face of the wall before drainage occurs. When drainage occurs the excess water in the film gets drained down to the element just below the element in question.

A final change in the data base is the specification of the layers to be displayed on the screen. This allows the model user to look at an hourly result of the progress of 12 of the 22 elements that now form the wall in question.

Sample Outputs of an Example Simulation

The attached output sheets give an indication of how the model has changed since the beginning of this project. The first output shows a list of the layers that now form the wall. There are 20 layers listed along with their thicknesses. Opposite layer #15, which is the glass fibre layer, are the 2 wood stud layers #21 and #22, shown in the example.

The next sample output was a status sheet printed out for October 1 after a full nine months of simulation of the drying capability of the wall. The wood-based layers are shown (i.e. elements 3, 5, 11, 12 and 21 - refer to the list of layers to identify these). These wood layers started off at 30% moisture content in January. The sheathing layer, #11, started at about 80% due to the trapped water behind the sheathing paper. The 2 siding elements have dried off - elements 3 and 5. The exterior and middle layers of

the sheathing have dried, but not completely. The top part of the exterior face of the sheathing is now dry but the middle to lower portion have a considerable way to go before reaching a "dry" condition. Similarly, the top and bottom portions of the middle layer of the sheathing have showed some drying whereas the middle to lower portion has not moved since January. The stud layer 21 has dried rather uniformly by between 4 and 4.5 moisture content percentage points.

The next three printouts illustrate the effect of the new interior leakage module. If we start from the outside layer, #1, and move inward we can see the effect of wind velocity starting from the outside and the effective wind velocity acting at the surface shown in column 2. This is for a south wind - wind direction is 180°. The leakage velocities through the gaps in the siding are shown in column 6. Column 7 shows the air flow rate in the air space behind the siding. This is a strapped air space. The velocities in the upper portion of the wall are upward with air going out the opening at the top of the air space. The velocities in the lower portion of the wall are downward and leaking into the house, the speed through that leak into the house is shown in column 9 in this example. The next example is similar to the first one but here the wind direction is 30° from normal to the wall and the effective wind velocity at the surface of the wall is reduced as is indicated in column 2. On the other hand, the velocity through the inward leak is increased due to the higher overall wind effect which is depressurizing the inside of the house. Note that the wind depressurization of the interior of the house has not been made sensitive to wind direction.

A final example shows the affect of wind when the direction is away from the wall in question. Column #2 shows no local wind effect and the velocity distribution through the leakage sites in the siding shown in column 6 are very small. Again, the leakage rate at the bottom of the wall is a result of depressurization in the house which is not wind direction sensitive and is therefore dominant in this case.

In conclusion, all of the changes requested to be made in our agreement dated October 27, 1986, have been completed and await your review for finalization.

Yours truly,

SCANADA CONSULTANTS LIMITED

Michael C. Swinton, P. Eng.

MCS:smm

DATA USED IN THE DRYING WALL MODEL

TITLE:
HALIFAX SOUTH WALL - WITH STRAPPING: PAINTED EXTERIOR SURFACE OF THE SIDING

NUMBER OF ELEMENTS UP THE WALL (NV) AND LAYERS THROUGH THE WALL (NE)
9,20

SELECTION OF MATERIALS FOR EACH LAYER (SEE PROPERTIES DATABASE FOR #)
1,15,20,16,16,4,5,4,6,6,10,10,10,17,17,17,9,21,4,9

THICKNESS OF EACH LAYER (in m)
1,0.002,0.005,0.005,0.005,0.002,0.02,0.002,0.00025,0.00025,0.004,0.004,0.004,0.030,0.030,0.030,0.0001,0.0095,0.002,1

SELECTION OF MATERIALS FOR THE STUD LAYERS (SEE PROPERTIES DATA BASE FOR #)
16,16

LATERAL THICKNESS OF STUD LAYERS
0.019,0.019

LOCATION OF THE STUDS: NEXT TO THE INSULATION LAYER (LAYER #)
15

WALL HEIGHT (z), WALL LENGTH (m)
6,9

Siding Gap Characteristics: WIDTH(m) ! bottom to top (9 elements + opening)
0.001,0.001,0.001,0.001,0.001,0.001,0.001,0.001,0.001,0.02

Siding Gap Characteristics: FLOW PATH LENGTH(m) ! bottom to top (9 + opening)
0.01,0.01,0.01,0.01,0.01,0.01,0.01,0.01,0.01,0.04

Siding Gap Characteristics: FLOW EXPONENT ! bottom to top (9 elements + opening)
0.9,0.9,0.9,0.9,0.9,0.9,0.9,0.9,0.9,0.6

INWARD LEAK: ELEMENT # (0 IF NONE), INDOOR WIND PRESSURE COEFF, HEIGHT OF NPP(m)
1,-0.3,3

AIR SPACE CHARACTERISTICS: NUMBER OF THE LAYER, FLOW EXPONENT
7,0.8

(+/- 22.5) WIND PRESSURE COEFFICIENTS ! bottom to top (9 elements + opening)
22.5, 0.1,0.2,0.3,0.4,0.5,0.5,0.4,0.3,0.2,0.1

(+/- 45) WIND PRESSURE COEFFICIENTS ! bottom to top (9 elements + opening)
45.0, 0.05,0.1,0.15,0.2,0.25,0.25,0.2,0.15,0.1,0.05

(+/- 67.5) WIND PRESSURE COEFFICIENTS ! bottom to top (9 elements + opening)
67.5, 0.025,0.05,0.075,0.1,0.125,0.125,0.1,0.075,0.05,0.025

(OTHER DIRECTIONS) WIND PRESSURE COEFF! bottom to top (9 elements + opening)
180., 0.0,0.0,0.0,0.0,0.0,0.0,0.0,0.0,0.0,0.0

WALL ORIENTATION (DEGREES FROM NORTH): N:360, E:90, S:180, W:270
180

...cont'd

DATA USED IN THE DRYING WALL MODEL

MOISTURE SOURCE STRENGTH IN kg/hr, & LOCATION: LAYER # & ELEMENT NUMBER
0.,10,5

MOISTURE CONTENT FOR FORMATION OF SURFACE FILM, FILM THICKNESS THRESHOLD(m)
35,1

SIMULATION START AND END (DAY OF THE YEAR)
1,365

NUMBER OF ITERATIONS BETWEEN THE 3 MAJOR SUB MODELS
2

NUMER OF LAYERS DISPLAYED IN SCREEN (MAX 12); SPECIFY LAYER NUMBERS
12, 1,2,3,5,6,7,9,10,11,12,21,20

NAME OF THE WEATHER DATA FILE (INCLUDE THE DRIVE SPEC: e.g. A:DWEATH.SOU)
D:HAL.SOU

NAME OF OUTPUT FILE FOR PLOTTING (e.g. GRAPGH.PRN)
GRF.PRN

NAME OF THE TABULAR OUTPUT FILE (e.g. DRY3.PRN; "LPT1:" PRINTS TO PRINTER)
DRY3.PRN

CHARACTERISTICS OF THE WALL

No.	ELEMENT	THICKNESS(mm)
1	OUTDOOR AIR	1000.0
2	EXTERIOR AIR FILM	2.0
3	PAINTED WOOD SIDING	5.0
4	WOOD-BASED SIDING	5.0
5	WOOD-BASED SIDING	5.0
6	INTERIOR AIR FILM	2.0
7	AIR SPACE	20.0
8	INTERIOR AIR FILM	2.0
9	SHEATHING PAPER	0.3
10	SHEATHING PAPER	0.3
11	PLYWOOD(DOUGLAS FIR)	4.0
12	PLYWOOD(DOUGLAS FIR)	4.0
13	PLYWOOD(DOUGLAS FIR)	4.0
14	GLASS FIBER INSULATION	30.0
15	GLASS FIBER INSULATION	30.0
16	GLASS FIBER INSULATION	30.0
17	POLYETHYLENE	0.1
18	GYPSUM	9.5
19	INTERIOR AIR FILM	2.0
20	INDOOR AIR	1000.0

(21 WOOD STUD 19 mm)
(22 WOOD STUD 19 mm)

PRESS RETURN TO CONTINUE...

HOUR	M/D/H	TEMP (C)	RH (%)	SOLAR (W/m2)	WIND (km/h)	WIND DIRECTION DEG FROM NORTH
6464	SEP/27: 0	12.2	99.0	43.0	18.0	330.0

ACCUMULATED SOLAR INCIDENCE (MJ/sq.m.) 424.8

REFERENCE TEMP DISTRIBUTION: CONDUCTION WITH NO AIR FLOW IN AIR SPACE

12.2 12.9 13.0 13.3 13.4 13.6 13.8 13.8 13.9 13.9 17.0 20.0

No.	VELOCITY (m/s)	DISTRIBUTION THROUGH AND UP THE WALL									
	1	2	3	5	6	7	9	10	11	12	21	20
9	5.00				0.02	-0.04						
8	5.00				0.04	-0.04						
7	5.00				0.06	-0.04						
6	5.00				0.08	-0.04						
5	5.00				0.10	-0.05						
4	5.00				0.12	-0.05						
3	5.00				0.15	-0.06						
2	5.00				0.17	-0.07						
1	5.00					-0.07	1.40					

INSTANTANEOUS RATE OF MOISTURE FLOW FROM WALL = 0.498 (g/(m2.h))

NET CUMULATIVE AVERAGE RATE OF MOISTURE FLOW = -0.224 (g/(m2.h))

PRESS RETURN TO CONTINUE...

HOUR	M/D/H	TEMP (C)	RH (%)	SOLAR (W/m2)	WIND (km/h)	WIND DIRECTION DEG FROM NORTH
6449	SEP/26: 17	12.8	94.0	0.0	19.0	150.0

ACCUMULATED SOLAR INCIDENCE (MJ/sq.m.) 424.6

REFERENCE TEMP DISTRIBUTION: CONDUCTION WITH NO AIR FLOW IN AIR SPACE

12.8 12.8 12.9 13.2 13.4 13.5 13.8 13.8 13.8 13.9 16.9 20.0

No.	VELOCITY (m/s) DISTRIBUTION THROUGH AND UP THE WALL											
	1	2	3	5	6	7	9	10	11	12	21	20
9	5.28	1.67			0.26	0.14						
8	5.28	2.04			0.48	0.13						
7	5.28	2.36			0.70	0.10						
6	5.28	2.64			0.92	0.07						
5	5.28	2.64			0.92	0.02						
4	5.28	2.36			0.71	-0.02						
3	5.28	2.04			0.49	-0.06						
2	5.28	1.67			0.27	-0.08						
1	5.28	1.18				-0.10	1.92					

INSTANTANEOUS RATE OF MOISTURE FLOW FROM WALL = -0.617 (g/(m2.h))
NET CUMULATIVE AVERAGE RATE OF MOISTURE FLOW = -0.221 (g/(m2.h))
PRESS RETURN TO CONTINUE...

HOUR	M/D/H	TEMP (C)	RH (%)	SOLAR (W/m2)	WIND (km/h)	WIND DIPECTION DEG FROM NORTH
6498	SEP/20: 18	15.6	70.0	0.0	16.0	180.0

ACCUMULATED SOLAR INCIDENCE (MJ/sq.m.) 466.0

REFERENCE TEMP DISTRIBUTION: CONDUCTION WITH NO AIR FLOW IN AIR SPACE

15.6 15.6 15.7 15.9 15.9 16.1 16.2 16.2 16.2 16.3 18.1 20.0

No.	VELOCITY (m/s)		DISTRIBUTION THROUGH AND UP THE WALL								
	1	2	3	5	6	7	9	10	11	12	21	20
9	4.44	1.99			0.33	0.22						
8	4.44	2.43			0.63	0.20						
7	4.44	2.81			0.92	0.17						
6	4.44	3.14			1.21	0.13						
5	4.44	3.14			1.20	0.07						
4	4.44	2.81			0.90	0.00						
3	4.44	2.43			0.59	-0.04						
2	4.44	1.99			0.26	-0.07						
1	4.44	1.41				-0.08	1.65					

INSTANTANEOUS RATE OF MOISTURE FLOW FROM WALL = -0.216 (g/(m2.h))

NET CUMULATIVE AVERAGE RATE OF MOISTURE FLOW = -0.195 (g/(m2.h))

PRESS RETURN TO CONTINUE...

APPENDIX C

APPENDIX C

ADDENDUM OF SEPTEMBER 19, 1987
THE RESULTS OF TASK 3
'AIR FLOW COEFFICIENTS ALONG THE WALL'

The coefficients tabulated in this addendum relate flow rate Q to pressure drop ΔP along the airspace behind the siding according to the relation:

$$Q = A_1 \times \Delta P^{0.5} + A_2 \times \Delta P$$

The A_1's and A_2's are presented in raw form as they apply to the wall specimens tested and also in normalized form to apply to a wall of any size. To achieve this the volume flow rate, Q has been divided by the width, W, of the tested wall specimen and the pressure drop has been converted to a pressure drop per siding board, i.e. dividing by N, the number of siding boards. Therefore the A_1's are multiplied by $W/\sqrt{N}$ and the A_2's by W/N.

In applying these results to a real wall a measure of ΔP along the wall would have to be divided by the number of siding panels between pressure taps. This outcome could then be related to Q per unit width of wall when the ΔP's are multiplied by the appropriate A_1 and A_2 coefficients.

The computer model of wall drying uses both formulations of the volume versus pressure drop relations, i.e.

$Q = f(\Delta P)$ and $\Delta P = f(Q)$.

Coefficients for the latter relation are also presented in this Appendix.

TABLE 1: ALONG THE WALL COEFFICIENTS

MATERIAL: PINE

SPACING (mm)	FLOW DIRECTION	RAW COEFFICIENTS A1	RAW COEFFICIENTS A2	NORMALIZED COEFF. A1	NORMALIZED COEFF. A2
1	UP	4.388E+00	6.778E-01	1.590E+00	1.098E-01
2	UP	3.160E+01	1.965E+00	1.145E+01	3.184E-01
3	UP	8.889E+01	6.504E-01	3.220E+01	1.054E-01
5	UP	1.880E+02	1.084E+00	6.809E+01	1.756E-01
1	DOWN	5.820E+00	9.466E-01	2.108E+00	1.534E-01
2	DOWN	3.977E+01	1.602E+00	1.441E+01	2.594E-01
3	DOWN	9.816E+01	4.273E-01	3.556E+01	6.923E-02
5	DOWN	2.088E+02	-5.154E-01	7.563E+01	-8.349E-02

TABLE 2: ALONG THE WALL COEFFICIENTS

MATERIAL: MASONITE

SPACING (mm)	FLOW DIRECTION	RAW COEFFICIENTS A1	RAW COEFFICIENTS A2	NORMALIZED COEFF. A1	NORMALIZED COEFF. A2
1	UP	1.965E+01	3.258E-01	7.118E+00	5.278E-02
2	UP	4.993E+01	7.965E-01	1.809E+01	1.290E-01
3	UP	8.676E+01	9.350E-01	3.143E+01	1.515E-01
5	UP	1.616E+02	4.439E+00	5.853E+01	7.192E-01
1	DOWN	1.940E+01	7.791E-01	7.026E+00	1.262E-01
2	DOWN	5.492E+01	2.287E+00	1.989E+01	3.704E-01
3	DOWN	1.138E+02	2.550E+00	4.121E+01	4.130E-01
5	DOWN	2.184E+02	7.785E+00	7.911E+01	1.261E+00

TABLE 3: ALONG THE WALL COEFFICIENTS

MATERIAL: VINYL

SPACING (mm)	FLOW DIRECTION	RAW COEFFICIENTS A1	RAW COEFFICIENTS A2	NORMALIZED COEFF. A1	NORMALIZED COEFF. A2
1	UP	2.520E+01	1.514E-01	7.215E+00	1.533E-02
2	UP	5.693E+01	3.560E-01	1.630E+01	3.605E-02
3	UP	8.631E+01	8.641E-01	2.472E+01	8.749E-02
5	UP	1.726E+02	3.662E+00	4.943E+01	3.707E-01
1	DOWN	3.012E+01	-1.769E-01	8.625E+00	-1.791E-02
2	DOWN	6.068E+01	4.673E-01	1.738E+01	4.732E-02
3	DOWN	9.689E+01	6.603E-01	2.775E+01	6.685E-02
5	DOWN	1.767E+02	3.435E+00	5.061E+01	3.478E-01

TABLE 4: ALONG THE WALL COEFFICIENTS

MATERIAL: TENTEST BACKED ALUMINUM

SPACING (mm)	FLOW DIRECTION	RAW COEFFICIENTS A1	RAW COEFFICIENTS A2	NORMALIZED COEFF. A1	NORMALIZED COEFF. A2
1	UP	8.353E+00	3.026E-02	3.383E+00	6.129E-03
2	UP	2.974E+01	5.550E-01	1.204E+01	1.124E-01
3	UP	5.597E+01	5.905E-01	2.267E+01	1.196E-01
5	UP	1.492E+02	1.580E+00	6.044E+01	3.199E-01
1	DOWN	2.897E+00	2.821E-01	1.173E+00	5.713E-02
2	DOWN	3.169E+01	4.615E-01	1.284E+01	9.346E-02
3	DOWN	7.491E+01	4.713E-01	3.034E+01	9.544E-02
5	DOWN	1.684E+02	1.843E+00	6.821E+01	3.732E-01

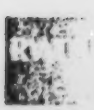

ALONG THE WALL NORMALIZED COEFFICIENTS

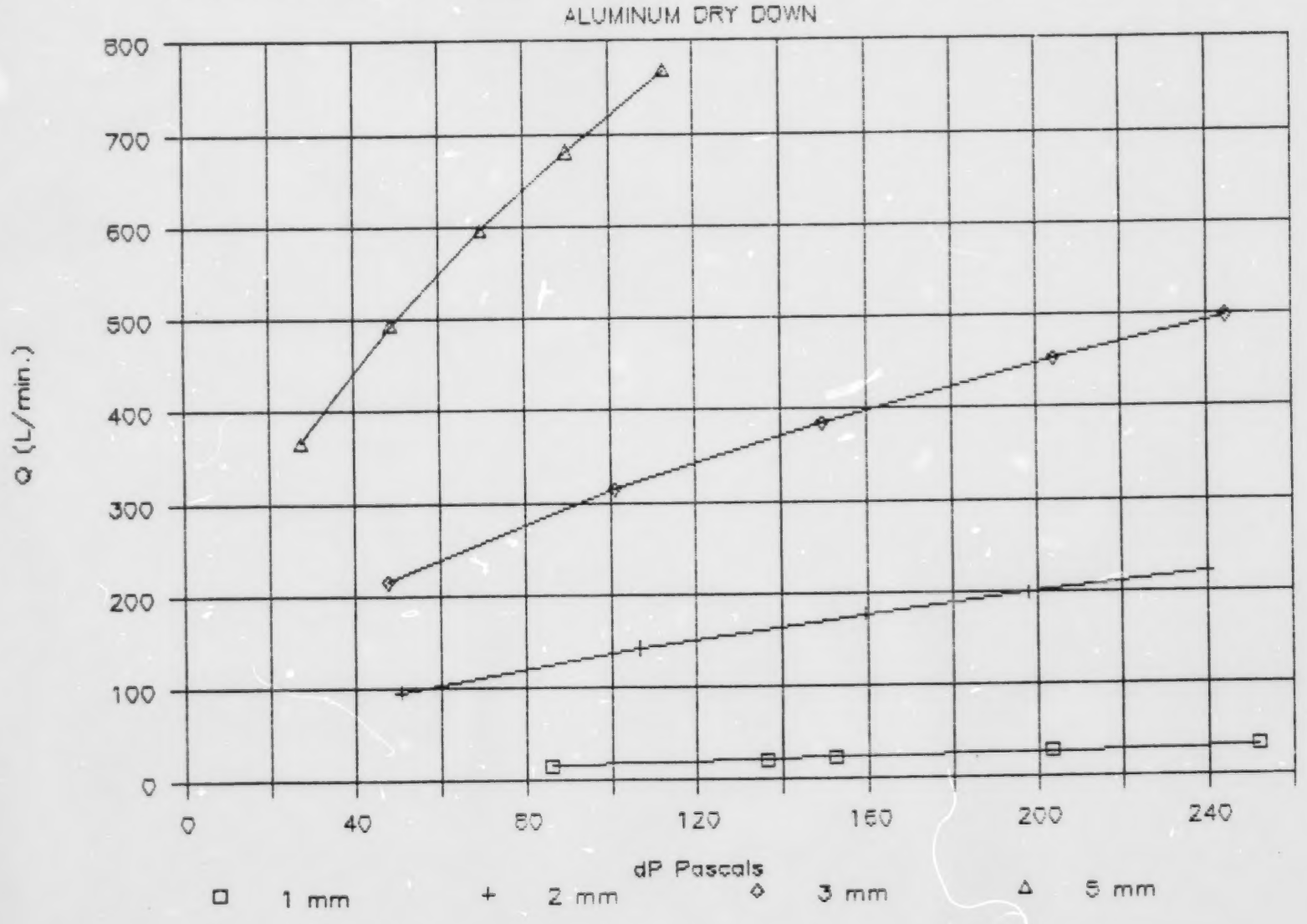

ALONG THE WALL NORMALIZED COEFFICIENTS

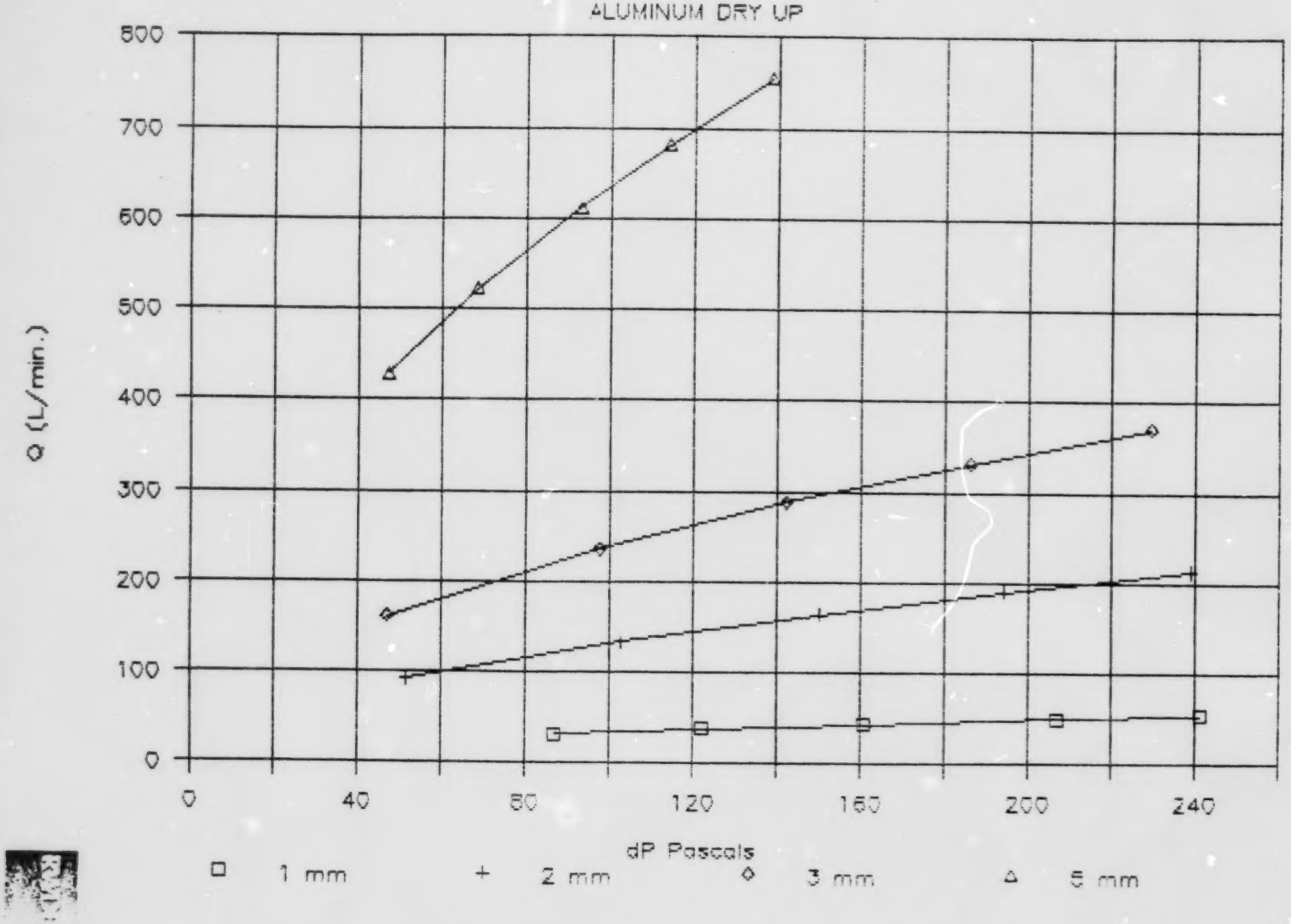

ALONG THE WALL NORMALIZED COEFFICIENTS

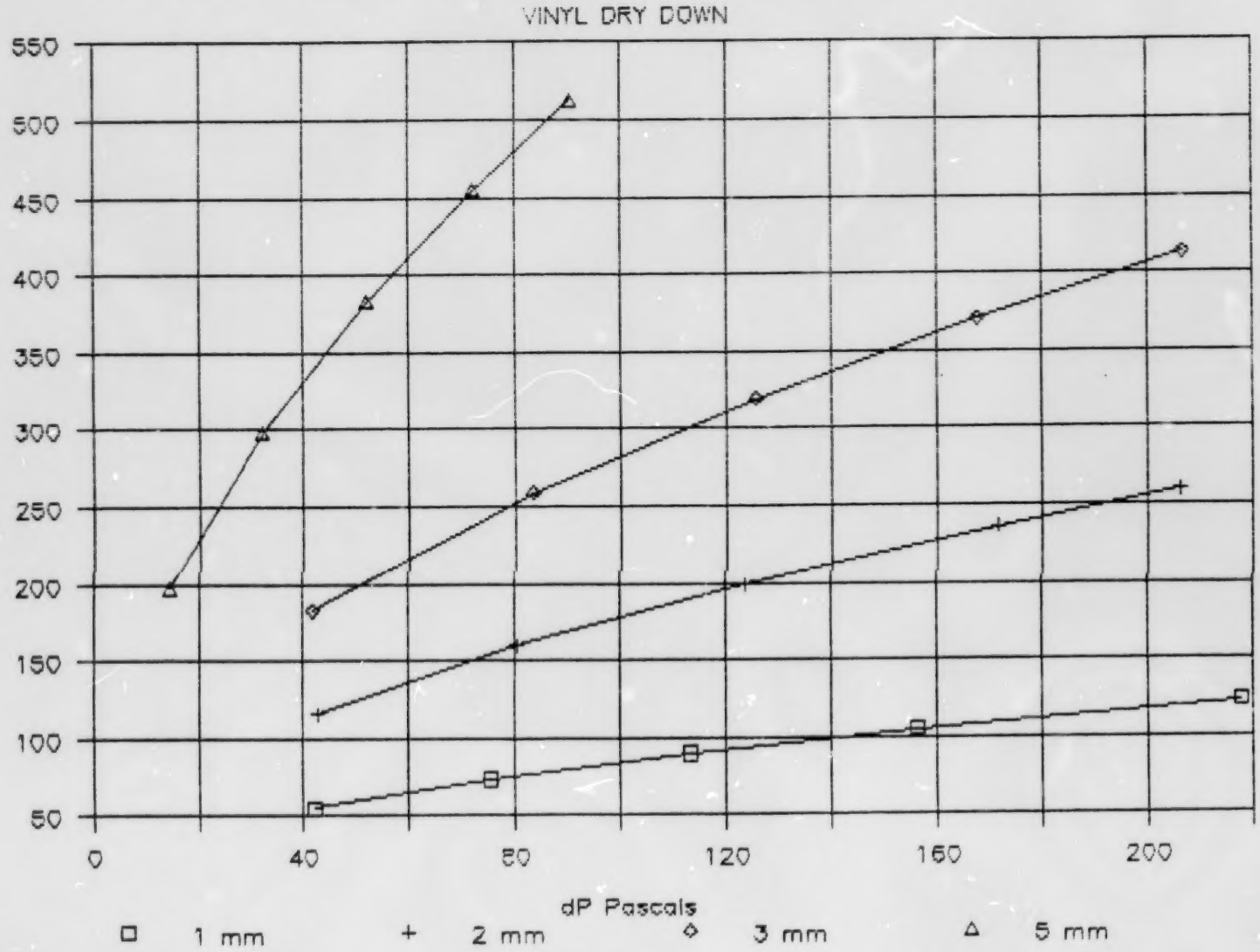

ALONG THE WALL NORMALIZED COEFFICIENTS

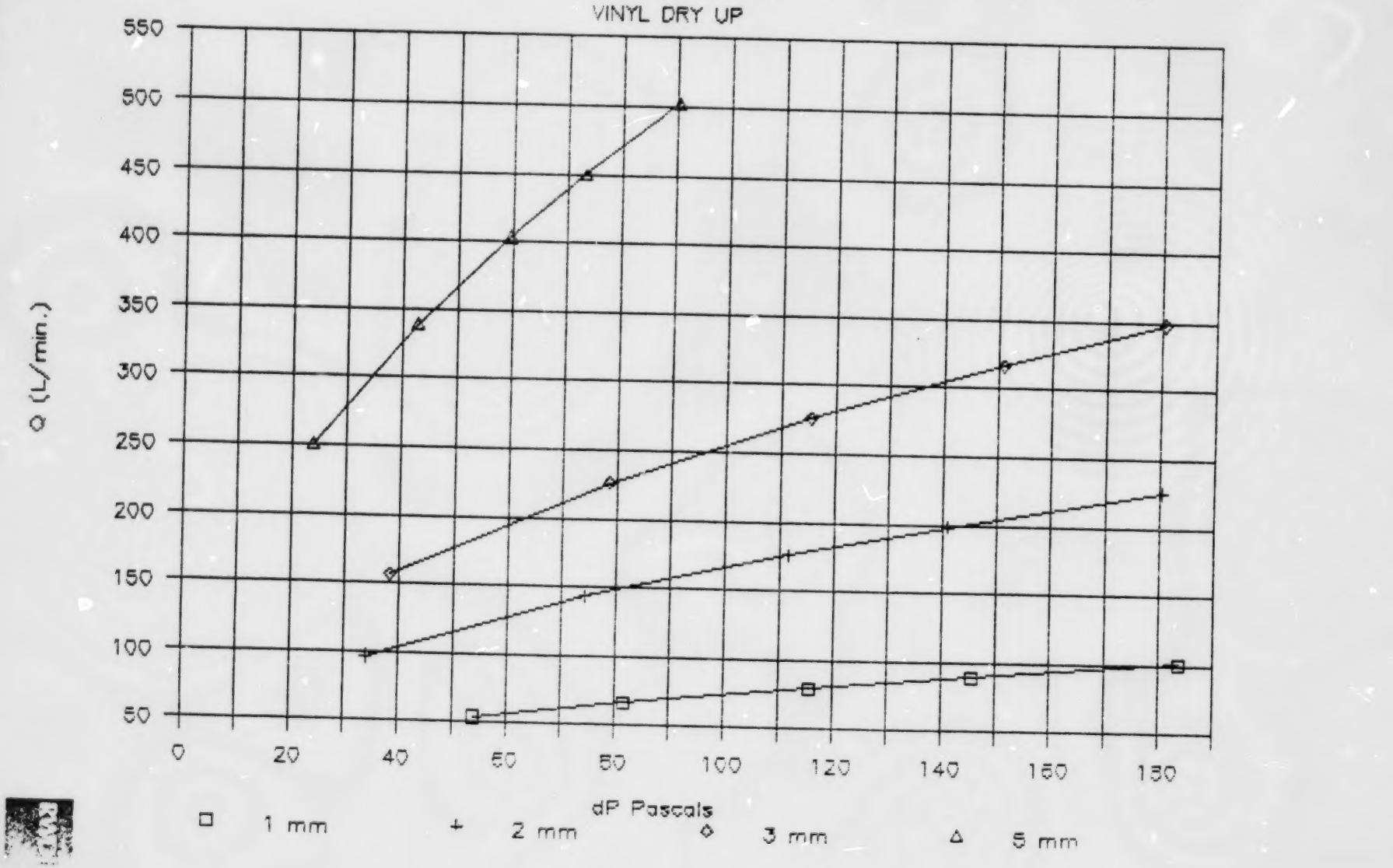

ALONG THE WALL NORMALIZED COEFFICIENTS

MASONITE DRY DOWN

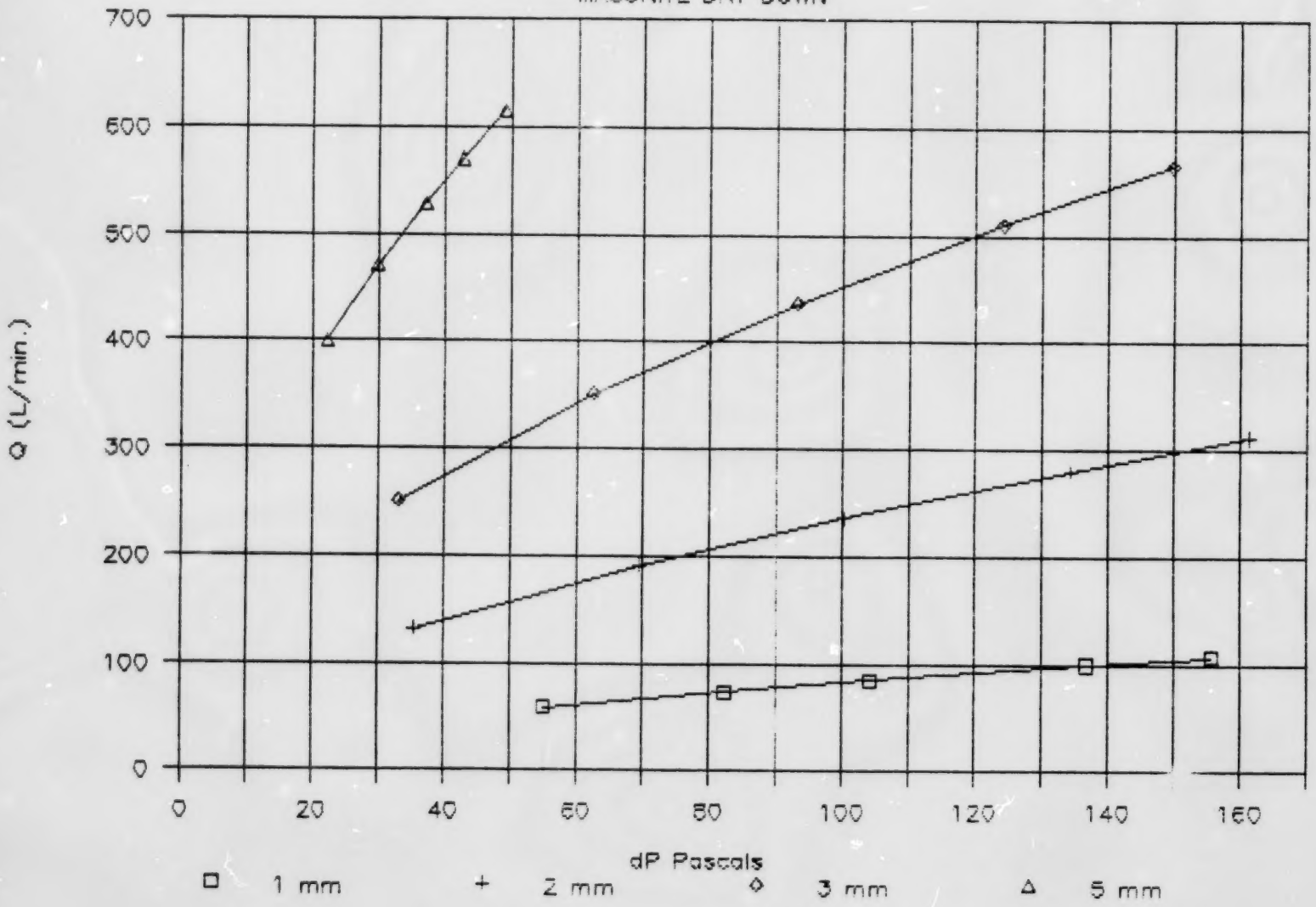

ALONG THE WALL NORMALIZED COEFFICIENTS

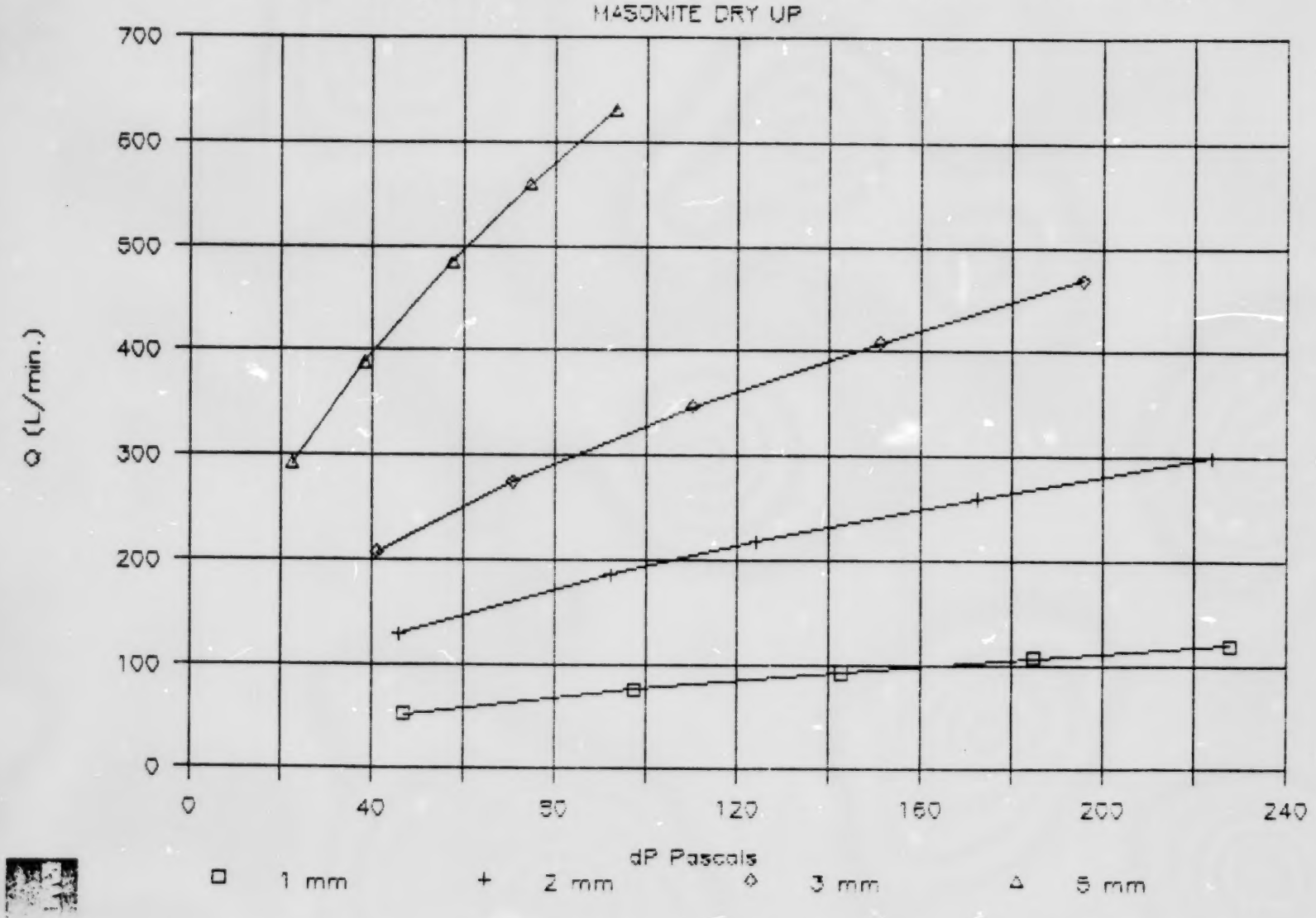

ALONG THE WALL NORMALIZED COEFFICIENTS

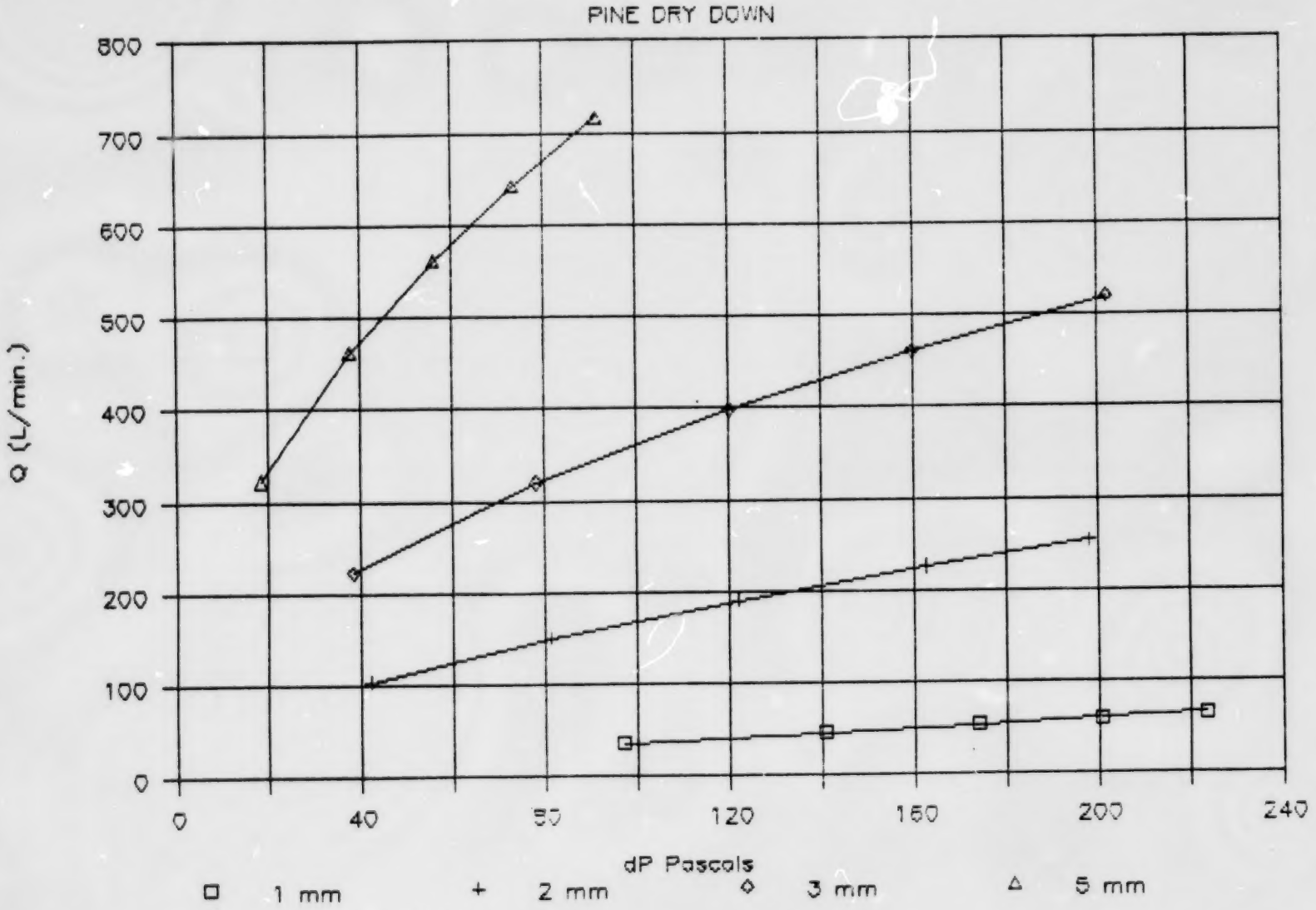

ALONG THE WALL NORMALIZED COEFFICIEINTS

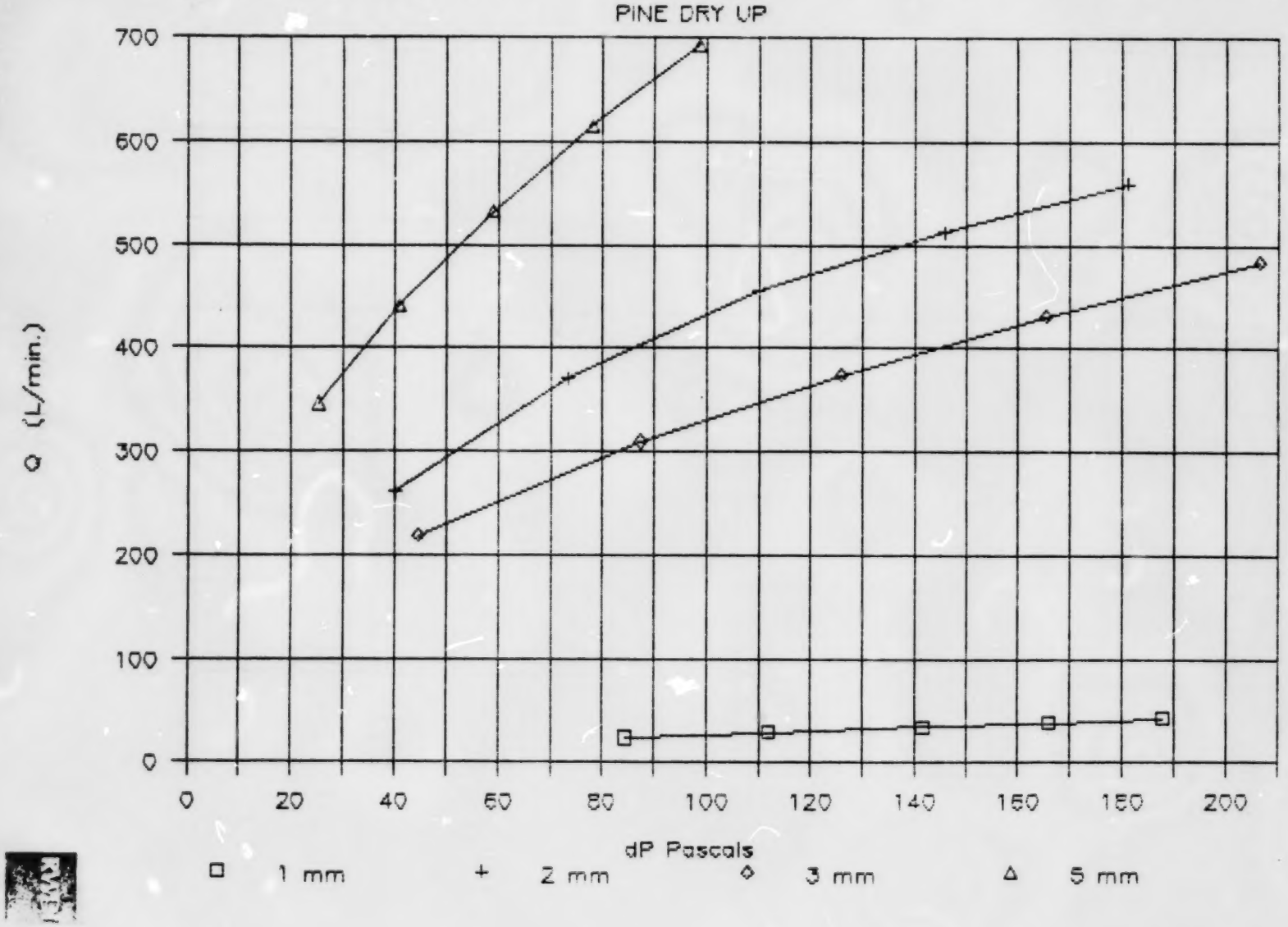

Rowan Williams
Davies & Irwin Inc.

June 26, 1987

Mr. Alvin J. Houston
Project Manager Canada Mortgage
and Housing Corporation
National Office
Montreal Road
Ottawa, Ontario
K1A 0P7

Re: Drying Characteristics in Walls of Low Rise Residential Housing - Addendum to Milestone Report Number 3, March 31, 1987

Dear Mr. Houston:

Since our last meeting of May 15, 1987 we have completed testing and verification for Task 3, which consists of determining air flow coefficients along the wall between the siding and backing for four different siding materials. These materials are; pine board, masonite, vinyl, and tentest backed aluminum. Results of these tests are included herein and discussed at length below. Testing details including methodology may be found in the original milestone report number 3, dated March 31, 1987.

During this interim period we have also completed testing for Task 4 which has involved the determination of air flow coefficients across the wall (ie. perpendicular to the wall) for the same four materials. These tests were performed for each siding material in both air-dry and wetted conditions. These results will be reported on separately, including testing details, in milestone report number 4 by July 3, 1987.

Air flow in a wall, occurring between the siding and the backup sheathing, is produced in general by leakage paths across the siding material, at siding interfaces and at interfaces between the siding and other building materials. For experimental reasons the actual flow condition in a wall is modelled by two simpler laboratory conditions, namely;

(i) flow versus pressure drop along and behind the siding (Task 3) and
(ii) flow versus pressure drop across the siding (Task 4).

As indicated, only results of Task 3 are discussed in this summary.

The flow coefficients presented in Tables 1,2,3 and 4 are the results of Task 3

650 Woodlawn Road West. Guelph. Ontario N1K 1B8 • Tel. (519) 823-1311. Telex 069-56639. Fax (519) 823-1316

testing for along the wall flow for the materials noted. The purpose for obtaining these coefficients is to determine the mathematical relationship between pressure drop, P (Pascals) and flow rate, Q (liters/min). This relationship, arbitrarily treating Q as the independant variable (ie. the measured quantity) for a given P, may be expressed in the following form;

$$P = Ko + k1*Q + k2*Q^2 \qquad (1)$$

where Ko is an error term (usually small), K1 is the coefficient of the linear term in Q and K2 is the corresponding coefficient for the quadratic term in Q^2. Although other forms of this equation can be used, one advantage of this form is that relative magnitudes of K1 and K2 give some indication of relative proportions of laminar flow represented by Q and turbulent flow represented by Q^2 behind the siding.

These coefficients, in addition to those obtained for Task 4, are essential inputs to the air flow segment of our computer model developed as Tasks 1 and 2. The intent of this computer model, comprised of three sub-models, is to predict the drying characteristics of wood framed walls. The sub-models include a heat transfer model, an air flow model and a moisture flow model. Results from other portions of this project (Tasks 5 and 6) will be used in the moisture flow as well. Information from Task 7 (ie. experimental verification) will be used to test the accuracy and verstility of the numerical model.

The pressure drop P, described by equation (1) for along-the-wall flow, is produced to some degree by surface friction but mostly by the rapid contractions and expansions characteristic of the cross sectional geometry of some sidings. Figure 1 illustrates these geometries for typical siding samples used in this study. Only the pine board has a relatively even backside. The profiles of the remaining three materials are stepped. As will be seen, such differences in geometry are partly responsible for differing coefficients among siding materials.

As illustrated in Tables 1 through 4, tests have been performed considering the following parameters: siding material (4 types), flow direction (up and down the wall), and spacing between the siding and the backup sheathing. These results have been normalized to account for the small size of tested samples. Pressure drop P, along the sample has been normalized by the number of siding boards making up the sample. Flow rate has been normalized by the length of gap parallel to the siding in meters. Thus, the normalized coefficients in the tables are to be applied in conjunction with a pressure drop per siding board and a flow rate per meter of horizontal siding length.

DISCUSSION OF RESULTS

Numerous conclusions can be drawn from the results presented in Tables 1 through 4.

The Ko coefficients represent error terms which are small for any practical flow rates. These error terms correspond to the best fit quadratic curve to the measured experimental data.

The K1 coefficients corresponding to the linear term Q are consistently greater than the K2 coefficients corresponding to the square term by a factor of ten or more. Only for two instances in the case of the aluminum siding and 1mm spacing is the

difference less than ten. By inspecting these coefficients it becomes evident that the squared Q term quickly overcomes the relative factor of ten associated with the linear term. This suggests that the flow is largely laminar only for the lowest flow rates and becomes primarily turbulent for most of the flow regime. This outcome applies mainly to spacings of 2mm or more.

As may be expected the tables show that for all four siding materials the coefficients of both K1 and K2 consistently decrease with increase in spacing. This is a reasonable outcome which suggests that for a given pressure larger flow rates occur for larger spacings.

Comparing K1 and K2 coefficients for the 'up' and 'down' flow cases for each siding material indicates that the coefficients are in most cases less in the 'down' flow case. This implies that for a given flow rate, the pressure drop is less for downward flow than for upward flow. The effect is more pronounced for the larger spacing (ie. 3mm and 5mm). This is a reasonable outcome judging from the siding profiles illustrated in Figure 1 for masonite, vinyl and aluminum. For these cases downward flow has better pressure recovery as it crosses the 'steps' than upward flow. However, based on the same reasoning the pine sample should not exhibit any difference in pressure drop for either flow directions. Although the K1 coefficient is significantly different in the two directions for the pine siding, the K2 coefficients, which dominate for all but the lowest rates, are very similar for the two flow directions. Thus, the results are reasonable and consistent.

In comparing K1 and K2 coefficients among siding types it can be seen that:

(i) the K1 coefficients for 1mm and 2mm spacings in both 'up' and 'down' flow directions are largest for pine and diminish in order for masonite , aluminum , and vinyl . Thus, for a given pressure drop P, the flow rate is largest for vinyl and least for pine siding.

(ii) similarly, for the 3mm and 5mm spacings in both directions, K1 results suggest that for a given P, the flow rates are largest for the pine siding and decrese in order for aluminum, masonite and vinyl sidings.

(iii) using similar reasoning, the K2 coefficients for all spacings and both flow directions indicate that for a given P, the flow rate is largest for masonite and decreases in order for pine, vinyl and aluminum sidings.

(iv) since the flow rate squared term most often produces the major portion of the pressure drop for all but the lowest flows, the order determined by the K2 coefficients for flow rate among siding types will govern in most cases.

The use of the Ko term allows a non-zero pressure at zero flow. Although this provides the best fit at higher flow rates, it is obviously incorrect at very low flow rates. This non-zero Ko term leads to a negative K1 term in one instance (vinyl, 1mm, flow down). Reanalysis of the data, forcing a zero Ko term will probably eliminate this anomoly.

This completes the work for Task 3. Except for possible refinements to the coefficients or rearrangement of equation (1). Similar coefficients will be generated from the results of Task 4 to supplement those discussed above. In addition, the Task 4 milestone will address the effect of wetted sidings on air flow

coefficients across the samples.

Should you find the need, we would be pleased to discuss these results with you at your convenience.

Yours very truly,

ROWAN WILLIAMS DAVIES & IRWIN INC.

Vincent Ferraro, M.Eng., P.Eng.
Project Engineer

VF/ld

TABLE 1: ALONG THE WALL COEFFICIENTS

MATERIAL: PINE

SPACING (mm)	FLOW DIRECTION	RAW COEFFFICIENTS			NORMALIZED COEFFICIENTS		
		Ko	K1	K2	Ko	K1	K2
1	UP	3.000E-01	7.200E-01	1.530E-03	1.359E+00	4.027E+00	1.056E-02
2	UP	1.477E+00	9.220E-02	1.827E-04	6.691E+00	5.156E-01	1.261E-03
3	UP	2.200E-01	1.320E-02	9.484E-05	9.966E-01	7.382E-02	6.548E-04
5	UP	3.110E-02	2.850E-03	2.394E-05	1.409E-01	1.594E-02	1.653E-04
1	DOWN	-1.950E-02	5.640E-01	6.314E-04	-8.834E-02	3.154E+00	4.359E-03
2	DOWN	1.449E+00	6.940E-02	1.817E-04	6.564E+00	3.881E-01	1.255E-03
3	DOWN	8.810E-01	3.605E-03	9.351E-05	3.991E+00	2.016E-02	6.456E-04
5	DOWN	-1.050E-01	-6.914E-04	2.438E-05	-4.757E-01	-3.867E-03	1.683E-04

TABLE 2: ALONG THE WALL COEFFICIENTS

MATERIAL: MASONITE

SPACING (mm)	FLOW DIRECTION	RAW COEFFFICIENTS			NORMALIZED COEFFICIENTS		
		Ko	K1	K2	Ko	K1	K2
1	UP	-6.740E-02	1.260E-01	1.334E-03	-3.121E-01	7.202E-01	9.414E-03
2	UP	-1.950E-01	4.912E-02	2.110E-04	-9.029E-01	2.808E-01	1.489E-03
3	UP	4.040E-01	1.656E-02	8.913E-05	1.871E+00	9.466E-02	6.290E-04
5	UP	1.070E-01	1.113E-02	1.832E-05	4.954E-01	6.362E-02	1.293E-04
1	DOWN	3.860E-02	1.630E-01	7.370E-04	1.787E-01	9.317E-01	5.201E-03
2	DOWN	9.120E-02	5.200E-02	9.490E-05	4.223E-01	2.972E-01	6.697E-04
3	DOWN	2.120E-01	1.764E-02	3.810E-05	9.816E-01	1.008E-01	2.689E-04
5	DOWN	-2.770E-02	6.722E-03	9.951E-06	-1.283E-01	3.842E-02	7.022E-05

TABLE 3: ALONG THE WALL COEFFICIENTS

MATERIAL: VINYL

SPACING (mm)	FLOW DIRECTION	RAW COEFFFICIENTS			NORMALIZED COEFFICIENTS		
		Ko	K1	K2	Ko	K1	K2
1	UP	1.280E-01	4.000E-02	1.242E-03	1.024E+00	3.951E-01	1.514E-02
2	UP	-1.540E-02	1.710E-02	2.433E-04	-1.232E-01	1.689E-01	2.967E-03
3	UP	-4.000E-02	1.695E-02	9.204E-05	-3.200E-01	1.674E-01	1.122E-03
5	UP	-5.600E-02	8.570E-03	1.907E-05	-4.480E-01	8.464E-02	2.325E-04
1	DOWN	1.242E+00	-7.510E-02	1.497E-03	9.936E+00	-7.417E-01	1.825E-02
2	DOWN	7.000E-01	1.620E-02	2.050E-02	5.600E+00	1.600E-01	2.500E-01
3	DOWN	3.280E-01	1.056E-02	8.190E-05	2.624E+00	1.043E-01	9.986E-04
5	DOWN	3.700E-01	5.315E-03	2.035E-05	2.960E+00	5.249E-02	2.481E-04

TABLE 4: ALONG THE WALL COEFFICIENTS

MATERIAL: TENTEST BACKED ALUMINUM

SPACING (mm)	FLOW DIRECTION	RAW COEFFFICIENTS			NORMALIZED COEFFICIENTS		
		Ko	K1	K2	Ko	K1	K2
1	UP	-1.800E-01	1.200E-01	1.200E-02	-7.200E-01	5.926E-01	7.316E-02
2	UP	3.270E-01	8.793E-02	5.395E-04	1.308E+00	4.342E-01	3.289E-03
3	UP	2.720E-01	3.043E-02	2.081E-04	1.088E+00	1.503E-01	1.269E-03
5	UP	4.195E-02	9.024E-03	3.107E-05	1.678E-01	4.456E-02	1.894E-04
1	DOWN	-1.412E-02	1.170E-01	1.200E-02	-5.648E-02	5.778E-01	7.316E-02
2	DOWN	2.534E-02	7.387E-02	5.461E-04	1.014E-01	3.648E-01	3.329E-03
3	DOWN	2.620E-01	1.554E-02	1.364E-04	1.048E+00	7.674E-02	8.316E-04
5	DOWN	8.225E-02	5.967E-03	2.545E-05	3.290E-01	2.947E-02	1.552E-04

APPENDIX D

APPENDIX D

ADDENDUM OF SEPTEMBER 1987
THE RESULTS OF TASK 4
'AIR FLOW COEFFICIENTS ACROSS THE WALL'

The coefficients tabulated in this addendum relate flow rate Q to pressure drop ΔP across the siding according to the relation:

$$Q = A_1 \times \Delta P^{0.5} + A_2 \times \Delta P$$

The A_1's and A_2's are presented in raw form as they apply to the wall specimens tested and also in normalized form to apply to a wall of any size. To achieve this the volume flow rate Q has been divided by the product of the number of siding gaps N and the width of the wall W, i.e. N x W. Therefore, both the raw A_1's and A_2's are multiplied by N x W to obtain their normalized counterparts.

In applying these results to a real wall, a measure of ΔP across the wall would give a value of Q per unit width of wall, per siding panel when multiplied by the appropriate A_1's and A_2's.

The computer model of wall drying uses both formulations of the volume versus pressure drop relations, i.e.

$$Q = f(\Delta P) \text{ and } \Delta P = f(Q)$$

Coefficients for the latter relation are also presented in this Appendix.

TABLE 1: ACROSS THE WALL COEFFICIENTS

MATERIAL: PINE

CONDITION	RAW COEFFICIENTS		NORMALIZED COEFF.	
	A1	A2	A1	A2
DRY	5.412E+01	1.769E+00	1.753E+02	5.730E+00
WET 1	3.352E+01	4.255E+00	1.086E+02	1.379E+01
WET 2	5.238E+01	1.218E+00	1.697E+02	3.945E+00

TABLE 2: ACROSS THE WALL COEFFICIENTS

MATERIAL: MASONITE

CONDITION	RAW COEFFICIENTS		NORMALIZED COEFF.	
	A1	A2	A1	A2
DRY	1.308E+01	5.457E-01	4.028E+01	1.681E+00
WET 1	4.230E+00	8.732E-01	1.303E+01	2.690E+00
WET 2	8.620E+00	8.032E-01	2.655E+01	2.474E+00

TABLE 3: ACROSS THE WALL COEFFICIENTS

MATERIAL: VINYL

CONDITION	RAW COEFFICIENTS		NORMALIZED COEFF.	
	A1	A2	A1	A2
DRY	3.196E+00	1.992E-01	7.431E+00	4.632E-01
WET 1	-9.550E-01	2.566E-01	-2.220E+00	5.966E-01
WET 2	1.824E+00	8.808E-02	4.240E+00	2.048E-01

TABLE 4: ACROSS THE WALL COEFFICIENTS

MATERIAL: ALUMINUM

CONDITION	RAW COEFFICIENTS		NORMALIZED COEFF.	
	A1	A2	A1	A2
DRY	1.022E+01	5.805E-01	2.377E+01	1.350E+00
WET 1	-2.576E+00	5.283E-01	-5.989E+00	1.228E+00
WET 2	-9.747E-01	7.465E-01	-2.266E+00	1.736E+00

TABLE 5: ACROSS THE WALL COEFFICIENTS

MATERIAL: PINE RUN 2 AUG/87

CONDITION	RAW COEFFICIENTS		NORMALIZED COEFF.	
	A1	A2	A1	A2
DRY	2.486E+01	1.054E+00	8.055E+01	3.415E+00
WET 1	4.700E+01	2.764E+00	1.523E+02	8.955E+00
WET 2	7.000E+01	1.415E+00	2.268E+02	4.586E+00
WET 3	5.611E+01	1.576E+00	1.818E+02	5.106E+00
WET 4	3.741E+01	2.015E+00	1.212E+02	6.529E+00
WET 5	2.883E+01	1.891E+00	9.341E+01	6.127E+00

ACROSS THE WALL NORMALIZED COEFFICIENTS

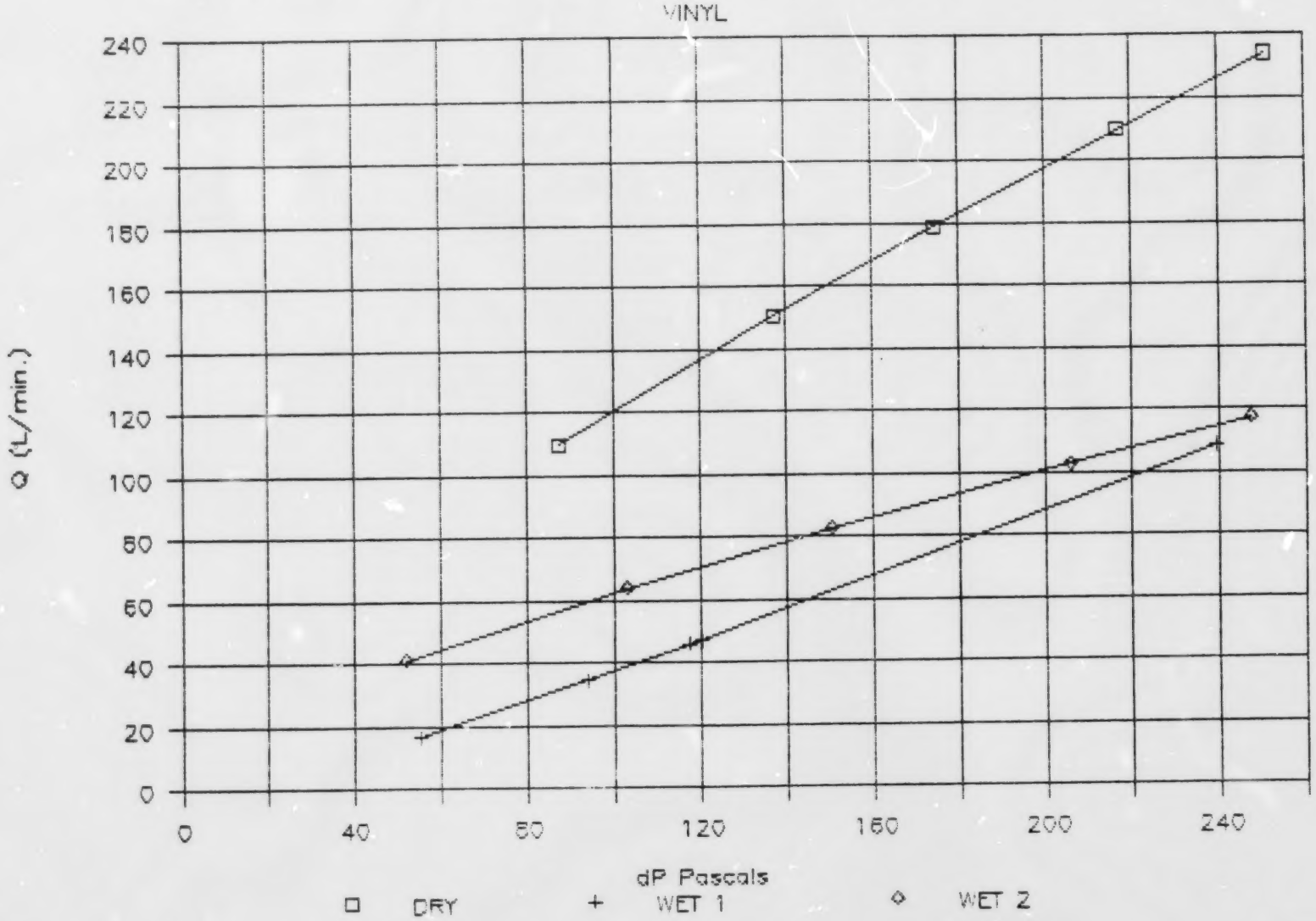

ACROSS THE WALL NORMALIZED COEFFICIENTS

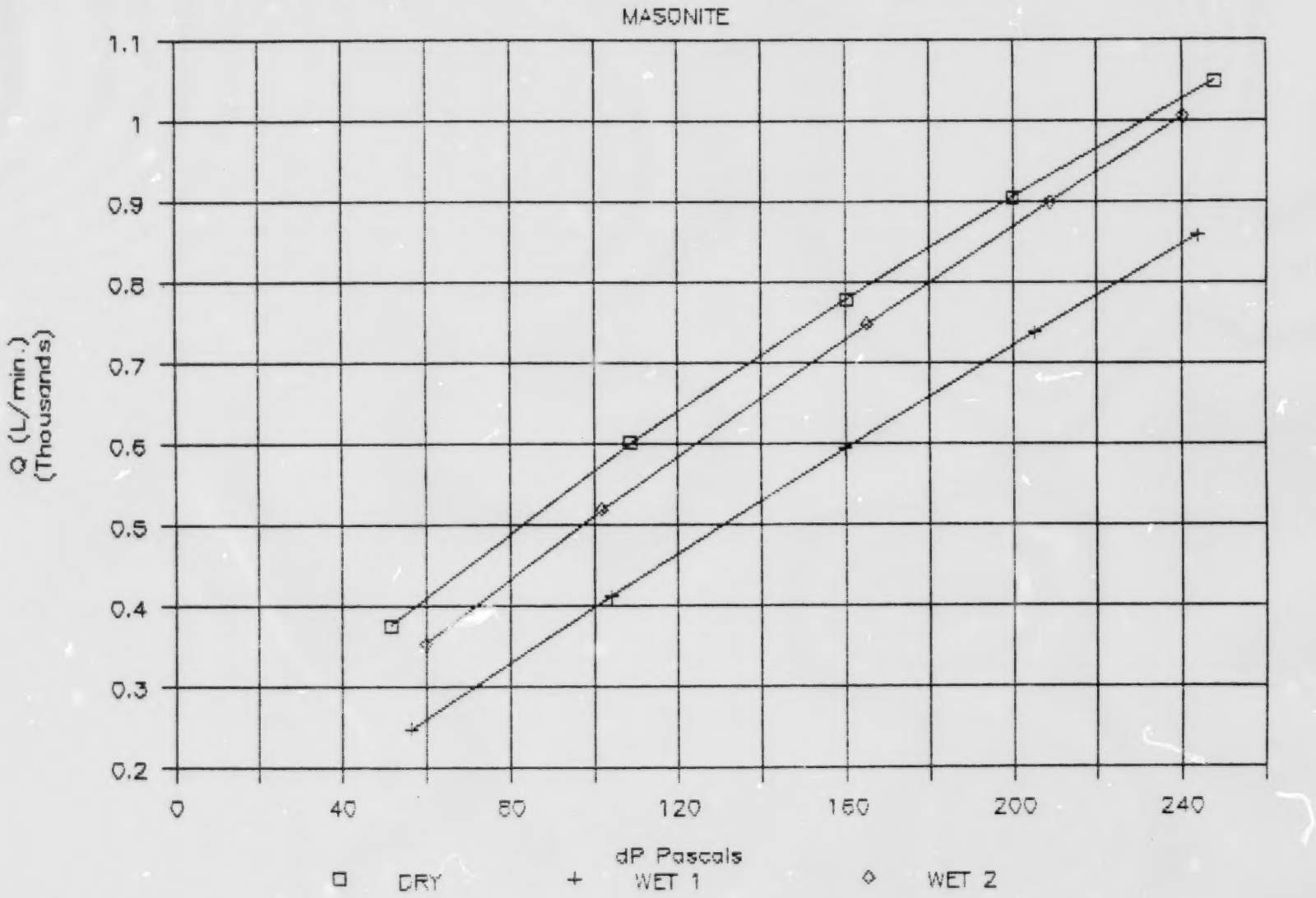

ACROSS THE WALL NORMALIZED COEFFICIENTS

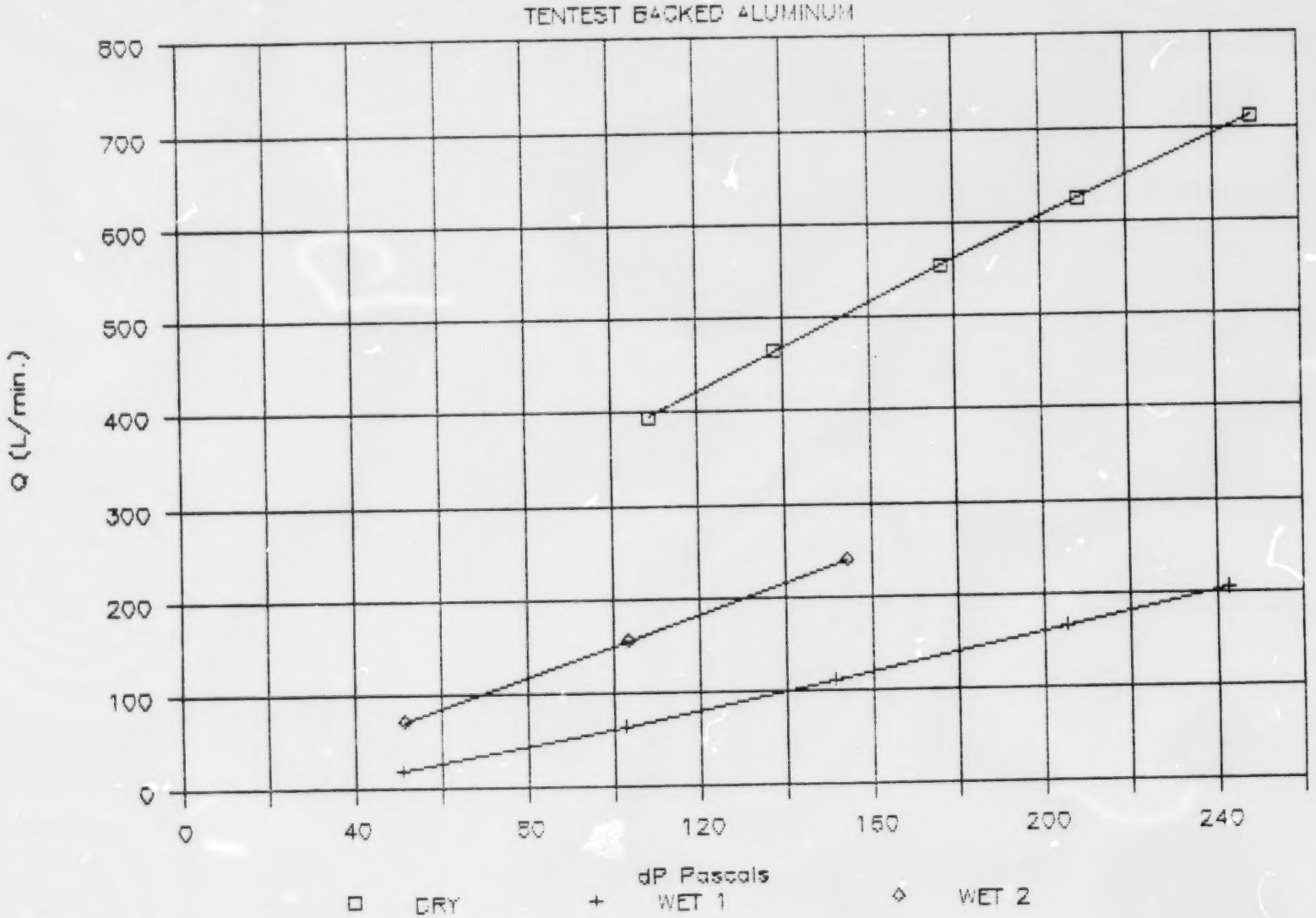

ACROSS THE WALL NORMALIZED COEFFICIENTS

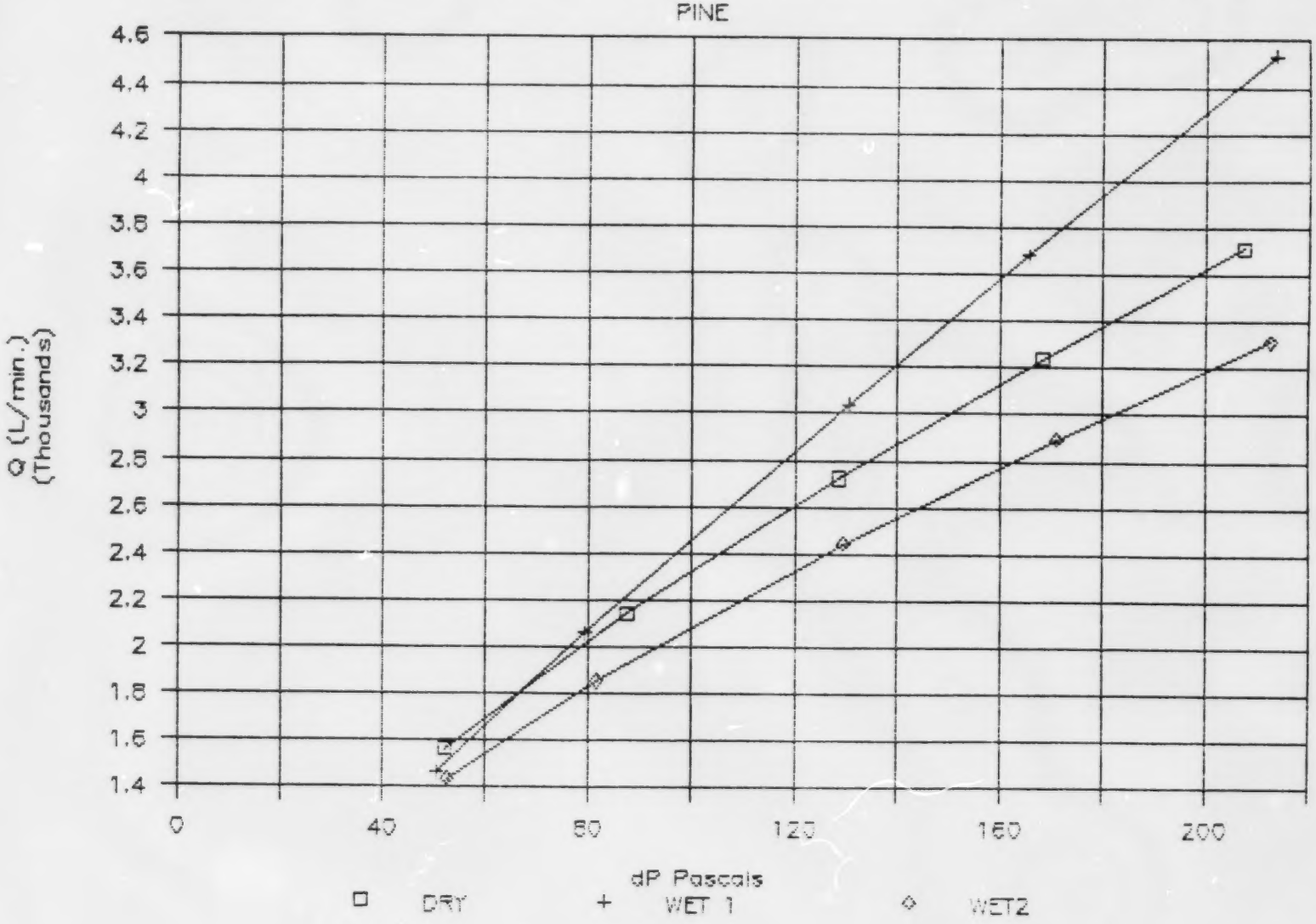

ACROSS THE WALL NORMALIZED COEFFICIENTS

PINE RUN 2/AUG 87

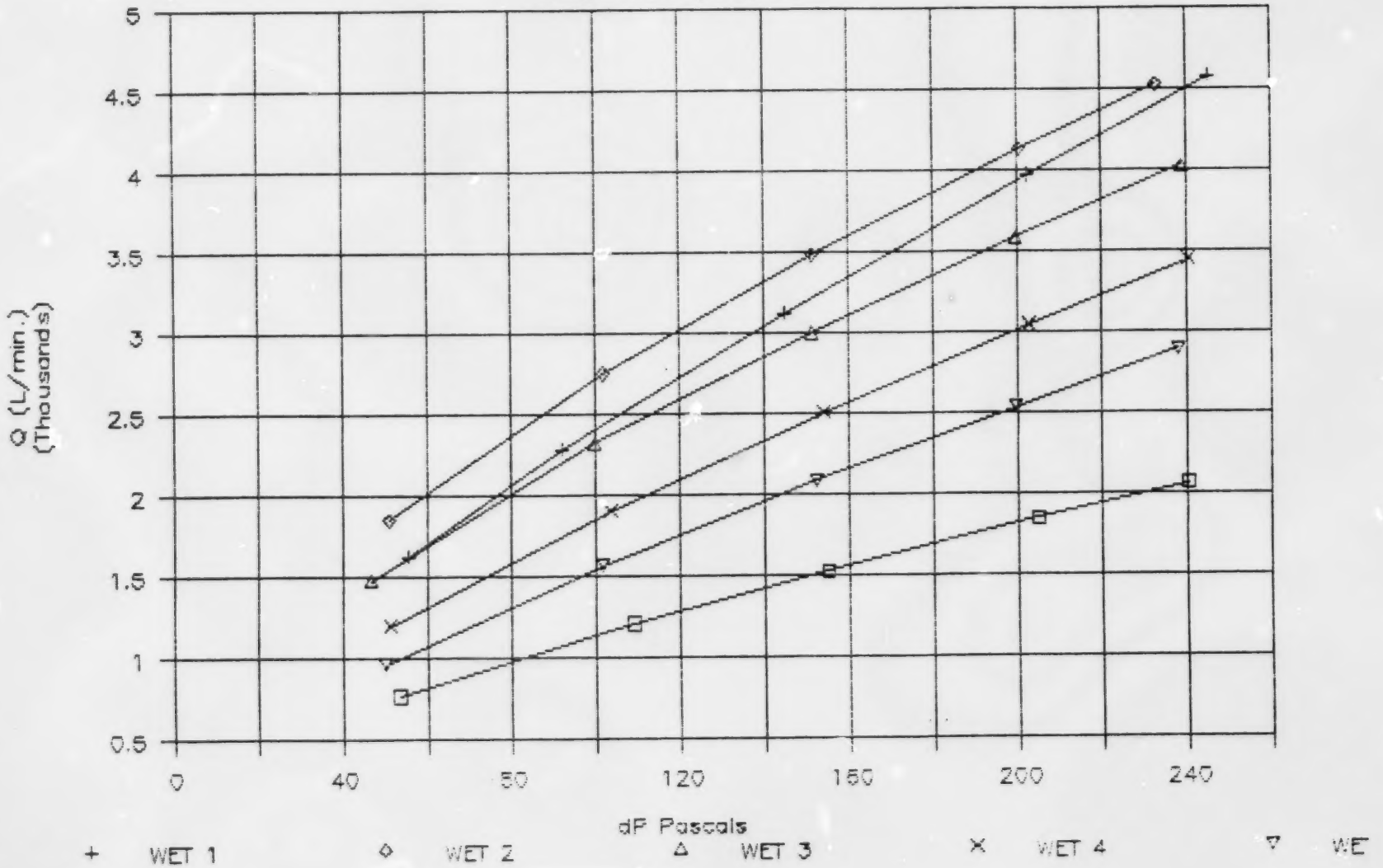

DRYING CHARACTERISTICS IN WALLS OF LOW-RISE RESIDENTIAL HOUSING

MILESTONE REPORT FOR TASK 4

July 3, 1987

Report 48714002

Submitted to:

CANADA MORTGAGE AND HOUSING CORPORATION

By:

ROWAN WILLIAMS DAVIES & IRWIN Inc.

GUELPH, ONTARIO

TABLE OF CONTENTS

		Page No.
1.	INTRODUCTION	1
2.	BACKGROUND	1
3.	METHODOLOGY	3
	3.1 Experimental Apparatus	3
	3.2 Experimental Procedure	3
	3.3 Description of Siding Samples and Deviation From Real Walls	5
4.	DISCUSSION OF RESULTS	6
5.	CONCLUSIONS	9

1. INTRODUCTION

This milestone report describes details of the work performed for Task 4 of the present contract. The objectives of this task are to measure air flow coefficients which relate pressure drop across various sidings to flow rate for (i) air-dry siding materials and (ii) siding materials when wetted by rain. The results and conclusions derived for this task compliment those of Task 3 and provide, among other items, inputs to the simulation computer program developed in Tasks 1 and 2.

2. BACKGROUND

Air flow in a wall, occurring between the siding and the backup sheathing, is produced in general by leakage paths across the siding material, at siding interfaces and at interfaces between the siding and other building materials. For reasons relating to experimentation and computer simulation, the actual flow condition in a wall is modelled and investigated by two simpler laboratory conditions, namely:

(i) flow along and behind the siding versus pressure drop (Task 3) and

(ii) flow across the siding versus pressure drop (Task 4).

Results of Task 3 are discussed in milestone report number 3 dated March 31, 1987 and in the accompanying addendum dated June 26, 1987. The flow coefficients for the present Task 4, illustrated in Tables 1(a) through 1(d), are discussed herein.

The purpose for obtaining these coefficients is to determine the mathematical relationship between pressure drop, P (Pascals) and flow rate, Q (liters/min). This relationship, arbitrarily treating Q as the independent variable (ie. the measured quantity) for a given P, may be expressed in the following form;

$$P = K1*Q + K2*Q^2 \qquad (1)$$

where K1 is the coefficient of the linear term in Q and K2 is the corresponding coefficient for the quadratic term in Q^2. Although other forms of this equation can be used, one advantage of this form is that relative magnitudes of K1 and K2 give some indication of relative proportions of laminar flow represented by Q and turbulent flow represented by Q^2 behind the siding.

These coefficients, in addition to those obtained for Task 4, are essential inputs to the air flow segment of our computer model developed as Tasks 1 and 2. The intent of this computer model, comprised of three sub-models, is to predict the drying characteristics of wood framed walls. The sub-models include a heat transfer model, an air flow model and a moisture flow model. Results from other portions of this project (Tasks 5 and 6) will be used in the moisture flow model as well.

The pressure drop P, described by equation (1) for across-the-wall flow, is produced to a small extent by material surface friction but mainly by expanding and contracting flow through the horizontal gaps or weep holes between siding panels. Figures 1(a) through 1(d) illustrate these geometries for the typical siding samples used in this study. As will be seen, such differences in geometry and gap spacings are largely responsible for differing coefficients among siding materials.

As illustrated in Tables 1(a) through 1(d), tests have been performed considering the following parameters: siding material (4 types), one flow direction from the outside towards the wall cavity, and the siding in air-dry and wetted states. These results have been normalized to account for the small size of tested samples. Flow rate has been normalized by the total length of gaps parallel to the siding in meters (i.e. total gap length = width of sample x number of horizontal gaps). Thus, the normalized coefficients in the tables are to be applied in conjunction with a flow rate per meter of horizontal siding length. Air flow coefficients derived for flow along-the-siding (Task 3) and flow across the siding (Task 4) have been normalized to produce the same units (i.e. dimensions of the coefficients). Thus, the coefficients for either case can be input to the computer simulation without modification.

3. METHODOLOGY

The air flow coefficients were determined with the use of an experimental set-up consisting of a pressure chamber, an orifice plate flowmeter, a vacuum source and associated instrumentation. The pressure chamber was constructed at the Guelph laboratory of RWDI.

3.1 Experimental Apparatus

The experimental arrangement used to measure air flow coefficients arising from air flow through the horizontal gaps between siding panels is described below.

A 0.81m square sample of siding consisting of numerous siding panels was mounted, with the weathering surface facing outward, into a rigid frame which was fitted into a cubical pressure chamber. Attached to the face opposite the sample siding was a 7.6cm orifice plate flowmeter used to measure the volume flow rate drawn out of the chamber by a vacuum source. The flow range of the vacuum was from a minimum of approximately 2 litres/minute (l/min) to a maximum of 2000 l/min. The orifice plate flowmeter was calibrated using rotameters traceable to NBS standards in a range of pipe flow Reynolds numbers of 1500 to 3000. This corresponds to a flow rate range of approximately 80 l/min to 200 l/min flowing through the pipe. In order to maintain accuracy in flow measurement, the rotameters themselves were substituted for the orifice plate flowmeter whenever the flow rate decreased below 100 l/min. Pressure measurements relative to laboratory (i.e. ambient) were taken behind the siding. Pressure differences were measured with a Validyne pressure transducer and associated control and display instrumentation.

3.2 Experimental Procedure

The siding materials tested include; masonite (a prefabricated compressed wood fibre), wood fibre backed aluminum, feather-edged lumber (referred to as

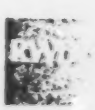

pine-board), and vinyl. Figures 1(a) through 1(d) illustrate the details and overall dimensions of these specimens.

Each siding specimen with pressure taps attached was placed in its unique rigid wood frame and set into place occupying one face of the pressure chamber. The remaining steps of the test procedure are itemized below:

(i) Once the sample was mounted into the test chamber a tare run was performed by sealing the siding face with a polyethylene sheet. This step, performed for the maximum pressure difference, measured the amount of leakage caused by the test apparatus excluding the test siding.

(ii) The polyethylene sheet was removed and a test run was performed with the siding in an air-dry condition for five pressure drops covering a practical full-scale range up to 300 Pa.

(iii) Next, the wall was sprayed continuously for 15 minutes with tap water from a standard hose to simulate rain hitting the siding. During the entire spraying period a pressure difference across the siding of 50 Pa was maintained.

(iv) The wetted siding was allowed to drain for 5 minutes without a pressure difference across it and a repeat test as in step (ii) was performed for five pressure drops.

(v) At the end of Step (iv) the sample was allowed to drain for 15 minutes more and then retested as in step (ii) for five pressure drops. This step was inserted into the procedure to investigate the effect of drying on restoring the original pressure regime.

These steps constitute a complete test procedure performed on all four different siding material types.

3.3 Description of Siding Samples and Deviation From Real Walls

As indicated previously four sidings are considered in this portion of the study, namely: masonite, wood fibre backed aluminum, pine board and vinyl. Although the dimensions of each sample vary slightly the test chamber which receives the samples is 0.81m square. Any variation in sample dimensions is accommodated by the rigid frame insert.

Differences in sample size and attachment details between model and full scale could potentially introduce differences in gap spacings and associated measurement errors under large pressures or when material expands abnormally from moisture absorption. However, the geometry of the test apparatus, sample size and test parameters were selected to minimize any significant errors due to model scale. In particular, the maximum test pressure, was maintained at relatively low values (i.e. maximum pressure of 300 Pa) to represent frequently occurring wind speeds (i.e. one or more occurrences per day). These pressures would not produce significantly different siding deflections between model and full scale. These considerations do not influence weep holes, which also serve as ventilation holes, existing in vinyl and aluminum siding samples, see Figures 1(b) and 1(d).

All four siding samples have a continuous horizontal gap at every panel interface. Masonite panels have the largest overlap of approximately 2.8cm. Aluminum, pine and vinyl panels have 2.2cm, 1.6cm and 1.3cm overlaps respectively. In addition to horizontal gaps, vinyl and aluminum samples have small weep holes (ventilation holes) as shown in Figures 1(b) and 1(c).

Horizontal gaps play an important role in determining air flow rate and pressure drop across the sidings (i.e. air flow coefficients). This is particularly true in view of the effects of pressure differences in changing the gap spacing and water filling the gaps.

The pine siding sample was assembled using flat head nails at panel edges and where panels overlap. This deviates from practice where round head nails are

commonly used to produce significantly wider gaps. However, the pine sample with narrower gaps was tested because it represents a more severe test of air flow and drying potential. As will be seen below, the outcome of this test indicates that of the four materials tested, pine siding has the greatest air flow and associated drying capacity. Air flow and drying potential are expected to be significantly greater with round head nails and the resulting larger gaps.

Details of geometry and mounting are illustrated in Figures 1(a) through 1(d).

4. DISCUSSION OF RESULTS

Numerous useful conclusions can be drawn from the tabulated coefficients in Tables 1(a) through 1(d) and plotted curves illustrated in Figures 2(a) through 2(d).

The K_1 coefficients corresponding to the linear term in Q are consistently greater than the K_2 coefficients corresponding to the square term by a factor of 500 or more. Only in one instance for vinyl siding does this factor drop to 315. By inspecting these coefficients in relation to equation (1) it becomes evident that the linear term in Q dominates for flows less than 315 l/min per meter of wall (in the case of vinyl) and the squared term in Q influences higher flow rates. This suggests that flow is increasingly laminar below 315 l/min/m and increasingly turbulent above that level.

The K_1 coefficients for all materials are lowest for the dry run, increase for the first wet run (very little drying time) and decrease again for the second wet run (greater drying time). This K_1 progression is inversely related to flow rate. Thus, the flow is largest for the dry case, decreases dramatically in the first wet run and increases to near the dry level for the second wet run. This observation applies in varying degrees to all samples and suggests that for a given pressure difference the flow decreases when water plugs the gaps and increases again when the gaps dry out (or drain). Further, the wetting and drying cycle for some materials (i.e. adsorbing materials such as wood or wood fiber products) may cause permanent or at least long lasting deformations in siding geometry and gap spacing. In other

words, a hyterisis effect may exist in some materials. This effect is best illustrated by wood fibre backed aluminum siding because of the loose and fibrous nature of the backing. The normalized coefficients in Figure 1(d) indicate that the coefficients for the second wet run are significantly greater than the original dry run. Evidently, this material requires more drying time to return to its original flow regime. These characteristics are qualitatively illustrated in Figures 2(a) through 2(d).

Depending on the relative magnitudes of K_1 and K_2 for a particular siding, equation (1) indicates that at high flow rates the $K_2 \times Q^2$ term, representing turbulent flow, significantly influences the flow regime. But at lower flow rates, the $K_1 \times Q$ term, representing laminar flow, dominates the flow. This outcome suggests that flow across siding gaps for most cases is mainly laminar and that the flow becomes increasingly so as the air flow rate and gap spacings are reduced by water retention along the gap.

In comparing air flow coefficients among the four different siding materials the following observations are made:

(i) in the air-dry cases both K_1 and K_2 coefficients are largest for vinyl and decrease for aluminum, masonite and pine. Thus, flow rates through the gaps of these siding materials, which are inversely proportional to the coefficients, are largest for pine and least for vinyl.

(ii) the same ordering of coefficients and flow rates occurs for both the first and second wet runs after 5 minutes and 15 additional minutes of drying time respectively.

The coefficients, as illustrated in Tables 1(a) through 1(d), have been used in equation (1) to generate representative plots in Figures 2(a) through 2(d). These figures graphically illustrate the effect of water on siding samples over practical ranges of flow rate and pressure drop. For a given pressure drop the flow rate is greatest for the dry sample, is least for first wet run (least drying time) and is

intermediate for the second wet run (greater drying time). The spread of the curves qualitatively indicates the magnitude of the effect of wetting and the rate of drying. Thus, the masonite siding seems to return to its near air-dry condition most quickly followed by vinyl and aluminum which show similar behavior.

Figure 2(d) suggests that pine siding presents somewhat of a special case. Over a smaller pressure range (0-200 Pa), as compared to other siding materials, the three curves for pine siding are much less separated, especially for the lower half of the flow rate scale (500 l/min). Thus, the effect of water, either absorbed or retained by capillary forces, is less pronounced in pine siding. Furthermore, at flow rates above approximately 500 l/min pine siding illustrates unexpected behavior. The first wet run, having the least drying time, allows more flow than either the air-dry sample or the sample after a longer drying period. This outcome, although not yet understood, can likely be explained by the material properties of pine siding, the rate of moisture absorption and dimensional changes under pressure and moisture absorption.

The curvature of plots for all four samples indicates the effects of the $K_2 \times Q^2$ term in equation (1). Curves for pine, masonite and vinyl which are concave upwards have a positive K_2 coefficient. Two curves for aluminum and one curve for vinyl, which are concave downward, have a negative K_2 coefficient. A negative K_2 coefficient suggests that flow through the gap increasingly occurs by blowing through the water layer at high pressure drops. This is evident in the wet #1 curve of aluminum siding which shows significantly more flow at its upper end with decreasing pressure differences. Conversely, a positive K_2 coefficient suggests that pressure differences are not sufficient to blow through the water layer and hence build up with little increase in flow rate.

5. CONCLUSIONS

The above discussion leads to the following conclusions:

(i) In all cases the $K_1 \times Q$ term dominates the fitted relationship within the measured range of flow rate Q versus pressure drop P. This implies that, in most cases, the flow across the siding gaps is mainly laminar and only at the highest flow rates does the flow become significantly turbulent as influenced by the $K_2 \times Q^2$ term.

(ii) The flow rates through siding gaps for wet and dry runs are greatest for pine followed by masonite, aluminum and vinyl. This suggests that the drying potential for the inner wall (i.e. the components behind the siding) is greatest for the pine siding. The drying characteristics of pine siding are expected to be better yet for the gap spacings determined by round head nails found in practice.

(iii) Each of the four siding materials demonstrates, to a varying degree, the tendency to much lower flow rates through the siding gaps of wetted siding and a return to near normal (i.e. normal implying the dry state) flow rates upon drying. The drying time for a siding to return to a normal (air-dry) condition and drying capacity can be estimated to be in the order of several hours depending on siding material.

(iv) A hysterisis effect may be responsible for permanent or long term geometrical distortion of some siding materials susceptible to large moisture retention.

ROWAN WILLIAMS DAVIES & IRWIN Inc.

Vincent Ferraro, P.Eng.
Project Engineer

Glenn D. Schuyler, P.Eng.
Principal

Table 1(a): COEFFICIENTS FOR FLOW THROUGH WALL

MATERIAL: masonite

TEST CONDITION	RAW COEFFICIENTS		NORMALIZED COEFFICIENTS	
	K1	K2	K1	K2
dry	2.872E-01	1.320E-03	1.097E-01	1.925E-04
wet #1	7.053E-01	5.967E-04	2.694E-01	8.706E-05
wet #2	4.353E-01	9.413E-04	1.663E-01	1.373E-04

Table 1(b): COEFFICIENTS FOR FLOW THROUGH WALL

MATERIAL: vinyl

TEST CONDITION	RAW COEFFICIENTS		NORMALIZED COEFFICIENTS	
	K1	K2	K1	K2
dry	1.432E+00	1.058E-02	6.429E-01	2.130E-03
wet #1	6.628E+00	-3.539E-02	2.975E+00	-7.129E-03
wet #2	2.140E+00	5.593E-02	9.603E-01	1.126E-02

Table 1(c): COEFFICIENTS FOR FLOW THROUGH WALL

MATERIAL: aluminum

TEST CONDITION	RAW COEFFICIENTS		NORMALIZED COEFFICIENTS	
	K1	K2	K1	K2
dry	4.362E-01	1.243E-03	2.025E-01	2.678E-04
wet #1	4.087E+00	-1.586E-02	1.897E+00	-3.418E-03
wet #2	1.727E+00	-2.366E-03	8.015E-01	-5.097E-04

Table 1(d): COEFFICIENTS FOR FLOW THROUGH WALL

MATERIAL: pine

TEST CONDITION	RAW COEFFICIENTS		NORMALIZED COEFFICIENTS	
	K1	K2	K1	K2
dry	6.399E-02	1.031E-04	2.101E-02	1.112E-05
wet #1	9.468E-02	4.345E-05	3.109E-02	4.685E-06
wet #2	5.922E-02	1.464E-04	1.945E-02	1.578E-05

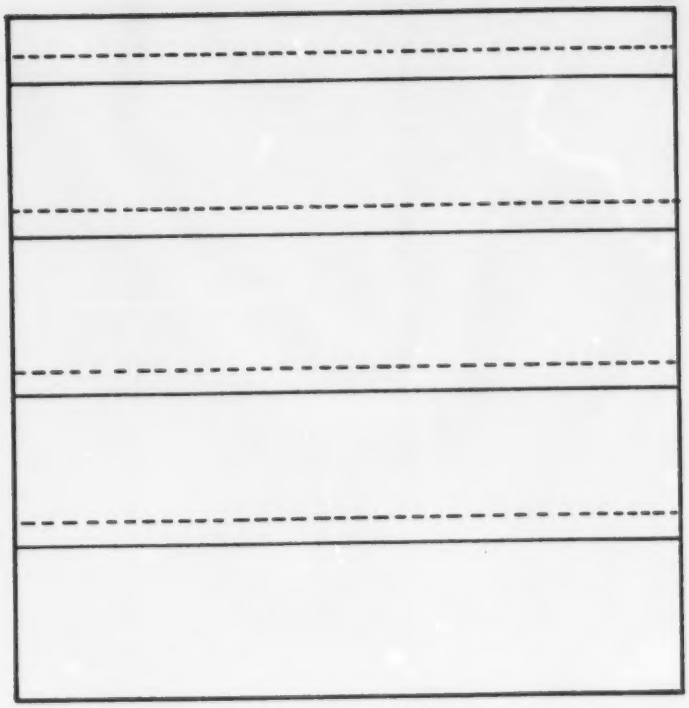

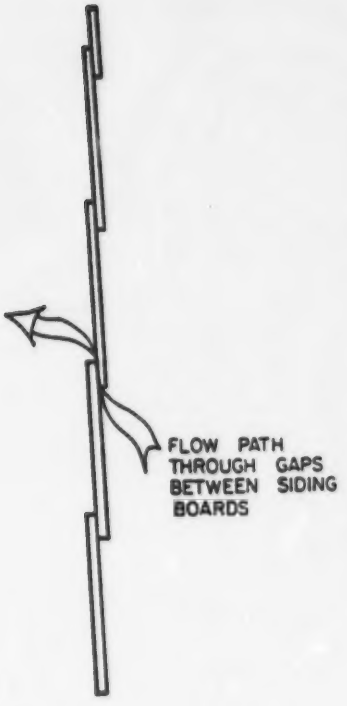

FIGURE I(A) MASONITE SIDING

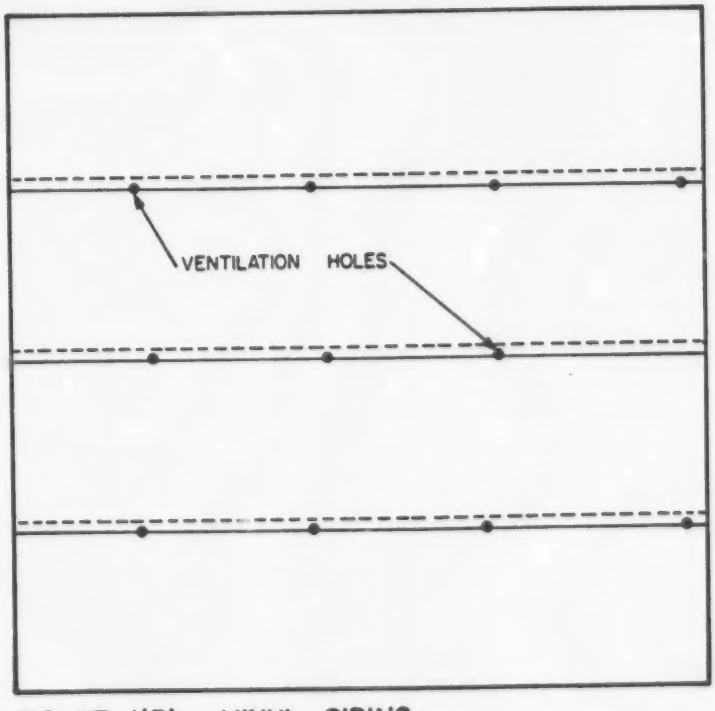

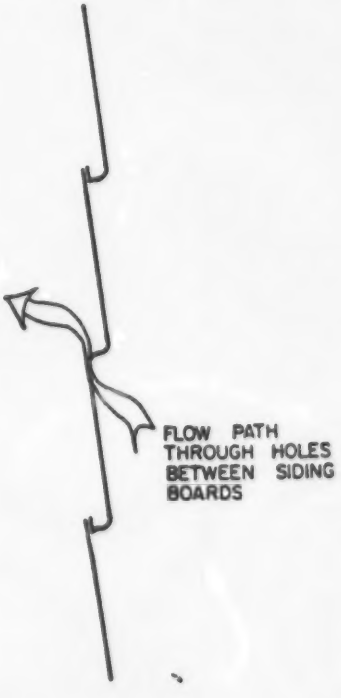

FIGURE I(B) VINYL SIDING

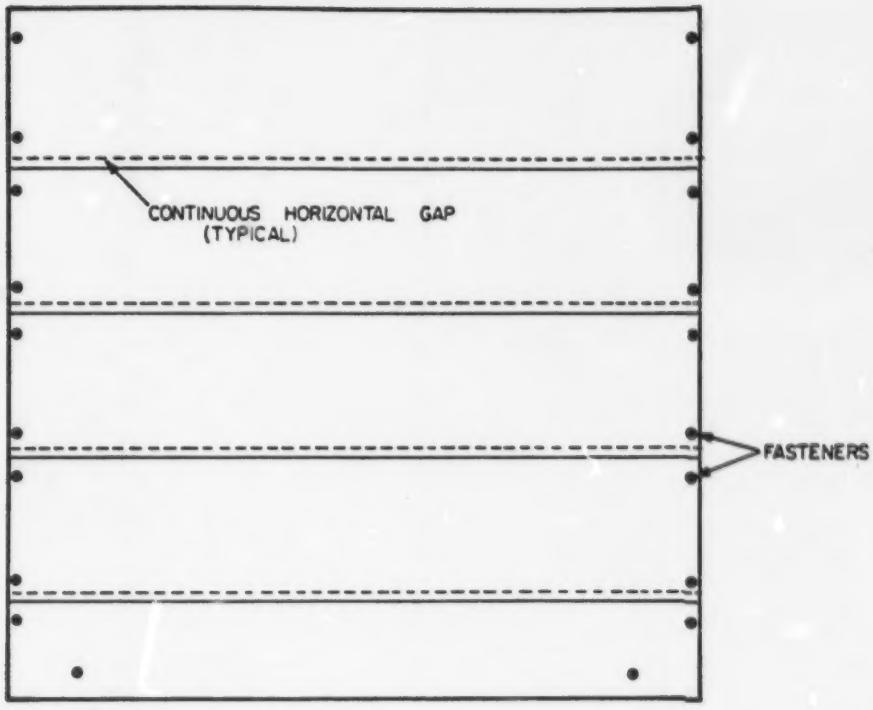

FIGURE I(C) PINE SIDING

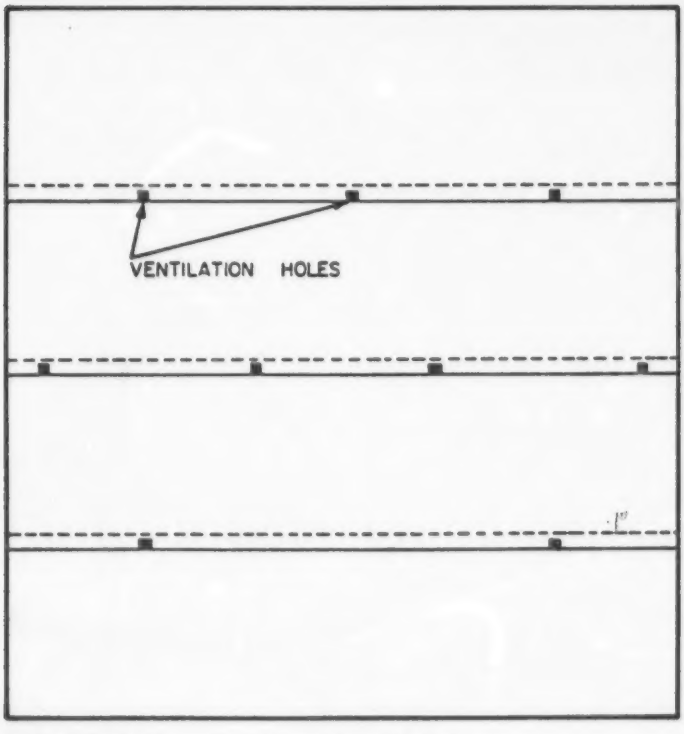

FIGURE I(D) ALUMINUM SIDING
(BACKED WITH TENTEST)

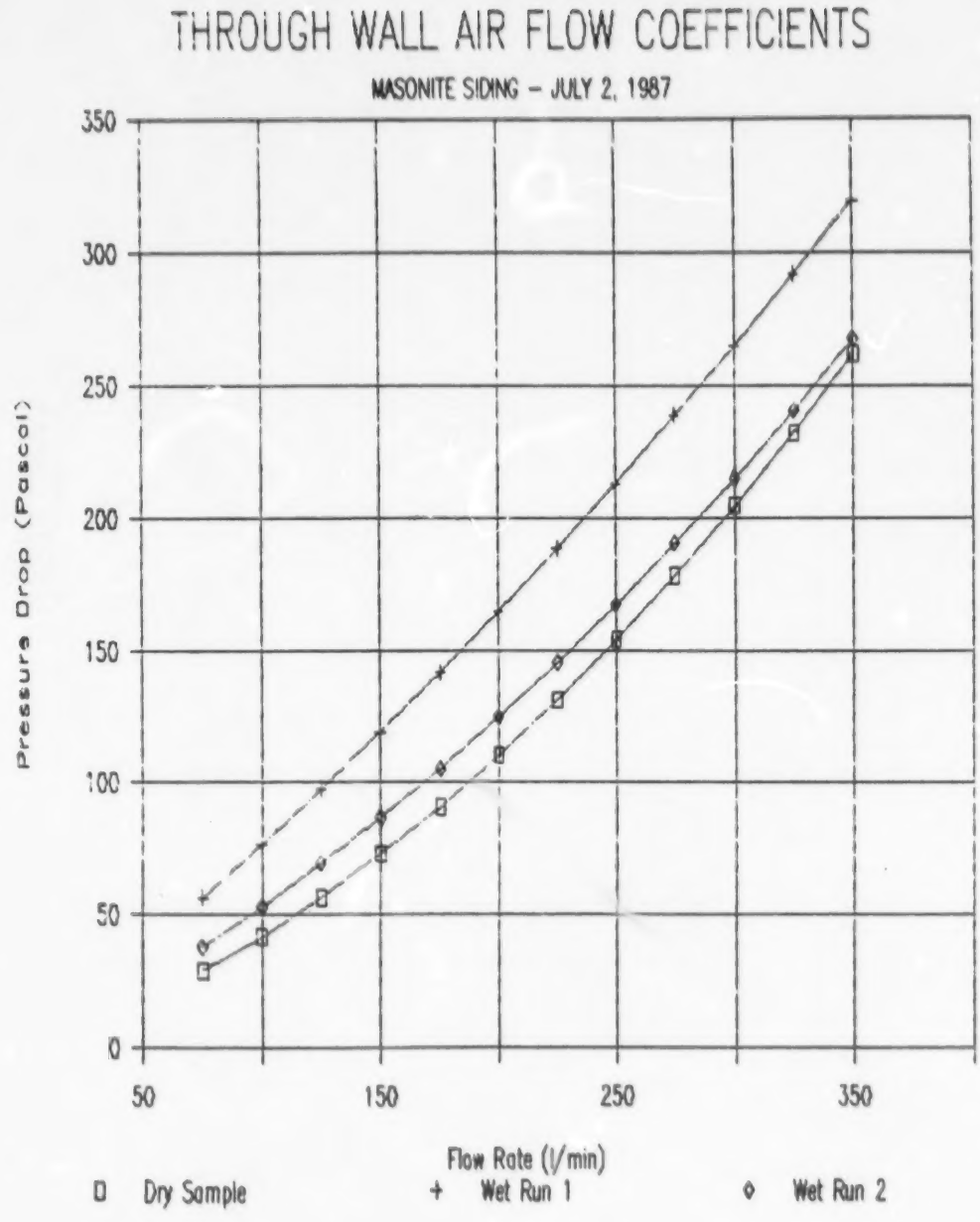
THROUGH WALL AIR FLOW COEFFICIENTS
MASONITE SIDING – JULY 2, 1987
Pressure Drop (Pascal)
350
300
250
200
150
100
50
0
50
150
250
350
Flow Rate (l/min)
Dry Sample
Wet Run 1
Wet Run 2

FIGURE 2(a)

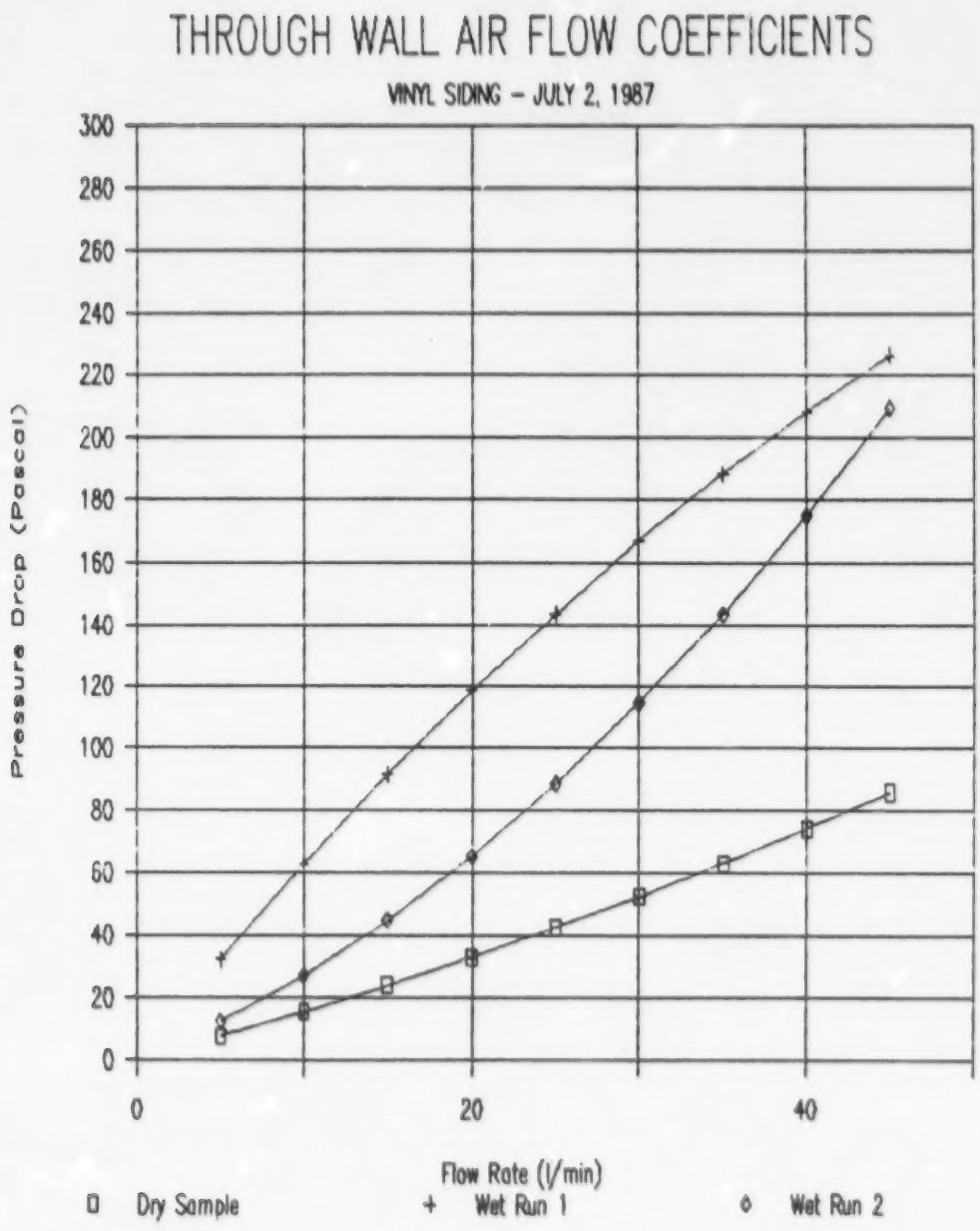
THROUGH WALL AIR FLOW COEFFICIENTS
VINYL SIDING - JULY 2, 1987
Pressure Drop (Pascal)
300
280
260
240
220
200
180
160
140
120
100
80
60
40
20
0
0
20
40
Flow Rate (l/min)
Dry Sample
Wet Run 1
Wet Run 2

FIGURE 2(b)

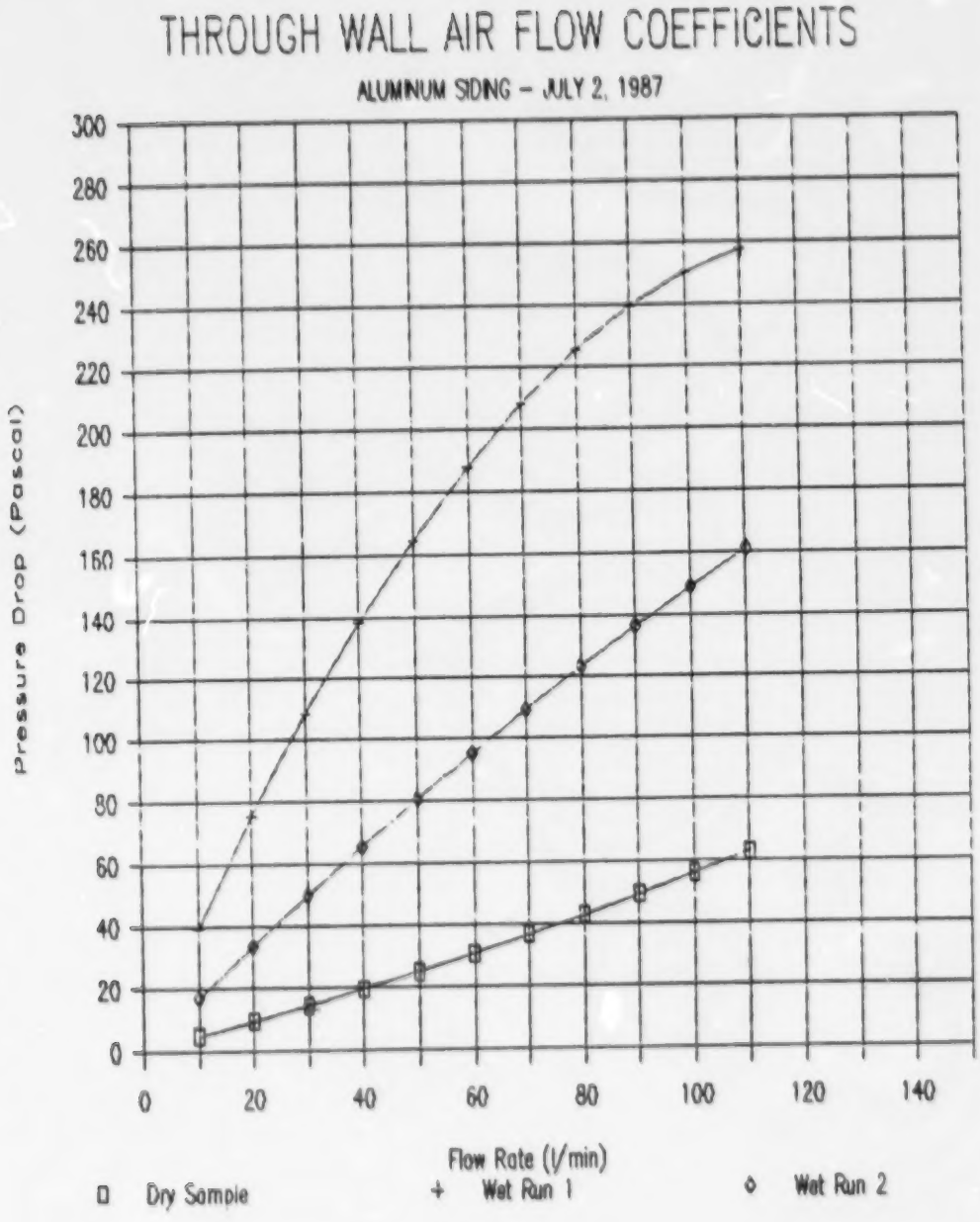
THROUGH WALL AIR FLOW COEFFICIENTS
ALUMINUM SIDING – JULY 2, 1987
Pressure Drop (Pascal)
300
280
260
240
220
200
180
160
140
120
100
80
60
40
20
0
0
20
40
60
80
100
120
140
Flow Rate (l/min)
Dry Sample
Wet Run 1
Wet Run 2

FIGURE 2(c)

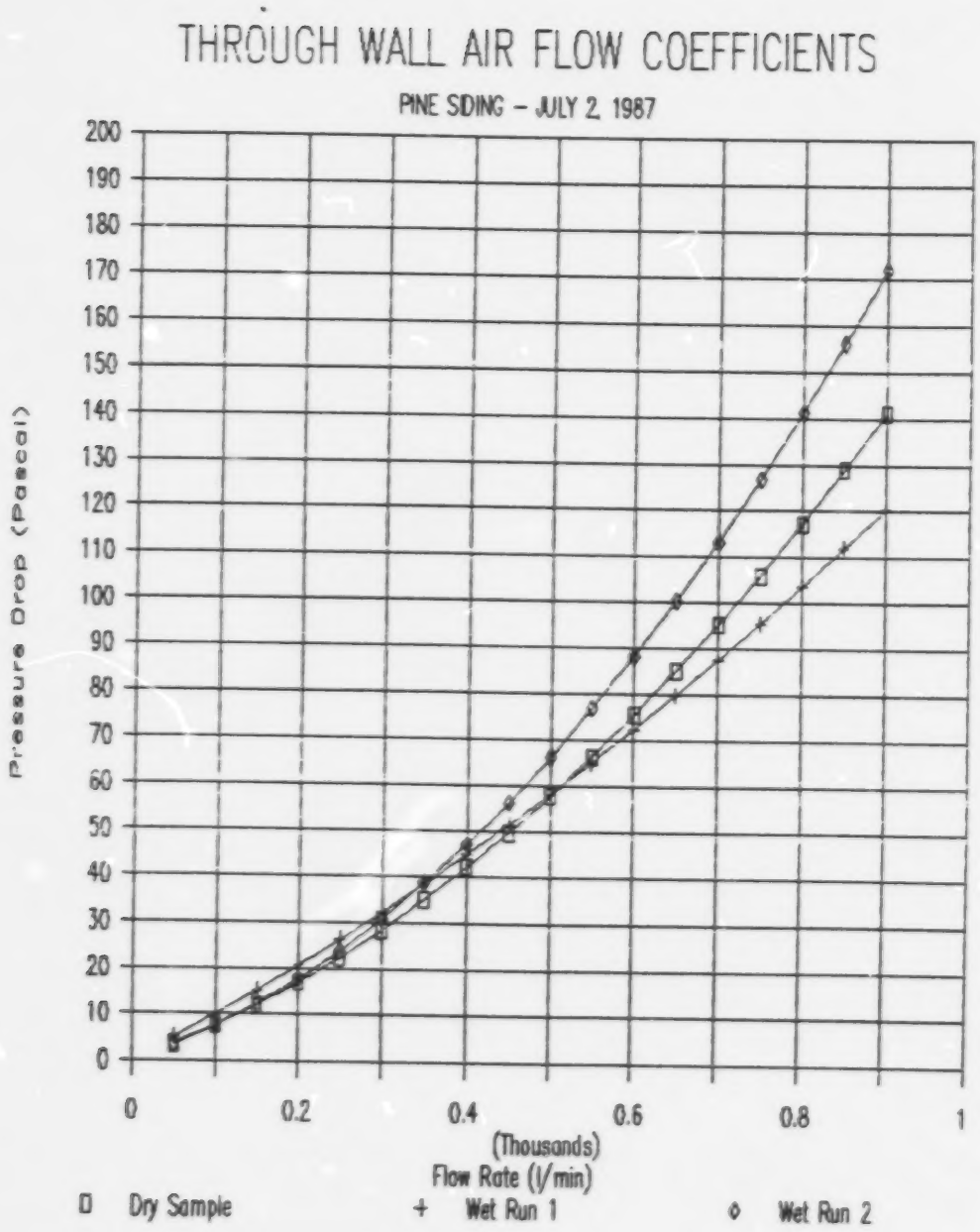
THROUGH WALL AIR FLOW COEFFICIENTS
PINE SIDING – JULY 2, 1987
Pressure Drop (Pascal)
200
190
180
170
160
150
140
130
120
110
100
90
80
70
60
50
40
30
20
10
0
0
0.2
0.4
0.6
0.8
1
(Thousands)
Flow Rate (l/min)
Dry Sample
Wet Run 1
Wet Run 2

FIGURE 2(d)

APPENDIX E

DRYING CHARACTERISTICS IN WALLS OF LOW RISE RESIDENTIAL HOUSING

MILESTONE REPORT FOR TASK 5: WATER ADSORPTION OF VARIOUS BUILDING MATERIALS

December 21, 1987
Report 48714005

Submitted to:
CANADA MORTGAGE AND HOUSING CORPORATION

By:
ROWAN WILLIAMS DAVIES & IRWIN Inc.
GUELPH, ONTARIO

TABLE OF CONTENTS

	Page No.
1. INTRODUCTION	1
2. BACKGROUND	1
3. METHODOLOGY	2
3.1 Experimental Apparatus	2
3.2 Experimental Procedure	3
3.3 Description of Samples and Experimental Difficulties	4
4. DISCUSSION OF RESULTS	5
5. CONCLUSIONS	7

1. INTRODUCTION

This milestone report describes details of the work performed for Task 5 of the present contract. The objectives of this task are to investigate and measure the moisture adsorption characteristics of various building materials commonly used in residential wood frame wall construction. Results and conclusions derived from this task provide inputs, along with those from other tasks, to the computer simulation developed in Tasks 1 and 2. Evaporation characteristics of building materials will be investigated in Task 6.

2. BACKGROUND

The interior components of wood framed walls can be wetted in various ways; the most common being leakage of moist interior air through interior walls and penetration of wind driven rain through the exterior building envelope (i.e. siding). In order for moist inside air leakage to significantly wet materials the temperature inside the wall must be below its dew point. Depending on the length of the wetting period, various building materials will adsorb moisture at different rates until their saturation point is reached. The amount of moisture adsorbed and time required to reach saturation depend on the initial moisture content, the volume of internal voids and the magnitude of adhesive and surface tension forces acting between the water molecules and the material matrix. Any further wetting will allow beads of water to form which will eventually be drained by gravity along the surface of the material. If the material is not completely saturated, the beads will be partially or completely adsorbed as they move over the unsaturated area. This procedure will continue until the material is saturated. Beyond the saturation point, moisture will drain down the face of the material and drip away along the bottom edge. This drainage effect has been modelled in the simulation, but no information on the level at which it takes place is available from the literature. This task attempts to give some representative numbers that can be used pending more detailed investigations.

The purpose of tests performed for Task 5 is to measure the amount of water which can be adsorbed or retained (i.e. by beading) by various building materials used in residential wood frame construction. Results are presented on a percentage weight basis. This investigation was not concerned with determining the rate at which moisture is adsorbed.

The intent of the computer simulation program, comprised of three submodels, is to predict the drying characteristics of wood framed walls. These submodels are: a heat transfer model, an air flow model and a moisture flow model. Results from the present work will be used as input to the moisture flow sub-model to set an upper limit to the amount of water capable of being held (i.e. by adsorption and surface tension) by the material. The model retains any water above the material fiber saturation in a surface layer. Since the hygroscopic material can only begin to dry when the surface layer disappears, the model monitors evaporation from or condensation to this layer on an hourly basis. Task 6 results will also provide input to this submodel. Input parameters for the air flow sub-model have been generated in Task 3 and 4.

Six building materials have been investigated. These include: Tentest (weather side), Tentest (back side), "15 lb" building paper, pine veneer, industrial poplar veneer and a mohogany veneer. Sample dimension and test procedures are described in the following section.

3. METHODOLOGY

The moisture adsorption characteristics were determined with the use of a humidity box, a heat source and water to generate water vapour and a strain gauge with associated instrumentation to continuously measure sample weight. The weight was monitored with a video camera and recorded over the testing period with a video recorder.

3.1 Experimental Apparatus

The experimental arrangement used to measure material moisture capacity is illustrated in Figure 1 and in Photographs 1 and 2.

Samples of the six materials described previously were cut to 25 cm x 25 cm sizes. The veneer samples were all approximately 4 mm in thickness. The Tentest samples were cut to approximately 4mm thicknesses from commercially available 15 mm tentest boards. Building paper ("15 lb") was also cut from commercially available stock. The thinnest possible materials were selected or cut to represent a thin surface layer consistent with the computer simulation. The samples were tested for 16 to 24 hours.

Once cut, the samples were glued to a plexiglass backing plate which was strenthened by galvanized steel 'Z' sections to prevent warping. In this way only one surface of the material could adsorb moisture. The plate and sample assembly were hung onto a metal rod which was fixed into a concrete block wall. Strain gauges were mounted onto the rod and calibrated to measure sample weight. The strain gauge was electrically connected to a power source and amplifier. The output from the amplifier was fed to a voltmeter for continuous monitoring by a video camera and video tape recorder.

Water vapour was generated by heating a tank of water to near the boiling point. The vapour was conducted to the humidity box, constructed of 5 cm styrofoam insulation, and allowed to flow over the sample. The humidity box with a flexible connection to the vapour source, was brought into close proximity to the sample and plate assembly hanging from the strain gauge scale. Typically, the gap between the sample and the box was set to 5mm. Water vapour was directed towards the bottom edge of the sample equally along a narrow horizontal gap in the humidity box. The water vapour passed over the relatively cool sample, partially condensing over it and the remainder escaping around the sides and top of the sample. No moisture was seen to condense on any part of the plate assembly except for the intended sample face. The entire set-up is illustrated in Figure 1 and Photographs 1 and 2.

The experiment was conducted in an area whose temperature and relative humidity were measured to be 30°C and 70% respectively.

3.2 Experimental Procedure

The test procedure followed for each sample building material started by obtaining the weight of the air dry sample. Contact cement was then applied to both the back side of the sample and to the backer plate. After a short drying period the two glued surfaces were brought into contact under uniform pressure for a minimum 12 hour period. The entire assembly was weighed to obtain a total dry weight before testing. The plate assembly was hung onto the strain gauge weigh scale. Finally, a relative adjustment of the humidity box and the plate assembly was required to set the gap between the two components at approximately 5mm. The total weight of the assembly was recorded continuously by a video camera observing a voltmeter attached to the strain amplifier output. The video recordings were later manually analyzed and subsequently plotted (i.e. % sample weight gain versus elapsed time). The difference between the instantaneous weight of the assembly and the dry weight constituted the moisture adsorbed. These steps constituted a complete test procedure performed on all six samples.

3.3 Description of Sample Selection and Experimental Difficulties

Sample types were selected based on the materials typically forming the inside wall cavity in wood frame construction. The overall sample dimensions were chosen somewhat arbritraiiy but mainly for convenience of constructing the test apparatus. One veneer of a standard 15mm plywood (i.e. approximately 5mm) with the backside covered in glue, representing the glue layer in the plywood, was used for testing in the case of the pine, poplar and mahogany samples. The intention of glueing the backside of samples to the plate was in part to provide support, but also to prevent moisture from forming on inside surfaces of the plate assembly.

The experimental procedure followed in the present tests provides a source of water vapour which differs from natural sources occurring in actual walls. The

vapour produced in the experiment is generated by boiling water. This hot vapour is different from vapour in actual walls in two ways. Firstly, the relatively hot condensed water is lower in viscosity as compared to water found in walls by factors ranging from 3 for the lowest inside wall temperatures expected to 1.5 for the warmest temperatures expected. Using thermocouples, temperatures measured at numerous locations on the sample surfaces were found to be near 50°C in comparison to inside wall temperatures ranging between -10°C to 30°C. A second consequence of using heated steam is that higher sample temperatures cause the sample dimensions and pore sizes to increase.

Since we are dealing with large fluctuations in moisture content, the effect of temperature on pore size is a relatively small effect. In the cross-grain dimension, the dimensional variation due to moisture content changes would be at least an order of magnitude greater than that due to temperature variation.

The reduced viscosity of water in the experiment due to the higher temperature would cause a higher rate of drainage within the fibres of the material. Since this experiment is dealing with the magnitude of moisture storage, the internal drainage rate is immaterial. If the internal drainage is retarded, then surface drainage would be increased.

Since surface tension and density vary only slightly with temperature (i.e. less than 10% over the expected temperature range), the effect on water bead size and surface storage is expected to be small.

4. DISCUSSION OF RESULTS

The results of the present task are presented in Figures 2 through 7. These figures generally illustrate continuously increasing material weight due to moisture adsorption over time until equilibrium is reached.

The Tentest samples, both with the weather face and inner face exposed, adsorb the greatest percentage of water of all six materials tested. The amount of

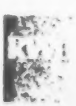

water adsorbed for both cases is approximately 2.8 times the sample weight, i.e. 280%. As shown by the relative slopes of the two samples, both surfaces adsorbs moisture at approximately the same rate. Photographs numbers 7 and 8 illustrate the backside of the Tentest material immediately after testing. A visual examination during and after testing revealed no beading on the surface of either samples. Instead, when saturation was achieved, condensed water seemed to flow by gravity to the bottom of the sample and drip away along the edge. Water accumulation can be seen in the photographs as the dark horizontal band near the bottom of the sample. The height of this band, referred to here as the capillary height, is governed by a system of forces which are of similar magnitude irregardless of sample size. Therefore, the capillary height, seen in the small test samples, is expected to be the same in actual wall sheathing of the same material. As a result, the moisture content in the area above this height would be lower than the average calculated herein and the moisture content within the capillary height area would be at a higher level than calculated.

The Mahogany veneer sample adsorbs approximately 80% water based on the sample weight. Photograph 4 illustrates the Mahogany sample at test completion. Beading and drainage of water was clearly observed during testing.

The Pine veneer sample adsorbed approximately 120% water based on the sample weight. Photograph 3 illustrates the sample at completion of testing. Beading was observed only on segments of the sample at any time during testing. This is thought to be caused partly by the horizontal orientation of the grain and partly by the material properties themselves. At completion of testing the lowest horizontal segment seemed to be heavily laiden with water: an indication of internal drainage.

For the building paper sample (15 lb variety) the relative weight increase was approximately 65%. As illustrated in Photographs 5 and 6 beading and surface drainage of condensed water occurred significantly after saturation of the sample.

The poplar veneer sample adsorbs approximately 75% water based on the air-dry sample weight. Only localized beading of water was observed during the testing. Much like the pine and mahogany samples, drainage occurred internally through the material to the bottom edge of the sample.

The troughs illustrated in the moisture adsorption curves of pine and building paper are caused by the lag time required to begin vapourizing water added to a depleted tank. They are therefore not related to material performance.

Determining material properties for wood products can be expected to generate results having significant scatter. This scatter and lack of accurate repeatibility result from the influences of the multitude of natural forces responsible for tree growth as well as from the variations in processing wood to produce commercial products. These effects manifest themselves in the variations of material properties such as differences in long grain versus across grain properties, wood density and material inhomogeneity such as knots. As well changing properties under repeated influences, such as temperature, i.e. hyterisis, also increases scatter in measurements.

Capillary rise is directly related to capillary diameter. Within wood fibres the equilibrium capillary height is enormous because of the small capillary diameter. However, in a dried and processed surface layer of sawn lumber, the large voids and surface checks constitute large diameter capillaries resulting in the very high moisture content band observed in the test samples.

Internal drainage and capillary rise are internal flow mechanisms existing in the porous materials studied. Drainage in porous materials consists of internal and surface components. Whereas the internal drainage rate is constant above a certain amount of moisture availability, surface drainage largely depends on the rate of moisture supplied. Capillary rise is a moisture retention mechanism which depends on material pore structure and relative humidity (RH). Thus, every

material having a unique pore structure will have a characteristic capillary height at a specified RH. The relative humidity near samples of the present test is assumed to be 100% since vapour-saturated air is used to wet the materials. Based on this discussion, moisture adsorption by materials may be considered to comprise moisture retained on the surface and moisture adsorbed by the internal pore structure.

A separate test was performed to identify the approximate capillary heights of four samples as well as the moisture retention, i.e. weight of moisture retained within and above the capillary height. The four samples include veneers of; industrial Poplar, laboratory prepared Poplar, Mahogany and Tentest. These results are presented in Table 1. It is emphasized that the results are approximate, being derived from one sample of each material. Results will vary considerably from sample to sample and a complete test would require a much larger sample population.

According to the results and discussion above, the bottom edges of sheathing in actual walls can be expected to accumulate water in greater proportion relative to equal areas above. The forces producing this effect, identically to the laboratory samples, are internal drainage driven by gravity, and capillary forces (i.e. adhesion between the material and water as well as cohesion among water molecules). This second effect is also responsible for retaining additional water in the bottom layer. Furthermore, the amount of moisture retained by a sample and the height of the band is dependant on the bottom edge geometry. For instance, a bevelled bottom edge may promote drainage and cause less surface water retention as compared to a squared edge. Since the magnitudes of the forces per unit width of material are similar in the test samples as in the real wall materials, the capillary heights are also expected to be similar for a given edge geometry. Therefore, small material samples used to represent actual sizes will give somewhat erroneous moisture content readings because of the incorrect proportion of water held near the bottom of a material as compared to the total adsorbed moisture.

In actual walls, a free edge is not likely to exist. Nevertheless, the same mechanisms are expected to produce moisture banding wherever a horizontal interface exists, between two segments of the same or different materials, or where a sheathing element contacts a horizontal surface. The consequences of this outcome in actual walls is to keep the bottom layers of sheathing at a higher moisture content than the remaining surface. Consequently, these areas would be more likely to suffer deterioration as compared to the remainder of the surface. In addition, adjacent or supporting components, studs for instance, may also suffer some deterioration due to the moisture present in the sheathing material.

Water that accumulates on horizontal surfaces can largely be removed by mechanical drainage to the outside. With this in mind, any material or construction practice that improves drainage, either by internal or surface flow, and that maintains some moisture diffusion capacity for local drying, should be considered. For instance, minimizing horizontal joints in sheathing would promote internal drainage in some materials. Since moisture flow along the sheathing is unaffected by vertical joints, their placement could be according to convenience. Clearly, materials which have poor internal drainage, relying mostly on surface drainage to discharge water would not be affected, nor would suffer, from such a practice.

The above discussion considering the possible benefits or harmful effects of the horizontal banding of water highlights the difficulty of drawing conclusions of real walls system by considering only a few parameters or outcomes in isolation. For instance, the effect of moisture accumulation may be considered harmful in one case where deterioration is foreseen in baseplates, say, and beneficial in another because most of the sheathing is well drained. The eventual outcomes in an actual wall will depend on the relative importance of all effects and their influences on each component of the wall.

The outcomes of this segment of the study will influence the computer model simulation program and our overall understanding of the problem as well. The surface drainage of porous materials under gravity forces can easily be treated in the computer model. Moisture overflow in one vertical element during one time

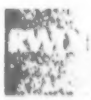

increment (i.e. one hour) could in part be passed to the element below according to the moisture contents in the previous hour. Furthermore, elements forming the bottom layer can be maintained at a consistently higher moisture content. Any water tending to puddle at the base of a wall layer can also be represented as a moisture source and sink. Any air leaking into or out of the cavity would also be influenced by this moisture source/sink.

5. CONCLUSIONS

Work performed for this task can be summarized by the following conclusions:

(i) the order of water adsorption based on weight of dry sample is: Tentest, either side 280%, pine veneer 120%, mahogany veneer 80%, poplar veneer 75% and building paper 65%.

(ii) although not a primary concern in this experiment, the order for the time required to reach 90% of saturation is: Tentest, both sides 5.5 hrs, poplar veneer 8.5 hrs, building paper 10 hrs, pine veneer 13 hrs and mahogany 14 hrs. These adsorption rates have been adjusted where appropriate to account for the time required to vaporize water.

(iii) in some cases, for Tentest, pine and poplar samples, beading was not observed or observed in small quantities. For others such as mahogany veneer and especially building paper, beading occurred in greater amounts.

(iv) as observed in most samples drainage of condensed water either through the sample material or over its surface (i.e. beading) produced a horizontal area at the bottom of all samples which retained a larger amount of water than the remainder of the sample. This same effect is expected to occur in actual walls and will be roughly the same height. The amount of moisture retained in this layer is also dependant on the bottom edge geometry.

(v) the outcome described in (iv) along with its consequences can easily be included into the computer simulation of wall drying. For instance excess water draining from one element can be input to the element below.

(vi) water migration to the bottom layer by internal or surface drainage in the sheathing, can delay drying and accelerate deterioration in that material as well as adjoining components.

ROWAN WILLIAMS DAVIES & IRWIN Inc.

Vincent Ferraro, M.Eng., P.Eng.
Project Engineer

Glenn D. Schuyler, P.Eng.
Principal

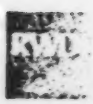

TABLE 1

SAMPLE WEIGHT GAIN AND CAPILLARY HEIGHT

SAMPLE	DIMENSIONS (cm)	WEIGHT GAIN/DRY WEIGHT TOTAL	TOP	BOTTOM	CAPILLARY HEIGHT (cm)
Industrial Poplar	25.9 x 26.9	0.925	0.891	1.281	3.3
Prepared Poplar	25.0 x 26.4	0.871	0.814	1.187	3.8
Mahogany	25.1 x 26.0	0.665	0.625	0.786	3.4
Tentest	26.9 x 12.3	2.187	2.140	2.490	2.6

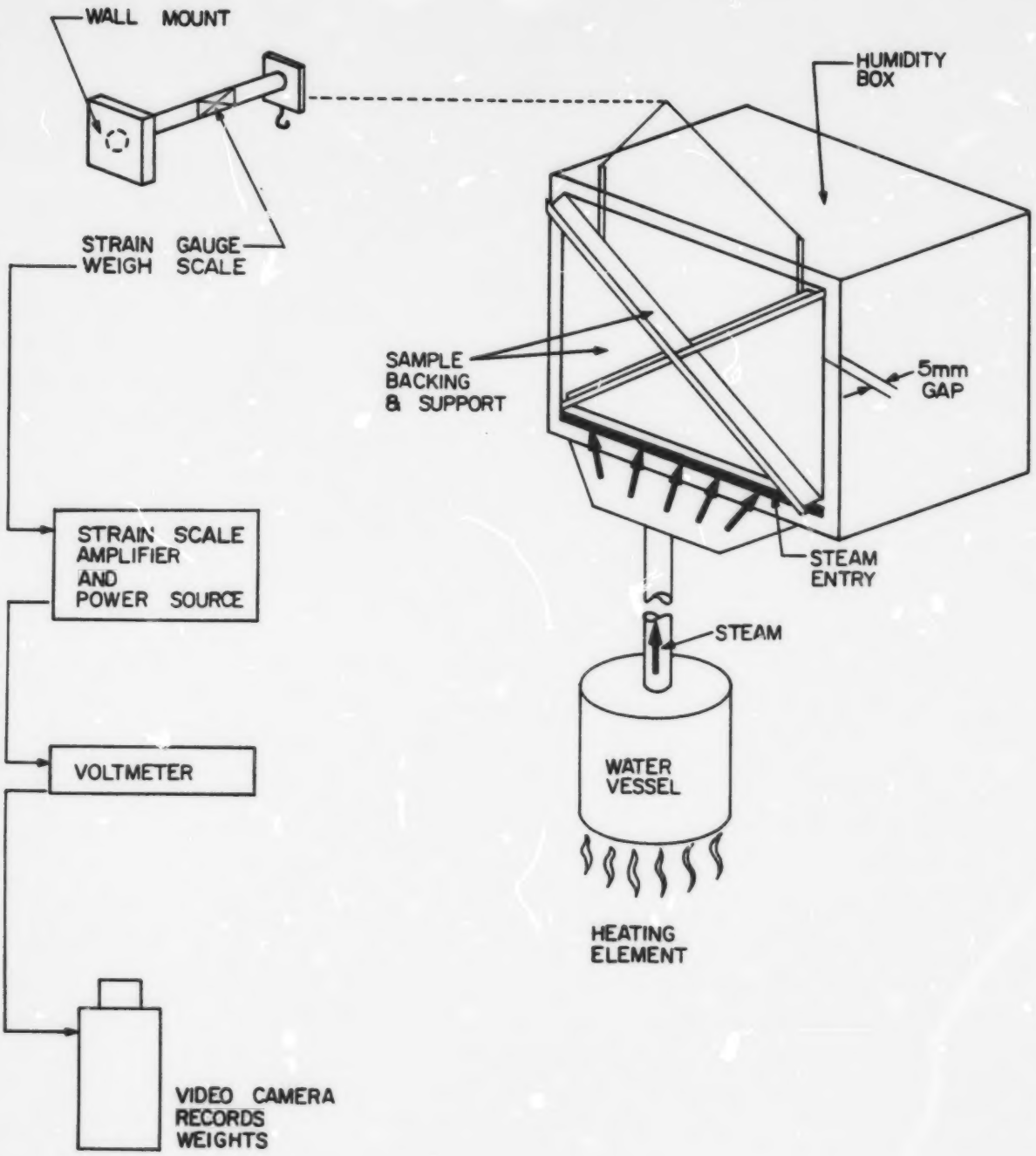

FIGURE 1
TEST APPARATUS FOR TASK 5

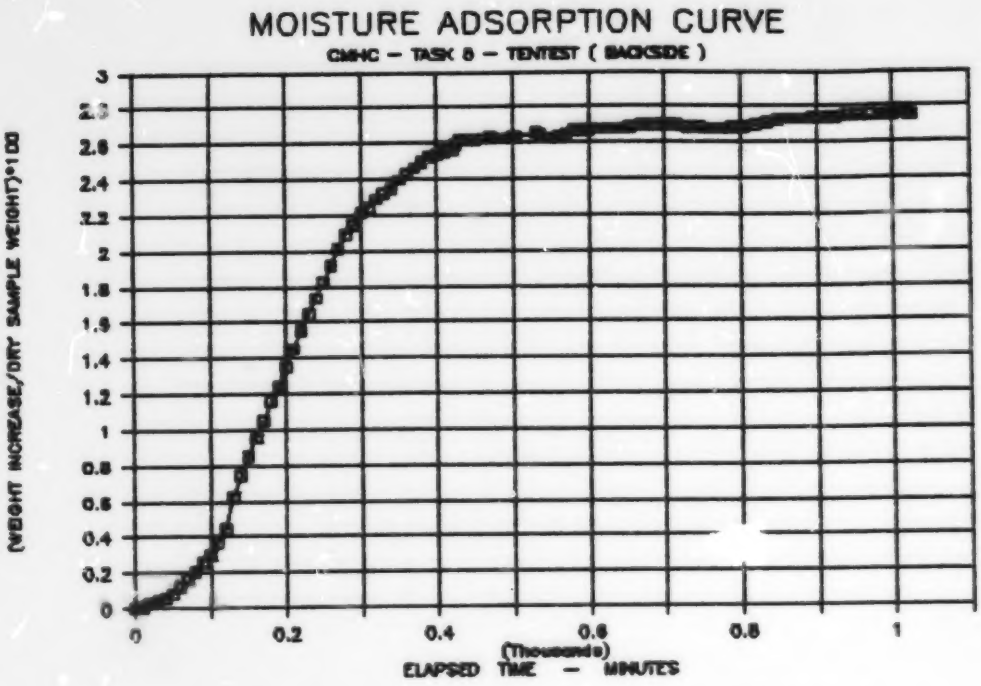

FIGURE 2: TENTEST (BACKSIDE)

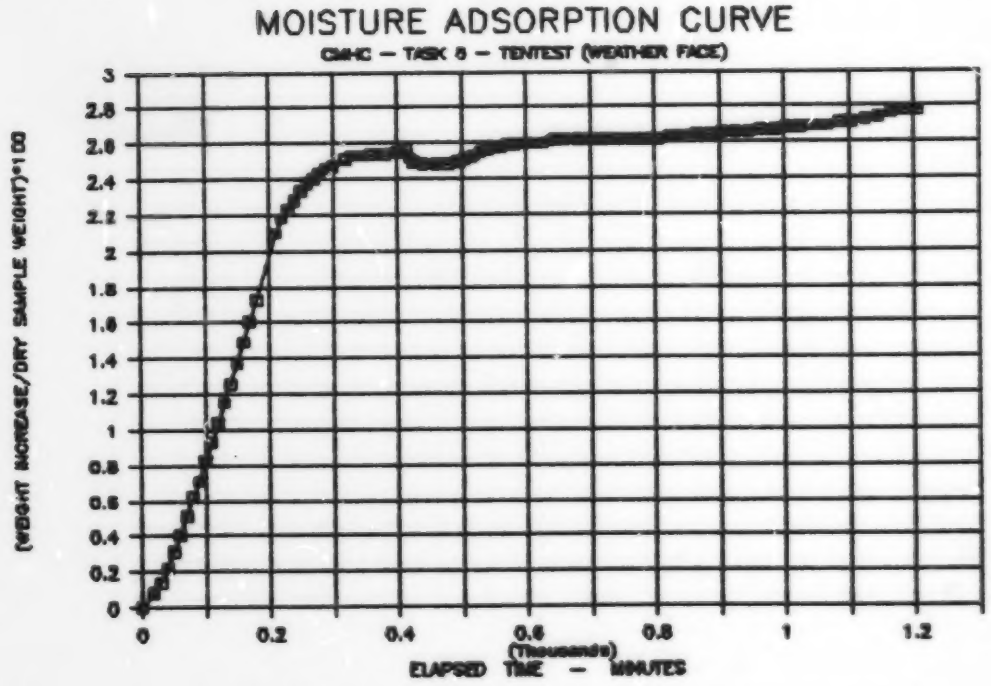

FIGURE 3: TENTEST (WEATHER FACE)

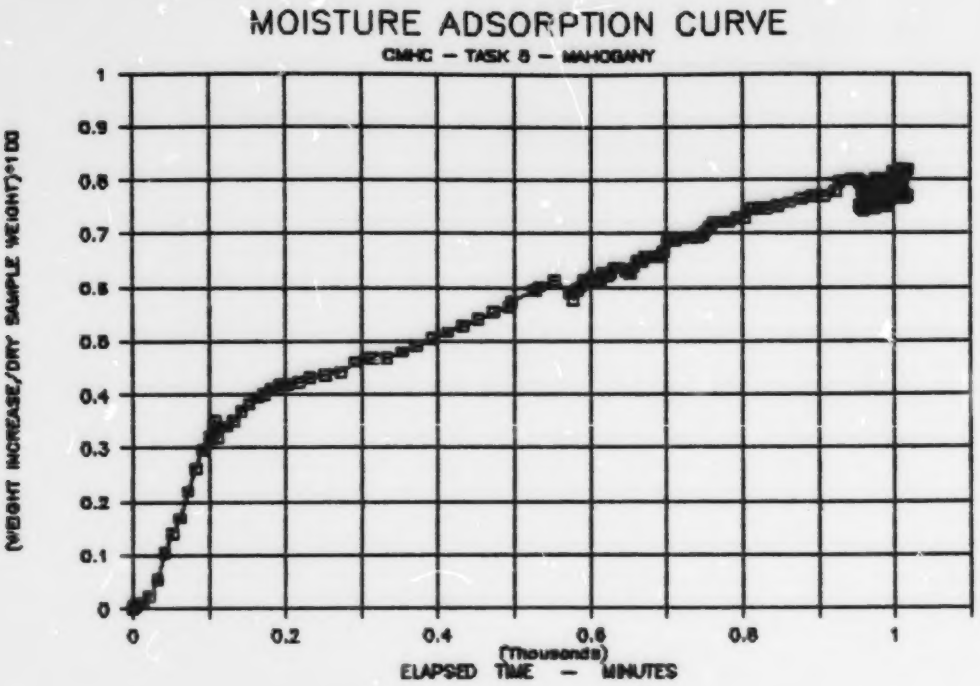

FIGURE 4: MAHOGANY VENEER

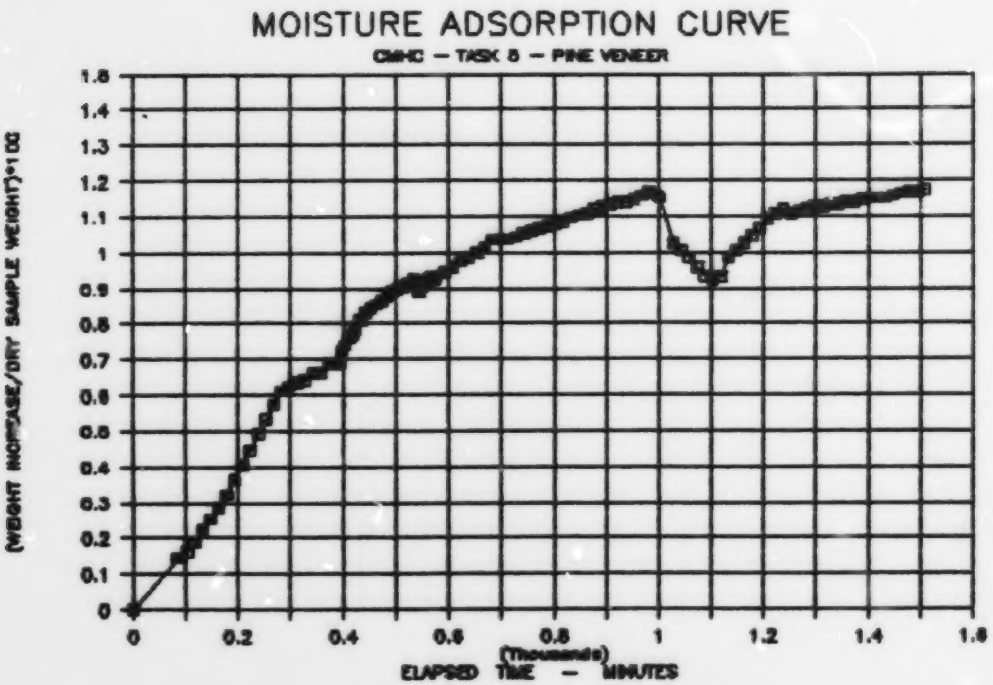

FIGURE 5: PINE VENEER

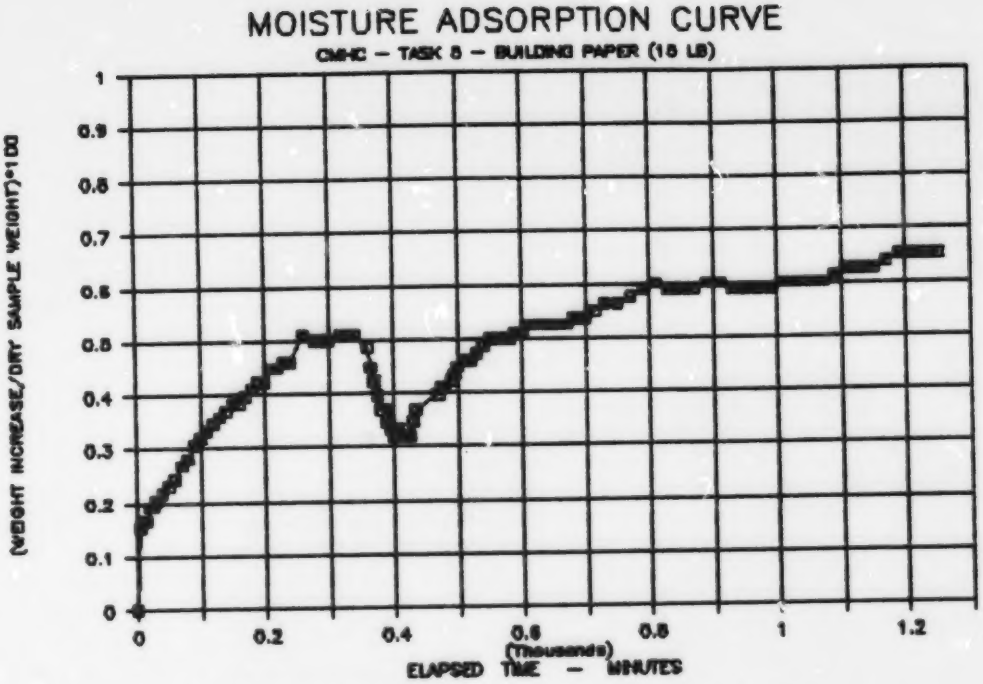

FIGURE 6: BUILDING PAPER (15 lb)

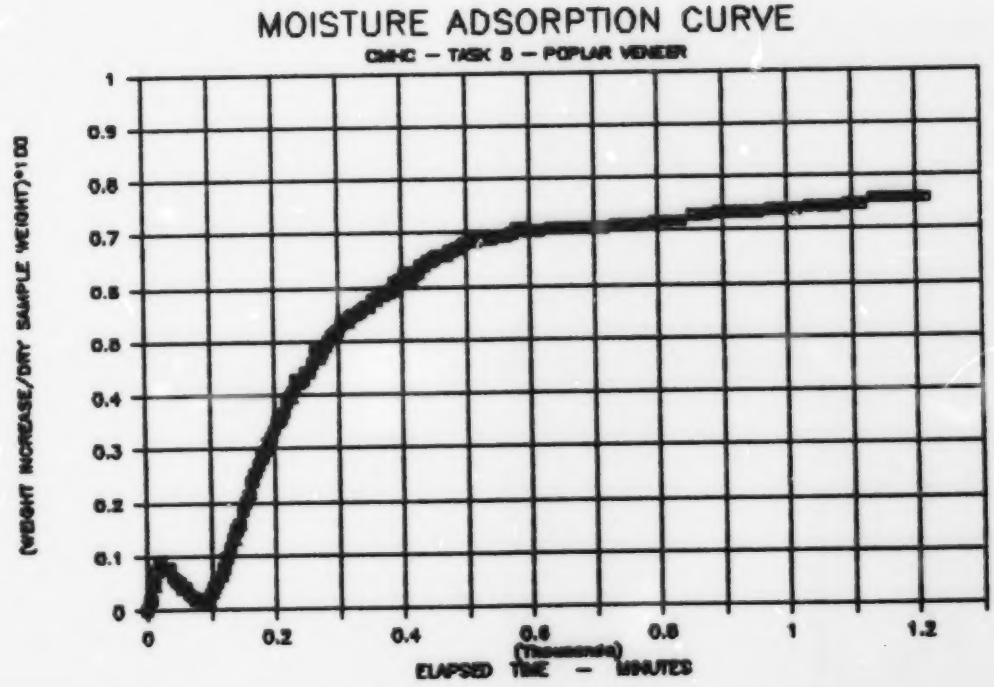

FIGURE 7: POPLAR VENEER

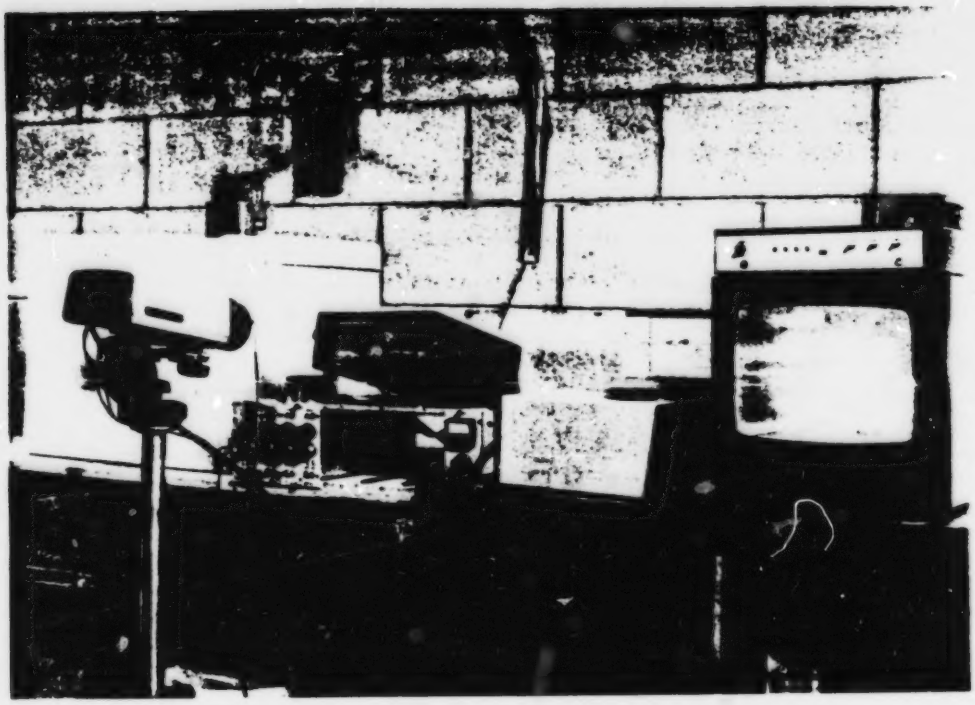

PHOTO #1
COMPONENTS OF
THE EXPERIMENTAL
SETUP

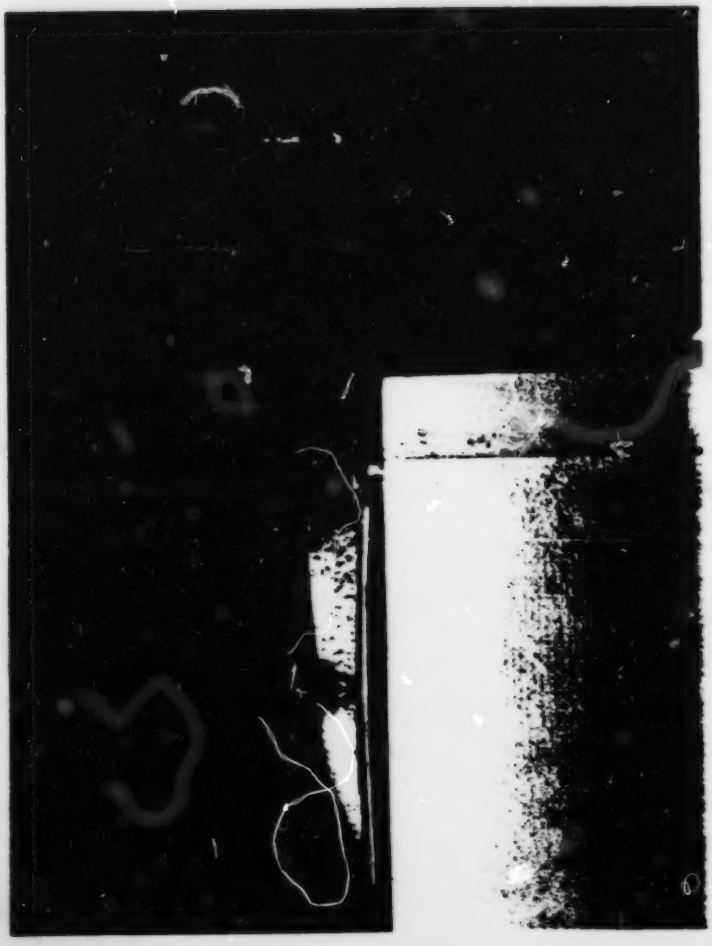

PHOTO #2
DETAILS OF STRAIN
GAUGE WEIGH SCALE
AND SAMPLE ARRANGEMENT

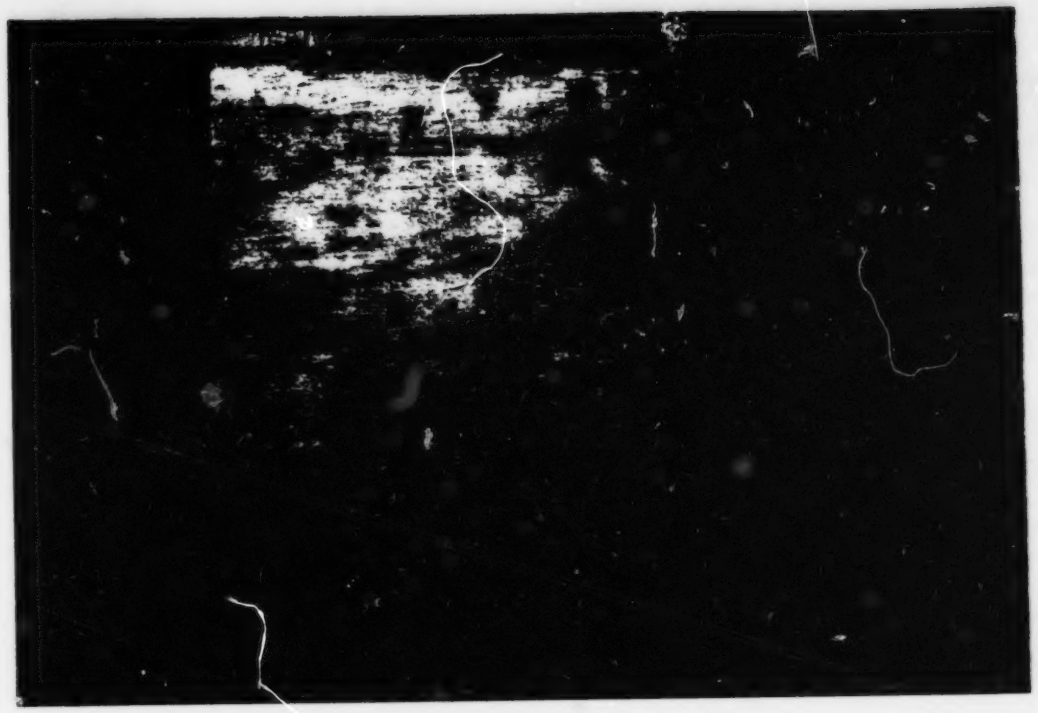

PHOTO #3
PINE SAMPLE AT TEST COMPLETION

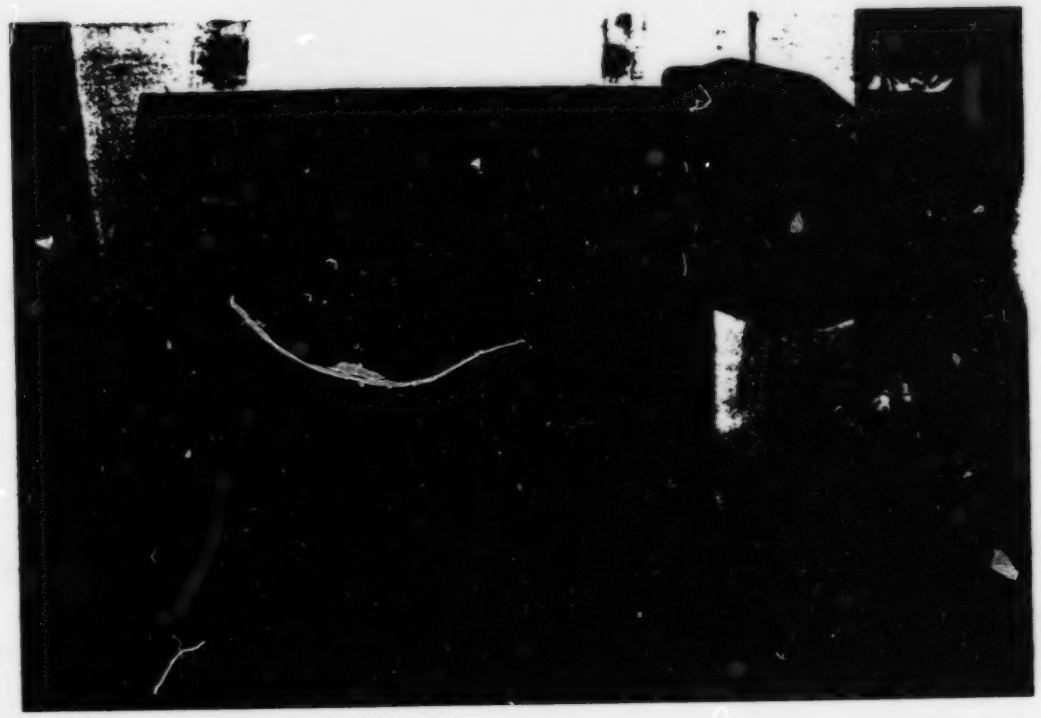

PHOTO #4
MAHOGANY SAMPLE AT TEST COMPLETION

BUILDI

BUILDING PAPER CL

PHOTO #5
G PAPER BEFORE TESTING

PHOTO #6
E–UP ILLUSTRATING BEAD FORMATION

PHOTO #7
TENTEST BACKSIDE SAMPLE AT TEST COMPLETION

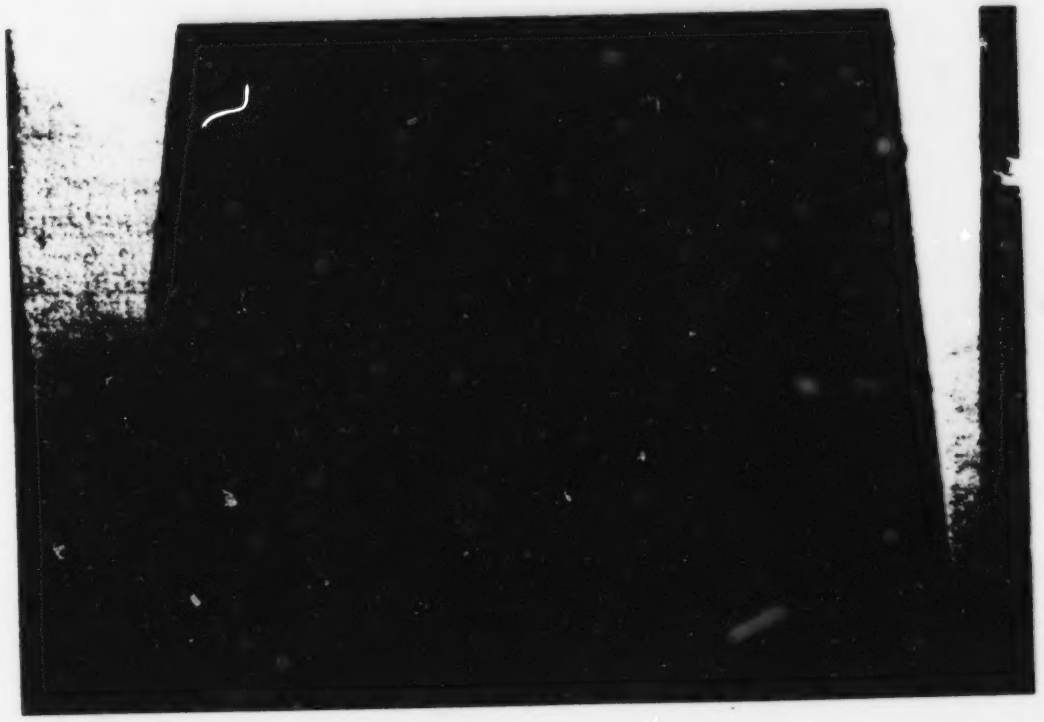

PHOTO #8
TENTEST BACKSIDE SAMPLE CLOSE–UP

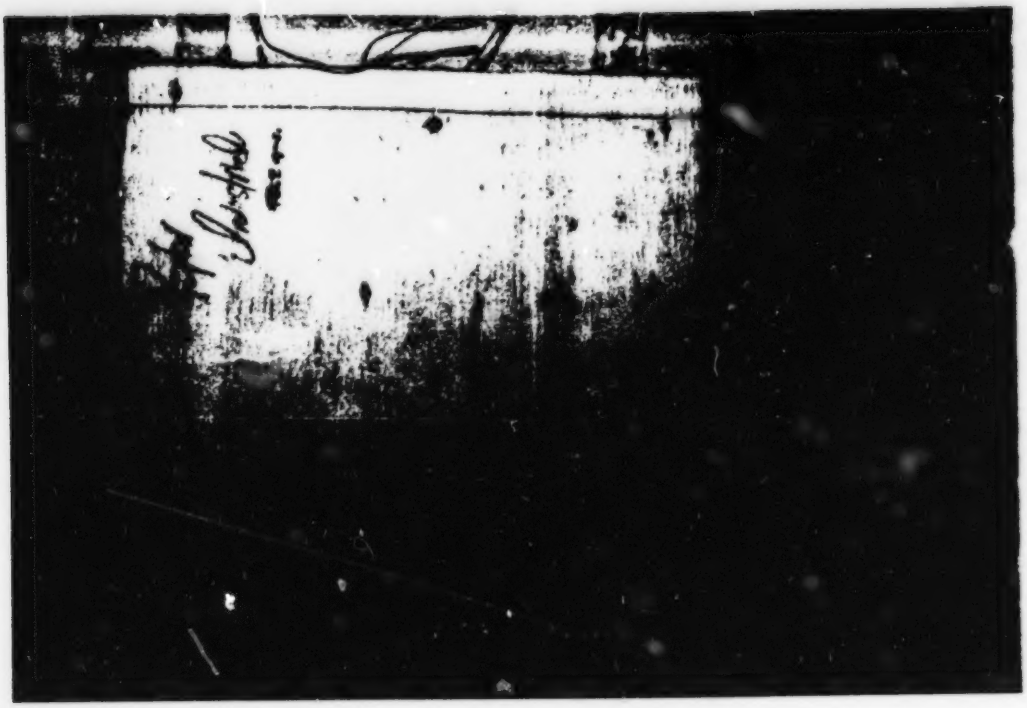

PHOTO #9
POPLAR SAMPLE AT TEST COMPLETION

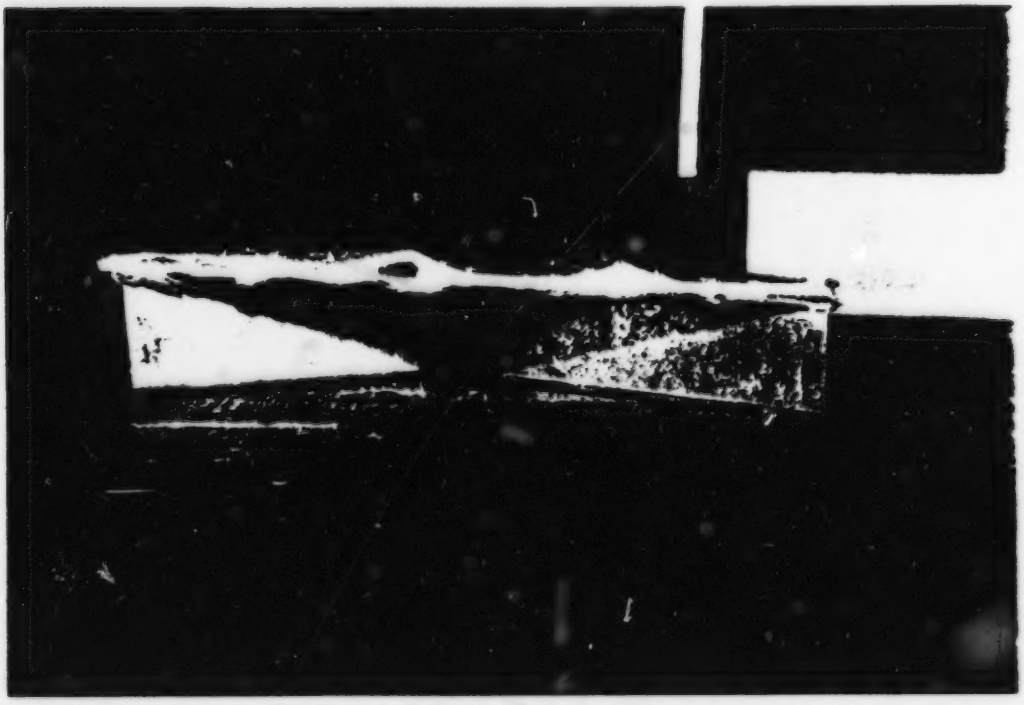

PHOTO #10
POPLAR SAMPLE: EFFECT OF MOISTURE EXPANSION
ON SEPARATING SAMPLE FROM BACKING

APPENDIX F

DRYING CHARACTERISTICS IN WALLS OF LOW-RISE RESIDENTIAL HOUSING
MILESTONE REPORT FOR TASK 6:
EVAPORATION RATE OF BUILDING MATERIALS AT VARIOUS TEMPERATURES

September 18, 1987

Report 48714006

Submitted to:

CANADA MORTGAGE AND HOUSING CORPORATION

By:

ROWAN WILLIAMS DAVIES & IRWIN Inc.

GUELPH, ONTARIO

TABLE OF CONTENTS

	Page No.
1. INTRODUCTION	1
2. BACKGROUND	1
3. METHODOLOGY	3
3.1 Sample Preparation	3
3.2 Experimental Apparatus	4
3.3 Experimental Procedure	5
3.4 Experimental Difficulties	6
4. DISCUSSION OF RESULTS	7
4.1 General	7
4.2 Current Theory of Evaporation	8
4.3 Discussion of Results and Applicability to the Computer Model	10
5. CONCLUSIONS	16
REFERENCES	
TABLE	
FIGURES	

1. INTRODUCTION

This milestone report describes details of the work performed for Task 6 of the present contract. The objectives of this task are to investigate and measure the evaporation rate of various building materials used in residential wood framed construction over a practical range of temperatures. In particular, the main goal is to determine whether or not the evaporation behaviour at below freezing temperatures is fundamentally different from that above freezing. The answer to this question will be useful in assessing the evaporation algorithm used in the moisture flow model of the computer simulation program developed in Phase I of the present research contract. As well, the results of this work provide estimates of surface moisture resistivities used in the moisture and heat flow models forming part of this simulation program. The materials studied include; veneers of poplar, pine and mahogany as well as building paper (15 lb variety) and fiberboard sheating material (i.e. Tentest). The mechanism thought to be at work in the moisture evaporation from porous materials will be summarized in relation to the results of this work. The computer program which performs the simulations will be validated, as part of the next and final task, Task 7, with controlled measurements on a typical full scale wall assembly.

2. BACKGROUND

Interior components of wood framed walls can become wet over a period of time from penetration of wind driven rain through the exterior envelope or by leakage of moist air from interior spaces. As well, moisture present during construction may be trapped inside the wall cavity. In each case, drying of the material and the air space (ie. moisture evaporation) will only occur under suitable conditions which will in part be controlled by the outdoor environment (ie. the weather). Other parameters which control the amount and rate of drying in porous building materials include; wall cavity temperature, relative humidity, air flow over the material surface, as well as pore sizes and pore size distribution which influence moisture resistivity in the material.

Over a free surface, with no convection of air, water will evaporate or condense (ie. drying or wetting) depending on the relative vapor pressures over the water surface and in the air. Three conditions may exist: the vapour pressure in the air can be equal to, less than or greater than that immediately over the water surface (ie. the equilibrium vapor pressure). If the vapour pressures are equal no moisture transfer will occur. If the vapor pressure in the air is greater than or less than the equilibrium pressure immediately over water then water will condense from the air or evaporate into the air respectively. The equilibrium relative humidity over a flat water surface is, by definition 100%. The equilibrium vapor pressure over a water surface is determined by the temperature.

A similar mechanism is at work in drying or wetting of porous materials with the added complication that the equilibrium vapour pressure over water held in pores is reduced as compared to that over free water because of capillary forces existing within the pores. Therefore every material having a unique pore structure (i.e. amount and distribution of pores) will have a characteristic equilibrium vapour pressure at a given temperature. The drying mechanism in porous materials is discussed in more detail in Section 4. Tabulated data relating equilibrium moisture content, temperature and relative humidity, from which equilibrium vapour pressure can be derived, are readily available for wood (see Reference 1). The same data is not available for individual species because the values do not differ appreciably among them. Similar data for wood products such as wood fiber board and building paper were not available.

The purpose of the present tests performed for Task 6 is to determine the evaporation rate from a surface layer of six building materials over a range of temperatures above and below freezing. The intent in considering only a thin surface layer at moisture contents above fiber saturation is to identify any fundamental differences in evaporation rate behaviour above and below the freezing point of water compared to that over a free surface. Hence, sample thickness and test duration (i.e. the period allowed for drying) were governed by the fact that freezing would first occur in surface water and large pore water before occurring in bound water (i.e. water held below fiber saturation). Drying

RWDI

rate data are plotted on three different ordinates; two versus elapsed drying time and the third versus temperature. The first groups of plots 1(a) throught 1(f), present raw evaporation rates on a unit area basis. Figures 2(a) through 2(f) present the same evaporation rates in coefficient form. These data are obtained by dividing the evaporation rate data of Figures 1(a) through 1(f) by the vapour pressure difference between the equilibrium value above the samples and that in air. These vapour pressures are determined from the moisture content versus relative humidity and temperature curves for wood and air temperature. Figures 3(a) through 3(f) illustrate the variation of average evaporation rates over the test period for different temperatures. For all figures plots (a) through (f) correspond to each of six materials tested.

The work performed for this task is in general intended to improve our understanding of evaporation performance of building materials and in particular to address the issue of the effect of temperature on evaporation. This work has direct influence on confirming the algorithm used in the computer program developed during Phase I of the project. As well, surface moisture resistivities, required in the moisture flow submodel of the computer program, can be derived from evaporation rate data obtained in this task.

3. METHODOLOGY

The evaporation rates were determined at six different temperatures with the use of a temperature controlled chamber. The data was recorded manually for each of six samples every hour for an eight hour period.

3.1 Sample Preparation

The materials forming the outer portion of walls in residential wood framed construction (i.e. sheathing paper and sheathing materials) were selected as samples for this test. The 25 cm x 25 cm sample dimensions were chosen arbitrarily and mainly for convenience of constructing the test apparatus. The thicknesses of the samples were selected, except for building paper, to represent

RWDI

the surface drying layer of in-situ materials. Although the material and its pore structure among other factors, determine evaporation rate, the thickness of this layer determines the amount of moisture adsorbed, and the time required to approach room-dry conditions and will also affect operation of the apparatus.

The solid wood veneers were not available nor could be conveniently prepared at less than 5 mm thickness. Tentest fiberboard (10 mm thick) and 15 lb building paper were obtained from commercial stock. The Tentest was sliced to 3mm thickness.

Each sample material was weighed in its room-dry state and after twelve hours of oven drying at temperatures not exceeding 105°C. Oven dried samples were not used for the actual test. A similar set of samples was prepared for testing. One surface of each material was covered with a 3 mm - 4 mm layer of silicone which was allowed to harden over a period of a week. A backing of aluminum foil was also applied over the silicone. This sample preparation was intended to constrain evaporation to occur from one surface only and to model roughly the active surface layer described above. The room-dry and oven-dry sample weights were measured along with the weights of room-dry samples plus backing for the six materials. The total oven-dry sample weights, including backing were derived from these measurements.

3.2 Experimental Apparatus

The experimental assembly used in this study is illustrated in Photographs 1(a) and 1(b). The assembly consists of (a) an air conditioning unit, (b) a heater, (c) a mixing chamber and (d) the test chamber. Selected temperatures were attained by controlling the combined inputs of the heater and the a/c unit into the mixing chamber. A fan between the mixing and test chambers supplied constant temperature air to the test chamber and maintained air flow over the samples. Air velocities over the samples ranged between 3.5 and 4 meters/second. Temperatures were measured using thermocouples (e) at numerous locations within the apparatus and were controllable to within ± 1 degree C during 85% of the drying

period. To periodically weigh the test samples, the apparatus had to be opened momentarily. The test chamber required 10 minutes to regain its setpoint condition. During this period, constituting 15% of the time, the temperature ranged from 3 to 14 degrees C above the desired temperature. Relative humidities in the test chamber were measured with a chilled mirror dew point meter (f). Sample weights were determined with the use of a triple beam balance accurate to 0.5 grams.

3.3 Experimental Procedure

The desired temperatures were obtained in the test chamber by combining the output air stream from the heater and the a/c unit. An initial period of approximately one hour was required for the chamber temperature to stabilize at the start of the test.

Once the samples were prepared and weighed as described in Section 3.1, they were submerged overnight in a shallow bath of tap water and allowed to adsorb as much water as possible. The samples were removed from the water bath and allowed to drain for three minutes at room temperature before testing. The samples were weighed immediately before placement into the test chamber, set to one of six temperatures, to obtain the total saturated weight. Sample weights were subsequently recorded every hour over a period of eight hours. At the end of each consecutive hour of drying the test chamber was opened to remove, weigh and replace the samples. This procedure caused the temperature in the chamber to rise between 3 and 14 degrees C above the desired value for approximately 15% of the total drying time. During the rest of the time the temperature was maintained within ± 1 degree C. Overall, including the weighing time, samples spent 50 minutes out of every hour at the selected temperature and 10 minutes above the temperature. This procedure, which required eight hours of testing for each temperature, was repeated for all six temperatures using the same samples after resaturating. The six dry bulb temperatures selected for testing were measured with a type 'T' thermocouple meter. Corresponding dew point temperatures in the

test chamber were measured with the chilled mirror dew point meter. Relative humidity was derived from these temperatures. The results are tabulated below:

TEMPERATURE (°C)		RELATIVE
DEW POINT	DRY BULB	HUMIDITY (%)
-9.8	- 5.6	70
-6.7	- 2.2	70
-6.4	0	59
-2.4	3.9	62
7.2	15.6	60
15.6	23.2	70

The experimental difficulty of temperature rise was most important at low temperatures and of decreasing concern as the room temperature test was approached (i.e. 23°C). For this test, the heating and cooling units were turned off but the air flow over the samples was maintained as before. The range of dry bulb temperatures tabulated above was selected for testing mainly to confirm the applicability of the evaporation model (forming part of the computer simulation program) over a wide temperature range. Evaporation rate data was also used to derive surface moisture resistivities required by the simulation program.

3.4 Experimental Difficulties

Equalization of the sample temperature to that of the chamber at test start-up and removal of the samples from the test chamber for weighing at hourly intervals with the associated temperature changes were the main difficulties encountered during the experiment. At the end of each hour of drying, the test chamber was opened to room air, samples were removed, weighed and returned to the chamber. During the few seconds that the test chamber was opened, to remove and then to return the sample, the chamber temperature increased by between 3 and 14°C depending on the selected test temperature. In all cases, the apparatus required less than seven minutes to re-establish the desired temperature. The

RWDI

samples were exposed to room temperature for an additional three minutes as they were being weighed. The room environment was generally at 23°C and 60% RH. The relative humidity difference between room air and test chamber was less than ±15%.

These effects of temperature, as estimated in section 4.3, are significant at the lowest test temperature and become negligible on approaching the room temperature test case.

The intent of backing the samples with silicone and aluminum foil was to constrain moisture evaporation to occur from one surface only. Although aluminum is impervious to moisture, silicone can adsorb small amounts of moisture. Further acetic acid, which probably serves as a carrier solvent for silicone caulking, depresses the boiling point of water when in solution by an amount depending on its concentration. For instance, a 3% acetic acid solution in water depresses the boiling point by approximately 24°C, from 100°C to 76.6°C. Since the vapour pressure of this mixture would be different from that of retained moisture the effect on drying was unknown. However, the effect on moisture evaporation from the veneers would be expected to be small and restricted to the first soak/dry cycle.

4. DISCUSSION OF RESULTS

4.1 General

The raw data resulting from the present work are presented in several different ways. Figures 1(a) through 1(f) illustrate evaporation rate, grams of water per meter^2 per hour, versus drying time. The mass of water held by the sample at time zero is taken to be the saturated moisture content of the samples. Figures 2(a) through 2(f) illustrate the same data but dimensionalized to gm/(m^2 x Pa x hr). The vapour pressure difference between the air value and the equilibrium value over the material is used to generate these figures. The results at time zero, indicate the maximum amount of water capable of being held by the sample.

RWDI

Although one might expect the amount of water adsorbed would be the same after each overnight soaking period, the result shows significant differences among the six runs. This behavior after repeated soaking and drying cycles (i.e. hysteresis) is attributed to the variable amount of water held on the material surface as well as the variable quantity of air trapped in pores of the material matrix. Figures 3(a) through 3(f) illustrate data of Figures 2(a) through 2(f) averaged over the test period and plotted versus temperature.

4.2 Moisture Evaporation Theories

The evaporation of moisture from porous materials follows the 'S' shaped curve commonly referred to as a sorption isotherm. These curves are characteristic of evaporation of moisture from porous materials and to the first order are functions of relative humidity only for any particular material sample. Existing theories, which attempt to explain the drying mechanism, rely in varying proportions on the thermodynamics of heat and moisture exchange processes and the physics of evaporation at microscopic and molecular levels. Those which emphasize the molecular approach, generally converge to describe a similar mechanism occurring in the bulk materials.

In general, this drying mechanism involves at least two stages. These are: (i) evaporation of water held in capillaries and pores to the equilibrium layer, and (ii) diffusion of water vapour from a layer in dynamic equilibrium with the material surface. Whereas the diffusion mechanism is commonly accepted, differences in the theories mainly occur in the evaporation step with respect to how water molecules are bonded to the pore and capillary surfaces. The diffusion phase is believed to be driven by the vapour pressure difference between the equilibrium value of the vapour layer and that of the surrounding air. Above the fiber saturation point, about 30% MC in wood, water and saturated vapour fill small and large pores and are continually transported to a thin surface layer by liquid and vapour diffusion under vapour pressure gradients and capillarity under relative humidity gradients. Drying rate in this range of MC is thought to be constant and controlled mainly by vapour pressure differences between the vapour layer and its

surroundings for a given sample. A constant drying rate is borne out by experiment (Reference 3) over some portion of the drying regime when the moisture content is above the fiber saturation point.

Below the fiber saturation point water in the liquid state is held in pores and capillaries, more or less strongly depending on the sizes of the voids, the relative humidity within the voids and the molecular bonding between water layers and the wood fibres. As evaporation proceeds beyond this point, it becomes increasingly more difficult to extract water from these spaces. This period of drying is also confirmed by experiment (Reference 3) as having rapidly decreasing drying rate with time.

Diffusion of vapour away from a material occurs when a vapour pressure difference exists between the equilibrium value in the material vapour layer and the value in air. The equilibrium relative humidity depends on the moisture content of the wood and only slightly on its temperature, therefore the vapour pressure in the equilibrium layer is controlled by the temperature (i.e. assuming a system in thermal equilibrium) and by the moisture content (relative humidity) of the material. Increasing the air temperature will produce larger differences in the two vapour pressures and correspondingly faster drying.

For example, suppose a system initially in thermal equilibrium with air at 16°F and 60% relative humidity (RH) surrounding a wood sample whose moisture content is above the fibre satuation level (i.e. equilibrium RH = 100%) is brought into a 24°C environment. The equilibrium RH stays at 100% so the equilibrium vapour pressure eventually rises from 1896 Pa to 3072 Pa. However, the vapour pressure of the ambient air remains 1116 Pa. Thus the vapour pressure difference increases by 150% from 780 Pa to 1956 Pa with a corresponding increase in drying rate. The significance of this two step drying process (i.e. from material to equilibrium layer based on RH only and then from equilibrium layer to ambient air based on vapour pressure difference) becomes clear when one considers a material at a temperature above that of the ambient air. In that case, even if the RH of the

ambient air equals the equilibrium RH of the material, drying can still take place since there is still a vapour pressure difference.

An important effect of moving air over the material surface is to generate a turbulent mixing layer (i.e. boundary layer) which influences heat and moisture transfer coefficients across the material - air interface. This mixing layer will have varying influences on evaporation of moisture from material surfaces depending on wind speed and material surface roughness. Samples in the test chamber were exposed to air velocities of between 3.5 and 4 meters/second.

It should be noted that moisture contents which have been calculated in Table 2, represent average values through the thickness of each specimen. Recent work by Forintek Canada has shown that for moisture contents (MC), below fiber saturation, a moderate MC gradient exists below a 3mm depth but that in addition, a steep gradient also exists near the surface which is more closely in equilibrium with surrounding air. This demonstrates that a layer of unknown moisture diffusion resistance exist near the surface of these specimen. The behaviour for specimens having MC above fiber saturation is not known. Therefore, based on sample thicknesses used in this work evaporation rates and moisture diffusivities may be representative of a surface layer thicker than actually existing.

4.3 Discussion of Results and Applicability to the Computer Model

The figures and tables presented here are of practical interest with regard to quantifying the behaviour of the specific materials used in real walls. Figures 3(a) through 3(f) illustrate the variation of average evaporation rate, i.e. drying rates, with temperature. These figures are useful in regard to understanding and attempting to explain the processes underlying the drying mechanism.

Based on Figures 1(a) through 2(f) the evaporation performance of building paper seems to be somewhat different from any of the other five materials including: Tentest and veneers of solid mahogany, pine, industrial and laboratory prepared poplar. The relatively large initial drying rates of building paper over the

first hour followed by relatively constant drying rates over the next seven hours, suggests that much of the water is held on the surface. Since surface water is more easily evaporated than water held in pores, distinctive evaporation rates would be expected for building paper. Drying rates for the remaining materials vary less consistently during the eight hour drying period because a much smaller proportion of water is held on the surface.

This outcome tends to support the choice made in the computer model to ignore adsorbed moisture in building paper because of the large proportion of surface water. In addition, building paper has a small moisture holding capacity as compared to other materials comprising actual walls. For these reasons and because building paper is found adjacent to the air space behind the siding, drying in real walls may first be apparent at this layer and may also be expected to occur quickly in relation to other layers. Contrary to this however, building paper may serve an important function in blocking the removal of moisture from inner layers by presenting itself as a surface on which condensation can occur. Practical experience with building paper suggests that the vapour permeance may be a great deal lower in many cases than expected. These possibilities could have significant implications to the drying of the sheathing layer, depending on the amount of air leakage across the building paper layer.

The computer model simulation distinguishes between slow processes which take longer than an hour, moisture migration through Tentest for instance, and rapid changes lasting less than an hour, moisture diffusion through an air space for example. When boundary conditions remain unchanged, parameters in a rapid process need only be evaluated once as an average over the period. However, with the same fixed boundary conditions, a slowly varying process needs to be monitored at every time step (i.e. every hour in this case). Drying of building paper may be a borderline case where much of the drying occurs during the first hour but some drying can occur after that.

Some of building paper's behaviour with respect to initial drying may be attributed to experimental error. The size of the sample and the small amount of

water adsorbed make this material particularly sensitive to experimental difficulties. For instance, any jolting of the sample as it is initially weighed and introduced into the test chamber could shake relatively large proportions of loosely held water free of the sample. This effect would be most serious for building paper at the beginning of testing. This problem disappears for all samples when some drying has occurred.

The evaporation rates of the remaining five materials generally decrease with time while some variability is evident. As indicated in Figure 1(f) mahogany demonstrates the most consistently declining evaporation rate with time.

Figures 2(a) through 2(f) are obtained from Figures 1(a) through 1(f) by dividing vapour pressure differences calculated at each temperature into the evaporation rates for each of the six temperatures tested.

Consideration of Figures 2(a) through 2(f) indicate that by dividing the vapour pressure differences between the value in air and the equilibrium value over the material for a given temperature, signficiantly reduces the apparent scatter of evaporation rates presented in the previous figures. For all materials tested the initial evaporation rates dimensionalized in this way are largest and diminish over time as drying progresses. No one material stands out as having unusual initial drying characteristics. Therefore, this outcome suggests that water held on the surface of the materials tested is evaporated at roughly the same rate. Building paper shows significantly less scatter in evaporation rates over the remainder of the testing period simply because less water is left to be evaporated. It is further concluded that compared to the other materials, building papers retains a larger proportion of its moisture as surface water. This outcome is not surprising for two reasons; first, on a mass quantity basis, less material is available to retain water in building paper and second, the asphaltic component of building paper changes its surface and to some extent its internal fiber characteristics. Data used to calculate vapour pressure differences are presented in Table 1.

Figures 2(a) through 2(f) also show the interesting result that on averaging evaporation rates over the test temperatures two different rates are apparent. One is the initial faster rate discussed above resulting from surface water evaporation. The second is a relatively constant rate occurring over the remaining seven test hours. With the exception of building paper, this evaporation rate is relatively constant among all materials and has a value of approximately 0.15 grams/(m^2 x hr x Pa). The approximate average secondary rate for building paper is 0.05 grams/(m^2 x hr x Pa). Thus, the moisture diffusivity is roughly the same for all materials tested except building paper. The influences of a smaller proportion of internal moisture and the asphalt component in building paper are likely responsible for this difference. No clear differences results for Tentest which also has asphaltic material components as well as being a manufactureed product consisting of compressed small wood particles.

Figures 3(a) through 3(f) illustrate the variation of evaporation rates with temperature during the first hour as well as averaged over the entire eight hour period and averaged over a seven hour period as well. Variation of first hour, i.e. initial evaporation rates for all materials indicate a definite trend of decreasing rates with increasing temperature.

Average evaporation rates, either the eight or seven hour averages, shown in Figures 3(a) through 3(f) illustrate a similar and less pronounced variation of evaporation rates with temperature for all materials studied. In general, average evaporation rates decrease with increasing temperature. A typical variation for instance is given by the pine veneer sample to be 0.19 g/(m^2 x hr x Pa) at -2°C to 0.07g/(m^2 x hr x Pa) at 23°C. As shown in these figures the variation is not monotonic. A trough in the curves appears for each sample tested.

The fact that normalizing by ΔP does not collapse all curves for different temperatures onto one constant evaporation rate curve indicates that vapour pressure differences at the various temperatures tested may not be the only forces driving the drying process.

The moisture adsorption capacities of the solid wood samples and tentest are all greater than building paper based on the oven dry weight of the material. As indicated in Table 2 building paper has the lowest % moisture content of 57% followed by pine 76%, mahogany 89%, laboratory prepared poplar 105% industrial poplar 125% and tentest 370%. Tentest adsorbs the most moisture relative to its dry weight both because of its ability to retain water but also because of its relatively low density.

Saturation moisture content and evaporation rate are two parameters which can offer important insight into the behaviour and suitability of materials in real wall assemblages. However, the influence of other factors such as: exterior climate, wall cavity temperatures and solar radiation cannot be ignored in assessing the appropriateness of materials.

In general, the numerous parameters derived in this and previous tasks must be considered together in the wall system both as modelled numerically by the simulation computer program or physically in the real wall.

An important outcome can be drawn from these results, particularly for the solid wood samples. This is, that the evaporation rates, when normalized by the vapour pressure differences shown in Table 1, are only moderately different for temperatures below freezing down to -5.6°C as compared to those above freezing.

5. CONCLUSIONS

Considering evaporation rates of the various materials at different temperatures normalized by vapour pressure differences, the following comments are appropriate:

(i) the evaporation rate normalized by vapour pressure difference appears to be only mildly affected by temperature.

RWD

(ii) the low end of the test range is representative of common temperatures likely to be experienced by actual sheathing material in most Canadian localities for much of the time. Although outdoor temperatures can often drop significantly below this level, sheathing material is often insulated by an air space and siding and consequently spends less time below -5.6°C.

(iii) vapour pressure difference is partially successful in collapsing evaporation rate curves for any material at the six temperatures tested.

(v) for all materials tested two significantly different evaporation rates are distinguished: an initial rate corresponding to evaporation of surface water followed by a secondary rate controlled by the moisture diffusivity of the surface layer and the associated moisture content gradient.

(vi) all materials tested indicate a similar initial moisture evaporation rate. Secondary evaporation rates are lower for building paper as compared to the remaining materials.

(vii) the consequences of these outcomes on real walls cannot be determined without looking at the wall as an interrelated system.

ROWAN WILLIAMS DAVIES & IRWIN Inc.

Glenn D. Schuyler, P.Eng.
Principal

Vincent Ferraro, M.Eng., P.Eng.
Project Engineer

References

1. Simpson, W., 'Sorption Theories Applied to Wood' Forest Products Laboratory. U.S. Department of Agriculture December 1979.

2. Hutcheon, N.B., 'Building Science for a Cold Climate', John Wiley & Sons, Handegord, G.O. 1983

3. Berger, D., Pei, D.C.T., 'Drying of Hygroscopic Capillary Porous Solids - A Theoretical Approach' University of Waterloo, Waterloo, Ontario, Canada Int. of Heat and Mass Transfer, Vol. 16, pp. 293-302.

RWDI

TABLE 1

VAPOUR PRESSURE DIFFERENCES ABOVE WOOD SURFACES

EQUILIBRIUM TEMPERATURE (°C)	EQUILIBRIUM RELATIVE HUMIDITY OF WOOD	RELATIVE HUMIDITY OF AIR (%)	EQUILIBRIUM VAPOUR PRESSURE OVER WOOD (Pa)	VAPOUR PRESSURE IN AIR (Pa)	ΔP (Pa)
-5.6	100%	70	406.	284.	122.
−2.8	"	70	537.	375.	162.
0.	"	60	639.	385.	254.
3.9	"	60	842.	507.	335.
15.6	"	60	1896.	1115.	781.
23.2	"	70	3072.	2128.	944.

ΔP = equilibrium vapour pressure over wood - vapour pressure in air

CMHC - TASK 6

TABLE 2: RAW MOISTURE EVAPORATION DATA

MATERIAL	TEMP deg. C	/-------- MASS (g) -------/ Initial Conditions DRY	TOTAL OVEN DRY	SATURATED	HOURS - ELAPSED DRYING TIME 1.0	2.0	3.0	4.0	5.0	6.0	7.0	8.0
					Drying Mass : grams							
Building Paper	-5.6	24.1	274.1	287.9	284.5	283.3	282.5	281.6	280.8	280.3	279.6	279.3
			MC % --->	57.3	43.2	38.2	34.9	31.1	27.8	25.7	22.8	21.6
	-2.2	24.1	274.1	284.8	280.0	278.7	277.4	277.0	276.5	276.3	276.1	276.0
			MC % --->	44.4	24.5	19.1	13.7	12.0	10.0	9.1	8.3	7.9
	0.0	24.1	274.1	283.3	279.2	278.0	277.3	276.4	276.4	276.4	276.0	275.9
			MC % --->	38.2	21.2	16.2	13.3	9.5	9.5	9.5	7.9	7.5
	3.9	24.1	274.1	285.1	281.1	278.6	278.5	277.7	277.4	277.0	276.7	276.5
			MC % --->	45.6	29.0	18.7	18.3	14.9	13.7	12.0	10.8	10.0
	15.6	24.1	274.1	285.5	280.1	278.5	277.9	277.0	276.5	276.2	275.5	275.5
			MC % --->	47.3	24.9	18.3	15.8	12.0	10.0	8.7	5.8	5.8
	23.3	24.1	274.1	285.8	279.2	276.9	276.0	275.8	275.4	275.0	274.8	274.7
			MC % --->	48.5	21.2	11.6	7.9	7.1	5.4	3.7	2.9	2.5
Tentest	-5.6	35.5	218.9	313.7	307.5	305.1	304.0	302.8	301.6	300.8	299.6	298.5
			MC % --->	267.0	249.6	242.8	239.7	236.3	233.0	230.7	227.3	224.2
	-2.2	35.5	218.9	338.1	332.8	330.0	326.4	323.7	321.5	319.4	318.0	314.5
			MC % --->	335.8	320.8	313.0	302.8	295.2	289.0	283.1	279.2	269.3
	0.0	35.5	218.9	327.8	321.6	319.3	316.3	314.0	312.3	309.8	306.8	304.0
			MC % --->	306.8	289.3	282.8	274.4	267.9	263.1	256.1	247.6	239.7
	3.9	35.5	218.9	336.4	331.1	327.5	324.7	320.6	316.5	311.0	306.0	302.3
			MC % --->	331.0	316.1	305.9	298.0	286.5	274.9	259.4	245.4	234.9
	15.6	35.5	218.9	338.1	329.7	325.8	321.2	312.2	305.7	296.9	289.9	282.7
			MC % --->	335.8	312.1	301.1	288.2	262.8	244.5	219.7	200.0	179.7
	23.3	35.5	218.9	348.7	338.1	331.6	326.8	323.6	320.5	316.5	310.8	307.5
			MC % --->	365.6	335.8	317.5	303.9	294.9	286.2	274.9	258.9	249.6
Pine	-5.6	93.3	209.1	280.4	275.6	273.8	272.6	271.0	269.5	268.0	266.7	265.5
			MC % --->	76.4	71.3	69.3	68.1	66.3	64.7	63.1	61.7	60.5
	-2.2	93.3	209.1	277.3	271.7	269.4	267.1	264.8	261.7	260.4	258.5	256.0
			MC % --->	73.1	67.1	64.6	62.2	59.7	56.4	55.0	52.9	50.3
	0.0	93.3	209.1	277.6	273.4	271.5	268.7	266.1	264.7	262.1	259.2	256.1
			MC % --->	73.4	68.9	66.9	63.9	61.1	59.6	56.8	53.7	50.4
	3.9	93.3	209.1	277.3	273.0	269.7	266.1	261.5	257.7	251.7	248.2	245.1
			MC % --->	73.1	68.5	65.0	61.1	56.2	52.1	45.7	41.9	38.6
	15.6	93.3	209.1	272.7	262.5	257.0	251.5	245.2	241.6	237.1	234.0	231.0
			MC % --->	68.2	57.2	51.3	45.4	38.7	34.8	30.0	26.7	23.5
	23.3	93.3	209.1	277.2	268.6	263.5	258.5	255.3	251.7	248.3	242.8	240.2
			MC % --->	73.0	63.8	58.3	52.9	49.5	45.7	42.0	36.1	33.3

TABLE 2: CONTINUED

Industrial	-5.6	100.5	233.3	348.2	341.4	339.5	338.3	337.4	335.3	334.0	332.6	331.7
Poplar			MC % --->	114.3	107.6	105.7	104.5	103.6	101.5	100.2	98.8	97.9
	-2.2	100.5	233.3	354.4	348.7	344.8	341.0	339.3	336.0	333.8	331.9	328.7
			MC % --->	120.5	114.8	110.9	107.2	105.5	102.2	100.0	98.1	94.9
	0.0	100.5	233.3	348.9	343.7	341.1	338.4	335.0	333.0	330.3	326.6	322.7
			MC % --->	115.0	109.9	107.3	104.6	101.2	99.2	96.5	92.8	89.0
	3.9	100.5	233.3	349.8	345.0	340.9	338.6	333.8	329.7	323.5	319.8	315.5
			MC % --->	115.9	111.1	107.1	104.8	100.0	95.9	89.8	86.1	81.8
	15.6	100.5	233.3	346.1	336.6	332.8	327.9	320.2	314.2	305.7	300.0	294.5
			MC % --->	112.2	102.8	99.0	94.1	86.5	80.5	72.0	66.4	60.9
	23.3	100.5	233.3	358.3	351.5	346.1	341.1	337.7	334.0	330.5	324.4	320.9
			MC % --->	124.4	117.6	112.2	107.3	103.9	100.2	96.7	90.6	87.2
Prepared	-5.6	68.3	176.4	241.8	237.0	235.1	234.0	232.7	231.2	229.7	228.2	226.7
Poplar			MC % --->	95.8	88.7	85.9	84.3	82.4	80.2	78.0	75.8	73.6
	-2.2	68.3	176.4	241.9	236.8	233.0	230.7	228.9	226.3	225.1	223.2	220.8
			MC % --->	95.9	88.4	82.9	79.5	76.9	73.1	71.3	68.5	65.0
	0.0	68.3	176.4	243.6	239.4	236.5	233.9	231.3	229.7	227.8	225.7	222.8
			MC % --->	98.4	92.2	88.0	84.2	80.4	78.0	75.3	72.2	67.9
	3.9	68.3	176.4	247.8	241.5	238.7	235.6	231.9	228.4	223.4	220.1	217.0
			MC % --->	104.5	95.3	91.2	86.7	81.3	76.1	68.8	64.0	59.4
	15.6	68.3	176.4	244.9	233.5	229.5	225.8	219.1	214.6	210.0	206.3	202.8
			MC % --->	100.3	83.6	77.7	72.3	62.5	55.9	49.2	43.8	38.7
	23.3	68.3	176.4	247.9	241.1	235.6	230.7	227.6	225.1	222.1	217.4	215.1
			MC % --->	104.7	94.7	86.7	79.5	75.0	71.3	66.9	60.0	56.7
Mahogany	-5.6	75.8	187.3	254.7	250.5	245.4	242.5	239.5	238.2	236.2	235.2	233.8
			MC % --->	88.9	83.4	76.6	72.8	68.9	67.2	64.5	63.2	61.3
	-2.2	75.8	187.3	241.5	236.5	233.8	231.2	229.2	226.7	225.4	223.8	221.5
			MC % --->	71.5	64.9	61.3	57.9	55.3	52.0	50.3	48.2	45.1
	0.0	75.8	187.3	250.1	244.9	241.8	239.0	236.4	235.1	233.4	230.4	228.0
			MC % --->	82.8	76.0	71.9	68.2	64.8	63.1	60.8	56.9	53.7
	3.9	75.8	187.3	251.3	246.5	243.1	240.0	236.2	233.5	229.3	226.3	223.5
			MC % --->	84.4	78.1	73.6	69.5	64.5	60.9	55.4	51.5	47.8
	15.6	75.8	187.3	248.7	239.3	236.2	232.6	227.3	222.9	218.3	215.1	212.3
			MC % --->	81.0	68.6	64.5	59.8	52.8	47.0	40.9	36.7	33.0
	23.3	75.8	187.3	243.4	236.9	232.4	228.5	226.1	223.3	221.6	217.9	216.3
			MC % --->	74.0	65.4	59.5	54.4	51.2	47.5	45.3	40.4	38.3

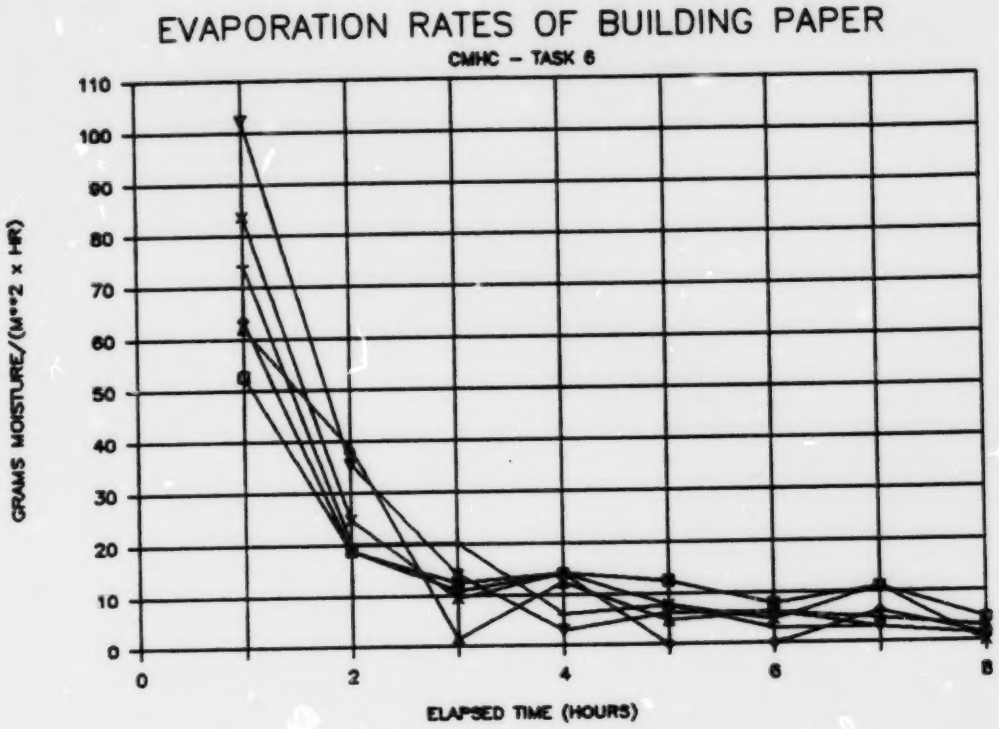

FIGURE 1(a)

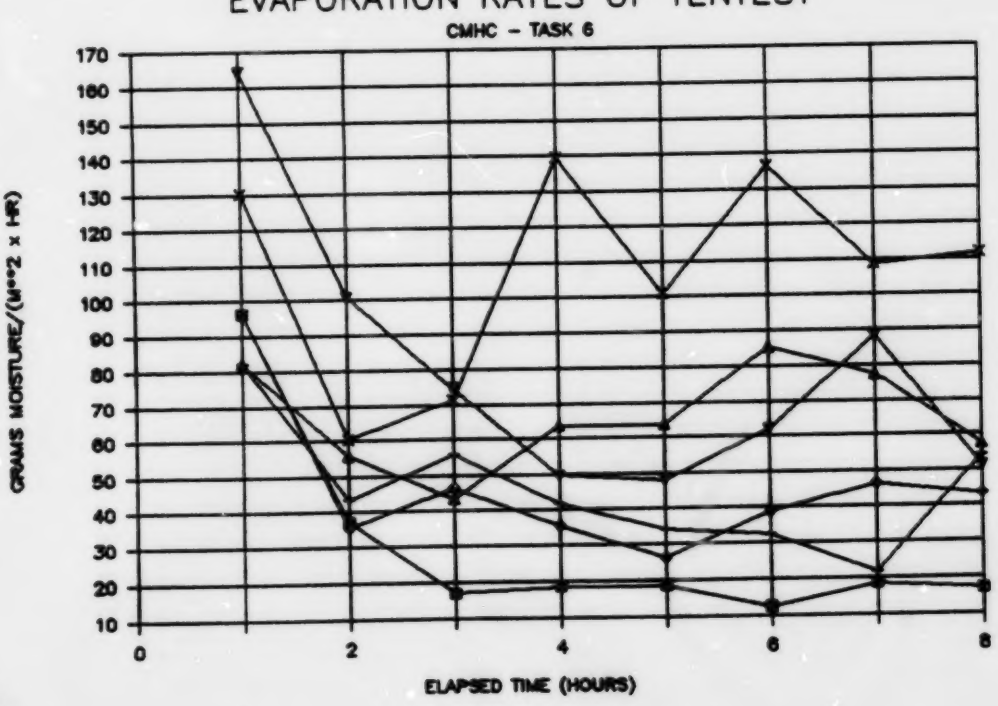

FIGURE 1(b)

RWDI

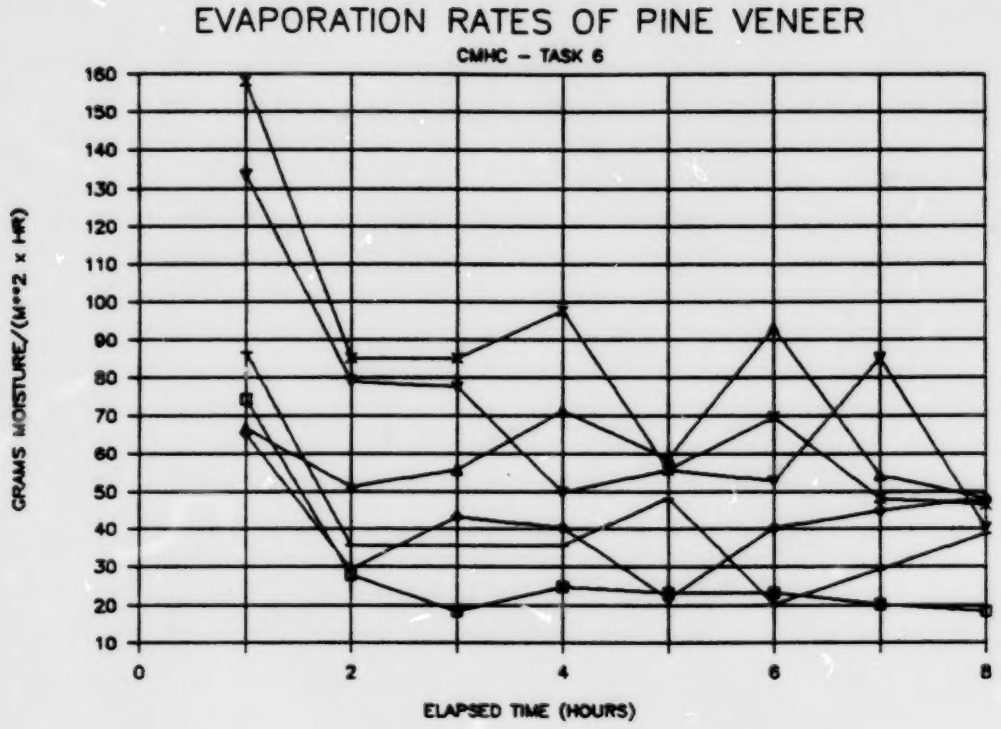

FIGURE 1(c)

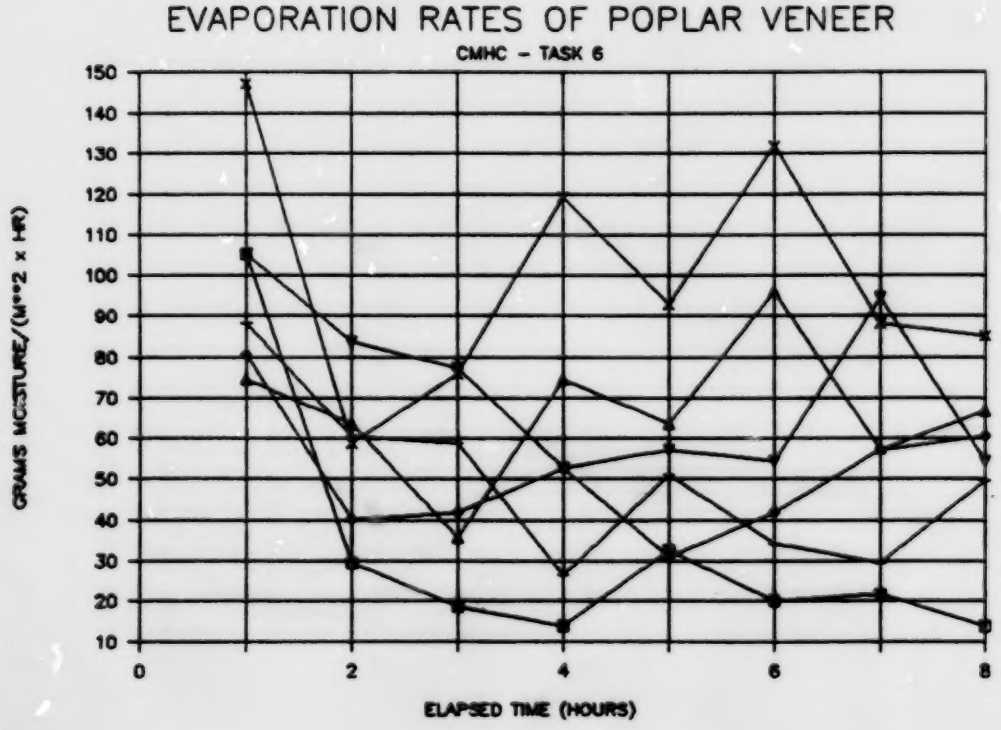

FIGURE 1(d)

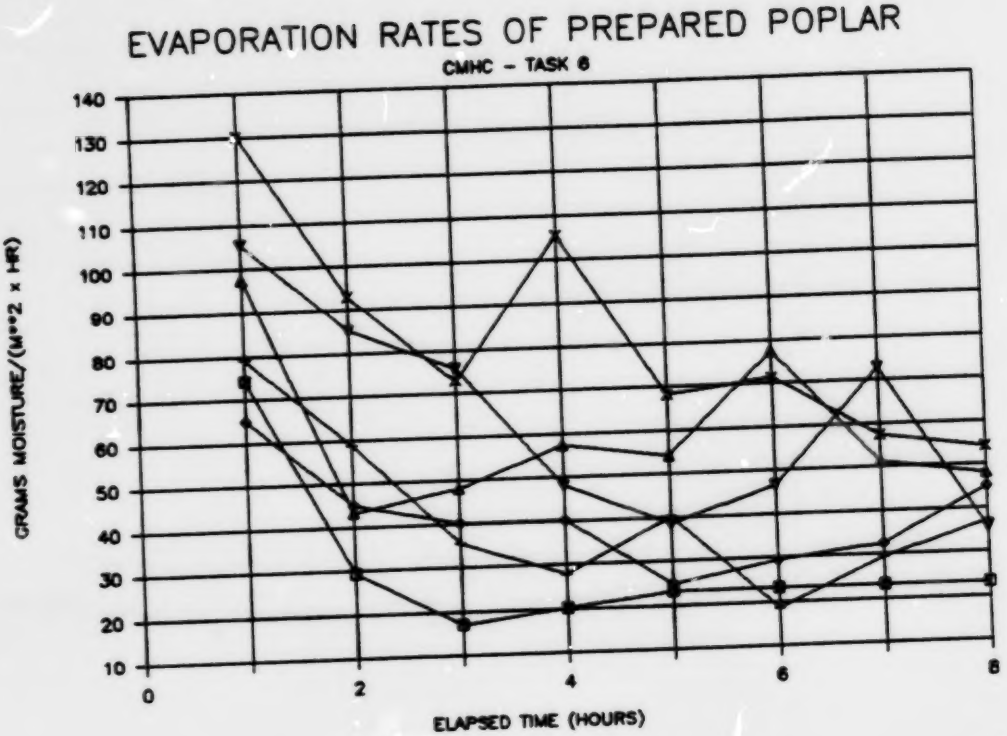

FIGURE 1(e)

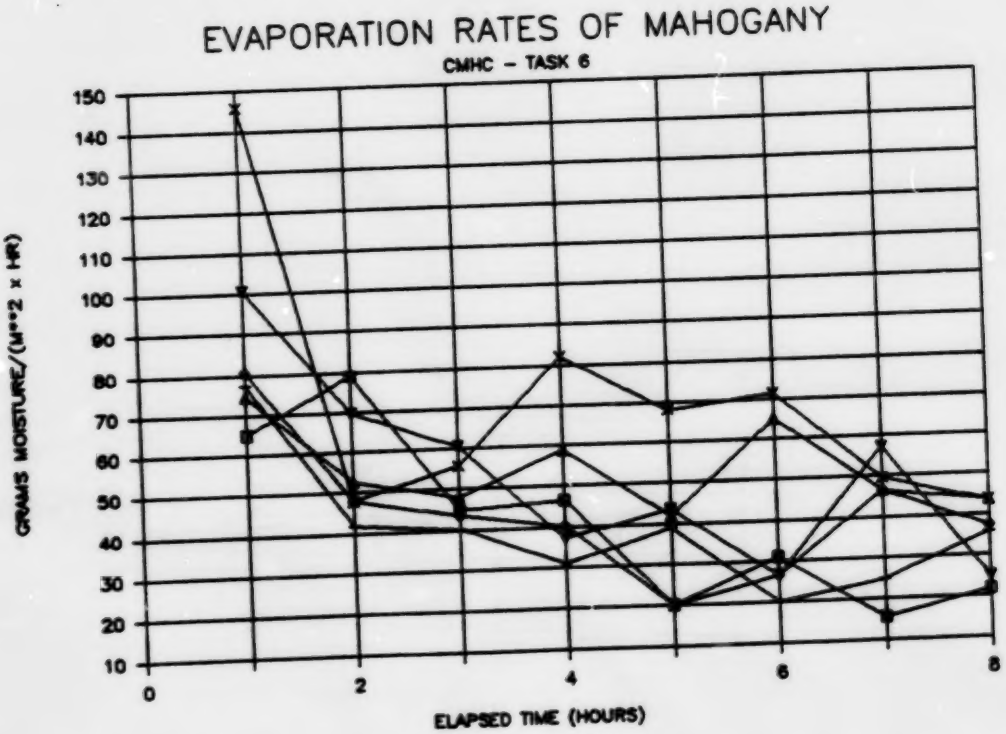

FIGURE 1(f)

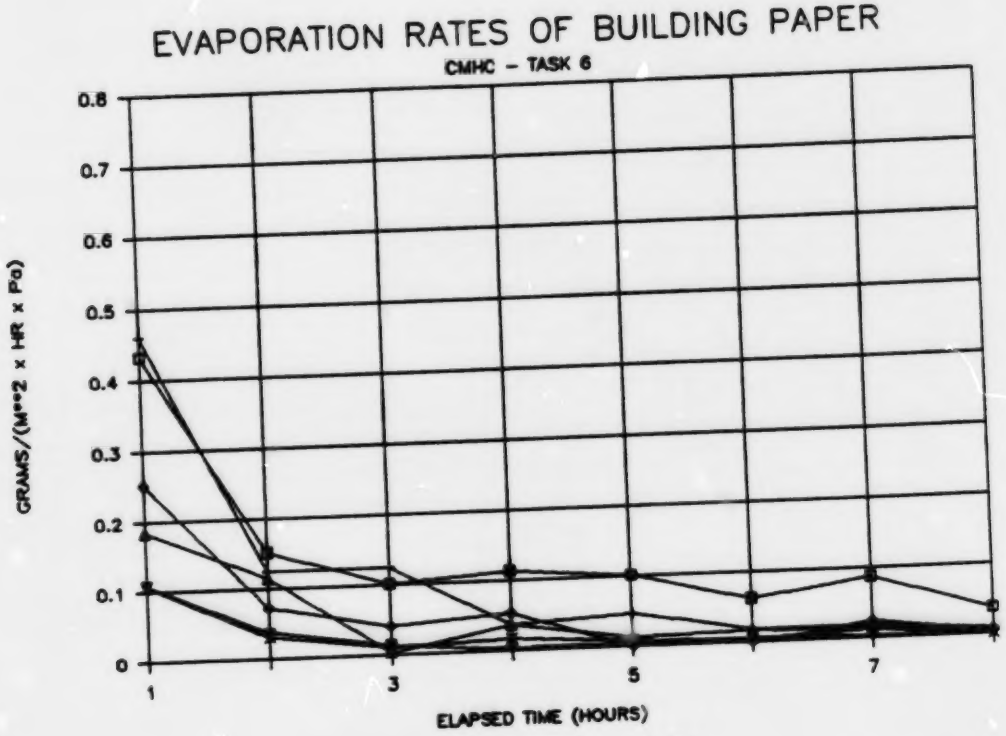

FIGURE 2(a)

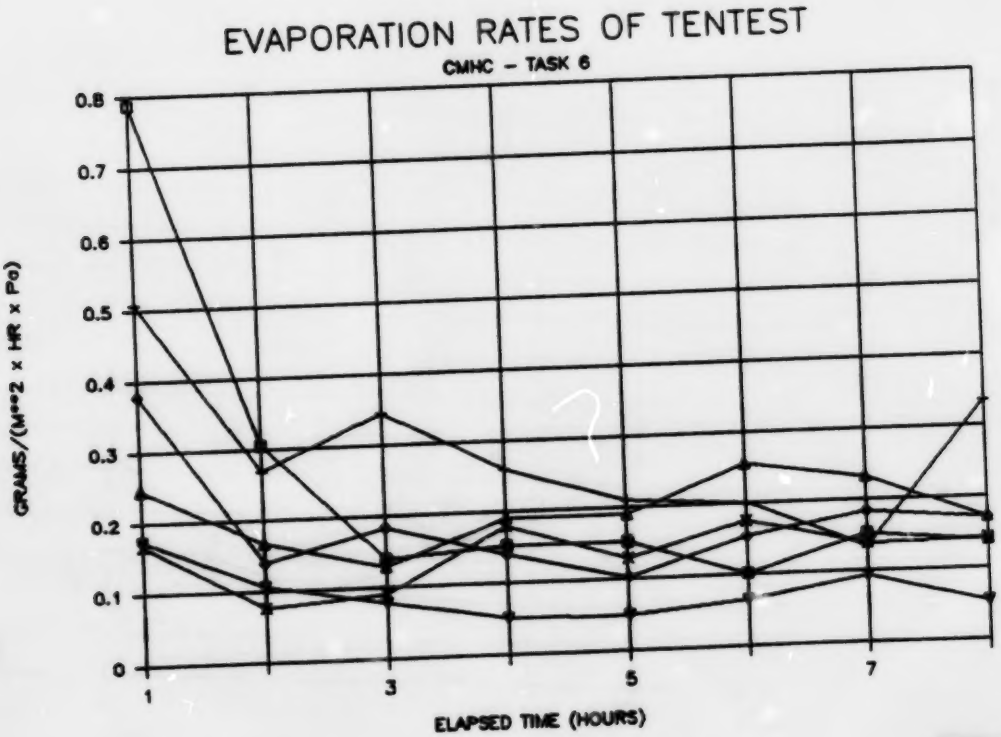

FIGURE 2(b)

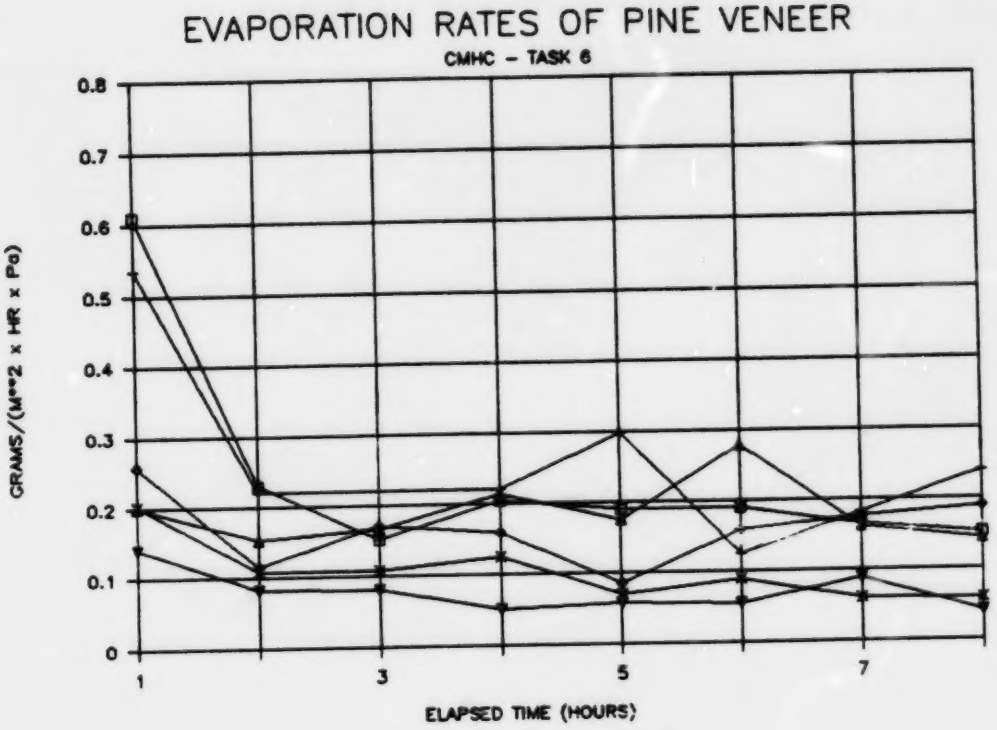

FIGURE 2(c)

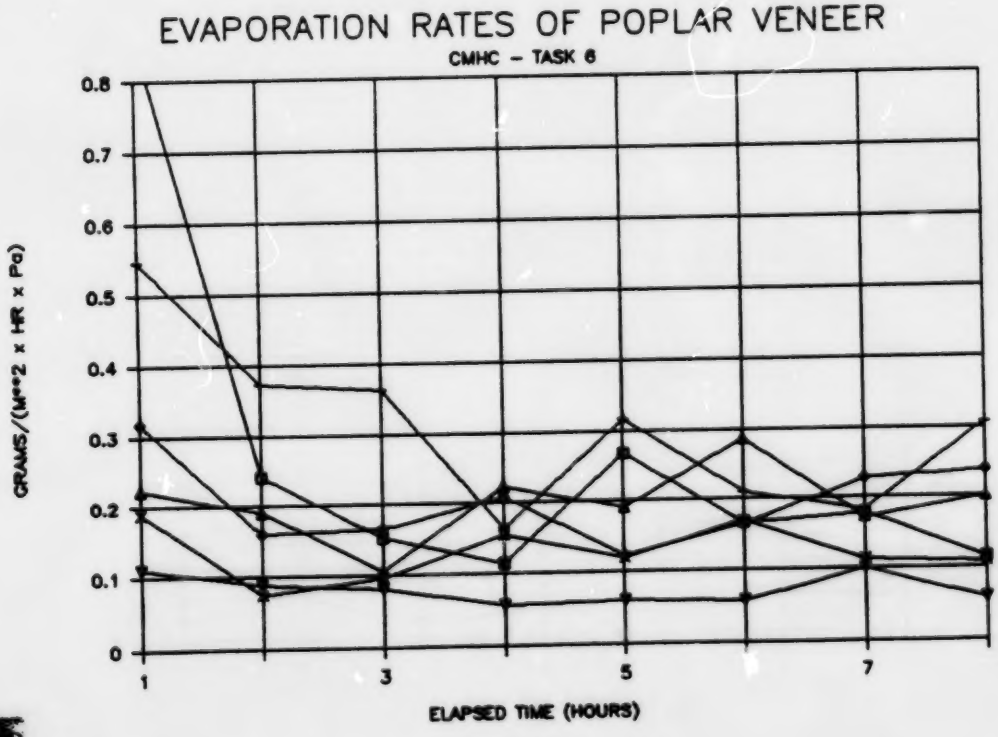

FIGURE 2(d)

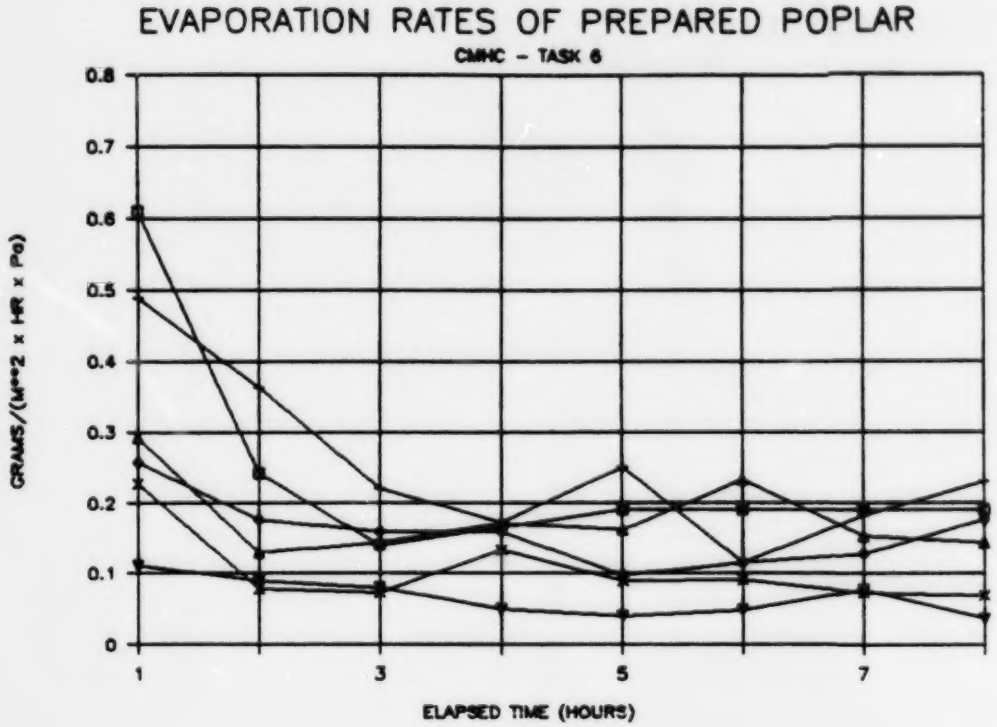

FIGURE 2(e)

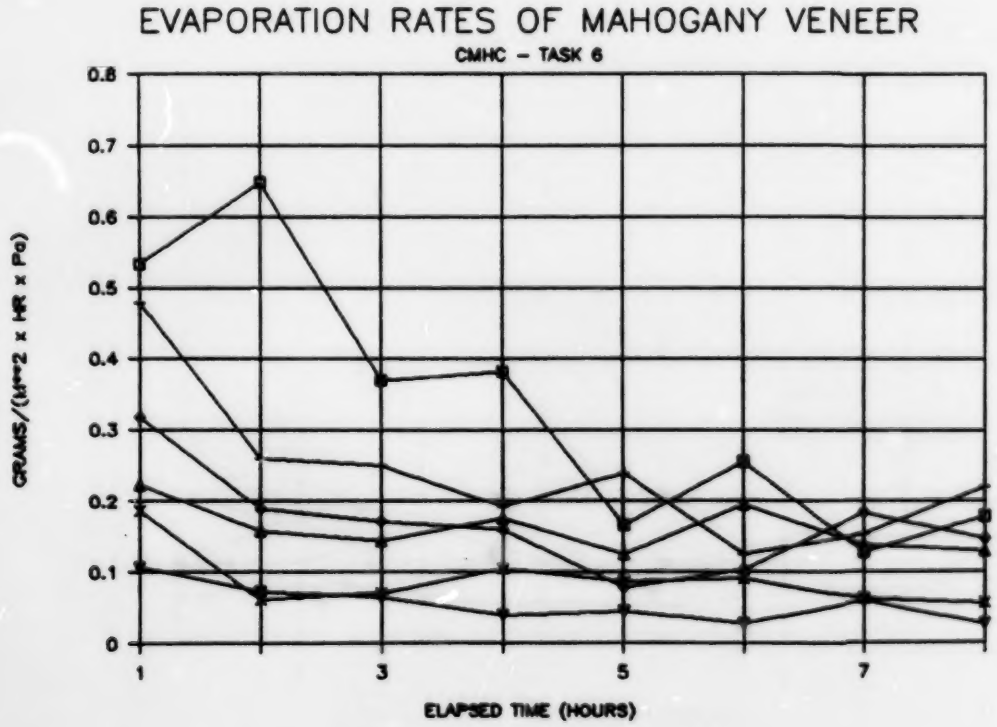

FIGURE 2(f)

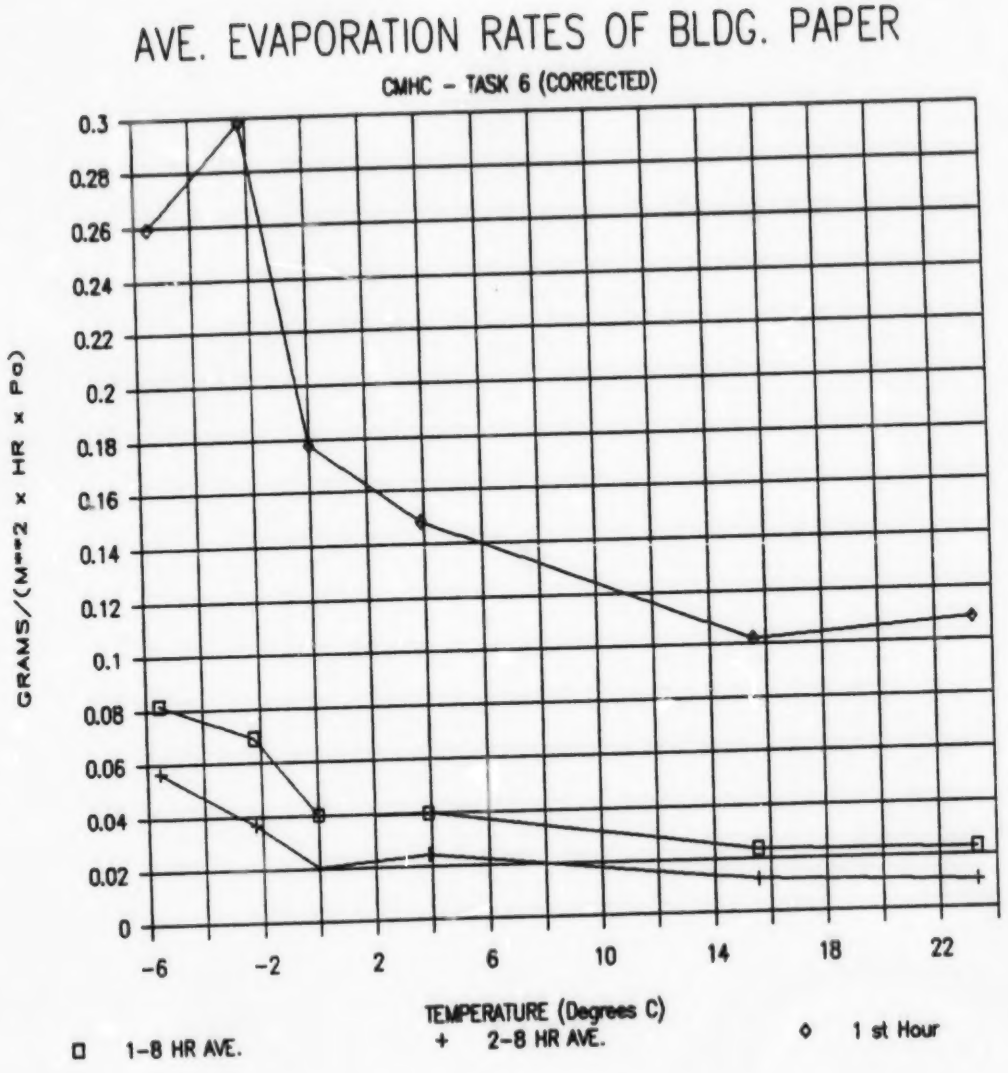
AVE. EVAPORATION RATES OF BLDG. PAPER
CMHC - TASK 6 (CORRECTED)
GRAMS/(M**2 x HR x Pa)
0.3
0.28
0.26
0.24
0.22
0.2
0.18
0.16
0.14
0.12
0.1
0.08
0.06
0.04
0.02
0
-6
-2
2
6
10
14
18
22
TEMPERATURE (Degrees C)
1-8 HR AVE.
2-8 HR AVE.
1 st Hour

FIGURE 3(a)

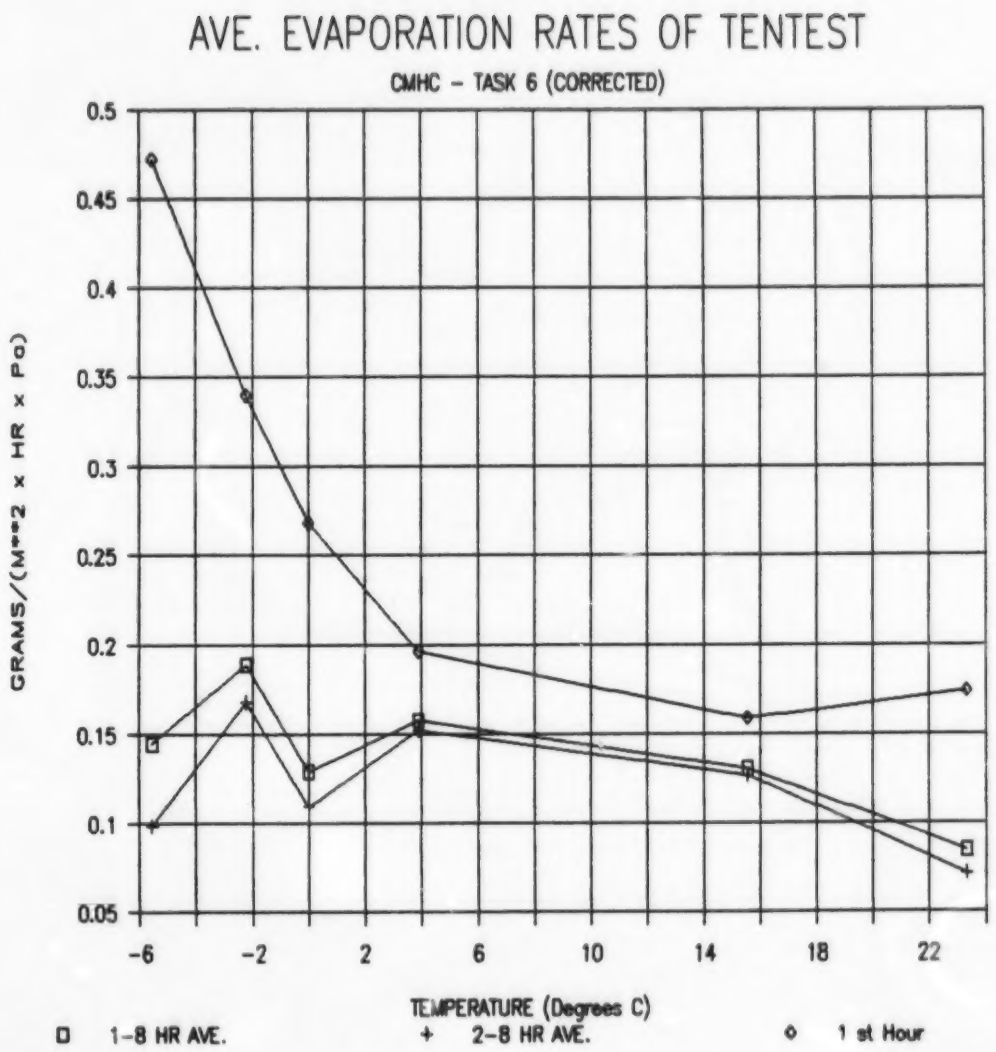
AVE. EVAPORATION RATES OF TENTEST
CMHC – TASK 6 (CORRECTED)
GRAMS/(M**2 x HR x Pa)
0.5
0.45
0.4
0.35
0.3
0.25
0.2
0.15
0.1
0.05
-6
-2
2
6
10
14
18
22
TEMPERATURE (Degrees C)
1-8 HR AVE.
2-8 HR AVE.
1 st Hour

FIGURE 3(b)

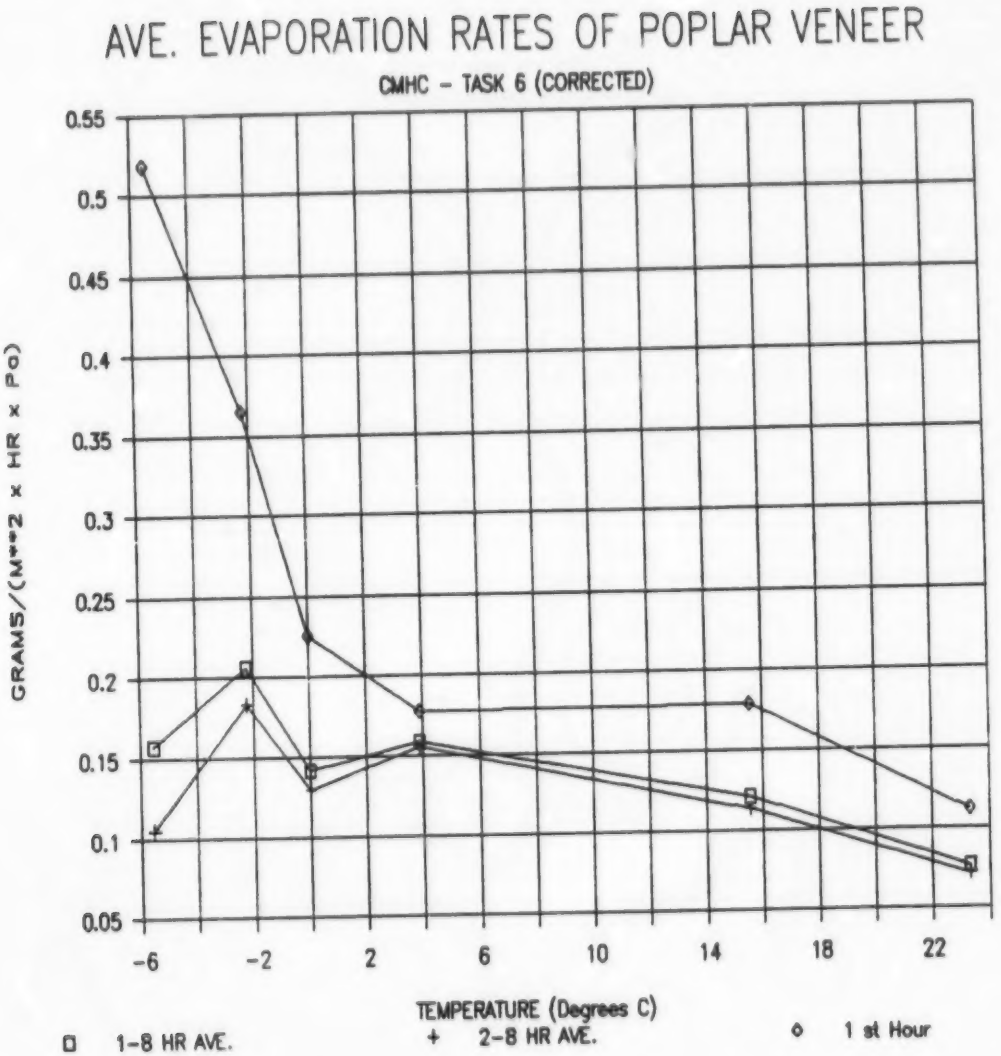
AVE. EVAPORATION RATES OF POPLAR VENEER
CMHC - TASK 6 (CORRECTED)
GRAMS/(M**2 x HR x Po)
0.55
0.5
0.45
0.4
0.35
0.3
0.25
0.2
0.15
0.1
0.05
-6
-2
2
6
10
14
18
22
TEMPERATURE (Degrees C)
1-8 HR AVE.
2-8 HR AVE.
1 st Hour

FIGURE 3(c)

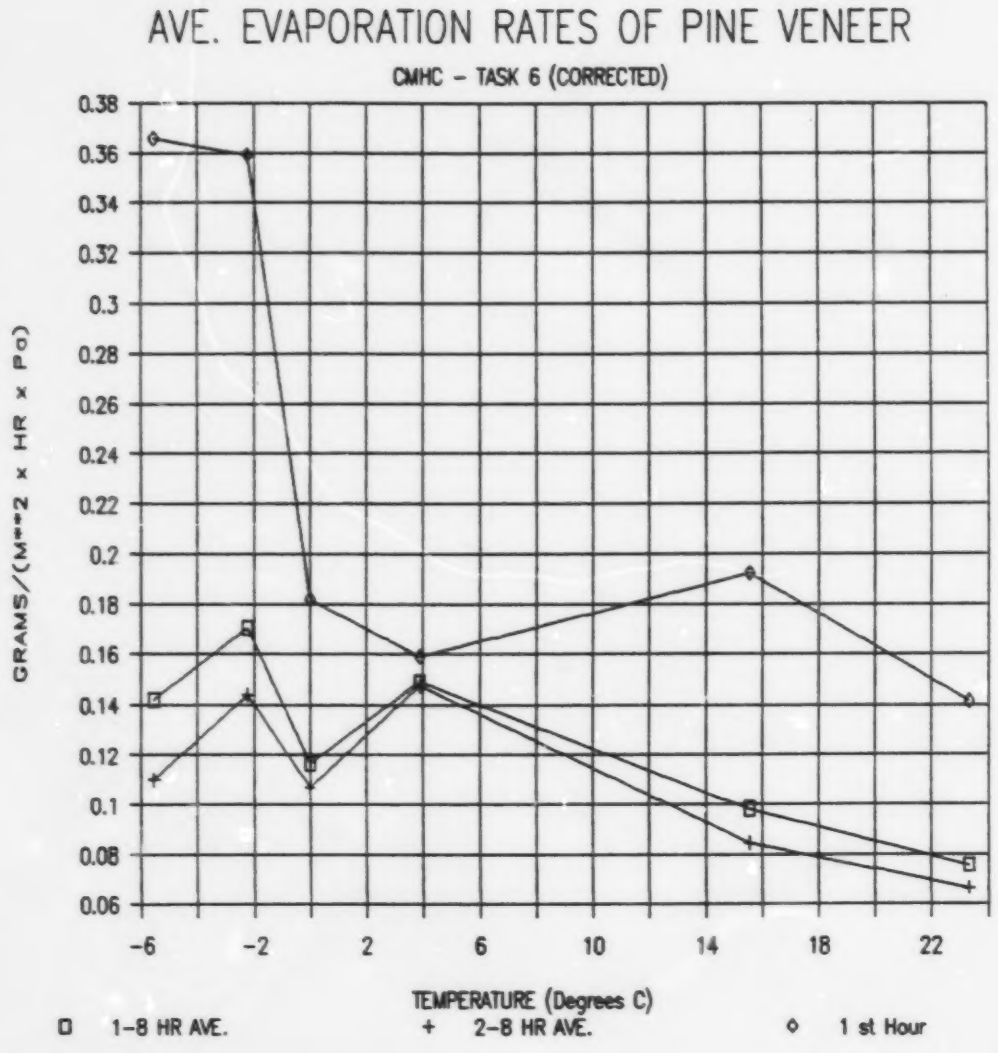
AVE. EVAPORATION RATES OF PINE VENEER
CMHC - TASK 6 (CORRECTED)
GRAMS/(M**2 x HR x Po)
0.38
0.36
0.34
0.32
0.3
0.28
0.26
0.24
0.22
0.2
0.18
0.16
0.14
0.12
0.1
0.08
0.06
-6
-2
2
6
10
14
18
22
TEMPERATURE (Degrees C)
1-8 HR AVE.
2-8 HR AVE.
1 st Hour

FIGURE 3(d)

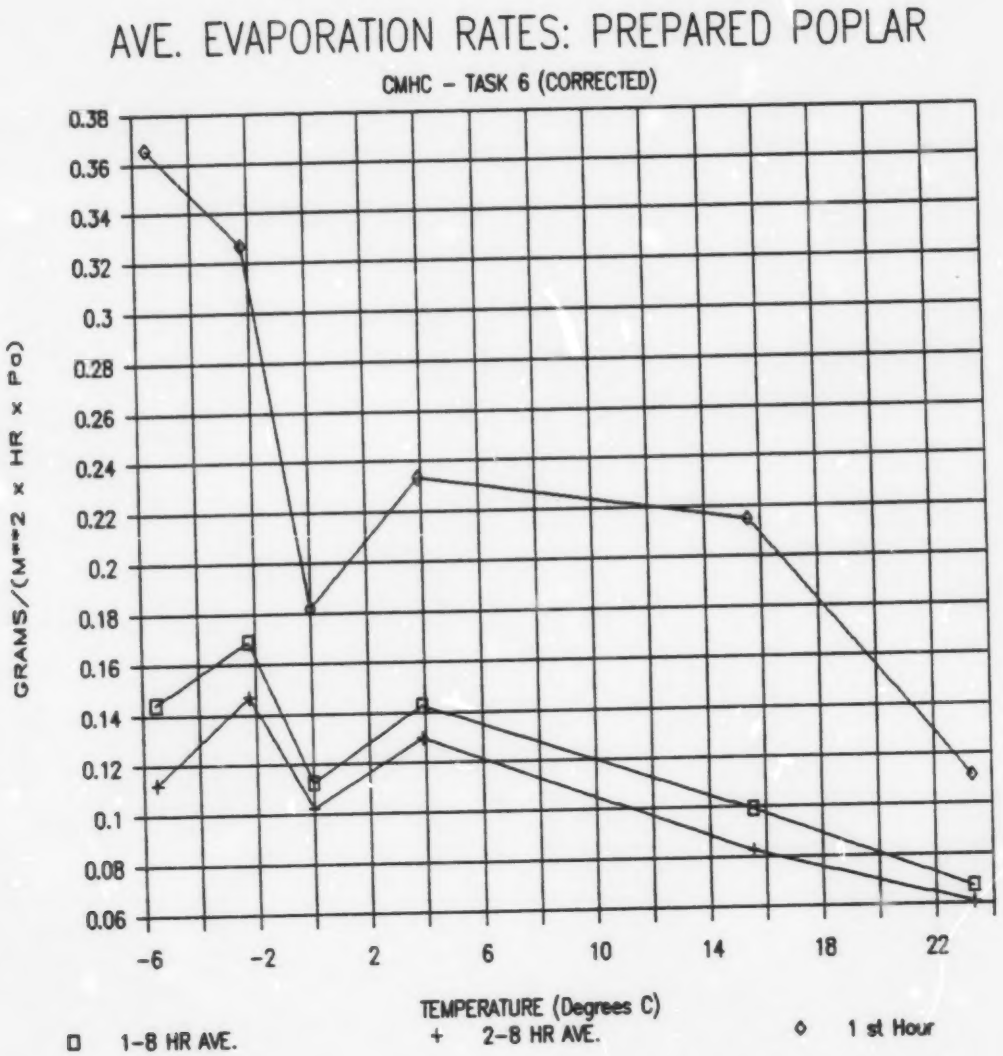
AVE. EVAPORATION RATES: PREPARED POPLAR
CMHC - TASK 6 (CORRECTED)
GRAMS/(M**2 x HR x Po)
0.38
0.36
0.34
0.32
0.3
0.28
0.26
0.24
0.22
0.2
0.18
0.16
0.14
0.12
0.1
0.08
0.06
-6
-2
2
6
10
14
18
22
TEMPERATURE (Degrees C)
1-8 HR AVE.
2-8 HR AVE.
1 st Hour

FIGURE 3(e)

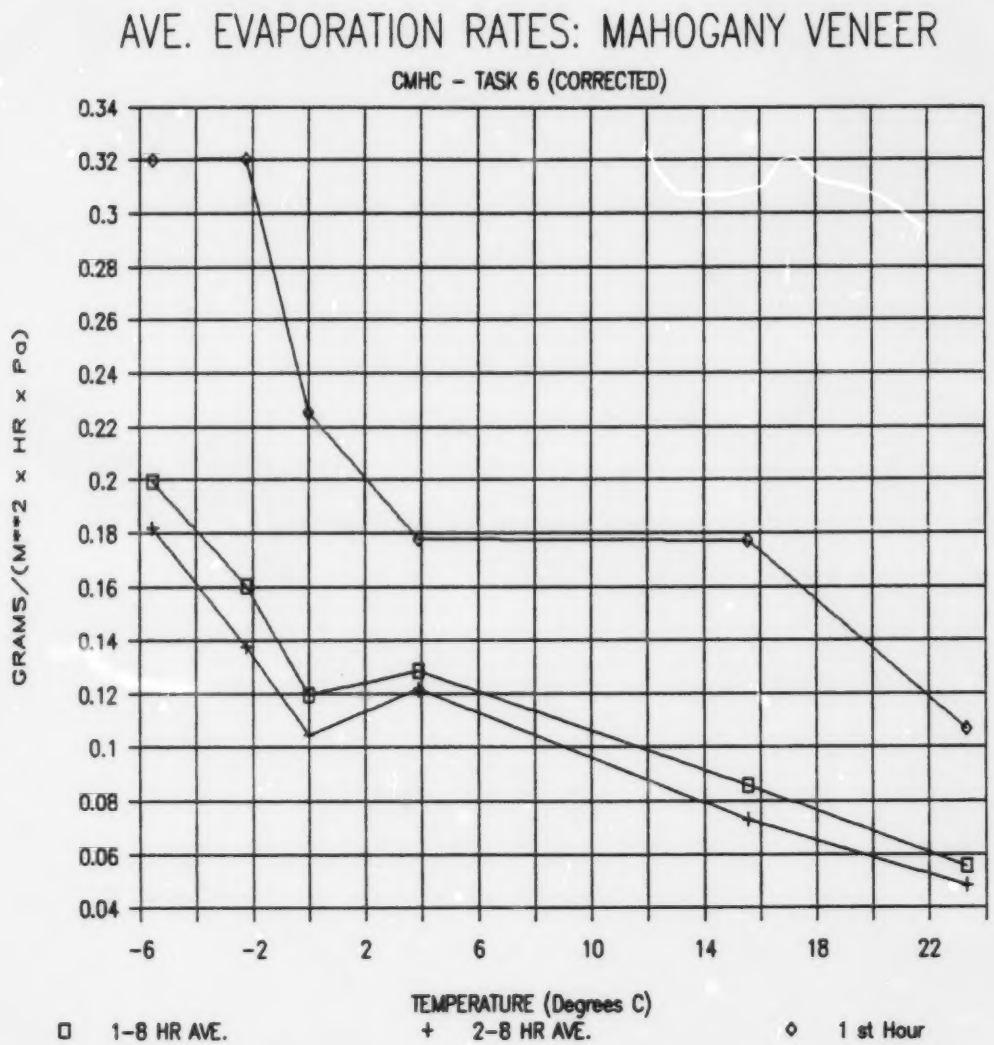
AVE. EVAPORATION RATES: MAHOGANY VENEER
CMHC – TASK 6 (CORRECTED)
GRAMS/(M**2 x HR x Pa)
0.34
0.32
0.3
0.28
0.26
0.24
0.22
0.2
0.18
0.16
0.14
0.12
0.1
0.08
0.06
0.04
-6
-2
2
6
10
14
18
22
TEMPERATURE (Degrees C)
1-8 HR AVE.
2-8 HR AVE.
1 st Hour

FIGURE 3(f)

(A)

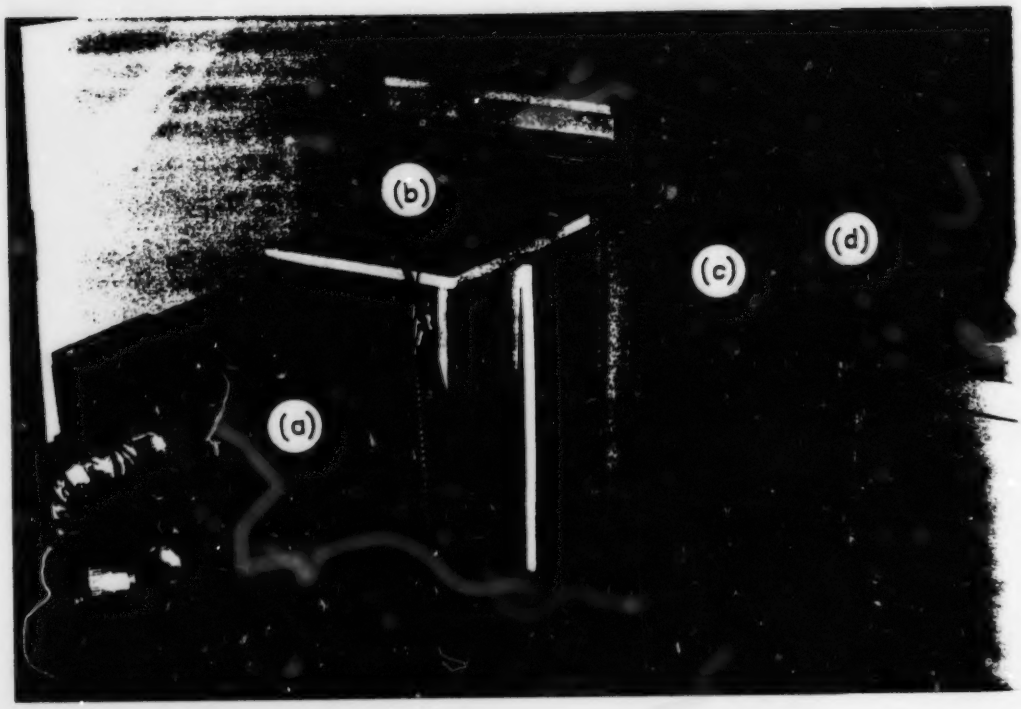

(a) A/C UNIT (b) HEATER CONTROL (c) MIXING CHAMBER (d) TEST CHAMBER

(B)

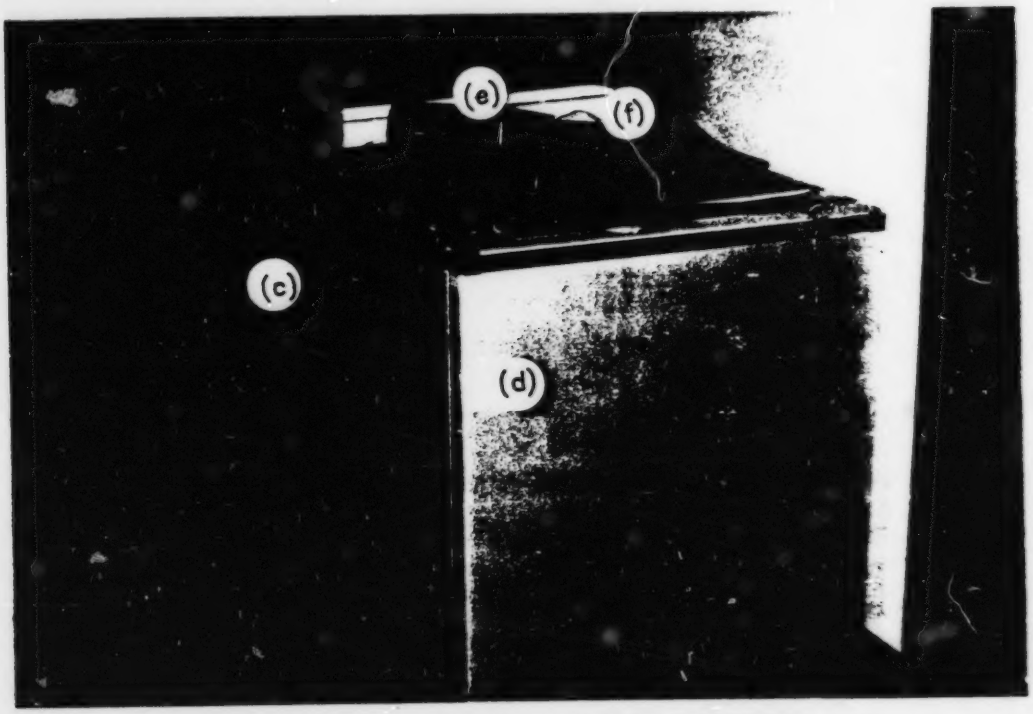

(c) MIXING CHAMBER (d) TEST CHAMBER
(e) THERMOCOUPLE RECORDER (f) RELATIVE HUMIDITY SENSOR

PHOTOGRAPHS (A) & (B): EXPERIMENTAL APPARATUS